

DETERMINATION OF DRAINAGE RATES OF HEAVY MEDIA FOR DIFFERENT APERTURE SIZES ON A VIBRATING SCREEN

By

Kabondo Leonard

*Thesis presented in partial fulfilment
of the requirements for the degree
of*

MASTER OF ENGINEERING

(EXTRACTIVE METALLURGICAL ENGINEERING)



UNIVERSITEIT
In the faculty of Engineering
STELLENBOSCH
UNIVERSITY
at Stellenbosch University



Supervisor:

Dr. Neil Snyders

Co-Supervisors:

Prof. Steven Bradshaw

Prof. Guven Akdogan

March 2018

DECLARATION

By submitting this thesis electronically, I declare that the entirety of the work contained therein is my own, original work, that I am the sole author thereof (save to the extent explicitly otherwise stated), that reproduction and publication thereof by Stellenbosch University will not infringe any third-party rights and that I have not previously in its entirety or in part submitted it for obtaining any qualification.

March 2018

Copyright © 2018 Stellenbosch University

All rights reserved

ABSTRACT

Media losses are a significant contributor to the operational cost in a dense media separation (DMS) circuit. Of these losses, up to 80 wt% can occur on the drain and rinse vibrating screens. Although these screens are an integral part of any DMS circuit, surprisingly little work can be found in open literature regarding the effect of different screening panels on medium recovery, and particularly on ferrosilicon. Hence, considering the cost implication of heavy medium to the DMS circuit, the project focused on the recovery of medium particles. In this case, the effect of slurry density, volumetric flowrate and slot size variation were investigated.

To execute the thesis, experimental works were conducted on a 0.6 x 1.2 m vibrating screen with polyurethane, rubber, and poly-wedge slot apertures at slurry density between 1.6 – 2.7 kg/L and volumetric flowrate of 18 – 26 m³/h for both magnetite and ferrosilicon. Medium drainage rates were established with and without ore material for the entire underflow stream. Samples from the feed, underflow and overflow streams were collected for particle size distribution analysis, percent moisture, medium carryover and mass balance calculations.

Results obtained showed that increasing volumetric flowrate from 19.9 – 23.7 m³/h led to an increase in ferrosilicon drainage rate, percent moisture and medium carryover. However, once a critical volumetric flowrate was exceeded, a further increase in volumetric flowrate led to a decrease in drainage rate with a sharp increase in moisture and medium bypass to the oversize stream. A shift in the critical volumetric flowrate from 23.7 m³/h for fresh ferrosilicon to 24.5 m³/h for degraded material was observed. Comparable results obtained on magnetite showed different critical volumetric flowrates for different screen panels with 1x13 mm and 0.8x8.8 mm at 20.8 m³/h, 1x12 mm rubber panels and 0.63 mm poly-wedge at 21.3 m³/h, and 0.63x12 mm and 0.63x8.8 mm at 20.4 m³/h.

The increase in ferrosilicon slurry density from 1.9 to 2.45 kg/L led to a gradual decrease in medium drainage rate with increase in moisture and medium bypass to the oversize stream. However, a sharp drop in the drainage rate coupled with a significant increase in moisture and medium carryover was observed at slurry density between 2.45 – 2.7 kg/L. Conversely, increase in magnetite slurry density from 1.64 to 1.84 kg/L led to a gradual decrease in medium drainage rate across all the panels tested.

On the other hand, aperture size increase from 0.63x8.8 mm to 0.8x8.8 mm to 1.0x13 mm resulted in an increase in ferrosilicon drainage rate of about 1.4 - 1.9 m³/m²/h with a reduction in moisture and medium carryover of about 1.0 – 1.2 w/w% and 14.1 – 20.2 kg/t/m

respectively depending on the volumetric flowrate. The increase in slot width from 0.63 to 0.8 mm led to an increase in magnetite drainage rate of about 1.0 - 1.4 m³/m²/h at volumetric flowrate between 20.4 – 22.8 m³/h. However, the increase in slot length from 8.8 to 12 mm led to an increase in magnetite drainage rate of about 0.1 - 0.5 m³/m²/h at volumetric flowrate between 19.94 – 22.8 m³/h.

Increase in slurry density from 1.9 to 2.45 kg/L led to a steady decrease in the sharpness of separation with the cut sizes becoming finer postulating a rise in moisture and medium carryover to the oversize stream. Beyond 2.45 kg/L, a sharp decrease in the efficiency of separation and cut sizes with an increase in water split was observed. Increase in volumetric flowrate from 21.8 to 24.5 m³/h led to a drop in the sharpness of separation and cut size values with an upsurge in water carryover to the oversize stream. However, higher volumetric flowrate and slurry density led to a sharp decrease in the sharpness of separation and cut sizes with a marked increase in moisture bypass.

ACKNOWLEDGEMENTS

Want to thank God Almighty for giving me the strength and will to pursue this research project.

Would also like to give sincere gratitude and thanks to the following individuals and institutions:

- Project supervisors, Dr. Neil Snyders, Prof. Steven Bradshaw and Prof. Guven Akdogan, for according me the opportunity to pursue a Master's degree and for their technical support and input.
- Multotec, Copperbelt University and the Department of Process Engineering, Stellenbosch University for the financial and material support.
- My wife, sons (Chikombe and Bukata), mum, Cynthia, Sydney and nieces (Chanda and Patricia) for the unwavering support and words of encouragement.

TABLE OF CONTENTS

DECLARATION	i
ABSTRACT	ii
ACKNOWLEDGEMENTS	iv
LIST OF FIGURES	xii
LIST OF TABLES	xvi
LIST OF SYMBOLS	xvii
1 INTRODUCTION.....	1
1.1 Background and problem statement	1
1.2 Objectives of the study	3
1.3 Project significance.....	3
2 LITERATURE REVIEW.....	5
2.1 Purpose of screening.....	5
2.1.1 Medium recovery in a dense medium circuit	7
2.1.2 Significance of medium recovery	10
2.1.3 Section summary	10
2.2 Screen panels	11
2.2.1 Types of screen panels	11
2.2.1.1 Woven wire or wedge wire screens	12
2.2.1.2 Polymeric screen panels.....	13
2.2.1.2.1 Rubber panels	13
2.2.1.2.2 Polyurethane panels	14
2.2.2 Screen panel accessories	14
2.2.3 Section summary	14
2.3 Mechanisms of screening	15
2.4 Screen performance	16
2.4.1 Screen efficiency	17
2.4.2 Efficiency curve properties	19

2.4.2.1	Water bypass to the oversize stream (R_f).....	19
2.4.2.2	Cut size (D_{50})	19
2.4.2.3	Sharpness of separation (α).....	19
2.4.3	Effects of operating variables on screening rate	20
2.4.3.1	Screen aperture shape	21
2.4.3.2	Screen aperture size	22
2.4.3.3	Slurry density	22
2.4.3.4	Feed rate.....	23
2.4.3.5	Vibration intensity	23
2.4.3.6	Angle of inclination	25
2.4.3.7	Particle size distribution.....	26
2.4.3.8	Open area	28
2.4.3.9	Screen length and width.....	28
2.4.3.10	Material bed depth	28
2.4.3.11	Material flowability	29
2.4.3.12	Material friability	30
2.4.3.13	Particle shape.....	30
2.4.3.14	Particle density	31
2.4.4	Section summary	31
3	RESEARCH METHODOLOGY AND DESIGN.....	33
3.1	Introduction	33
3.2	Material preparation and characterisation	33
3.2.1	Material preparation	33
3.3	Design of experiments	35
3.4	Experimental set-up and procedure.....	37
3.5	Consideration of experimental variables	41
3.5.1	Feed rate	41
3.5.2	Slurry density	42

3.5.3	Aperture size	42
3.6	Results reproducibility.....	42
3.6.1	Medium drainage rate reproducibility.....	42
3.6.2	Moisture and medium carryover reproducibility	44
3.6.3	Viscosity reproducibility	45
4	RESULTS AND DISCUSSIONS	46
4.1	Introduction	46
4.2	Material characterisation	46
4.3	Effects of operating conditions on ferrosilicon recovery	48
4.3.1	Effects of feed rate variation on ferrosilicon recovery.....	49
4.3.1.1	Effects of volumetric flowrate variation on drainage rate.....	49
4.3.1.2	Effects of volumetric flowrate variation on moisture bypass	51
4.3.1.3	Effects of feed rate variation on ferrosilicon carryover	53
4.3.1.4	Section summary	54
4.3.2	Influence of slurry density variation on ferrosilicon recovery	55
4.3.2.1	Influence of slurry density variation on drainage rate.....	55
4.3.2.2	Influence of slurry density variation on moisture bypass	56
4.3.2.3	Effects of slurry density variation on medium carryover.....	58
4.3.2.4	Section summary	60
4.3.3	Effects of aperture size variation on ferrosilicon recovery	60
4.3.3.1	Influence of aperture size variation on ferrosilicon drainage rate.....	60
4.3.3.2	Influence of aperture size variation on moisture and medium carryover.....	61
4.3.3.4	Section summary	62
4.3.4	Influence of slot width on fresh ferrosilicon recovery	62
4.3.4.1	Influence of slot width on medium drainage rate.....	63
4.3.4.2	Influence of slot width on moisture bypass.....	63
4.3.4.3	Influence of slot width on medium carryover	64
4.3.4.4	Section summary	65

4.4	Ferrosilicon degradation	65
4.4.1	Possible causes of ferrosilicon degradation	65
4.4.1.1	Slime contamination.....	65
4.4.1.2	Solid concentration	67
4.4.1.3	Shear rate	69
4.4.1.4	Medium oxidation.....	70
4.4.1.5	Ferrosilicon disintegration	71
4.4.1.6	Section summary	72
4.4.2	Influence of operating conditions on degraded ferrosilicon recovery rate.....	73
4.4.2.1	Influence of volumetric flowrate on degraded ferrosilicon recovery rate ..	73
4.4.2.1.1	Influence of volumetric flowrate on deg ferrosilicon drainage rate	73
4.4.2.1.2	Influence of volumetric flowrate on moisture bypass	74
4.4.2.1.3	Influence of volumetric flowrate on degraded ferrosilicon carryover.....	75
4.4.2.1.4	Section summary	76
4.4.2.2	Effects of slurry density on degraded ferrosilicon recovery rate	76
4.4.2.2.1	Effects of slurry density on deg ferrosilicon drainage rate.....	76
4.4.2.2.2	Effects of slurry density on moisture bypass.....	77
4.4.2.2.3	Effects of slurry density on degraded ferrosilicon carryover	78
4.4.2.2.4	Section summary	80
4.4.2.3	Influence of aperture size on degraded ferrosilicon recovery rate.....	80
4.4.2.3.1	Influence of aperture size on deg ferrosilicon drainage rate	80
4.4.2.3.2	Influence of aperture size on moisture and medium carryover	81
4.4.2.3.4	Section summary	81
4.4.3	Influence of degradation on medium recovery	82
4.4.3.1	Influence of degradation on drainage rate	82
4.4.3.2	Influence of medium degradation on moisture bypass.....	82
4.4.3.3	Influence of degradation on medium carryover	83
4.4.3.4	Section summary	84

4.4.4	Effects of screen panel material on degraded medium recovery	84
4.4.4.1	Effects of screen panel material on degraded medium drainage rate	84
4.4.4.2	Effects of screen panel material on moisture bypass	85
4.4.4.3	Effects of screen panel material on degraded medium carryover	86
4.4.4.4	Section summary	86
4.5	Effects of operating conditions on magnetite recovery	87
4.5.1	Effects of feed rate variation on magnetite drainage rate	87
4.5.2	Effects of slurry density variation on magnetite drainage rate	88
4.5.3	Influence of slot width on magnetite drainage rate	90
4.5.4	Influence of slot length on magnetite drainage rate	90
4.5.5	Effects of deflectors on magnetite drainage rate	91
4.5.6	Effects of screen panel material on magnetite drainage rate	92
4.5.7	Influence of screening area on drainage rate	93
4.5.8	Section summary	95
4.6	Partition curves	96
4.6.1	Effects of slurry density and volumetric flowrate on the efficiency curve parameters	99
4.6.1.1	Effects of slurry density variation on the sharpness of separation (α)	100
4.6.1.2	Effect of slurry density variation on water split (R_f)	100
4.6.1.3	Effects of slurry density variation on cut size	101
4.6.1.4	Effects of feed rate variation on the sharpness of separation (α)	102
4.6.1.5	Effects of feed rate variation on water bypass (R_f)	103
4.6.1.6	Effects of feed rate variation on cut size	104
4.6.2	Section summary	104
4.7	Summary of results	105
4.7.1	Ferrosilicon recovery	105
4.7.2	Magnetite recovery	106
4.7.3	Partition curve parameters	107

4	CONCLUSIONS AND RECOMMENDATIONS.....	108
5.1	Conclusions	108
5.1.1	Effects of volumetric flowrate on medium recovery	108
5.1.2	Effects of slurry density on medium recovery	108
5.1.3	Combined effects of volumetric flowrate and slurry density on medium recovery	109
5.1.4	Effects of aperture size on medium recovery	109
5.1.5	Effects of screen panel material on medium recovery	109
5.1.6	Effects of particle curves on medium recovery.....	110
5.2	Recommendations	110
6	REFERENCES.....	111
7	APPENDICES.....	121
	Appendix A: Aperture pegging	121
	Appendix B: Influence of iron ore on medium drainage rate	121
	Appendix C: Effects of slimes contamination on medium viscosity	121
	Appendix D: Effects of feed rate variation on degraded ferrosilicon drainage rate	122
	Appendix E: Moisture bypass for 1x12 mm rubber panel.	122
	Appendix F: Media carryover for 0.8x8.8 mm (a), 0.63 mm (b) and 1x12 mm (c) screen panels.....	123
	Appendix G: Effects of volumetric flowrate variation on magnetite drainage rate	123
	Appendix H: Effects of slurry density variation on magnetite drainage rate.....	124
	Appendix I: Effects of slot width on magnetite drainage rate.....	125
	Appendix J: Effects of deflectors on magnetite drainage rate for 1x13 mm screen panels.	125
	Appendix K: Effects of screen panel material on magnetite drainage rate	125
	Appendix L: Drainage rate for fresh ferrosilicon only.....	126
	Appendix M: Drainage rate for fresh ferrosilicon and iron ore	134
	Appendix N: Drainage rate for degraded ferrosilicon and iron ore	142
	Appendix O: Drainage rate for magnetite only	148

Appendix P: Percent moisture and medium carryover for fresh ferrosilicon and iron ore	169
Appendix Q: Percent moisture and medium carryover for degraded ferrosilicon and iron ore.....	179
Appendix R: Particle size distribution calculation.....	192
Appendix S: Mass balance	202
Appendix T: Calculations for solid concentration	203

LIST OF FIGURES

Figure 1-1: Typical flowsheet for a dense medium circuit; redrawn from Wills & Napier-Munn (2006).....	2
Figure 2-1: Screening process	5
Figure 2-2: Typical dense medium circuit flowsheet; redrawn from Napier-Munn et al. (1995)	8
Figure 2-3: Multi-feed flow distribution, redrawn from Albuquerque et al. (2008).....	16
Figure 2-4: Actual Vs ideal efficiency curves.....	18
Figure 2-5: Quantifying the deviation from ideal performance	20
Figure 2-6: Deck and drive angles	25
Figure 2-7: Variation of effective length with angle of inclination, redrawn from Carnes & Olsen (2001).....	26
Figure 2-8: Particle size characterisation	27
Figure 3-1: Vibrating swico screen	33
Figure 3-2: Ten cup rotary splitter	34
Figure 3-3: Particle size distributions for iron ore, ferrosilicon and magnetite	35
Figure 3-4: Dimensions of the separating surface (a) and screen panel (b).....	37
Figure 3-5: Experimental setup	38
Figure 3-6: Blank panels (a), VFD (b), deflectors (c) and feed distributor (d) installed on the screen surface	38
Figure 3-7: Underflow tank.....	39
Figure 3-8: Magnetite drainage rate reproducibility for 0.63x8.8 mm polyurethane panels at 1.72 kg/L slurry density	43
Figure 3-9: Ferrosilicon drainage rate reproducibility for 1x13 mm polyurethane panels at 1.9 kg/L slurry density	43
Figure 3-10: Viscosity reproducibility for fresh (a) and degraded (b) ferrosilicon	45
Figure 4-1: Particle shapes of iron ore (a) and cavities (pores) on iron ore surface (b).....	47
Figure 4-2: Particle shapes of ferrosilicon (a) and magnetite (b).....	48
Figure 4-3: Effects of iron ore particles on ferrosilicon drainage rate for 1x13 mm polyurethane panels at 2.2 kg/L slurry density at 1:5 ore to medium ratio.....	49
Figure 4-4: Effects of volumetric flowrate on fresh ferrosilicon drainage rate for 1x13 mm (a) and 0.63x8.8 mm (b) polyurethane panels	50
Figure 4-5: Effects of volumetric flowrate on fresh ferrosilicon drainage rate for 0.8x8.8 mm polyurethane panels.....	51

Figure 4-6: Effects of volumetric variation on moisture carryover for 0.63x8.8 mm (a) and 1x13 mm (b) polyurethane panels	52
Figure 4-7: Effects of feed rate variation on medium carryover for fresh ferrosilicon for 1x13 mm polyurethane panels.....	54
Figure 4-8: Effects of feed rate variation on moisture and medium carryover on fresh ferrosilicon for 0.63x8.8 mm polyurethane panels	54
Figure 4-9: Effects of slurry density variation on fresh ferrosilicon drainage rate for 0.63x8.8 mm (a) and 1x13 mm (b) polyurethane panels	56
Figure 4-10: Effects of slurry density variation on moisture bypass for 1x13 mm (a) and 0.63x8.8 mm (b) polyurethane panels	58
Figure 4-11: Effects of slurry density variation on fresh ferrosilicon carryover for 0.63x8.8 mm (a) and 1x13 mm (b) polyurethane panels	59
Figure 4-12: Influence of aperture size variation on fresh ferrosilicon drainage rate at 2.2 kg/L slurry density	61
Figure 4-13: Influence of aperture size variation on moisture bypass for fresh ferrosilicon at 2.2 kg/L slurry density	61
Figure 4-14: Influence of screen aperture size on medium carryover for fresh material at 2.2 kg/L slurry density	62
Figure 4-15: Influence of slot width on fresh ferrosilicon drainage rate at 2.2 kg/L slurry density	63
Figure 4-16: Influence of slot width on moisture bypass for fresh ferrosilicon at 2.2 kg/L slurry density	64
Figure 4-17: Influence of slot width on medium carryover at 2.2 kg/L slurry density	64
Figure 4-18: Viscosity comparison for fresh and contaminated ferrosilicon at 3.45 S^{-1} shear rate	67
Figure 4-19: Viscosity variation with slurry density for degraded ferrosilicon.....	68
Figure 4-20: Viscosity variation with slurry density for fresh ferrosilicon.....	68
Figure 4-21: Viscosity variation with slurry density and shear rate for fresh (a) and degraded (b) ferrosilicon.....	69
Figure 4-22: Particle size comparison for fresh and degraded ferrosilicon after two months of running experiments with the same material.....	72
Figure 4-23: Effects of volumetric flowrate on degraded ferrosilicon drainage rate for 1x13 mm polyurethane panels.....	74
Figure 4-24: Effects of feed rate variation on moisture carryover for 1x13 mm polyurethane panels.....	74

Figure 4-25: Effects of volumetric flowrate on medium carryover on 1x13 mm polyurethane panels for degraded ferrosilicon.....	75
Figure 4-26: Effects of slurry density variation on degraded medium drainage rate for 1x13 mm polyurethane panels.....	77
Figure 4-27: Effects of slurry density variation on degraded ferrosilicon drainage rate for 1x12 mm rubber panels.....	77
Figure 4-28: Effects of slurry density on moisture bypass for 1x13 mm polyurethane panels.....	78
Figure 4-29: Effects of slurry density on moisture bypass for 1x12 mm rubber panels.....	78
Figure 4-30: Effects of slurry density variation on degraded medium carryover for 1x13 mm polyurethane panels (a) and 1x12 mm (b) rubber panels.....	79
Figure 4-31: Influence of aperture size on degraded ferrosilicon drainage rate at 2.2 kg/L slurry density.....	80
Figure 4-32: Effects of aperture size variation on moisture (a) and medium carryover (b) for degraded ferrosilicon at 2.2 kg/L slurry density.....	81
Figure 4-33: Influence of degradation on ferrosilicon drainage rate for 0.8x8.8 mm polyurethane panels at 2.0 kg/L slurry density.....	82
Figure 4-34: Influence of medium degradation on moisture bypass for 0.8x8.8 mm polyurethane panels at 2.0 kg/L slurry density.....	83
Figure 4-35: Influence of degradation on medium carryover for 0.8x8.8 mm screen panels at 2.0 kg/L slurry density.....	84
Figure 4-36: Effects of screen panel material on degraded ferrosilicon drainage rate at 1.9 kg/L slurry density.....	85
Figure 4-37: Effects of screen panel material on moisture bypass at 1.9 kg/L slurry density.....	85
Figure 4-38: Effects of screen panel material on degraded medium carryover at 1.9 kg/L slurry density.....	86
Figure 4-39: Magnetite drainage rates for various screen panels at 1.64 kg/L slurry density.....	87
Figure 4-40: Effects of feed rate variation on magnetite drainage rate for 1x13 mm polyurethane panels.....	88
Figure 4-41: Effects of slurry density variation on magnetite drainage rate for 1x13 mm polyurethane panels.....	89
Figure 4-42: Effects of slurry density on magnetite drainage rate for 0.63x8.8 mm polyurethane panels.....	89

Figure 4-43: Influence of slot width on magnetite drainage rate at 1.64 kg/L slurry density90

Figure 4-44: Influence of slot length on magnetite drainage rate at 1.64 kg/L slurry density.. 91

Figure 4-45: Effects of material deflectors on magnetite drainage rate for 1x13 mm screen panels at 1.72 kg/L slurry density 92

Figure 4-46: Effects of screen panel material on magnetite drainage rate at 1.72 kg/L 92

Figure 4-47: Effects of screen panel material on magnetite drainage rate at 1.84 kg/L slurry density 93

Figure 4-48: Comparison of the screen panel set up for multotec and current work 94

Figure 4-49: Drainage rate comparison between current and Multotec's work at 0.186 m² screen area for 0.63x8.8 mm (1.6 kg/L) and 1x12 mm (1.64 kg/L) rubber panels 95

Figure 4-50: Actual efficiency curve vs Whiten model curve for 1x13 mm at 1.90 kg/L slurry density 98

Figure 4-51: Effects of volumetric flowrate on partition curves for 0.8x8.8 mm polyurethane panels at 2.2 slurry density for degraded ferrosilicon 98

Figure 4-52: Effects of slurry density variation on efficiency curves for 1x13 mm polyurethane panels at 23.7 m³/hr volumetric flowrate for fresh ferrosilicon..... 99

Figure 4-53: Effects of slurry density variation on the sharpness of separation for fresh ferrosilicon 100

Figure 4-54: Effects of slurry density variation on water recovery to the oversize stream for fresh ferrosilicon 101

Figure 4-55: Effects of slurry density variation on cut size for fresh ferrosilicon 102

Figure 4-56: Effects of feed rate variation on the sharpness of separation for fresh ferrosilicon 103

Figure 4-57: Effects of feed rate on water split for fresh ferrosilicon..... 103

Figure 4-58: Effects of feed rate variation on cut size for fresh ferrosilicon 104

LIST OF TABLES

Table 2:1: Aperture sizes for inclined screens	22
Table 3:1: Experimental plan	36
Table 3:2: Screen panel sizes and material of construction	36
Table 3:3: Measured vibrating screen parameters.....	37
Table 3:4: Reproducibility assessment for 0.63x8.8 mm polyurethane panels on drainage rate at 1.72 kg/L slurry density.....	43
Table 3:5: Reproducibility assessment for 1x13 mm polyurethane panels on drainage rate at 1.9 kg/L slurry density	44
Table 3:6: Results reproducibility on the overflow stream for percent moisture (a) and medium carryover (b) for 1x13 mm screen panels	44
Table 4:1: Elemental analysis of fresh and slime contaminated ferrosilicon.....	66
Table 4:2: Medium oxidation.....	71
Table 4:3: Influence of screen area on drainage rate	95

LIST OF SYMBOLS

Nomenclature	Meaning	Units
a	Aperture size	m
B	Bulk density	g/mL
C	Water split to the undersize	m ³ /h
d	Particle diameter	m
D	Bed depth	m
D ₅₀	Cut size	m
D _{50c}	Corrected cut size	m
E _{OC}	Corrected efficiency to the oversize	%
f	Weight fraction of the feed	-
F	Feed rate	m ³ /h
G	Vibration intensity or G-force	Rev ² /m
K _v	Material velocity	m/s
M _f	Mass flow rate of the feed	m ³ /h
M _o	Mass flow rate of the oversize	m ³ /h
M _u	Mass flow rate of the undersize	m ³ /h
n	Opportunity times a particle contacts the screen surface	-
P	Probability of particle passage	-
Q	Drive angle	Degree
R	Angle of inclination	Degree
R _f	Water split to the oversize	m ³ /h
S	Frequency	rpm
T	Amplitude	cm
W	Screen width	m
W _{aw}	Weight of sample after washing, rinsing and drying	kg
W _{bw}	Weight of sample before drying	kg
Wt ₁	Weight of wet sample	kg
Wt ₂	Weight of dry sample	kg
α	Sharpness of separation	
β	Whiten fish hook parameter	
β*	Whiten fish hook parameter	

Acronym	Meaning
B	Half size
C	Near size particles
C_o	Critical oversize
C_u	Critical undersize
DMC	Dense medium circuit
DMS	Dense medium separation
K_{100}	Maximum particle size
kg/L	Kilogram per litre
kg/t/m	Kilogram of medium per tonne of feed per screen width
m ³ /h	Cubic meter per hour
m ³ /m ² /h	Cubic meter per square meter per hour
O	Oversize particles
O/S	Oversize stream
PSD	Particle size distribution
t/m ³	tonne per cubic meter
U	Undersize particles
U/S	Undersize stream
v/v %	Volume percent
VFD	Variable frequency drive
w/w %	Weight percent

Term	Meaning
Carryover/bypass	Refers to medium and or water to the oversize stream
Degradation	Refers to change in ferrosilicon behaviour
Medium or Media	Refers to ferrosilicon or magnetite particles
Screen media or panel	Refers to the separating surface
Screen area	Refers to the available space for material separation

1 INTRODUCTION

1.1 Background and problem statement

In a dense medium circuit (DMC) and the cyclone in particular, separation of ore particles is based on their differences in shape, particle size and density, with lighter particles recovered through the vortex finder and heavier ones through the apex (Bosman 2014). This is achieved by using the heavy medium as a medium of separation with relative density cutting between gangue and valuable minerals, and usually, the particle property that is used in distinguishing between the two minerals is density (Sripriya et al. 2006; Sripriya et al. 2003; de Korte, 2008). Valuable iron ore particles, for example, with a relative density of about 5.2 t/m^3 are separated from siliceous gangue material with a particle density of about 2.65 t/m^3 and valuable coal particles from gangue minerals such as clay, rock or shale with relative density of about 1.6 t/m^3 (Noble & Luttrell 2015). Typical media used in DMS circuits are either ferrosilicon or magnetite suspension, depending on the separation density (Bosman 2014). However, for separating density of higher than 2.0 kg/L , ferrosilicon is used, and below that, magnetite is used (Bosman 2014). Nonetheless, magnetite cannot entirely be used in processes with separation density above 2.0 kg/L as its relative density is too low for efficient particle separation. During the separation, water and medium particles adhere to the ore particles and are carried over to the cyclone float and sink product streams. The two product streams contain substantial amount of medium that must be recovered on a drain and rinse vibrating screen for reuse (Albrecht 1972).

In a typical DMS circuit, medium losses arise due to forces of attraction between the medium and ore particles, inefficient cyclone products washing on a drain and rinse vibrating screen, corrosion and abrasion of the medium, ore porosity, magnetic separation and classification inefficiencies, and excessive circuit loading during the addition of fresh medium to the cyclone (Sripriya et al. 2006). However, Williams & Kelsall (1992) and later Sripriya *et al.*, (2006) observed that a considerable quantity of about 70 - 80 w/w% is lost on a drain and rinse vibrating screen due to poor drainage characteristics. O'Brien & Firth (2005) established that for efficient medium recovery, 90 - 95 w/w% should be recovered on the drain section of the drain and rinse vibrating screen as there is minimal recovery on the rinse part of the screen. Medium losses are a significant contributor to the operational cost of a dense medium separation (DMS) circuit, accounting for 10 – 20 w/w% and 20 - 40 w/w% on magnetite and ferrosilicon respectively. It is worth noting that heavy medium plants are costly to run compared to native pan plants due to the high cost of the medium (Chastont & Napier-Munn 1972). Thus, to economically run the circuit, a strong emphasis is placed on the efficient and

effective medium recovery on the drain part of the drain and rinse screen for reuse in the cyclone. Hence, the drain section of the screen is vital in the drain and rinse applications. Figure 1-1 depicts a typical flowsheet for a dense medium circuit with a highlight on the medium recovery section.

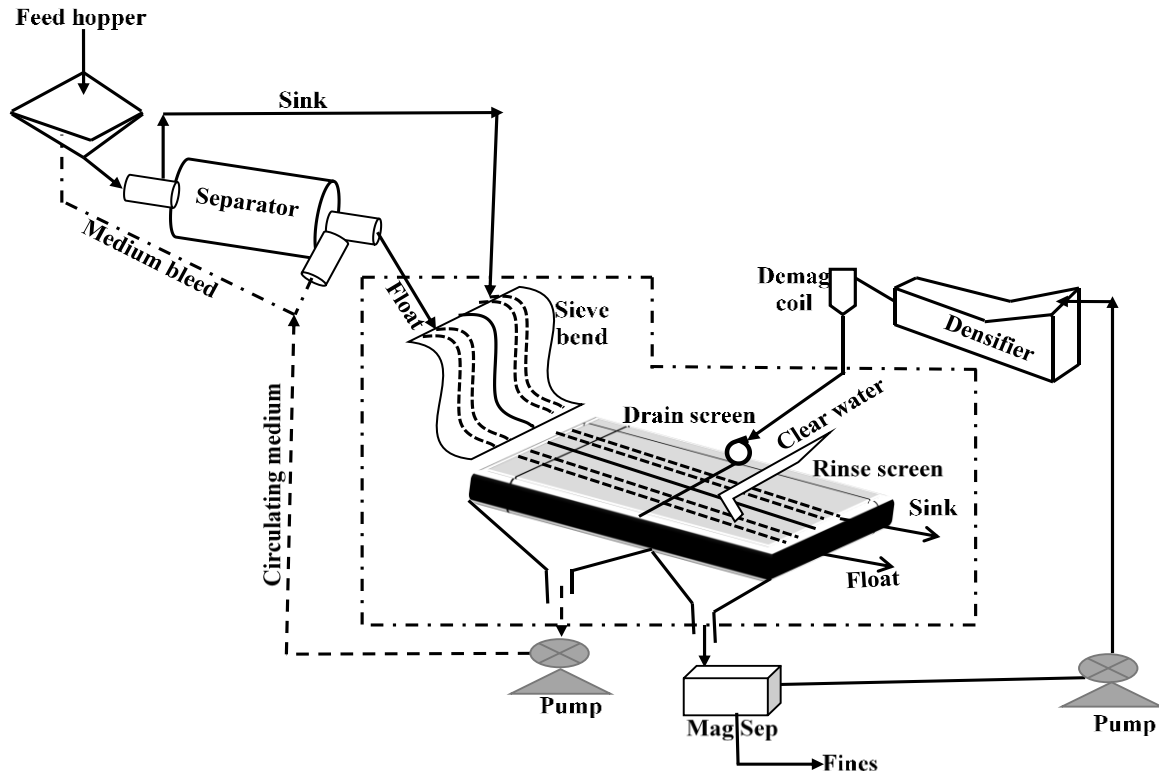


Figure 1-1: Typical flowsheet for a dense medium circuit; redrawn from Wills & Napier-Munn (2006)

While many factors such as screen slope, material feed rate, vibration intensity, screen size and shape, particle size, shape and density, viscosity and density of slurry, screen width etc (Liu, 2009) influence medium recovery on the drain part of the drain and rinse vibrating screen, the effects of feed rate, slurry density and slot size variation were investigated in this thesis. The feed rate of material onto the screen surface ranged from 18 - 26 m³/h, typical of those used in operating plants (O'Brien & Firth 2005; Mabote 2016; Mwale 2015). Feed rate was chosen as it is easily manipulated by operators on a plant and often changed to adapt to production requirements. The need to understand the feed rate with regards to screen installations is therefore of critical importance. The slurry density ranges chosen depicted the current dense medium operating conditions for the separation of coal particles using magnetite at 1.64 to 1.84 kg/L (i.e. from 49.5 to 57.9 w/w% solids) and iron or diamond ore using ferrosilicon at 1.65 to 2.7 kg/L (i.e. 47.1 to 75.3 w/w% solids). The slurry density range

chosen for ferrosilicon was due to the fact that no research work has been published so far in open literature on the recovery of ferrosilicon at slurry density above 2.0 kg/L. The panel sizes used are typically those used on a drain and rinse vibrating screen and included the 0.63x8.8 mm, 0.63x12 mm, 0.8x8.8 mm and 1x13 mm polyurethane panels, 1x12 mm rubber panels and 0.63 mm poly-wedge wire. These panels were used considering that no work has been published so far in open literature on the recovery of ferrosilicon through the rubber, polyurethane, and poly-wedge panels.

1.2 Objectives of the study

The aim of the study was to determine the medium drainage rates for different screen slot sizes for the drain part of a drain and rinse vibrating screen in a DMS circuit using a 0.6 x 1.2 m vibrating screen with polyurethane, rubber, and poly-wedge panels. To allow a better development on the understanding of medium recovery, the following specific objectives were set:

- 1) Investigate the effects of feed slurry density, volumetric flowrate, and slot sizes on the operation of the vibrating screen by measuring the medium drainage rate, percent moisture and medium carryover.
- 2) Investigate the effects of screen panel material on medium drainage rate, percent moisture and medium carryover to the overflow stream.
- 3) Establish the influence of feed rate and slurry density variation on the partition curve parameters i.e. cut size, the sharpness of separation and water split ratio.

1.3 Project significance

Although many researchers have investigated medium recovery in the dense medium circuit (Napier-Munn et al. 1995; Sripriya et al. 2006; O'Brien & Firth 2015), no research work has been published so far in open literature on the *fundamental principles* that affect the recovery of ferrosilicon on a vibrating screen. Hence, the results presented in this thesis will help in bridging the gap in knowledge and enhance the efficient recovery of ferrosilicon on a drain and rinse vibrating screen.

The effects of feed density on material recovery in general have been investigated by a number of researchers (Guerreiro et al. 2015; Albuquerque et al. 2008; Valine et al. 2009; O'Brien & Firth 2015) who observed a decrease in screening rate with increase in slurry density. While all the findings on slurry density variation were key to this thesis, no information was found in the open literature regarding a slurry containing ferrosilicon and iron ore. Further, separation of iron ore and or diamond particles using ferrosilicon is usually done at slurry density above 2.0 kg/L (60.2 w/w% solids), however, no research work has

been reported so far on a medium slurry with percent solids above 60 w/w %. Hence, the results obtained in this project holds potential benefits of adding valuable information to the existing body of knowledge on the drainage rate of medium at slurry density above 60 w/w % solids.

The effects of different screen sizes and shapes on material recovery in general have been investigated by, *inter alia*, (Mabote 2016; Mwale 2015; Grozubinsky et al. 1998; Li & Tong 2015). However, little work has been done so far in establishing how different aperture sizes affect medium drainage rates in a DMS circuit. From open literature, no research work has been done on ferrosilicon drainage rate through polymeric (polyurethane and rubber) and poly-wedge screen panels. Acknowledging the rapid increase in demand by most operating plants for customised screen aperture designs and sizes capable of delivering specific production goals, the results presented in this thesis provides information on the influence of different screen panels on medium drainage rate.

2 LITERATURE REVIEW

2.1 Purpose of screening

Material recovery using a screen is among the oldest separation processes that has been employed over the years in physical separation industries. Screening is basically an assemblage of chances where particles encounter a screen surface, and at each encounter, there exists a likelihood of undersize particles passing through the screen apertures (Dong et al. 2009). It can also be defined as a process in which a screen surface acts as a barrier between oversize and undersize particles, which in an ideal case; undersize particles easily pass through while oversize particles are retained, as shown in Figure 2-1 below. Undersize particles in this context refer to particles in a feed stream that are less than the screen aperture size and oversize particles as particles larger than the screen hole size. The evolution of screens and principles governing their operations over the decades has been from diminutive and simple equipment where one would use hands to shake a screen surface to modernistic designs that are capable of separating high volumes of material (Vorster et al. 2002). This evolution has been accompanied by the separation of not only coarse particles but also fine particles with the discovery of several industrial screens. However, vibrating screens have emerged more predominantly over the years than the other screen types because of their versatility in separating materials (Gupta & Yan 2006).

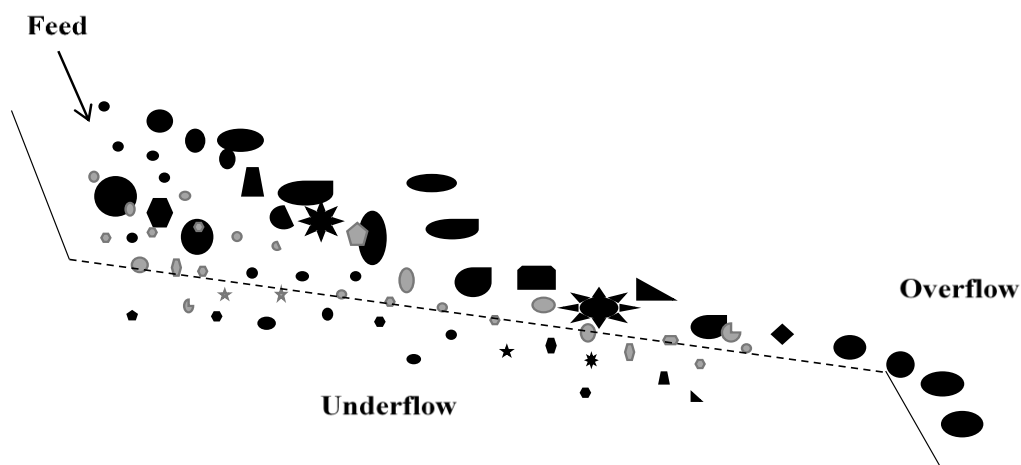


Figure 2-1: Screening process

A screening operation can also be defined by the rate of material conveyance across a screen length, stratification of fine particles through a thick bed of material and the rate of particle passage through the screen holes (Hudson et al. 1969). Material stratification is a process that involves the flow of undersize particles through spaces created by oversize particles onto a screen surface, thus, largely influenced by the concentration of fine particles in a particular

feed material (Soldinger 1999). Ferrara et al. (1988), however, established that the interactions among particles of different size fractions on a screen surface play a fundamental role in undersize stratification. On the other hand, Passage rate is the percolation of fine particles through the screen openings. Feller (1976) established that the probability of passage for a particular particle size fraction in the feed is largely dependent on the amount of that size fraction on a screen surface. However, Standish et al. (1986) observed that the probability (P) of particle passage is influenced by the relationship between particle diameter (d) and screen aperture size (a), as shown in Equation 2.1 below.

$$P = 1 - \left(\frac{d}{a}\right)^2 \dots \dots \dots 2.1$$

G. Subasinghe et al. (1989) further observed that the higher the relative size ratio (d/a) beyond 0.8, the slower the passage rate. Therefore, relative size ratio is a parameter that can be used to predict and differentiate passage rates for different particle size fractions (Feller 1976; Trumic & Magdalinovic 2011). Firth & O’Brien (2000) extended the likelihood of passage rate established by Standish et al. (1986) by incorporating the moisture content (or water quantity) (R_f) and the number of opportunities a particle contacts a screen (n) as shown in Equation 2.2 below. Hence, it was concluded that passage rate is largely influenced by the amount of moisture in the feed or on the screen surface as well as the opportunity times that undersize particles contact the screen surface for passage.

$$P = R_f + (1 - R_f) \left(\frac{d}{a}\right)^n \dots \dots \dots 2.2$$

However, there are distinct reasons for carrying out a physical separation through a screen surface, and these may include:

- 1) Grading; done on one or more screen decks stacked in decreasing aperture sizes to generate distinct size fractions of particles (DeCenso 2000).
- 2) Sizing; where particles of a particular feed are separated into different portions by size (Pieterse 1992).
- 3) De-sliming; process used to separate fine particles usually less than 0.5 mm from the ore material (Mohanty, 2003).
- 4) Trash removal; process used to remove unwanted particles from ore material.
- 5) Medium recovery; process used to recover heavy media particles from ore material.
- 6) Scalping; applied in the removal of coarse particles from the feed material.
- 7) Dewatering; usually applied in the removal of excess water from the ore particles.

Efficient physical separation requires minimal misplacement of materials during particle separation, thus, putting a great demand on the efficient operation of a screen surface. Misplaced materials arise in cases when particles smaller than the screen aperture are retained with oversize particles, and when the presence of oversize particles is spotted in the underflow stream (Soldinger 2000). Besides, setting up a screening section and its supporting infrastructure is one of the major capital expenditures in material processing plants (Pieterse 1992). Therefore, it is imperative that fundamental objectives of screening are entrenched before any physical separating process. While there are different objectives for performing a physical separation, this thesis solely focused on the recovery of media particles on the drain part of the drain and rinse vibrating screen in the dense medium circuit.

2.1.1 Medium recovery in a dense medium circuit

In a typical dense medium cyclone circuit (DMC), ore particles are separated based on their differences in densities, where lighter particles move towards the centre of the cyclone and are recovered through the vortex finder. These are referred to as floats. Heavier ones sink to the bottom and are recovered through the apex (Bosman 2014). They are commonly referred to as sinks. However, the separation is accomplished by the use of heavy media as medium of separation with relative density cutting between valuable and gangue minerals (Sripriya et al. 2006; Sripriya et al. 2003; de Korte, 2008). Archetypal media used in DMS circuits are either ferrosilicon or magnetite, depending on the density of separation. However, magnetite cannot entirely be used in processes with separation density above 2.0 kg/L since its relative density is too low for efficient particle separation.

During the separation, the solid particles and water that constitutes the heavy media adhere to the cyclone products making it necessary to be separated on the drain and rinse screen for re-use (Albrecht 1972). Many circuits are used for the recovery of media particles in a dense medium circuit. A simplified medium flowsheet is presented in Figure 2-2, showing the key streams with highlight on the drain and rinse vibrating screen (Wills & Napier-Munn 2006; Roller & Hazleton 1952). Christopher (2013) stated that drain and rinse screens can either be inclined or horizontal vibrating screens. However, in most cases, a horizontal or near horizontal screen surface with a low angle of inclination of up to 10-° or a reverse slope of 5-° is used to drain media particles (Wills & Napier-Munn 2006; Liu 2009). Sullivan (2013) established that horizontal screens have a greater particle sizing accuracy than inclined screens due to increased material residence time on the screen surface and are mostly used in sizing operations where screening efficiency of materials is very critical i.e. drain and rinse

operations (Parlar 2010). Nevertheless, horizontal screens have comparatively low capacity due to reduced velocity of particles along the screen length.

In most cases, horizontal screens are designed to work with either elliptical or linear motion produced by either double or triple shaft vibrators usually mounted above the screen surface (Makinde et al. 2015; Makinde 2014). Donaghy (2016) established that linear motion is by far better than elliptical motion owing to the high G-forces imparted onto the screen surface, with reduced screen blinding and enhanced conveyance of material across a screen length. Burke & Craig (2005) established that a horizontal screen surface coupled with a linear motion leads to an improved sizing accuracy due to the ‘popcorn effect’ created among the feed particles where the coarser particles are lifted off a screen surface while retaining the fine particles, thus, promoting undersize drainage rate. On the other hand, mounting a horizontal screen with linear motion requires less headroom compared with elliptical and or circular motion screens; hence, reduced material usage and space during pilot plant installation (Hailin et al. 2013).

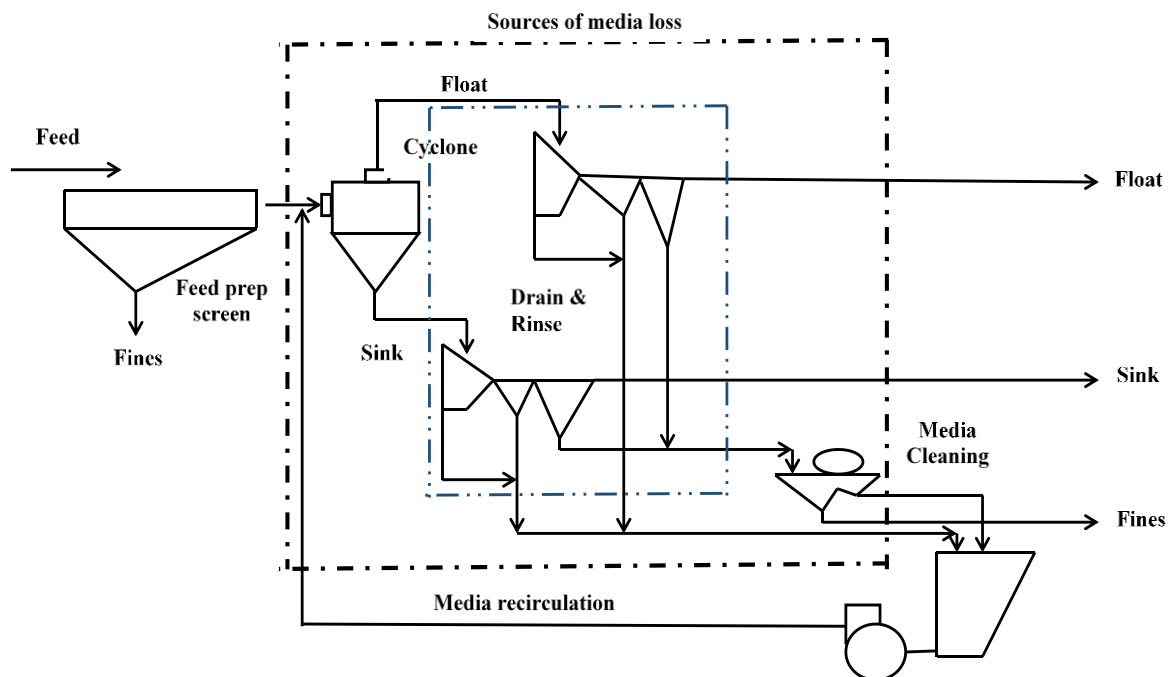


Figure 2-2: Typical dense medium circuit flowsheet; redrawn from Napier-Munn et al. (1995)

However, in a typical dense medium circuit, the drain and rinse vibrating screen is preceded by a profile of wire sieves (a sieve bend) to aid the media recovery process and reduce the quantity of ore and media particles to the vibrating screen, thereby, reducing the screen size (Holt 1978). The product is then passed on to the draining section where additional amount of media is expected to be recovered (Bevilacqua & Ferrara 1994). The fluid, comprising the media and water recovered on the sieve bend and draining section, is referred to as heavy

media and is directly recirculated back to the cyclone media feed circuit. The subsequent product from the drain section is then washed on the second half of the screen using a low-pressure spray of water (Wills & Napier-Munn 2006). This is done to rinse off the media particles still clinging on the cyclone products. The underflow products from the washing section referred to as dilute media comprising mostly of media, fines and wash water is too dilute and contaminated to be directly recirculated to the separating vessel for reuse. Therefore, it is treated separately in magnetic separators to recover magnetic particles from the non-magnetic particles. The reclaimed, cleaned media is then thickened to the desired density using a densifier before being redirected back to the cyclone media feed circuit. It is a customary practice to bleed off part of the circulating media to remove the fine and non-magnetic particles from the circuit. If not removed, they go into suspension and alter the physical properties of the heavy medium (Korte, 2000; Walker, 1943; Lawire & Needham 1949). The presence of these slimes has been known to have a constructive influence on medium stability and a detrimental effect on medium viscosity (Grobler et al. 2002). Highly viscous media is undesirable since it affects the separation process both in the cyclone and on the drain and rinse vibrating screen (Fourie et al. 1980; Marsh, 1945).

During normal operations, media losses arise due to corrosion and abrasion of the media particles, forces of attraction between the ore and media, ore porosity, housekeeping, inefficient washing of cyclone products on the rinse section of the drain and rinse vibrating screen, magnetic separation and classification inefficiencies, and excessive fresh medium addition to the cyclone (Sripriya et al. 2006). A lot of work has been done over the years, mostly by operating plants, to identify and quantify the causes of media loss and in turn, minimize the consumption. However, the task is complicated by the difficulty of finding an obvious media balance across the entire plant by sampling process streams. Napier-Munn et al. (1995) stated that a media balance replicating quantitatively the actual media consumption over period such as a month or a year within an abbreviated period is hardly established. This is due to the impact of factors such as media corrosion and house-keeping which are problematic, if not impossible, to quantify directly. On the other hand, media balance is made difficult by the fact that a momentous quantity of the loss often occurs in very short periods (owing to the flow surges or overloading) which are difficult to detect by all but most comprehensive high frequency or continuous sampling procedures (Napier-Munn et al. 1995).

Sripriya et al. (2006) established that while there are many possible points of media loss in the dense medium circuit, substantial quantity of about 70 - 80 w/w% is lost on a drain and rinse vibrating screen due to poor drainage characteristics. O'Brien & Firth (2005) further

established that for efficient media recovery, 90 - 95 w/w% must be recovered on the drain section of the drain and rinse vibrating screen since minimal media is recovered on the rinse part of the screen. Hence, to economically run the DMS circuit, a strong emphasis is placed on the efficient and effective media particles recovery on the drain part of the drain and rinse vibrating screen.

2.1.2 Significance of medium recovery

Replacing the lost media particles is a major operating cost accounting for 20 – 40 w/w% and 10 – 20 w/w% of the total operating costs for plants engaged in mineral separation using ferrosilicon and magnetite respectively (Sripriya et al. 2006). However, there are evidently incentives in minimising this loss and often probable with nominal capital expenditure through minor changes to plant configurations and improved operating procedures (Napier-Munn et al. 1995). Heavy medium plants are expensive to run compared to native pan plants due to the high cost of media; thence, to proficiently run these circuits, a sturdy importance is placed on efficient media particles recovery from cyclone products (Chastont & Napier-Munn 1972).

2.1.3 Section summary

Screening is a process in which particles encounter a screen surface, and at each presentation, there is a probability of passage through screen apertures. A screening operation can be defined by the rate of material conveyance across a screen length, stratification of fine particles through a thick bed of material and the rate of particle passage through the screen holes. The degree to which these processes affect the separation process hinges on the physical characteristics of the feed material and screen parameters. It is worth noting that screens are among the oldest and widely used particle separating devices with applications in trash removal, scalping, de-sliming, grading, sizing, media recovery and dewatering. While there are different goals for performing a physical separation, this thesis solely focused on heavy media recovery on the drain part of the drain and rinse vibrating screen. Despite the research works done so far on media recovery, it can categorically be pointed out that no research work has been published so far in open literature on the *fundamental principles* that affect the recovery of ferrosilicon on a vibrating screen.

During the recovery of media particles, different screen types are used. However, it has been established that horizontal or near horizontal vibrating screens coupled with a linear motion have a great ability of separating media particles due to maximisation of material residence time, effective slot size and thence, improved media drainage rate. While there many possible points in the dense medium circuit for medium recovery, great emphasis is placed on the drain

part of the drain and rinse vibrating screen where more than 90 w/w% of the medium particles is expected to be recovered for proficient running of the circuit.

2.2 Screen panels

A screen panel is a surface with holes that permits undersize particles to pass through while retaining oversize particles. It can also be defined as a replaceable surface that consists of one or more removable panels on a single screen deck. In any physical separation, the screen panel chosen to serve a specific screening objective largely affects the performance of a screen regarding efficiency, capacity and the cost of running a separation process (Satyenda 2015). Every screening application is distinct, and thus, the type of screen panels chosen is critical for success. Selecting a suitable screen panel is vital to delivering maximum plant throughput and maintaining screen size accuracy (Donaghy 2016). The choice of a separating surface primarily refers not only to selecting the correct aperture size and shape in reference to material cut size but also the wearing of these screen panels while in operation. Sullivan (2013) highlighted that even though selecting a suitable screen panel is fundamental in material separation; trial and error have obtained excellent results.

When choosing screen panels for a specific operation, open area and screen life expectancy are the two important factors considered. While there is a demand for screen panels with large open area and lower wear life, there is always a trade-off between the two parameters in the designing of screen aperture configurations. Wedge wire, for example, offers maximum open area for material separation but at the expense of wear life, and the opposite is true for polymeric screens. In light of recent and ongoing developments in material compounds, hybrid solutions such as urethane-encapsulated wires have in a way helped to swell the spectrum of this sweet spot and enabled most producers to enjoy the best of both parameters (Donaghy 2016). Kwade et al. (2012) highlighted that the best screen surface is one that can withstand high load and stress applied to it by the material weight and still maintain a high degree of resistance to corrosion and abrasion.

2.2.1 Types of screen panels

With increased demand for efficient material separation, there are several screen panels designed with varying aperture sizes and shapes, materials, open area and fixing systems (Donaghy 2016). Most screen manufacturers are striving consistently to make unique products by varying these specifications and dial in a functional and customised solution for different applications. However, the most common screen panels include woven wire mesh, perforated plates, polymeric (polyurethane and rubber), self-cleaning and hybrid panels.

These screen panels can be installed on a screen deck in many ways. However, an installation that involves tensioning and or tightening of the screen panels against the supporting frame is paramount in panel life extension. Polymeric screen panels, for example, are hammered and held in position by polymeric pins (Donaghy 2016). Even though polymeric screen panels have a higher initial cost per square meter compared to the standard wedge wire screens, they have a prolonged life in service. On the other hand, they are smaller and safer to handle, thus, making installation on a screen deck easier. Proper screen panel installation leads to prolonged life in service of screen panels, reduced plant down time and increased plant throughput. It is credible to note that improper installation is one of the common causes of premature screen panels failure while in operation, hence, its importance cannot be over emphasised. While screen panels installation is paramount in the physical separation process, limited work can be found in open literature regarding its impact on plant operations. While there are several types of screen panels used in heavy media separation in a dense medium circuit, discussed below are the panel types relevant to this thesis.

It is worth noting that a separating surface can be defined by at least two of the following four parameters; wire diameter or aperture thickness, opening size, mesh count and percent open area (DeCenso 2000). Mesh count, in this case, is the number of openings per linear inch. Percent open area is the ratio of the area of the screen openings to the total screen surface area. Whereas, subtracting wire diameter or aperture thickness from the inverse of mesh count gives the opening size.

2.2.1.1 Woven wire or wedge wire screens

Woven wire or wedge wire screens have traditionally been in use for centuries now as they are comparatively cheap. The wires used to make these screens are of uniform cross section for both the weft and warp strands, with the diameter of the weft usually lesser than that of the warp (Gupta & Yan 2006). The most common wire clothes that have been used over the years are the oil-tempered, high-carbon and stainless steel wires, each with its unique application benefits (Donaghy 2016). However, the wire material used typically depends on specific screening environments. Stainless steel, for example, is potent as an anti-blinding solution and advantageous in corrosion prone processes, while plain carbon steel wires are used for general screening purposes. Wedge wire screens have been known to offer maximum open area for screening though at the expense of wear life (Gupta & Yan 2006).

There have been several advancements in wedge wire design over the years that have centred on improving screen wear life and open area. For this reason, the slotted opening panels was

designed to work in operations with a significant demand for higher and improved screen open area and flat top woven wire cloth in operations where screen wear life is paramount (Gupta & Yan 2006). Nevertheless, the flat top woven wire cloth screens have not been extensively used due to the absence of knuckles, thus, leading to retardation in the passing rate of fine material. Other types such as the hybrid screens with threads or wires made of polyurethane or rubber are increasingly being used in areas that are strongly acidic, caustic, or mild to wet environments. These screen types offer the advantages of polymeric screen panels (improved wear life and noise reduction) without the need to convert to a modular deck and without great sacrifice on the open area. Since the discovery of different types of wires and threads in plastic form, industrial screens with fabricated plastic are now common with wire thickness ranging from 5 - 25 mm (Gupta & Yan 2006).

2.2.1.2 Polymeric screen panels

These are screen panels mostly used in high-volume applications and hot and humid environments. This is due to their adaption in operations with high screen surface depreciation as they have a higher resistance to wearing, thus, reducing plant stoppages due to constant changing and or maintaining of worn out screen panels. The most common polymeric screens include the rubber and polyurethane panels.

2.2.1.2.1 Rubber panels

Rubber panels are typically used in high-impact applications for both wet and dry operations. They are also recommended to work in separating natural sand and or gravel. Self-cleaning rubber screens, as an example, are used for fine and sticky material separation (Donaghy 2016). Due to high ductility, rubber panels are also employed in the separation of ore particles that are highly friable (Metso 2008). Among all the available screen panels, rubber panels offer the longest wear life in almost all challenging and aggressive applications. On the other hand, rubber material is also used in the cladding of perforated steel wire plates owing to their improved absorption of material weight, thus, improving the life span of the separating surface. Wills (1985) observed that wedge wire rubber cladding also leads to minimised effects of screen aperture blinding due to high elasticity of rubber. Similarly, Donaghy (2016) entrenched that cladding of wedge wire with rubber material leads to reduced noise levels by up to 9 decibels compared to the typical steel wire panels, culminating to about 50 % reduction as recorded by the human ear.

2.2.1.2.2 Polyurethane panels

Polyurethane panels have found great application mostly in wet conditions as they offer materials being separated extra lubrication in the presence of a fluid (Drake 1988). These screen types have a high resistance to surface wear in nearly all applications, reported to be about ten times better than the ordinary woven wire mesh (Wills & Napier-Munn 2006). With improvements in material compounds and chemical formulations, there exist several types of polyurethane screens in material separating industries such as the open-cast thermoset and injected-molded polyurethane panels. However, it has been observed that the open-cast thermoset polyurethanes have superior wear-life compared to the injection-molded polyurethanes due to the slow curing process that tend to create stronger molecular bonds in the material (Donaghy 2016).

2.2.2 Screen panel accessories

Special surface features such as deflectors, side liners, dams and skid bars are at times installed on a separating surface to enhance material separation (Donaghy 2016). Deflectors, for example, are used for redirecting material towards the middle of a screen surface, thus, improving material recovery. Skid bars are used in scalping operations to keep oversize particles off the screen surface, thereby, reducing screen surface wearing. Dams, on the other hand, are used to retard material flow on the screen surface, thus, improving material residence time for efficient undersize recovery. While all these accessories have been cited to be key in material recovery, no work can be found in open literature regarding their influence on medium recovery on a vibrating screen.

2.2.3 Section summary

With ever-increasing demand for higher throughputs in all screening operations; there exist several types of screen panels in today's material separating industries. The most common ones include the woven wire mesh, perforated plates, polymeric (polyurethane or rubber), self-cleaning, and hybrid panels. It is worth noting that in any separation process, the screen panels chosen is key in guaranteeing maximum plant throughput and keeping screen sizing accuracy. Each screening process is different. Hence, the type of screens chosen is critical for success. Although these screen panels are an integral part of any DMS circuit, astonishingly, little work can be found in open literature regarding their effect on media recovery. Even though many researchers have looked at the effects of different screen sizes and shapes on material recovery in general (Mabote 2016; Mwale 2015; Grozubinsky et al. 1998; Hilden 2007; Li & Tong 2015), in most cases, trial and error has obtained outstanding results (Sullivan 2013). On the other hand, no research work has been done so far on the recovery of

ferrosilicon particles through polyurethane, rubber and poly-wedge screen panels. Hence, considering the gap in knowledge and the increased demand by most material processing plants for efficient medium recovery with reduced misplacement, the thesis focused on showing the influence of polyurethane, rubber, and poly-wedge wire on ferrosilicon and magnetite recovery.

2.3 Mechanisms of screening

Industrial material sizing is used to separate particles into different size fractions ranging from 300 mm down to about 45 μm , though further than 45 μm is possible but at the expense of screening efficiency (Wills & Napier-Munn 2006). However, sizing beyond 45 μm at times can be challenging and expensive; hence, classification comes in handy as an alternative method to fine material separation. There is a thin line between material sizing using a screen and classification, and in most cases, the selectivity factor between the two processes rests on the particle size distribution of the feed; as particles finer than 45 μm require a large separating area (Wills 1985). The screening mechanism selected for a specific material separation process is largely dependent on the particle size distribution of the feed material and can either be dry or wet. In most cases, dry screening is customarily restricted to the separation of particles larger than 6 mm while wet screening can separate down to 45 μm . Drzymala & Konopacka (2012), however, established that dry screening down to 75 μm is possible though at the expense of screening efficiency. Aggregate industries have for many decades struggled with improving fine dry screening, and the problem has been compounded by the fact that most dry screening applications are rarely dry, with a typical process having a minimum of about 3 % moisture (Ondrias 1990). However, considering that particle separation in the dense medium circuit is accomplished in the presence of water and media, dry screening mechanism was therefore not an option in this thesis.

Studies done so far on wet screening have shown that it is more efficient to separate feed material with particles finer than 6 mm in the presence of the fluid (Mwale 2015; Mabote 2016; Valine et al. 2009). Wet screening is typically material separation in the presence of a liquid either on coarse or fine particles. During the separation process, fine particles are conveyed through the screen apertures by the fluid (Valine et al. 2009). Hence, the quantity of the fluid in the feed play a significant role in the efficient separation of particles. While screen length plays a key role during dry screening, Valine et al. (2009) proved that drainage rate of fine particles during wet screening can be achieved using a short screen length with feed slurry containing less than 20 v/v% solids, as most of the fluid volume carrying along fine particles pass through screen holes quite faster. Thus, for a feed slurry with less than 20 v/v%

solids, the screen width rather than its length plays a leading role in the recovery of fine particles. It was in the light of this fact that a multi-feed screen with increased capacity of about 1.5 - 2 times better than a single feed screen, as shown in Figure 2-3 below (Albuquerque et al. 2008; Barkhuysen 2009).

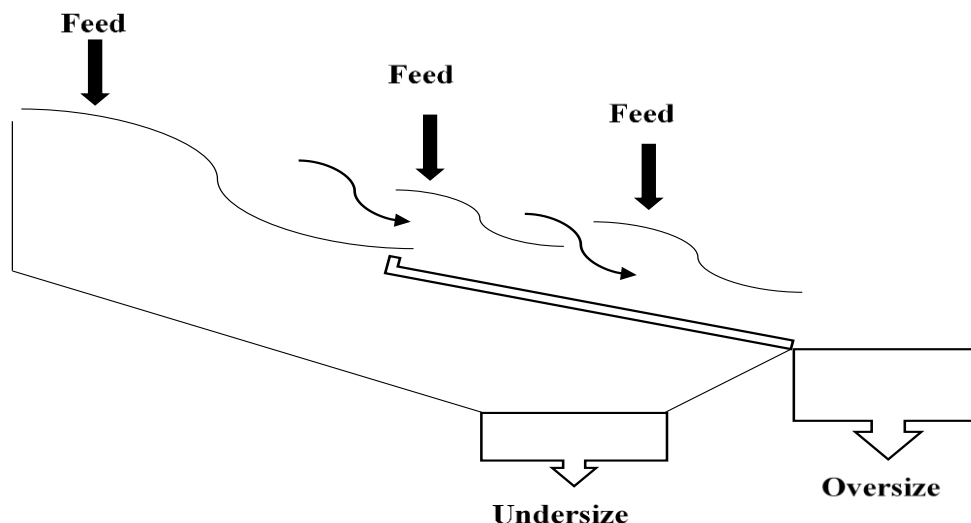


Figure 2-3: Multi-feed flow distribution, redrawn from Albuquerque et al. (2008)

2.4 Screen performance

Screen performance is primarily defined by the extent to which particles of feed material are separated into different size fractions (Wills & Napier-Munn 2006). The performance of every screen is governed by factors that affect the probability of particle passage through screen holes as well as those that affect opportunity times for particle contact with the screen surface. The screen performance can be assessed based on its capacity to handle a specific feed material and the corresponding efficiency (Gupta & Yan 2006).

Screen capacity, in this case, refers to the screen's ability to accept and handle a specific weight of feed material. The parameter is directly proportional to the screen area and calculated using standardised conditions of operation with presumed feed material (King 2000). Screen capacity rides on the variations of feed material properties and screen operating conditions characterised by capacity factors. Hence, it is a product of capacity factors and standard unit screen capacities. The ability of screen panels varies among different screen manufacturers depending on the applied assumptions, and the calculations are usually based on VSMA (vibrating screen manufacturers association) charts and formulas, as shown in Equation 2.3 below (Carnes & Olsen 2001). However, screen capacity cannot entirely be relied upon to give an objective overview of a screening operation as its calculation varies

among different screen manufacturers with specific assumptions. Hence, in this thesis, it was only referenced and maintained by choosing the screen length and width that provided a minimum screening area equivalent to the required screen capacity.

$$A = B \times S \times D \times V \times H \times T \times K \times Y \times P \times O \times W \times F \dots \dots \dots 2.3$$

Where

A- Is the screen capacity in tons/hour calculated per square foot of screen area.

B- Is the basic capacity/square foot in tons/hour

S- Angle of inclination

D- Screen deck

V- Oversize material

H- Half size particles

T- Aperture Shape

K- Feed condition

Y- Spray/wet screening

P- Particle shapes

O- Open area

W- Weight of material

F- Screening efficiency

2.4.1 Screen efficiency

In an ideal case, particles finer than the screen holes easily percolate through the apertures and coarse ones are retained. Given time and chance, screen panels can transmit all the available undersize particles in the feed. However, this is not feasible due to relatively high throughputs demanded in most material separating industries (Gupta & Yan 2006). Therefore, screen efficiency is used to express the percentage of a distinct size fraction in the feed material that reports either to the screen overflow or underflow stream (Sullivan 2013). An efficient classification device is one that can place most particles of a particular size fraction in the feed to the right stream for a specific screen aperture size. It is from this placement of particles that the fraction of a particular size class in the feed that reports either to the screen overflow or underflow stream is represented using either efficiency or partition curves. Partition curves are basically a graphical technique used to assess and account for misplaced particles either in the overflow or underflow stream. Gupta & Yan (2006) established that these classification curves can also be utilised in evaluating the separation efficiency on a size by size basis. Efficiency curves are obtained by performing a mass balance around a separator

and calculating the fraction of a particular size fraction in the feed that reports to the oversize (E_{oi}) using Equation 2.4 below (Wills & Napier-Munn 2006). Thus, the undersize efficiency can be established by subtracting E_{oi} from one.

$$E_{oi} = \left(\frac{O_i M_o}{f_i M_f} \right) \dots \dots \dots 2.4$$

Where;

E_{oi} = Actual recovery of particles of size i to the oversize stream

M_o = Mass flowrate of solids to the overflow stream

O_i = Weight fraction of material of size i in the oversize stream

M_f = Feed solids flowrate

f_i = Weight fraction of particles of size i in the feed

A typical efficiency curve shown in Figure 2-4 below for ideal and actual separation is drawn by plotting partition coefficients; defined as the percentage of particles of a specific size in the feed that reports to the oversize, against the geometric mean size of particles on a logarithmic scale (Gupta & Yan 2006). Ideal separation occurs when there is a perfect separation and at a separation size equal to the screen aperture size. Separation size value gives a brief glance of the performance of a separator, and a separation value close to the screen aperture size indicates efficient separation (Mwale 2015). Efficiency curves can also be used to model the performance of screens and for simulation and design purposes (Ferrara et al. 1987; Wills & Napier-Munn 2006; Subasinghe et al. 1989).

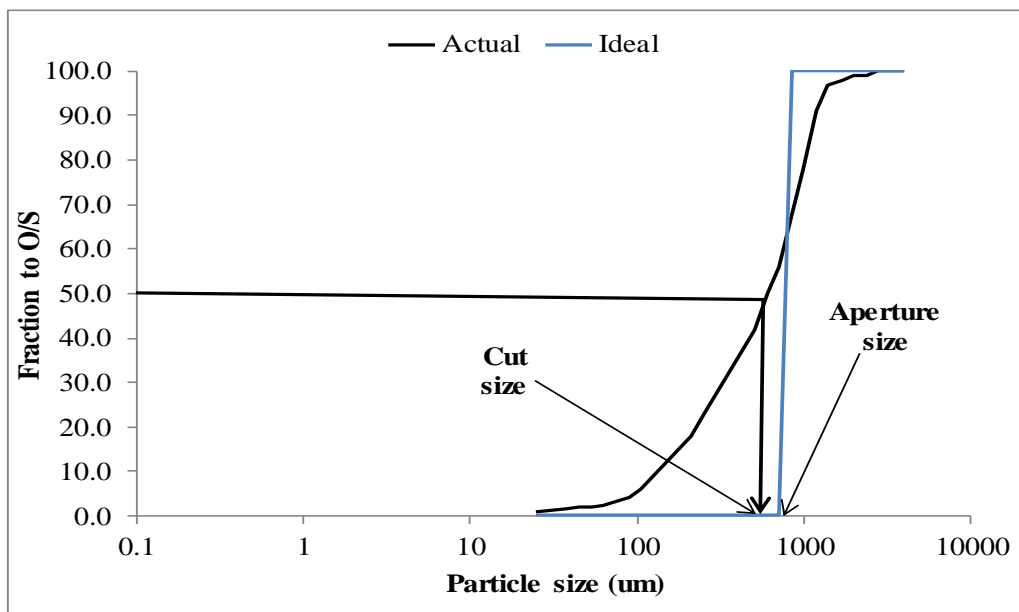


Figure 2-4: Actual Vs ideal efficiency curves

$$E_{oc} = 1 - C \left(\frac{e^\alpha - 1}{(e^\alpha \times \frac{d}{d_{50}}) - (e^\alpha - 2)} \right) \dots \dots \dots 2.6$$

Where;

E_{oc} = Recovery to the oversize stream

C = Fraction of water to undersize (thus fraction of water to oversize (R_f) = 1-C)

α = Sharpness of separation

d = Mean particle size

d_{50} = Cut size

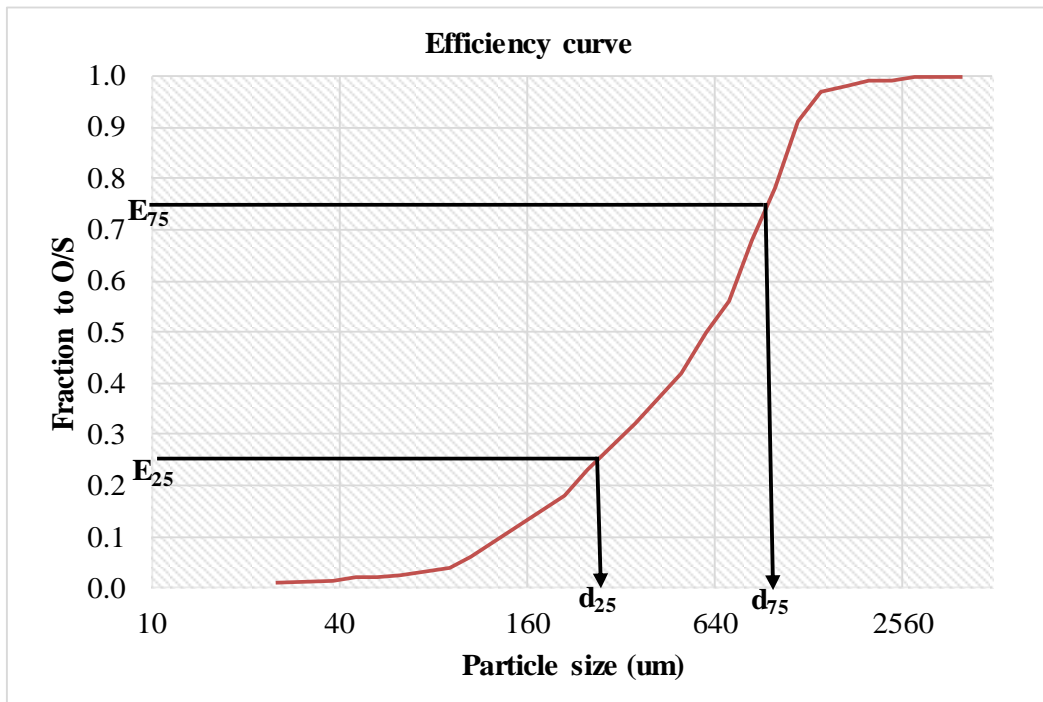


Figure 2-5: Quantifying the deviation from ideal performance

There are times when an efficiency curve exhibits a fish hook at finer particle sizes, and the phenomenon is known as the fish hook effect. However, this effect has been mostly observed in hydro-cyclones and less on screens (Plitt et al. 1990; Nageswararao 1999). Whitten used the parameter β to incorporate the fish hook effect in Equation 2.6 above, as shown in Equation 2.7 below.

$$E_{oc} = 1 - C \left(\frac{(1 + \beta\beta^*)e^\alpha - 1}{(e^{\alpha\beta^*} \times \frac{d}{d_{50}}) - (e^\alpha - 2)} \right) \dots \dots \dots 2.7$$

2.4.3 Effects of operating variables on screening rate

Many factors influence the drainage rate of fine particles and can be grouped into design or machine factors and operational factors (Firth & O’Brien 2000). Operational variables include

particle size distribution and shape, slurry density and viscosity, particle density, feed rate, material flowability and friability (Tsakalakis 2001). Design or machine variables include screen aperture shape and size, angle of inclination, open area, screen length and width, vibration intensity (frequency and amplitude) and material of the screen panels (Gupta & Yan 2006). All these factors are adjusted during material recovery to minimise the effects of screen blinding (occurs when undersize particles coagulate on a screen surface and block the apertures), aperture plugging (happens when critical size particles get lodged in the apertures) and material carryover (occurs when fine particles are carried over to the oversize stream).

This section reviews all the factors that have a bearing on the performance of the screen with emphasis on screen aperture shape and size, material feed rate and slurry density as the core parameters of the thesis. However, various concepts and thoughts that were used during experimental planning stage and results analysis were drawn from other factors not directly investigated, hence, the presentation of all the possible factors that influence the physical separation of material.

2.4.3.1 Screen aperture shape

Screen aperture shape is the shape of the openings of a screen panel. With significant advancement in screen technology, there exist different screen aperture designs with various shapes and configurations designed to meet specific material separation demands. The common ones include octagons, slots, hexagons, rhomboids, square, circular, tear drops and rectangular. However, complex screen aperture designs are more suited to handle operations compounded by screen pegging and or blinding. Wills & Napier-Munn (2006) established that most apertures are tapered at the bottom to make certain the passage of undersize and near-size particles, thus, improving material screenability. Cleary et al. (2009) further observed that the longer the tapered profile, the more likely that a particular particle will pass through.

Over the years, the slot, square and rectangular apertures have been the most widely used aperture designs. Slot and rectangular designs have found great applications in sizing and dewatering operations. They are also used in separating feed material with a lot of non-spherical particles since they are relatively resistant to pegging due to increased aperture flexibility (Wills & Napier-Munn 2006). Grozubinsky et al. (1998), however, established that these aperture shapes pose a substantial risk of passing elongated particles. Screening is widely a gravity driven operation, thus, placing a slot or rectangular panel on an inclined screen reduces its effective length and in turn, its efficiency in material recovery (Stairs 2014). Hence, slotted and rectangular screen apertures are best suited for horizontal or near

horizontal applications, where its full length can be maximised. Square openings, on the other hand, provide a higher open area but with reduced sizing accuracy as elongated particles can easily pass along the diagonal (Aplan et al. 2003).

2.4.3.2 Screen aperture size

Choosing a screen aperture size depends on the desired product size and downstream operations (Korte 2008). However, the maximum particle size that should be recovered obviously sets the minimum screen aperture size required (Sullivan et al. 1990). The effectiveness of any screen surface in separating specific particle size portions is reliant on how smaller such particles are in reference to the aperture size. Therefore, the establishment of separation cut point is fundamental prior to material separation. Normally, 0.25 - 0.5 mm aperture sizes are used in dewatering operations as they offer enough screening area for water to easily drain through a thick bed of material (Albrecht 2013). 0.5 - 3 mm aperture sizes are mostly used in sizing, desliming and media recovery operations. Recommended typical screen sizes that can be used on inclined screens with different screen panels are shown in Table 2:1.

Table 2:1: Aperture sizes for inclined screens

Material	Aperture size
Rubber	Required product size plus 25 - 30 % allowance
Polyurethane	Required product size plus 15 - 20 % allowance

Tsakalakis (2001) studied the effects of four different screen aperture sizes i.e. 0.6, 1.0, 2.0 and 4.0 mm on screening rate using crushed quartz. Screen panels of sizes 0.6 mm and 1.0 mm produced screening efficiencies of about 45 - 50 % and 75 - 80 % respectively. The decrease in screening efficiency for the 0.6 mm aperture was attributed to the high content of near-size particles in the feed as well as reduced screen capacity, as the ability of a screen surface reduces with aperture size. Aplan et al. (2003) established that as the screen aperture size changes for the same feed material, the proportions of undersize, oversize and near-size particles are in a way altered, hence, affecting screening rate.

2.4.3.3 Slurry density

Slurry density reflects the solid content of a slurry. Valine et al. (2009) established that the amount of water in a slurry plays a fundamental role in most material separating processes that work on the principle of gravity in separating particles of assorted sizes and densities. Guerreiro et al. (2015) investigated the effects of slurry density on screening rate at 1 - 3 v/v% solids and observed a decrease in recovery rate with increase in slurry density. During wet screening, drainage rate of undersize particles is aided by the presence of water in the slurry.

Hence, as the amount of water in a slurry reduces, there is a corresponding decrease in fine particles recovery. Kindig (1998) observed that high drainage rate is achievable with slurry containing between 10 - 20 v/v%. Furthermore, Albuquerque et al. (2008) and later Valine et al. (2009) investigated the effects of slurry density on material separation at 10 - 20 v/v% solids and established that undersize recovery reduces with increase in particle concentration in a slurry. While working on the application of banana screens in drain and rinse operations with slurry material containing between 33 - 60 w/w% solids, O'Brien & Firth (2015) determined that drain rate of magnetite reduces with increase in slurry density. Hence, the amount of water in a slurry plays a critical role in the efficient separation of undersize particles. While separation of diamond and or iron ore particles using ferrosilicon is done at slurry density above 2.0 kg/L (60.2 w/w % solids), however, no research work can be found in open literature on a slurry with percent solids above 60 w/w %.

2.4.3.4 Feed rate

Feed rate is expressed as a dry mass flow (t) of material onto a screen surface in a specified period (h) and is directly proportional to screen capacity (Albuquerque et al. 2008). Mbuyi et al. (2014) established that exceeding the capacity of a screen by over-feeding it leads to a reduction in the screening efficiency as most of the fine particles is misdirected to the oversize stream. This was attributed to a decrease in material residence time on the screen surface. King (2000) recommended that a screen surface should be fed with material at least up to 80 % of its capacity to efficiently recover fine particles. Burke & Craig (2005) observed that increasing material feed rate to a screen leads to high undersize recovery, but once an optimum point is exceeded, further increase leads to a reduction in the efficiency of separation. Even though low feed rate and longer screening period are ideal for efficient undersize recovery, this is not practical due to the high throughput demanded in most material separating industries.

Mabote (2016), Rogers & Brame (1985), Mwale (2015) among others investigated the effects of varying feed rate on material recovery rate and established that increasing feed rate onto a screen surface has a negative effect on the separation of undersize particles. O'Brien & Firth (2005) also investigated the effects of volumetric flowrate variation on magnetite recovery and observed a decrease in drainage rate with increase in feed flow rate.

2.4.3.5 Vibration intensity

The primary aim of introducing vibration motion to a screen surface is to enhance stratification of fine particles through a bed of material, dislodge particles pegging the

2.4.3.6 Angle of inclination

The angle of inclination represents the angle of elevation of a screen surface with respect to the horizontal and is achieved by tilting the feed end slightly up. In most cases, vibrating screens are operated with a reasonable angle of inclination less than 10 ° to aid in the transportation of material across the screen length (Metso 2008). With a slightly tilted feed end, oversize particles move off the screen surface easily, hence, creating room for undersize particles to stratify through a bed of material. However, Sawant et al. (2016) observed that the higher the angle of inclination, the greater the velocity of material on a screen surface. Aplan et al. (2003) established that material vertical acceleration on a screen surface can be calculated by considering the intensity of vibration (G) exerted on feed particles, the angle of inclination (R) and drive angle (Q), as shown in Figure 2-6 and Equations 2.9 and 2.10 below. It can be seen that particle velocity on the screen surface is largely influenced by the G-force, drive angle and angle of inclination.

$$K_v = \frac{G \times \sin (Q + R)}{\cos (R)} \dots \dots \text{for inclined screens} \dots \dots \dots 2.9$$

$$K_v = G \times \sin (Q) \dots \dots \text{for horizontal screens} \dots \dots \dots 2.10$$

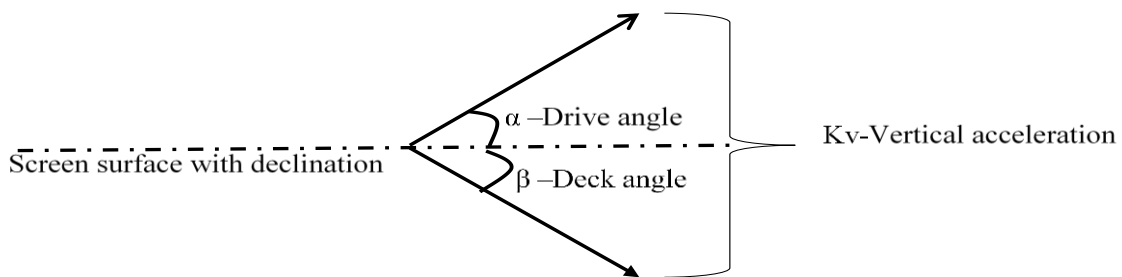


Figure 2-6: Deck and drive angles

Furthermore, Wills & Napier-Munn (2006) established that the effective aperture size of a screen at an elevation decreases by the cosine of the angle of inclination. For example, a screen panel with an aperture size of 2 mm and inclined at 40 ° has an effective aperture size of 1.5 mm, since the effective size is the product of actual aperture size and the cosine of the angle of inclination (DeCenso 2000). Carnes & Olsen (2001) compared the carrying capacities of the horizontal and inclined screens and proved that apertures of a horizontal screen appear larger than those for the inclined screen when viewed from the top, as shown in Figure 2-7.

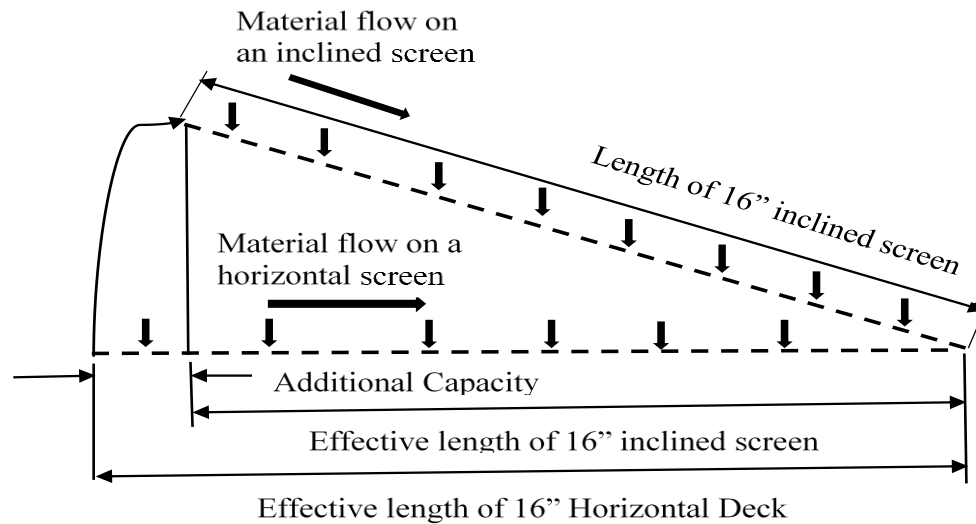


Figure 2-7: Variation of effective length with angle of inclination, redrawn from Carnes & Olsen (2001)

2.4.3.7 Particle size distribution

Particle size distribution (PSD) of feed material is one of the main factors that affects a separation process in terms of capacity as well as efficiency (Ma et al. 2000; Levoguer 2013). It describes the sizes of discrete particles in the feed. The influence of every particle size fraction on drainage rate is unique and differs for different screen aperture shapes and sizes, hence, categorising feed material into size fractions is fundamental.

While there are different size fractions i.e. fine, near size and oversize particles, Carnes & Olsen (2001) established that near size particles are very critical during screening. Near-mesh particles represent a group of particles in the feed that are $\pm 25\%$ of the aperture size, as shown in Figure 2-8. Adopting the established PSD model of Tsakalakis (2001) and redefining the critical undersize and oversize to conform to Carnes & Olsen (2001) definition, a modified PSD characterisation of the feed was developed with adjusted near-size particles (critical oversize (C_o) at $1.25a$ and critical undersize (C_u) at $0.75a$). Where (a) is the aperture size, (d) is the particle size, O is oversize, U is undersize, C is the near-size particles, B is the half size particles, A is undersize particles of size range ($0.5a < d < 0.75a$) and K_{100} is the maximum particle size. The adjustment was made to give a more representative characterisation of size fractions since Tsakalakis (2001) PSD model identified the critical undersize and oversize at -29% and $+50\%$ of the aperture size respectively.

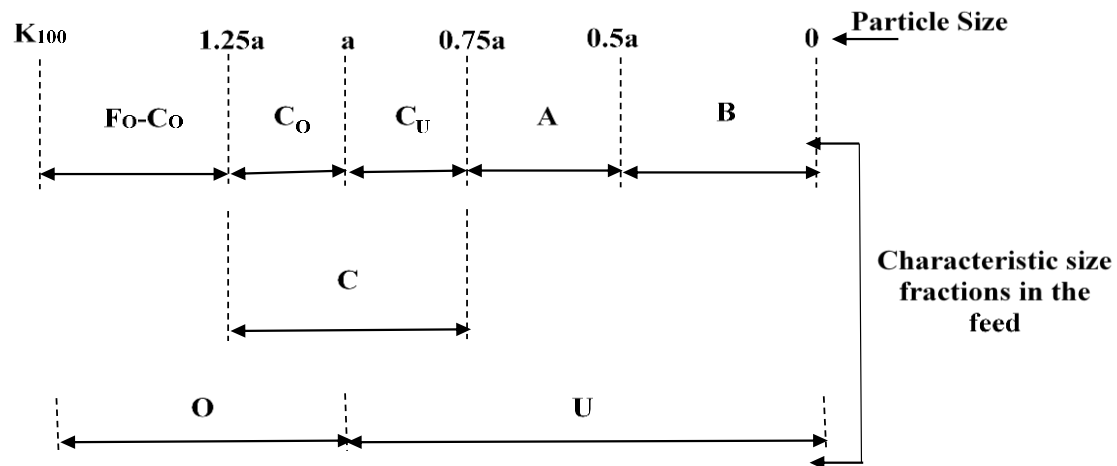


Figure 2-8: Particle size characterisation

Considering that particles bigger than the aperture size ($>1.25a$) are retained on the screen surface and particles finer than the screen openings ($<0.75a$) easily pass through the screen holes, passage rate is therefore dictated by the amount of near-size particles ($0.75a \leq d \leq 1.25a$) in the feed (Beunder & Rem 1999). Wodzinski (2003) observed that this group of particles is difficult to separate as they tend to peg the screen apertures, thus, reducing the screen carrying capacity. Carnes & Olsen (2001) observed that these particles also tend to roughen the screen surface, resulting in reduced material flowability. Thence, high proportions of near-size particles largely influence the screen's ability to recover fine particles efficiently. Standish et al. (1986) established that the passage rate of critical size particles can be aided by the presence of oversize particles ($>1.25a$) on the screen surface. Aplan et al. (2003) recognised that oversize particles on top of the material bed have a high ability to prevent fine particles from bouncing off a screen surface, thus, enhancing undersize passage rate. However, Soldinger (1999) and later Drzymala & Konopacka (2012) observed that too much oversize particles have a detrimental effect on the passage rate as they tend to carry along fine particles to the overflow stream. Conversely, Lawrence & Beddow (1969) and later Ferrara et al. (1987) observed that an increase in undersize particles in the feed leads to higher stratification, but beyond 60 %, stratification reduces due to increase in particle competition for passage. There is conflict in the literature regarding the influence of individual particle size fractions on recovery rate. Hence, understanding feed material gradation is essential for efficient material separation.

2.4.3.8 Open area

Open area is the percent ratio of the net aperture area to the entire screen area and ranges from 12 to 90 % depending on the screen characteristics and its projected usage (Aplan et al. 2003; Wills & Napier-Munn 2006). Schlemmer (2016) established that the percent open area of a screen panels is directly proportional to the screen aperture size. Gupta & Yan (2006) observed that open area increases with decrease in the wire thickness of the screen apertures. Gupta & Yan (2006) further emphasised that the available screening area for any screen surface is largely influenced by the thickness of the material surrounding the apertures. Hence, the thinner the aperture thickness, the higher the open area. This is due to the increase in the capacity and sizing accuracy of the screen, though at the expense of screen life.

2.4.3.9 Screen length and width

Wang & Tong (2011) established that increasing screen length during dry screening leads to efficient separation of undersize particles due to increase in material residence time. However, it has been established that higher drainage rate is attainable with feed slurry comprising of less than 20 v/v% solids within a short screen length since most of the fluid pass along with fine particles rather quickly (Valine et al. 2009). Satyenda (2015) observed that the width of a screen rather than its length plays a leading role in the wet screening of fine particles. Hence, screen width plays a significant role in wet screening than screen length. Furthermore, Stairs (2014) established that increasing screen width leads to a reduction in material bed depth on a screen surface, as this allows the spreading of material over a wider area at the feed end. Hence, more residence time for undersize particles to stratify and easily pass through the screen apertures. Normally, screen length is about 2 - 3 times the screen width (Tsakalakis 2001). As a rule of thumb, screen width is usually associated with screen capacity and screen length with efficiency (Aplan et al. 2003).

2.4.3.10 Material bed depth

Material bed depth is typically the thickness of material on a screen surface. When the material bed depth on a separating surface is thin, fluidization of particles is so high leading to easy stratification and separation of undersize particles. If the material bed depth is too thin, particles tend to bounce on the screen surface without stratifying, hence, reducing contact times with the screen surface for passage (Schlemmer, 2010). If the bed of material is too thick, there is a high reduction in the probability of passage due to insufficient stratification of undersize particles onto a screen surface (Donaghy 2016). Stairs (2014) established that an excessively deep bed depth of material is formed in the middle of a screen if the bed depth is too high at the feed end, resulting in inconsistent stratification and fines carryover to the

overflow stream. Material bed depth optimisation is therefore very critical since stratification of undersize particles starts as soon as material is introduced onto a screen surface.

Many researchers have recommended that for an efficient physical separation, material bed depth at the discharge end should be at least four times the screen hole size (Gupta & Yan 2006; Sullivan 2013; Tsakalakis 2001; Wills & Napier-Munn 2006). Aplan et al. (2003) recommended that the bed depth at the discharge end of a screen surface should not exceed 'n' times the screen aperture size, where $n = 2 + (0.02 \times \text{bulk density})$. However, O'Brien et al. (2010) observed that this principle does not entirely apply during wet screening as the percolation of fine particles through a bed of material is accomplished by hydraulic transport rather than stratification. Thus, evenly material distribution across the full-screen width is essential in ensuring that every particle has an opportunity to contact the screen surface at least more than once for passage.

Sullivan et al. (1990) stated that material bed depth (D) increases with feed rate (F) and reduces with increase in material velocity (v), bulk density (B) and net width of the screen at the discharge end (W), as shown in Equation 2.11. Since particle retention time is inversely proportional to material velocity along a screen length, it can be deduced that material bed depth is directly proportional to retention time. Mohanty et al. (2003) observed that increasing the retention time of particles on a screen surface enhances the passage of rightly oriented near-size and fine particles. Hudson et al. (1969), however, established that increase in material residence time leads to material build up on the screen surface and in turn, impair stratification and particle passage. Hence, optimisation of material bed depth on a screen surface is fundamental for efficient particle separation.

$$D = \frac{400F}{BVW} \dots \dots \dots 2.11$$

2.4.3.11 Material flowability

Material flowability is the flow of material on a screen surface and is largely influenced by the rheology properties of the material i.e. viscosity and stability (Collins et al. 1974). Slurry stability refers to the ability of solid particles to settle out in a slurry either by centrifugal forces or gravity. Slurry viscosity refers to the flow resistance of a fluid material (Collins et al. 1974). From literature, it has been observed these two parameters are influenced by the presence of ore slimes, solid concentration, shear rate accumulation, oxidation of medium surface, medium disintegration and shape of medium (Napier-Munn & Scott 1990; Poletto & Joseph. 1995; Alturki et al. 2013; Mangesana et al. 2008; Olhero & Ferreira 2004; Luckham & Ukeje 1999; Amiri et al. 2010; Boylu et al. 2004). Ideal heavy medium has low apparent

viscosity to maximise on pump and separation efficiency (Shi & Napier-Munn 2002; Grobler et al. 2002; Luckham & Ukeje 1999). Very viscous medium is undesirable on a screen surface due to reduced settling rate and flowability, hence, reducing the contact times particles make with the screen surface for passage. This, in turn, leads to increase in moisture and fine particles misplacement to the oversize stream.

2.4.3.12 Material friability

Friability refers to material disintegration on the screen surface. Even though there are physical similarities among most materials, their behaviour on a screen surface is different. Certain materials are highly friable with typical properties that cause them to break at critical sizes due to screen action (Anon 1978). If a large volume of such particles undergo degradation at a critical size equal to the aperture size, there will be a drastic drop in the separation efficiency of undersize particles due to aperture pegging (Govender & Van Dyk, 2003). However, some materials are highly friable and tend to break into smaller particles that can easily percolate through screen apertures (O'Brien et al. 2010). Corrosion in-situ of particles has a high ability to increase slurry viscosity due to the introduction of additional amounts of fines. However, Metso (2008) stated that this effect can be minimised by using polymeric screen panels as they have a high ability to reduce disintegration of highly friable materials.

Sciarone (1976) observed that materials such as ferrosilicon with 14 - 16 % silica have optimum properties with reduced friability. However, if the silicon content is less than 14 %, there is improved magnetic properties and specific gravity but with reduced corrosion resistance while above 16 %, there is deterioration in magnetic properties and specific gravity but with increased resistance to friability. Withal, Collins et al. (1974) observed that the higher the carbon content in the heavy media particles, the higher the friability as the amount of carbon adversely affect the relative density of particles.

2.4.3.13 Particle shape

During any screening process, it is obvious that particles larger than the screen hole will be retained while smaller particles easily pass through. At times, undersize and near-undersize particles are retained on a screen surface due to their shapes. Particle shapes of most materials include angular, acicular, flaky or slabby, spherical and ovaloid (Sullivan 2013). While it is a known fact that undersize spherical particles easily pass through the screen holes in any orientation, irregularly shaped particles passage largely depends on their orientation with which they hit a screen surface (Drzymala, 2007; Beunder & Rem, 1999). In some cases, they

present a small cross section and easily percolate through, while in other situations, a greater cross-section and are retained on a screen surface (Soldinger, 2000). Standish et al. (1986) studied the effects of different particle shapes on the screening process and established that screening time increases with egress from sphericity. Hence, appreciating the shapes of feed particles is decisive before conducting a physical separation process.

2.4.3.14 Particle density

Trumic & Magdalinovic (2011) observed that higher particle density leads to higher separation forces due to the high gravity forces induced by dense particles onto the separating surface. Heavy materials such as metal powders, for example, are separated quite readily even by fine screen sizes. However, lightweight materials such as sawdust exert low forces of gravity onto a screen surface and can only be screened at meagre feed rate (DeCenso 2000).

In a dense medium circuit, particles of ore material are separated based on the differences in density using heavy media i.e. magnetite or ferrosilicon with relative density cutting between gangue and valuable minerals (Marot, 1960; de Korte, 2008). In most cases, separating density higher than 2.0 t/m^3 , ferrosilicon is used, and below that, magnetite is used (Bosman 2014). Diamond ore, for example, with a relative density of about 3.6 t/m^3 is separated from either alluvial particles or kimberlite of density 2.65 t/m^3 (Noble & Luttrell 2015). Williams & Kelsall (1992), on the other hand, observed that due to over comminution and or production process, cavities are at times introduced on heavy media particles, and this reduces their effective density as most of them are liable to breaking during physical separation on the screen surface.

2.4.4 Section summary

The performance of every separating surface is primarily defined by the extent to which particles of feed material are separated into distinct size fractions. Screen performance is governed by the principles that hinge on the probability of particle passage through the screen apertures as well as those that affect opportunity times particles should contact a screen surface. While there are many ways of assessing the performance of a separating surface, in this thesis, drainage rate i.e. time taken to fill up a specific volume of the underflow tank before overflow, percent moisture and medium bypass were used. Drainage rate is a vital parameter in the drain and rinse applications as 90 - 95 w/w% of the media particles is expected to be recovered on the drain part of the drain and rinse vibrating screen. From literature, it has been established that very little recovery is achieved on the rinse part of the vibrating screen, hence, the economics of running the dense medium cyclone circuit is largely

dependent on the efficient recovery of media particles on the drain part of the screen for reuse in the cyclone.

Many factors influence the drainage rate of heavy media particles, and these include; screen aperture shape and size, PSD, material feed rate, percent solids, screen vibration intensity, the angle of inclination, slurry density, etc. A lot of work has been done so far on how most of these factors relate during physical separation of material in general (Guerreiro et al. 2015; Albuquerque et al. 2008; Valine et al. 2009; Mabote 2016; Mwale 2015; Grozubinsky et al. 1998; Li & Tong 2015). While all the findings were key to this thesis, no information was found in the open literature regarding the influence of relative density and especially above 60 w/w % solids, feed rate and screen panels on media drainage rates in a DMC circuit.

Therefore, this thesis focused on establishing the effects of slurry density, slot size and volumetric flowrate variation on medium recovery by calculating the medium drainage rate, water and medium bypass. While it is certain that the angle of inclination can be varied for maximum recovery, in cases where it was kept constant and at less than 5 ° with vibration intensity between 2 – 4G, excellent results were achieved (Guerreiro et al. 2015). Hence, this project assumed a horizontal screen surface with vibration intensity constant around 3.2G.

3 RESEARCH METHODOLOGY AND DESIGN

3.1 Introduction

This chapter outlines the experimental approach followed in evaluating the effects of varying volumetric flowrate, slurry density and aperture size on medium drainage rate. The experimental runs were conducted on a pilot plant discussed in section 3.4. In a typical dense medium circuit, the separation of heavy ore materials such as iron and diamond ore is accomplished by using ferrosilicon as medium, and for light particles like coal, magnetite is used. The choice of medium for a particular separation is largely dependent on the density of separation, where separation above 2.0 kg/L, ferrosilicon is used, and below that, magnetite is used. Thus, to depict current conditions and material combinations used in a dense medium circuit, ferrosilicon and magnetite suspensions were used. Iron ore was sourced from Sishen iron ore mine. The ferrosilicon used had about 15.23 w/w% silicon.

3.2 Material preparation and characterisation

3.2.1 Material preparation

The initial step in material preparation was to expose the iron ore, ferrosilicon and magnetite to the air and sun drying to ensure that all the inherent moisture was eliminated. Then the iron ore was sieved using a vibrating swico screen shown in Figure 3-1 below with 1.0 mm screen sieve to remove the minus 1 mm (non-magnetic) particles. The less than 1 mm particles have been known to have a negative effect on medium viscosity and positive influence on stability (Sripriya et al. 2001). Similar observations were also made by Fourie et al. (1980), Glastonbury & Jansen (1967), Marsh (1945) and Grobler et al. (2002). The iron ore, magnetite and ferrosilicon particles were then split down into 20 kg batches using the coning and quartering method adopted from Schumacher et al. (1990).



Figure 3-1: Vibrating swico screen

3.2.2 Material characterisation

Material characterisation in terms of particle size distribution (PSD) and particle shape is key to any physical separation process. Particle shapes and presence of cavities were determined for iron ore, ferrosilicon and magnetite using a Zeiss MERLIN Field Emission Scanning Electron Microscope at the Electron Microbeam Unit of Stellenbosch University's Central Analytical Facility. Prior to imaging, the samples were mounted on aluminium stubs with double sided carbon tape. The samples were then coated with a thin (~10nm thick) layer of gold, using an Edwards S150A Gold Sputter Coater. This was done in order to make the sample surface electrically conductive to avoid electron build-up on the sample surface which can cause electron charge. Beam conditions during the electron image analysis were 20 kV accelerating voltage (EHT (Extra-High Tension) target), with a working distance of 9.5 mm and a beam current of 11nA with an analytic column.

Particle size distribution was done using sieve analysis method. Firstly, small representative fractions of about 300 – 500 g for magnetite, ferrosilicon and iron ore were prepared using a ten-cup rotary splitter shown in Figure 3-2 below. Random sub samples were then combined until the required amount was obtained. Then all sieve sizes required for PSD analysis were collected and stacked in descending order with the largest sieve on top and the smallest sieve with a pan at the bottom, and the prepared sample poured onto the top sieve. The sieve sizes used included 4.0, 2.8, 2.36, 2.0, 1.7, 1.4, 1.18, 1.0, 0.85, 0.71, 0.6, 0.5, 0.355, 0.25, 0.212, 0.15, 0.106, 0.09, 0.063, 0.053, 0.045, 0.038 and 0.025 mm. The nested sieves were placed on the mechanical shaker for 10 - 15 minutes. Then the masses of particles retained on the sieves were measured to the nearest 0.1 g and recorded. Using the retained weights, the percent retained and cumulative percent passing were calculated for each sieve (DeCenso 2000). Then PSD graphs were generated for each material using the cumulative percent passing and geometric mean size on a logarithm scale, as shown in Figure 3-3.



Figure 3-2: Ten cup rotary splitter

Iron ore particles with a relative density of 4.0 g/mL had 90 % passing 2.80 mm with less than 1 % passing 1 mm sieve, as shown in Figure 3-3 below. Ferrosilicon material with 6.1 g/mL relative density had 90 % passing 90 microns, and magnetite with 4.72 g/mL relative density had 90 % passing 75 microns, as shown in Figure 3-3 below.

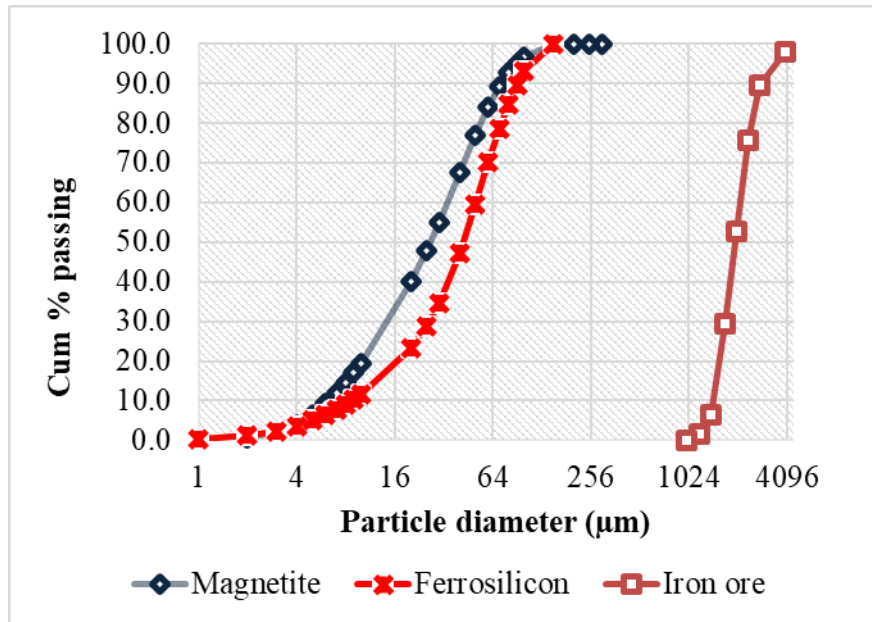


Figure 3-3: Particle size distributions for iron ore, ferrosilicon and magnetite

On the other hand, chemical composition of ferrosilicon before and after two months of experimental runs was established using an XRF spectrometry on a PANalytical Axios Wavelength Dispersive spectrometer at the Central of Analytical Facilities, Stellenbosch University, South Africa. The spectrometer was fitted with an Rh tube and with the following analyzing crystals: LIF200, LIF220, PE 002, Ge 111 and PX1. Major elements were analyzed on a fused glass disk using a 2.4kW Rhodium tube. Matrix effects in the samples were corrected by applying theoretical alpha factors and measured line overlap factors to the raw intensities measured with the SuperQ PANalytical software. The concentration of the control standards that were used in the calibration procedures for major element analyses fit the range of concentration of the samples. Amongst these standards were NIM-G (Granite from the Council for Mineral Technology, South Africa) and BE-N (Basalt from the International Working Group).

3.3 Design of experiments

Owing to the limited data on medium drainage rate in literature and the large number of permutations needed to cover a variety of typical operating conditions for the variables chosen, a comprehensive experimental design was adopted for the thesis, as shown in Table

3-1. It is worth noting that the initial plan was to run experiments on magnetite between 1.6 – 1.9 kg/L and ferrosilicon between 1.65 – 3.2 kg/L, although the highest density achieved for ferrosilicon was 2.7 kg/L due to material constraint. Hence, the table reflects the actual slurry densities after experimental runs. However, randomisation of experimental runs was not done due to restrictions presented by ore type and sump capacity, as the procedure involved the addition of water and or solids to the feed sump each time a sample was taken. Logistically, it was more resourceful to start with a high density and gradually dilute as samples were taken. On the other hand, randomisation would have meant repeatedly changing of screen panels for each combination of variables. It was more logical to test all combinations of feed rate and slurry density on one set of panels at a time. This procedure was followed for all the screen panels shown in Table 3-2 below. All the screen panels used were new with the same dimensions (305x305 mm) as shown in Figure 3-4 supplied by Multotec. Even though screen panels are not frequently changed in real time plants, it was done in this study to offer a wider perspective on medium drainage rate through different screen panels.

Table 3:1: Experimental plan

No	Relative density (kg/l)	% Solids by weight	% Solids by volume	% Solids v/v per screen area	Feed rate (m ³ /h)	Comment
1	1.64	49.50	17.21	33.68	18 to 26	Magnetite
2	1.72	53.10	19.37	37.91	18 to 26	
3	1.84	57.90	22.59	44.21	18 to 26	
4	1.65	47.10	12.08	23.63	18 to 26	Fresh and contaminated ferrosilicon
5	1.72	50.10	14.12	27.63	18 to 26	
6	1.85	55.00	16.67	32.62	18 to 26	
7	1.90	56.70	17.65	34.54	18 to 26	
8	2.00	59.80	19.61	38.38	18 to 26	
9	2.10	62.70	21.57	42.21	18 to 26	
10	2.20	65.20	23.53	46.05	18 to 26	
11	2.30	67.60	25.49	49.88	18 to 26	
12	2.45	70.80	28.43	55.64	18 to 26	
13	2.55	72.70	30.39	59.47	18 to 26	
14	2.70	75.30	33.33	65.23	18 to 26	

Table 3:2: Screen panel sizes and material of construction

No	Slot size (mm)	% Open area	Comment
1	0.63x8.8	15.16	Polyurethane
2	0.63x12	15.79	
3	0.8x8.8	15.55	
4	1x13	12.53	
5	1x12	16.25	Rubber
6	0.63	15.00	Polywedge wire

3.4 Experimental set-up and procedure

The experimental set up with specifications highlighted in Table 3:3 and Figure 3-4 comprised of the following main constituents, as shown in Figure 3-5.

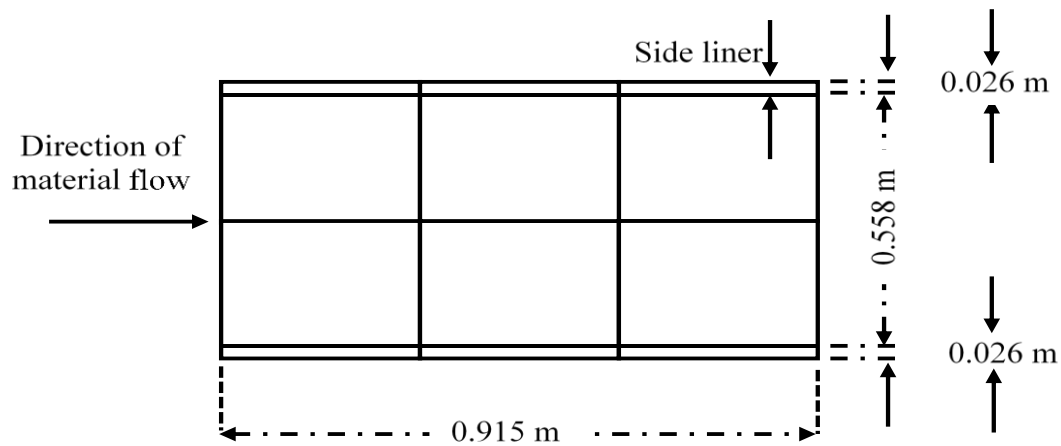
- 1) Feed tank (500 L) for material preparation as well as overflow and underflow sump collection.
- 2) Variable frequency drive (VFD) shown in Figure 3-6 (b).
- 3) Screen surface.

Two blank panels at the feed end (Figure 3-6 (a)), material deflectors (Figure 3-6 (c)) and feed distributor (Figure 3-6 (d)) were installed.

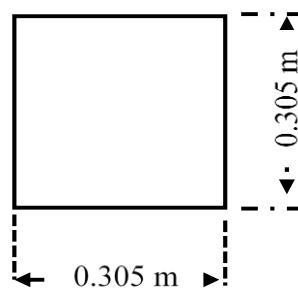
- 4) Underflow tank (101 L), as shown in Figure 3-7.
- 5) Movable overflow sample container (5 - 10 L).

Table 3:3: Measured vibrating screen parameters

No	Parameter	Comment
1	Screen area	Constant ($0.915\text{m} \times 0.558\text{m} = 0.511\text{m}^2$) (6 clear and 2 blank panels)
2	G-force	3.2 (3.2 mm amplitude and 50 Hz frequency)
3	Screen motion	Linear motion with 40° drive angle
4	Angle of inclination	Horizontal surface



(a)



(b)

Figure 3-4: Dimensions of the separating surface (a) and screen panel (b)

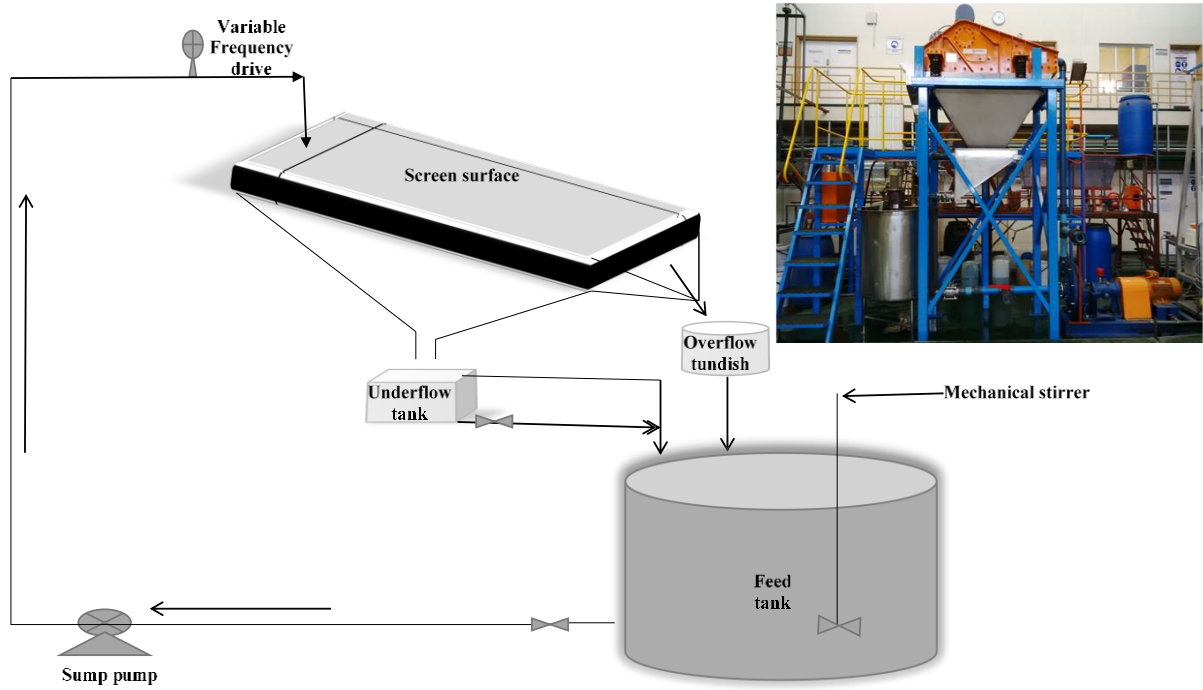


Figure 3-5: Experimental setup

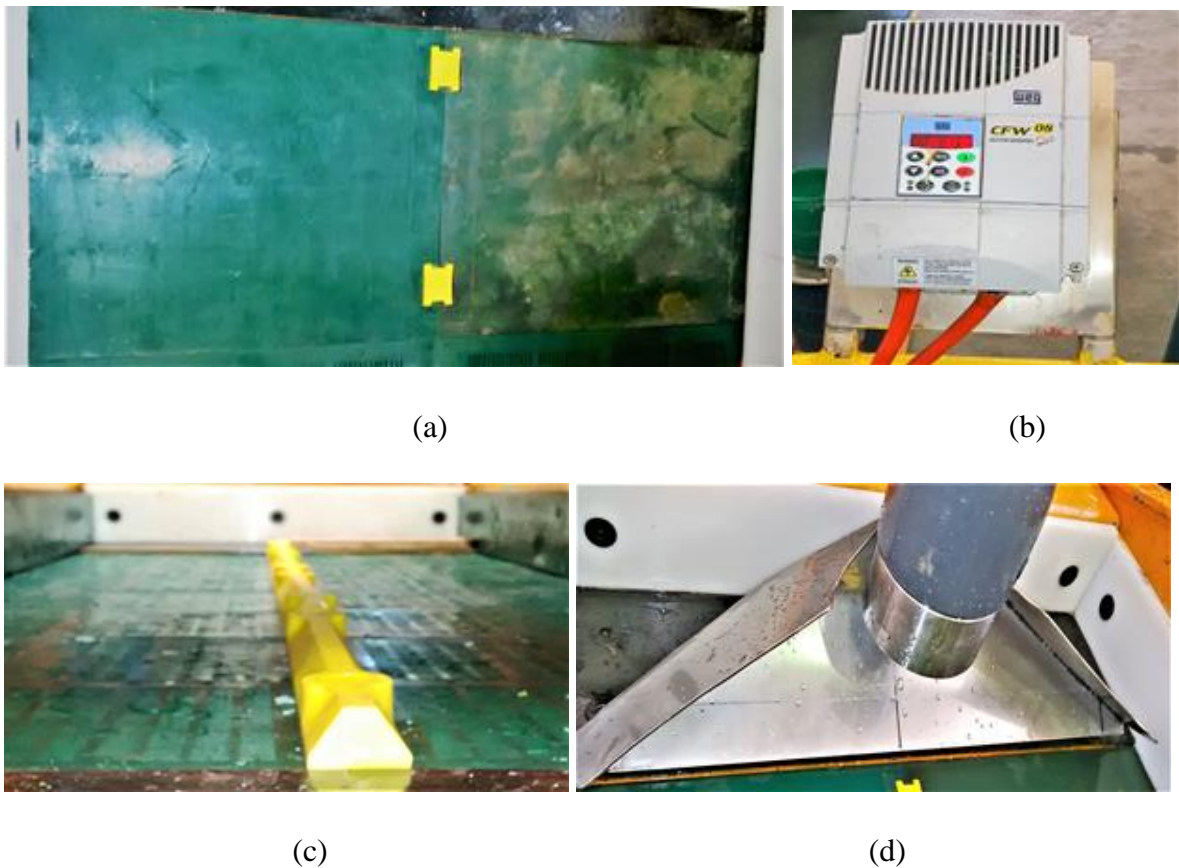


Figure 3-6: Blank panels (a), VFD (b), deflectors (c) and feed distributor (d) installed on the screen surface



Figure 3-7: Underflow tank

Before commencing experimental runs, screen panels with the required aperture size were installed on the screen. Then 310 - 350 L of a slurry containing either ferrosilicon or magnetite was prepared in a feed tank with a specific relative density and held under continuous mechanical agitation for at least 20 minutes to ensure uniform particle distribution. To guarantee manageable material handling, the slurry was used in a circulatory mode of operation. Once a uniform particle distribution was established in the feed tank, medium recovery commenced by starting the screen vibration, then opening the feed valve and starting the feed pump. The feed rates were measured prior to starting each set of experiments by removing the panels from the screen surface then adjusting the pump speed using the variable frequency drive (VFD) and establishing the time taken to fill up the underflow tank. On the other hand, the feed rates were confirmed by adding the medium drain rate and material flowrate to the overflow stream for each set point. Feed samples were taken from the feedline discharge point using a 10 L bucket for slurry density measurement. The slurry density was calculated by dividing the weight and volume of the sample. If the density was significantly lower or higher than the desired level, more solids or water was added to the feed tank respectively.

Once a steady flow of material was achieved by running for at least 20 - 30 minutes, medium drainage rate was established by closing the outlet valve at the bottom of the underflow tank and time to fill up a specific volume to the point of overflow recorded. The procedure was repeated at least two times at 10 minutes intervals for each experimental run and the average value for the three runs taken as the drainage rate. Drainage rate was established for a slurry containing medium (either magnetite or ferrosilicon) only and in the case of ferrosilicon, iron ore was later added at 1:5 (ore to medium ratio) and drainage rate established in the presence

of ore particles. At the end of each set of experiments, the feed tank content was emptied into 20 L buckets for storage.

For each experimental run on ferrosilicon and iron ore, samples from the feed, underflow and overflow streams were collected just after every drainage rate measurement using a 5 L bucket for particle size distribution, moisture content, media carryover and mass balance calculations. In terms of PSD measurement, the test samples were filtered, dried for 24 hrs at 105 - 110 °C in the oven and later de-lumped using steel rods and split down by means of a ten-cup rotary splitter shown in figure 3-2 to masses ranging between 300 - 500 grams for sieve analysis. Further, samples were collected from the feed stream and sent to the process engineering analytical laboratory for viscosity measurement using a rheometer.

To effectively execute the experimental works, the following response variables were calculated: -

1) Medium drainage rate

Drainage rate defined as the volume of material collected in the underflow tank from the entire drain stream just before overflow divided by the time taken and screen area expressed as m³/m²/h.

2) Percent moisture

Water being a driving force in wet screening, is used as an efficiency indicator for separating devices where a higher bypass shows inefficient separation and a lower value indicates efficient separation. Therefore, a representative sample was cut from the entire overflow stream using a 5 L bucket, weighed, filtered and later dried in an oven at about 105 - 110 °C for a minimum of 24 hours (Mariki 2000). After which, the difference in weights between the wet and dried material expressed as a percentage was taken as the percent moisture of the retained material, as shown in Equation 3.1 below.

$$\% \text{ Moisture} = \frac{[Wt_1 - Wt_2]}{Wt_1} \times 100 \dots \dots \dots 3.1$$

Where:

W_{t1}- Weight of wet sample and W_{t2}- Weight of dry sample

However, water bypass expressed as kilogram of water flow to the overflow stream per tonne of feed per screen width (kg/t/m) was calculated using Equation 3.2 below.

$$\text{Water bypass} = \frac{N \times O}{F \times W} \dots \dots \dots 3.2$$

Where;

N = % moisture, P = Overflow stream flowrate (kg/h), F = Feed rate (t/h) and W = Screen width (m).

3) Medium carryover

Medium carryover is a key parameter that is used to quantify the efficiency of separation of a screen surface in a dense medium circuit (Sripriya et al. 2006). Hence, a representative sample was cut from the overflow stream and weighed, then thoroughly washed on a sieve using pressurised water for a minimum of 10 minutes. The washed and rinsed material was then dried for at least 24 hrs at 105 - 110 °C and the difference in weights was used as a measure of percent medium carryover, as shown in Equation 3.3.

$$\% \text{ Medium carryover} = \left[\frac{W_{bw} - W_{aw}}{W_{bw}} \times 100 \right] - \% \text{ Moisture} \dots \dots \dots 3.3$$

Where;

Wbw- Weight before washing and Waw- Weight after washing, rinsing and drying

Furthermore, medium carryover expressed as kilogram of medium flow to the overflow stream per tonne of feed per screen width (kg/t/m) was calculated using Equation 3.4 below. While medium carryover to the overflow stream is a key parameter in the dense medium circuit, no information was found in the open literature on the calculation of this parameter on the screen surface. However, the calculation in kg/t/m was adopted from Sripriya et al. (2006) and Napier-Munn et al. (1995) who established that adhesion loss increases with screen loading. The effect was quite strong, and even moderately loaded screens showed a significant increase in loss (expressed in g/t/m of screen width) over lightly loaded screens.

$$\text{Medium carryover} = \frac{M \times O}{F \times W} \dots \dots \dots 3.4$$

Where;

M = % Medium carryover, O = Overflow stream flowrate (kg/h), F = Feed rate (t/h) and W = Screen width (m).

3.5 Consideration of experimental variables

3.5.1 Feed rate

Feed rate expressed as volumetric flow of material onto a screen surface over a specified period (m³/h) (O'Brien & Firth 2005). Albuquerque et al. (2008) stated that this parameter is directly proportional to the capacity of a screen surface. Hence, screen capacity in a way

dictates the volumetric flowrate of material onto a screen surface. King (2000) suggested that a screen surface ought to be fed with material at least up to 80 % of its handling ability to proficiently recuperate the fine particles. However, in this thesis, the volumetric flowrate varied between 18 to 26 m³/h for all the screen panels tested.

3.5.2 Slurry density

Slurry density is the weight of solids per unit volume of water expressed in kilogram per litre (kg/L). To depict the current dense medium operating conditions for the separation of coal particles using magnetite and iron or diamond ore using ferrosilicon, the feed slurry density varied from 1.64 to 1.84 kg/L (i.e. from 49.5 to 57.9 w/w% solids) for magnetite and 1.65 to 2.7 kg/L (i.e. 47.1 to 75.3 w/w% solids) for ferrosilicon. A maximum density of 2.7 kg/L for ferrosilicon attained was due to material constraint.

3.5.3 Aperture size

Choosing a screen aperture size appropriate for a separation process hinges on the anticipated product size and downstream processes (Korte 2008). Nonetheless, the maximum particle size that must be recovered sets the minimum screen aperture size required (Sullivan et al. 1990). The ability of any screen surface in separating particles is reliant on how much smaller such particles are relative to the hole size. Thus, the material cut point needs to be established before any physical separation. However, in this thesis, the panel sizes used are typically those used on a drain and rinse vibrating screen in the dense medium circuit, as shown in Table 3:2.

3.6 Results reproducibility

3.6.1 Medium drainage rate reproducibility

To assess the results reproducibility, the three test runs on medium drainage rate for both magnetite and ferrosilicon were repeated twice for selected experimental runs. Figure 3-8 shows the drainage rate of magnetite for the 0.63x8.8 mm screen panels at 1.72 kg/L slurry density and Table 3:4 shows the assessment of drainage rate using standard deviation. Similarly, Figure 3-9 shows the drainage rate reproducibility of ferrosilicon in the presence of iron ore for the 1x13 mm screen panels at 1.90 kg/L slurry density and Table 3:5 shows the assessment of drainage rate using the standard deviation. It can be seen that the results obtained were reproducible under the same experimental conditions with low standard deviation (SD) values for both magnetite and ferrosilicon with iron ore.

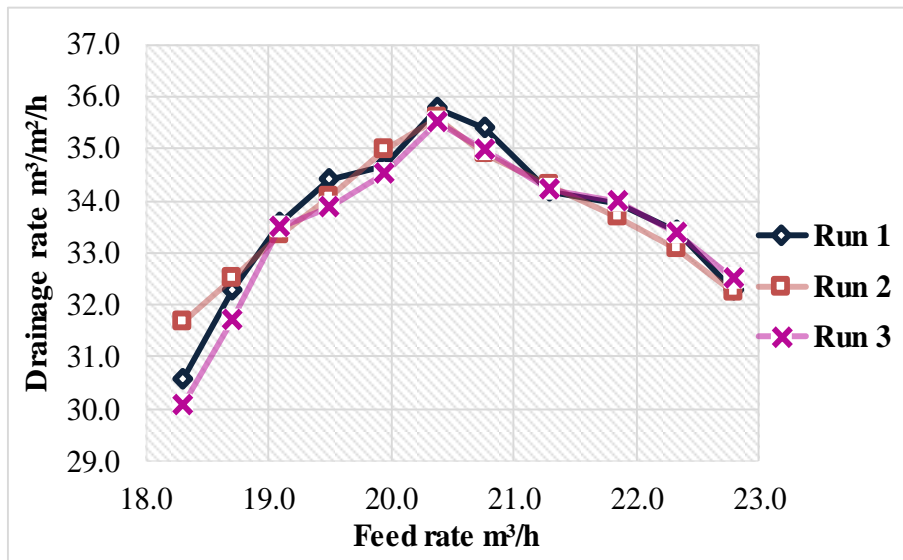


Figure 3-8: Magnetite drainage rate reproducibility for 0.63x8.8 mm polyurethane panels at 1.72 kg/L slurry density

Table 3:4: Reproducibility assessment for 0.63x8.8 mm polyurethane panels on drainage rate at 1.72 kg/L slurry density

Magnetite				
Feed rate (m³/h)	Drainage rate m³/m²/h			SD
	Run 1	Run 2	Run 3	
18.3	30.5	31.7	30.1	0.81
18.7	32.3	32.5	31.7	0.40
19.1	33.6	33.4	33.5	0.10
19.5	34.4	34.0	33.9	0.27
19.9	34.7	35.0	34.5	0.23
20.4	35.8	35.6	35.5	0.14
20.8	35.4	34.9	35.0	0.26
21.3	34.2	34.3	34.2	0.06
21.8	33.9	33.7	34.0	0.15
22.3	33.4	33.1	33.4	0.19
22.8	32.3	32.2	32.5	0.13

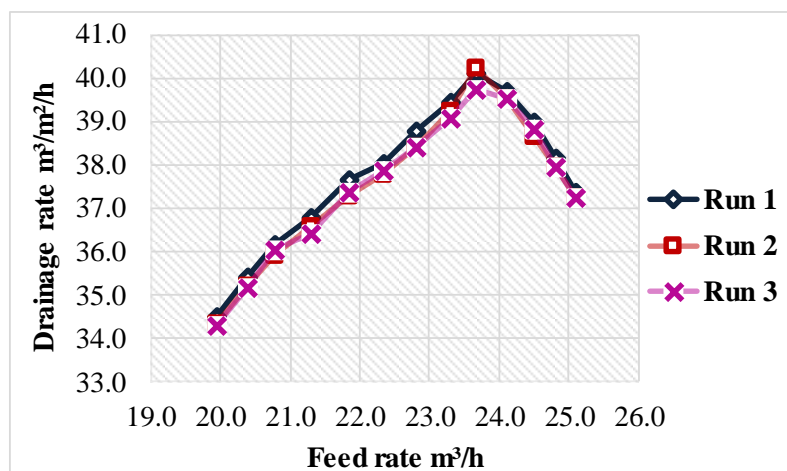


Figure 3-9: Ferrosilicon drainage rate reproducibility for 1x13 mm polyurethane panels at 1.9 kg/L slurry density

Table 3:5: Reproducibility assessment for 1x13 mm polyurethane panels on drainage rate at 1.9 kg/L slurry density

FeSi/Fe				
Feed rate (m ³ /h)	Drainage rate m ³ /m ² /h			SD
	Run 1	Run 2	Run 3	
19.9	34.5	34.3	34.3	0.12
20.4	35.4	35.2	35.2	0.13
20.8	36.2	35.9	36.0	0.13
21.3	36.8	36.6	36.4	0.19
21.8	37.6	37.3	37.4	0.19
22.3	38.0	37.8	37.9	0.12
22.8	38.8	38.4	38.4	0.22
23.3	39.5	39.2	39.1	0.19
23.7	40.1	40.2	39.8	0.24
24.1	39.7	39.6	39.5	0.08
24.5	39.0	38.7	38.8	0.17
24.8	38.2	38.0	38.0	0.12

3.6.2 Moisture and medium carryover reproducibility

Furthermore, selected experiments were repeated twice to assess the reproducibility of the results on the overflow stream. Consistency in results was assessed on the moisture and medium carryover to the oversize stream for the 1x13 mm screen panels by using the standard deviation (SD) as an indicator of reproducibility, as shown in Table 3:6 (a) and (b) below. Low SD values signify inconsequential differences among the results obtained while higher values indicate substantial variances. The standard deviation values obtained for both process responses were low signifying that the results obtained were reproducible under the same conditions. However, slight disparities were anticipated because of the errors presented through sample cutting.

Table 3:6: Results reproducibility on the overflow stream for percent moisture (a) and medium carryover (b) for 1x13 mm screen panels

Feed rate (m ³ /h)	% Moisture repeatability @2.70 kg/l			
	Run 1	Run 2	Run 3	SD
24.5	9.72	9.76	9.92	0.11
23.7	9.48	9.20	9.31	0.14
22.8	9.26	9.13	9.15	0.07
21.8	8.95	8.92	8.78	0.09
20.8	8.51	8.71	8.46	0.13
20.4	7.56	7.58	7.34	0.13

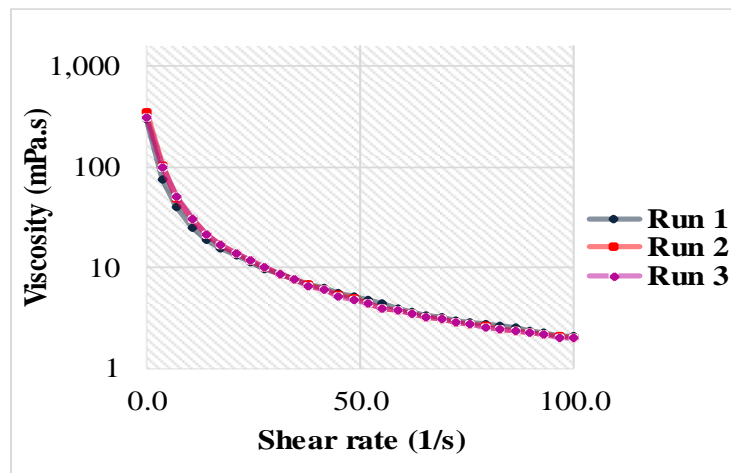
(a)

Feed rate (m ³ /h)	Media carryover repeatability (kg/t/m) @ 2.20 kg/l			
	Run 1	Run 2	Run 3	SD
24.5	19.32	19.89	19.67	0.29
23.7	14.33	14.81	14.82	0.28
22.8	13.80	13.73	13.52	0.14
21.8	12.38	12.44	12.48	0.05
20.8	11.74	11.77	11.90	0.09
20.4	11.43	10.96	10.82	0.32

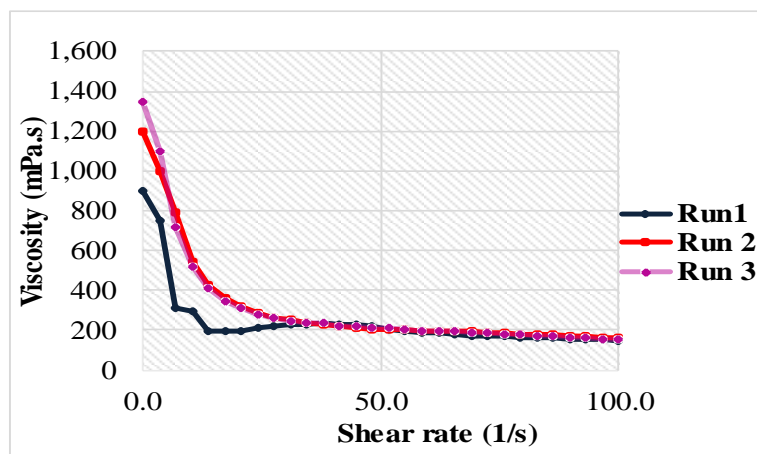
(b)

3.6.3 Viscosity reproducibility

Likewise, two replicates for the viscosity of both fresh and degraded ferrosilicon were done, as shown in Figure 3-10 (a) and (b) respectively. While there were minor disparities in the graphs obtained with repeats particularly at the low shear rate, it can, however, be deduced that the viscosity results were reproducible with minimal variances.



(a)



(b)

Figure 3-10: Viscosity reproducibility for fresh (a) and degraded (b) ferrosilicon

4 RESULTS AND DISCUSSIONS

4.1 Introduction

This chapter discusses the results obtained from the experimental work. The test work was conducted to show the effects of feed slurry density, volumetric flowrate, and slot sizes on the operation of the vibrating screen by measuring the medium drainage rate, percent moisture and medium carryover to the overflow stream. The results analysis also incorporated the influence of screen panel material on medium drainage rate, percent moisture and medium carryover. On the other hand, samples from the feed, underflow and overflow streams for ferrosilicon and iron ore were taken, dried, and processed for the establishment of particle size distribution. The PSDs for each stream were subjected to a Whitten fitting model to further show the influence of feed rate and slurry density on ferrosilicon recovery by extracting partition curve parameters i.e. cut size, the sharpness of separation and water split ratio.

The chapter is divided into five main subsections. Section 4.2 presents the characteristics of materials used in the thesis in terms of particle shapes. Section 4.3 deliberates on the effects of operating conditions on fresh ferrosilicon recovery regarding drainage rate, percent moisture and medium carryover. Section 4.4 discusses the possible contributors to the change in ferrosilicon behaviour on the screen surface. Presented in this section is the discussion on the effects of operating conditions on degraded ferrosilicon recovery. The subsections also discuss the effects of degradation and screen panel material on medium recovery in terms of drainage rate, moisture and medium bypass. Section 4.5 presents the influence of volumetric flowrate, slurry density and slot size variation on magnetite drainage rate and Section 4.6 presents a discussion on the consequences of slurry density and volumetric flowrate variation on Whitten model parameters for fresh and degraded ferrosilicon.

4.2 Material characterisation

Material characterisation in terms of particle shapes is key to any physical separation process. Before starting experimental runs, all materials were subjected to a scanning electron microscope for particle shapes and presence of cavities establishment.

Iron ore particles were elongated in shape with a few cavities or pores on the surface, as shown in Figure 4-1. Considering that slot apertures were used for medium separation; aperture pegging was probable, posing a substantial risk of passing elongated iron ore particles with a higher medium carryover to the oversize stream. While a horizontal screen surface was used to maximise on the effective slot size and reduce the possibility of slot

pegging, aperture pegging was seen on all the panels tested particularly at the feed end, as shown in Appendix A.

Bevilacqua & Ferrara (1994) established that the presence of cavities on the surface of ore material being separated acts as medium carriers to the oversize stream, as medium particles get entrapped in the pores of the ore material. Hence, the presence of pores on iron ore particles posed a significant threat of carrying medium particles to the oversize stream. On the other hand, Bowman et al. (2000) noted that cavities on ore particles act as sites for particle disintegration. This observation was consistent with Mikli et al. (2001). Further, Noble & Luttrell (2015) proved that particle disintegration of highly friable materials can be minimised by reducing the screen amplitude; hence, the screen amplitude was adjusted to 3.2 mm, as shown in Table 3:3. However, countable iron ore particles were observed in the underflow samples. Therefore, to minimise fine particles accumulation, iron ore was withdrawn after every experimental run and all the minus 1 mm particles sieved before conducting the next set of experiments.

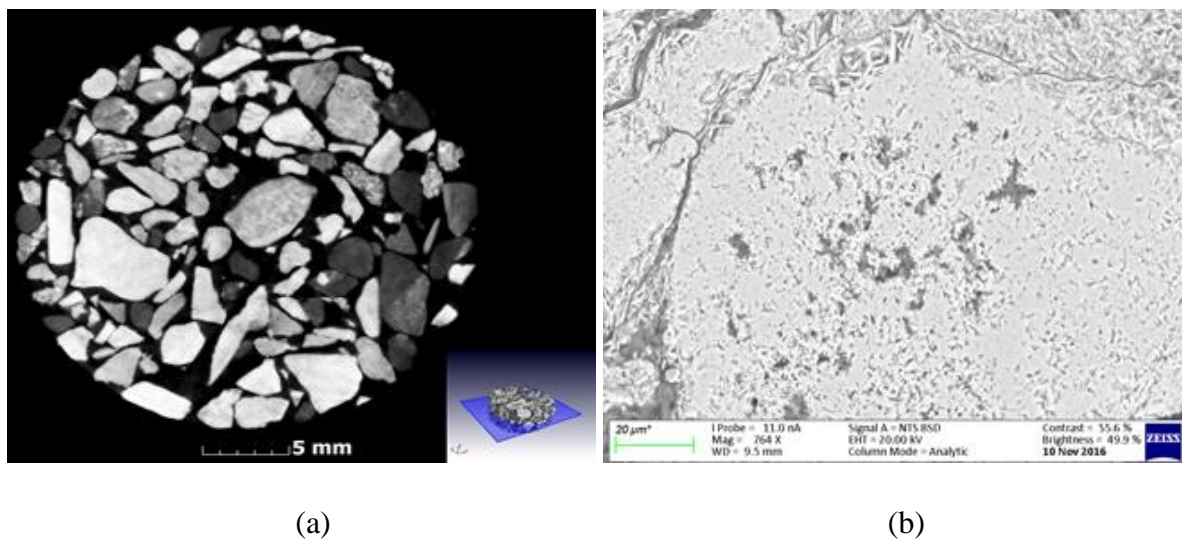
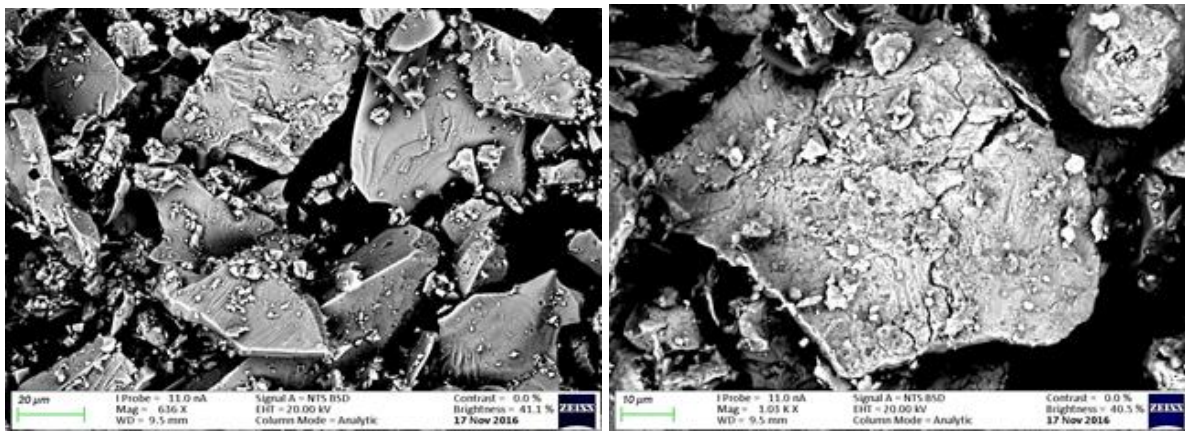
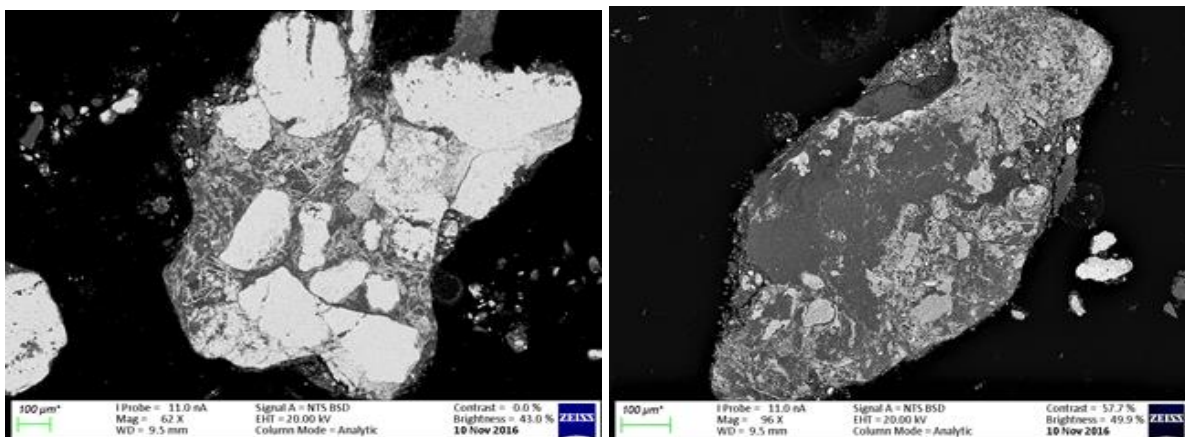


Figure 4-1: Particle shapes of iron ore (a) and cavities (pores) on iron ore surface (b)

Figure 4-2 (a) and (b) shows the particle shapes of ferrosilicon and magnetite respectively. Both materials were characterised by acicular and irregularly shaped particles, typical of milled ferrosilicon. From literature, it has been observed that irregularly shaped ferrosilicon particles have a larger surface area and hence, more susceptible to disintegration during normal plant operations (Collins et al. 1974; Williams & Kelsall 1992). Ferrosilicon particles were also characterised by the presence of crevices and sharp points, and Collins et al. (1974) established that these act as corrosion sites. Therefore, ferrosilicon disintegration and physiochemical surface oxidation were unavoidable with time.



(a)



(b)

Figure 4-2: Particle shapes of ferrosilicon (a) and magnetite (b)

4.3 Effects of operating conditions on ferrosilicon recovery

Presented in this section is the influence of volumetric flowrate, aperture size and feed density on the recovery of fresh ferrosilicon in terms of drainage rate, percent moisture and medium carryover. This section also discusses the influence of iron ore particles on ferrosilicon recovery by comparing the drainage rates for ferrosilicon only and ferrosilicon with iron ore particle.

Figure 4-3 for 1x13 mm polyurethane panels shows the influence of adding iron ore to ferrosilicon at 1:5 ore to medium ratio. It can be seen that the effect of iron ore particles on medium drainage rate was minimal due to probably the low amount of iron ore particles added to the circuit. Comparable results were obtained on the 0.63x8.8 mm and 0.8x8.8 mm screen panels, as shown in Appendix B.

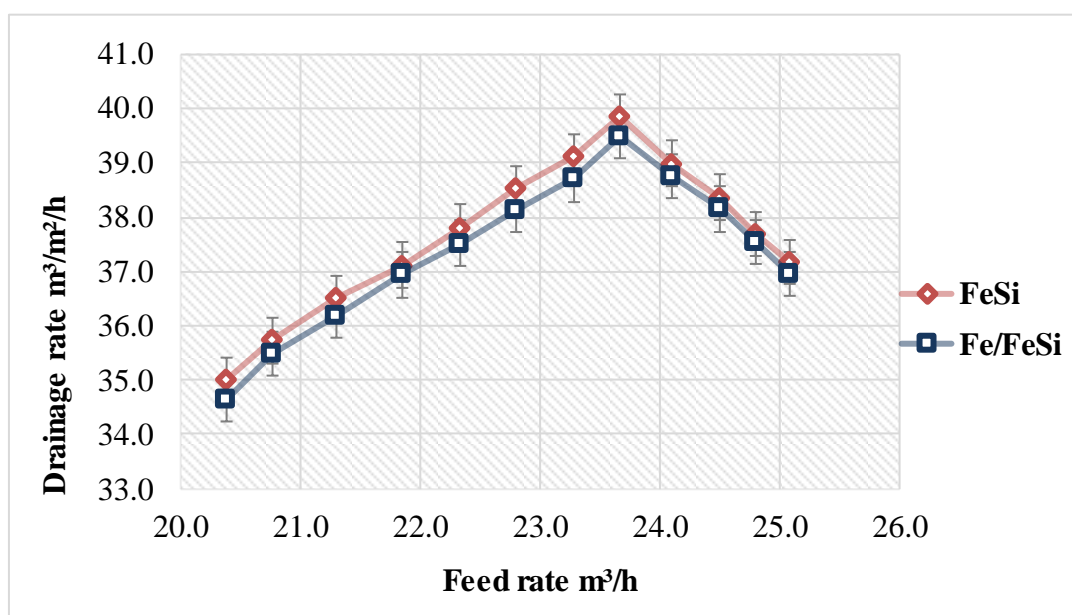


Figure 4-3: Effects of iron ore particles on ferrosilicon drainage rate for 1x13 mm polyurethane panels at 2.2 kg/L slurry density at 1:5 ore to medium ratio

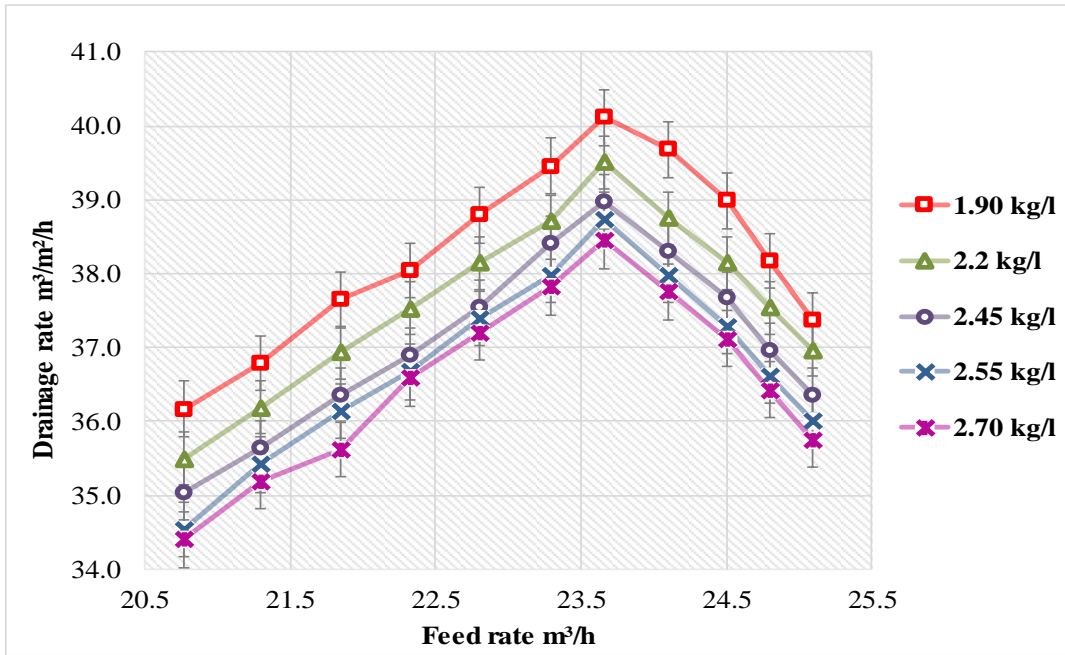
4.3.1 Effects of feed rate variation on ferrosilicon recovery

This section discusses the effects of varying volumetric flowrate on medium recovery regarding drainage rate, percent moisture and medium carryover to the overflow stream for fresh material.

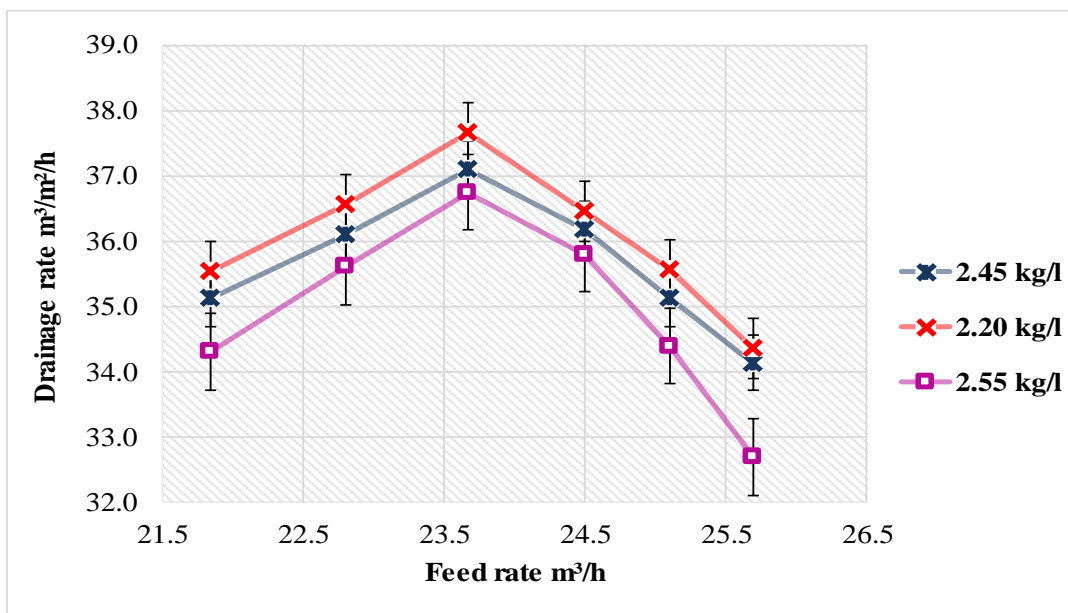
4.3.1.1 Effects of volumetric flowrate variation on drainage rate

The effects of feed rate variation on fresh ferrosilicon drainage rate assessment is shown in Figure 4-4 (a) for 1x13 mm screen panels. Increasing the volumetric flowrate from 20.8 – 23.7 m³/h of material onto the screen surface had a direct and positive influence on medium drainage rate. However, once a critical feed rate was reached, a further increase led to a decrease in medium drain rate. This trend was seen across all the panels tested on fresh ferrosilicon and iron, as shown in Figure 4-5 for 0.8x8.8 mm and Figure 4-4 (b) for 0.63x8.8 mm. Burke & Craig (2005) observed that increasing feed rate of material on to a screen leads to an increase in undersize recovery, but once a critical point is exceeded, screening rate reduces drastically. Hence, exceeding the capacity of a screen surface by overfeeding it leads to a reduction in medium drain rate as most of the particles are misdirected to the oversize stream due to reduced material residence time on the screen surface (Mbuyi et al. 2014). Therefore, the trend obtained was consistent with Burke & Craig (2005) and Mbuyi et al. (2014) results. The critical volumetric flowrate was the same for 1x13 mm, 0.63x8.8 mm and 0.8x8.8 mm polyurethane panels tested on fresh ferrosilicon at 23.7 m³/h showing that there were minimal variances in material handling capacity among the panels tested. However, this

was not expected as the panels had different open areas. While aperture pegging (shown in Appendix A) played a significant role in reducing medium drainage rate, the similarity in critical screen points among the panels tested can be attributed to the limits associated with the build-up of a bed of material on the screen surface and the permeability of that bed. Hence, the threshold is associated with the screen size. This is clearly a topic for further studies in order to elucidate the fundamental reasons behind this phenomenon.



(a)



(b)

Figure 4-4: Effects of volumetric flowrate on fresh ferrosilicon drainage rate for 1x13 mm (a) and 0.63x8.8 mm (b) polyurethane panels

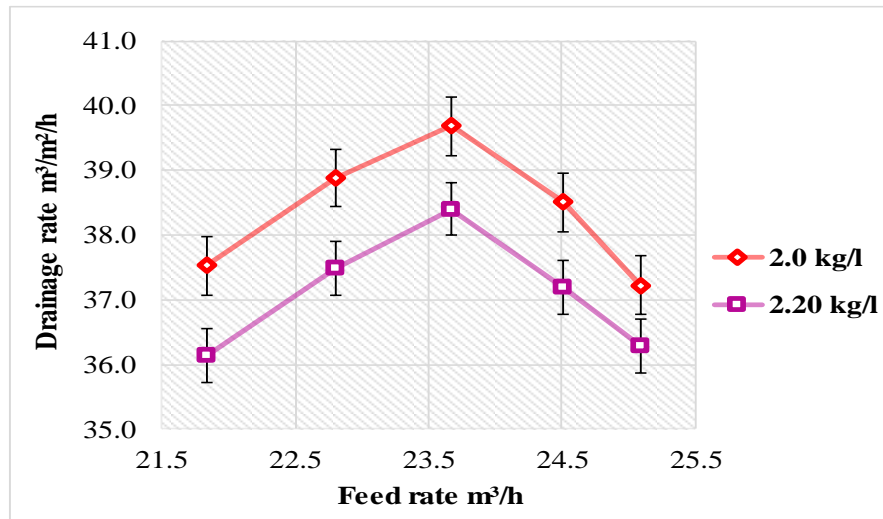
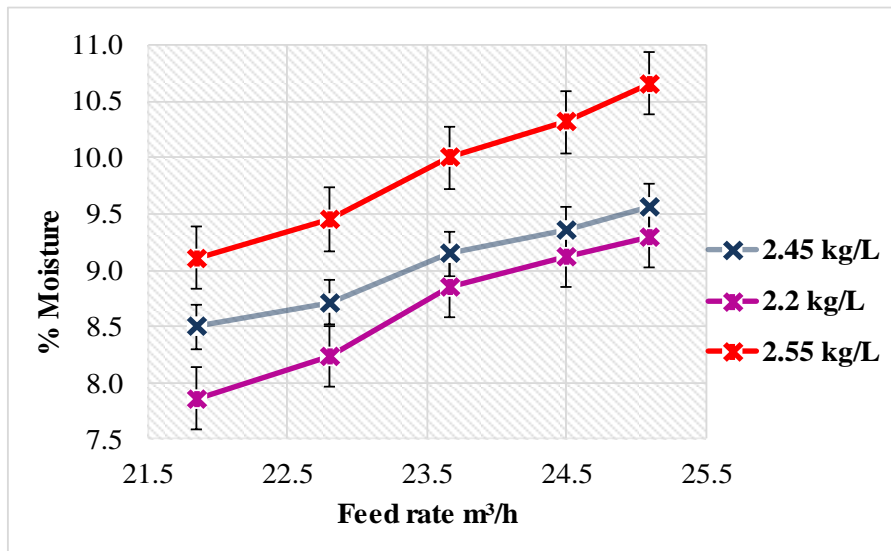


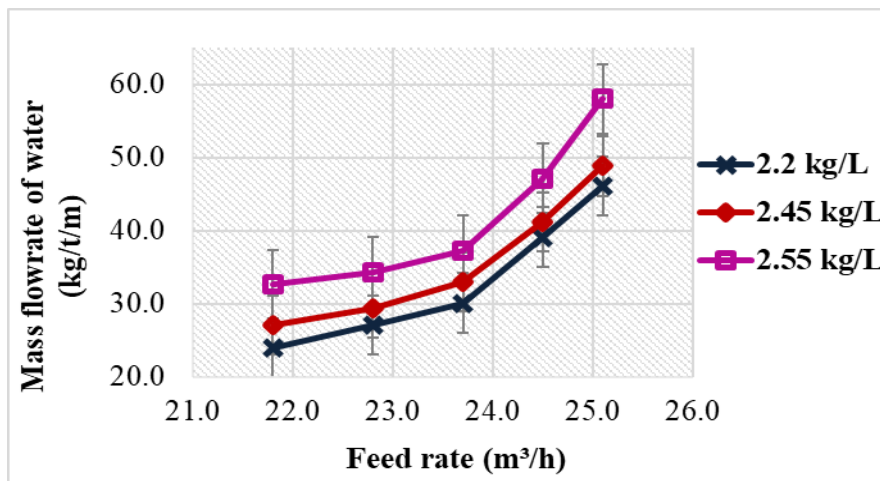
Figure 4-5: Effects of volumetric flowrate on fresh ferrosilicon drainage rate for 0.8x8.8 mm polyurethane panels

4.3.1.2 Effects of volumetric flowrate variation on moisture bypass

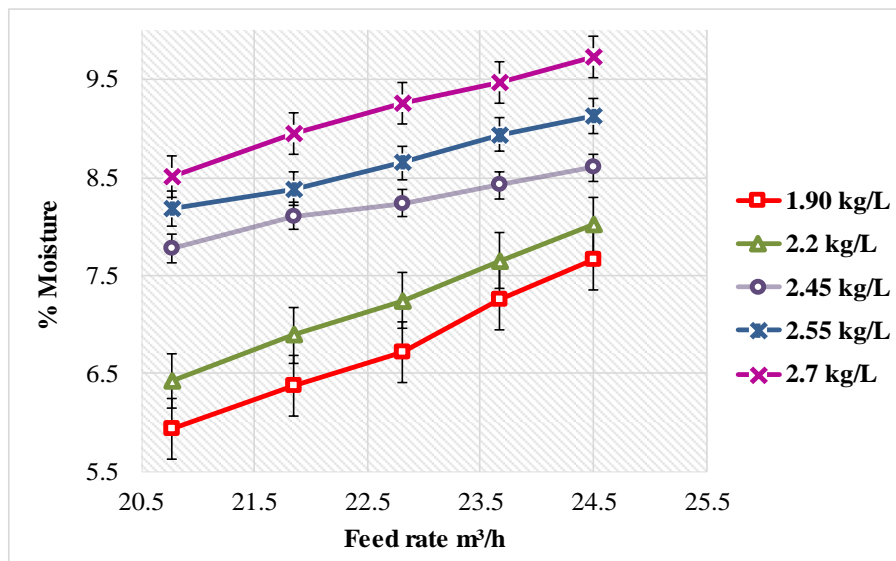
Moisture bypass is a parameter that is used to assess the performance of a separating surface. A higher value of water bypass is undesired since it is typically related to higher fine particles carryover to the overflow stream (Gupta & Yan 2006). Figure 4-6 (a) and (b) shows the influence of varying volumetric flowrate on the moisture bypass to the oversize stream for 0.63x8.8 mm screen panels. Increasing the volumetric flowrate from 21.8 – 25.1 m³/h led to an increase in percent moisture bypassing to the overflow stream with a sharp rise in the mass flowrate of water observed above 23.7 m³/h. A slight up-swing in percent moisture was seen between 22.8 – 23.7 m³/h and after which, a gradual increase with volumetric flowrate was observed. The rise in feed rate resulted in a drop-in material residence time on the screen surface. Hence, part of the water still trapped in the material bed bypassed to the overflow stream. The result obtained is consistent with Hudson et al. (1969) who established that increase in feed rate leads to an increase in material bed depth on the screen surface, thus, limiting the easy flow of water through the apertures. However, higher bed depth coupled with reduced material residence time due to increased volumetric flowrate led to an upswing in water bypass to the oversize stream. The result obtained by Hudson et al. (1969) was consistent with Sullivan et al. (1990) who established that material bed depth increases with feed rate. Hence, it can be postulated that increase in volumetric flowrate leads to an increase in moisture bypass due to a reduction in material residence time and increase in material bed depth on the screen surface. Related results obtained on 1x13 mm screen panels showed a slight up-swing in the moisture bypass beyond 22.8 m³/h, except 2.45 kg/L curve, as shown in Figure 4-6 (c).



(a)



(b)

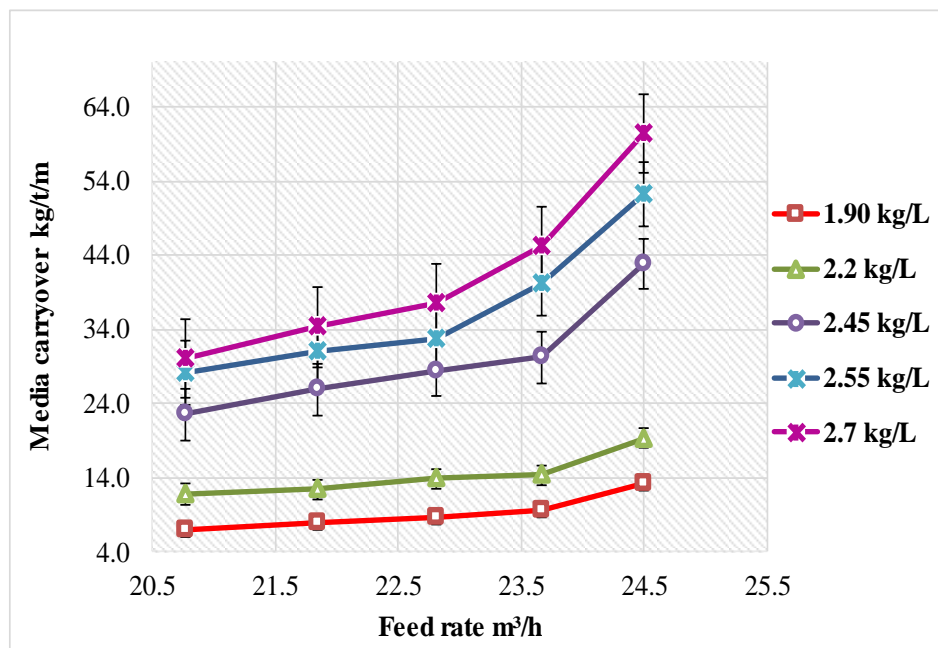


(c)

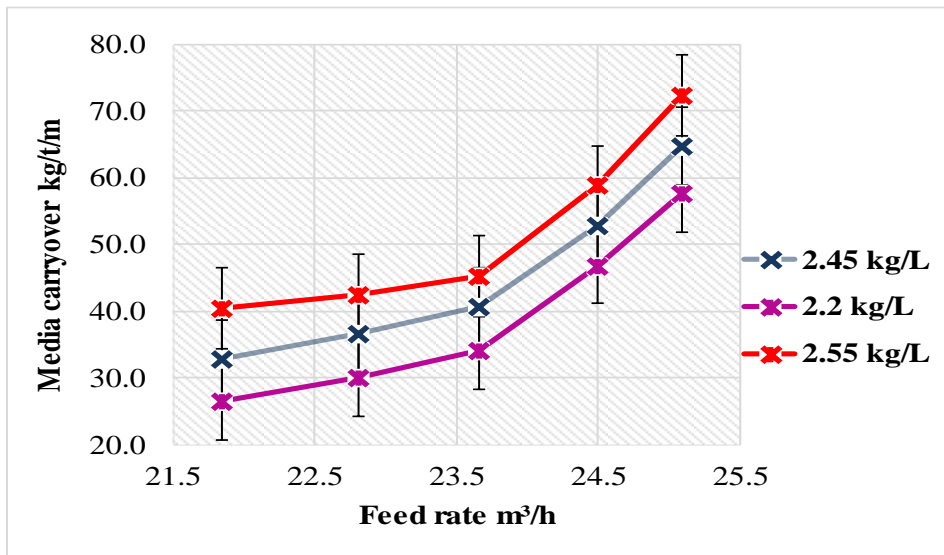
Figure 4-6: Effects of volumetric variation on moisture bypass for 0.63x8.8 mm (a) and (b) and 1x13 mm (c) polyurethane panels

4.3.1.3 Effects of feed rate variation on ferrosilicon carryover

Medium carryover to the overflow stream is used as an indicator of the efficiency of a separating surface. Higher amounts of fine particles reporting to the oversize indicate poor separation efficiency and lower amount shows efficient separation. An assessment of the effects of volumetric flowrate variation on medium carryover is provided in Figure 4-7 (a) for 1x13 mm screen panels. It can be seen that as the feed rate increased from 20.8 to 23.7 m³/h, there was an increase in medium carryover to the overflow stream. However, beyond the screen critical point of 23.7 m³/h, a sharp increase in medium carryover was observed, and more pronounced at slurry density above 2.2 kg/L. The result obtained was consistent with the drainage rate for the same set of panels with a drop in medium recovery observed with increase in volumetric flowrate beyond 23.7 m³/h, indicating a higher medium and water carryover to the oversize stream. Similar trend was observed on 0.63x8.8 mm screen panels with a sharp rise in medium carryover beyond 23.7 m³/h, as shown in Figure 4-7 (b). The result obtained is comparable with Mohanty (2003) who observed that increase in material feed rate leads to a reduction in retention time and passage rate of rightly oriented particles, thus, increasing fine particle carryover to the oversize stream.



(a)



(b)

Figure 4-7: Effects of feed rate variation on medium carryover for fresh ferrosilicon for 1x13 mm polyurethane panels

The interaction between moisture and medium carryover is shown in Figure 4-8 below for 0.63x8.8 mm polyurethane panels at 2.2 kg/L slurry density. It can be seen that an increase in moisture to the oversize stream led to an increase in medium carryover with an upswing beyond 8.9 % moisture.

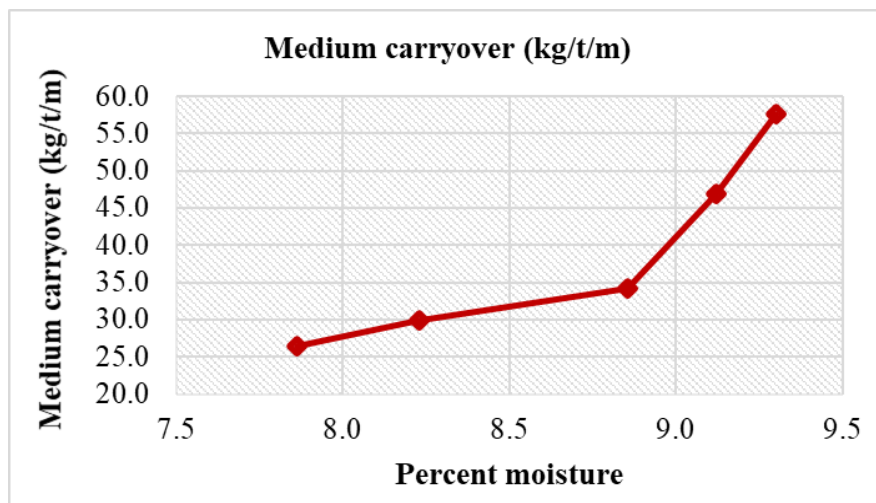


Figure 4-8: Interaction between percent moisture and medium carryover on fresh ferrosilicon for 0.63x8.8 mm polyurethane panels at 2.2 kg/L

4.3.1.4 Section summary

Increase in volumetric flowrate from 20.8 – 23.7 m³/h had a direct and positive influence on ferrosilicon drainage rate. However, beyond the screen critical point of 23.7 m³/h, a further increase in feed rate led to a decrease in ferrosilicon drain rate. Hence, it can be deduced that exceeding the capacity of a separating surface by overfeeding it leads to a reduction in

ferrosilicon recovery as most of the particles are misdirected to the oversize stream due to reduced material residence time on the screen surface. Hence, an increase in moisture and medium bypass to the overflow stream with an up-swing above the screen critical point. It is worth noting that the critical volumetric flowrate was the same for all the panels tested on fresh ferrosilicon at 23.7 m³/h.

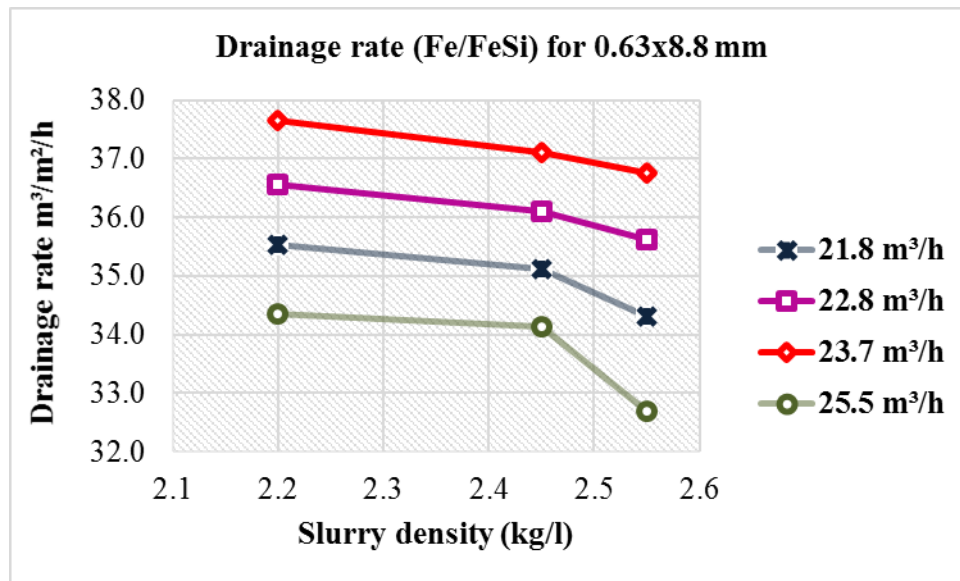
4.3.2 Influence of slurry density variation on ferrosilicon recovery

Valine et al. (2009) stated that the amount of water in a slurry play a significant role in the separation of fine particles. In wet screening, for instance, the percolation path of fine particulate matter through a bed of material is enhanced by the presence of a fluid. Hence, the quantity of the fluid in the feed is critical in the efficient separation of fine particles. This subsection presents a discussion on the effects of varying slurry density on drainage rate, percent moisture and medium carryover to the oversize stream.

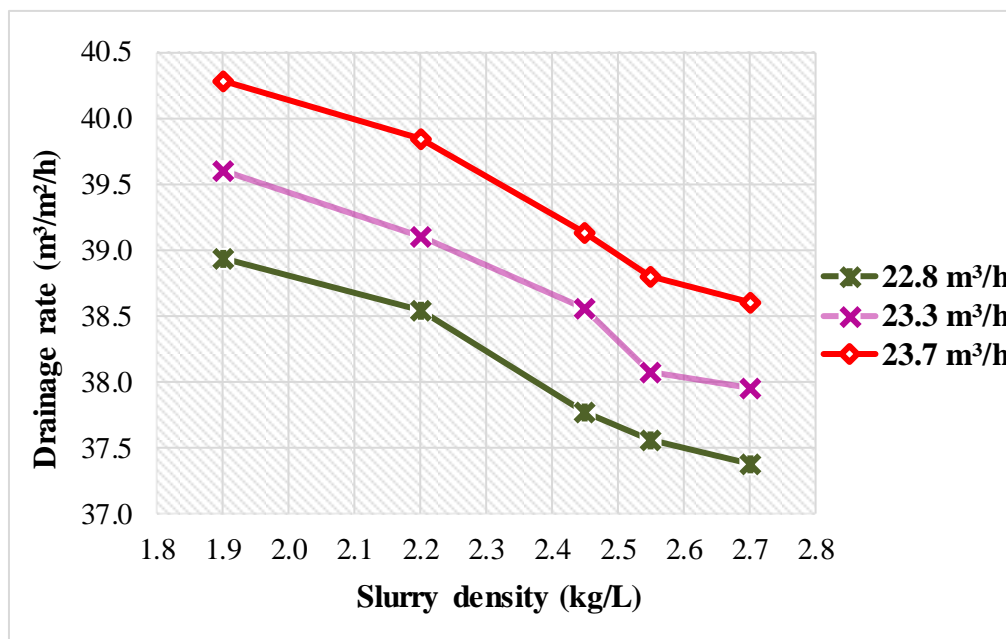
4.3.2.1 Influence of slurry density variation on drainage rate

Assessment of the effects of varying slurry density on the drainage rate of ferrosilicon is shown in Figure 4-9 (a) and (b). From Figure 4-9 (a) for 0.63x8.8 mm screen panels, it can be seen that as the slurry density increased from 2.2 to 2.55 kg/L, there was a gradual decrease in medium drainage rate up to 2.45 kg/L and thereafter, a sharp drop in medium drainage rate was observed. This point could be assumed to be the critical slurry density the screen could handle, and any further increase in solid concentration led to a sharp drop in the drainage rate of ferrosilicon particles. At higher slurry density, the particle bed of material on a separating surface builds up faster, thence, easily exceeding the capacity of a screen even at low volumetric flowrate. This result is consistent with Albuquerque et al. (2008) who established that increase in solid concentration from 10 - 20 v/v % leads to a reduction in the screening rate of undersize particles. A comparable trend obtained on 1x13 mm screen panels showed a gradual decrease in medium drain rate with a sharp decline between 2.2 – 2.45 kg/L as the density increased from 1.9 - 2.7 kg/L, as shown in Figure 4-9 (b). The significant decline in drainage rate between 2.2 – 2.45 kg/L can be attributed to the rise in the viscosity observed around the same slurry density range for fresh ferrosilicon. However, a further sharp drop in medium drainage rate was seen between 2.45 – 2.55 kg/L and after that, a point was reached where a further increase in the slurry density had minimal influence on medium drainage rate. Hence, the rate of decrease in medium drainage rate with density slows between 2.55 – 2.7 kg/L. This point could be due to the screen reaching its saturation point such that any further increase in slurry density led to minimal medium loss even if the loss was still incurred. The

result obtained is comparable with O'Brien & Firth (2015) who showed that an increase in slurry density leads to a reduction in medium drainage.



(a)



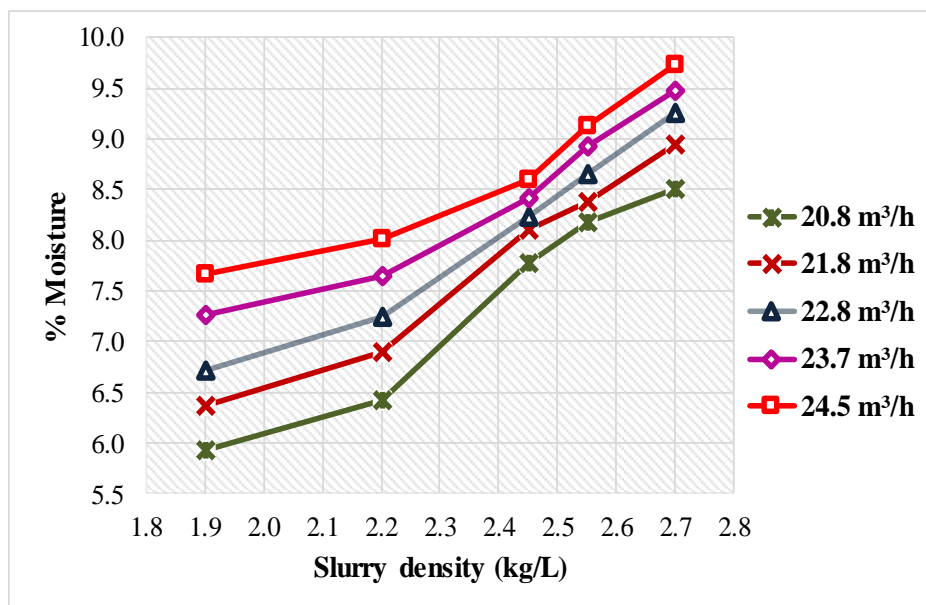
(b)

Figure 4-9: Effects of slurry density variation on fresh ferrosilicon drainage rate for 0.63x8.8 mm (a) and 1x13 mm (b) polyurethane panels

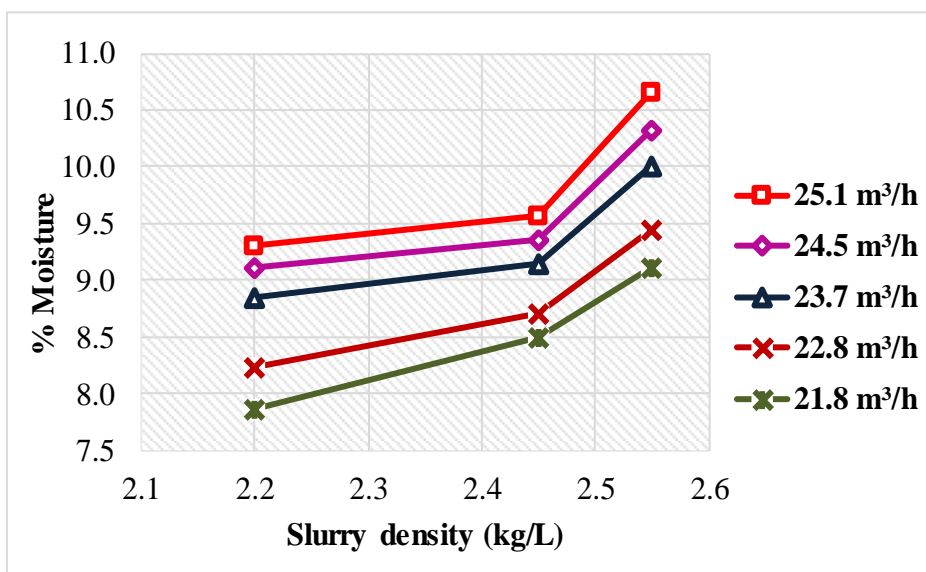
4.3.2.2 Influence of slurry density variation on moisture bypass

Figure 4-10 (a) and (b) shows the effects of varying slurry density on the moisture bypass to the oversize stream. Figure 4-10 (a) for 1x13 mm screen panels indicate that as the slurry density increased from 1.9 to 2.7 kg/L, there was a corresponding increase in water bypassing

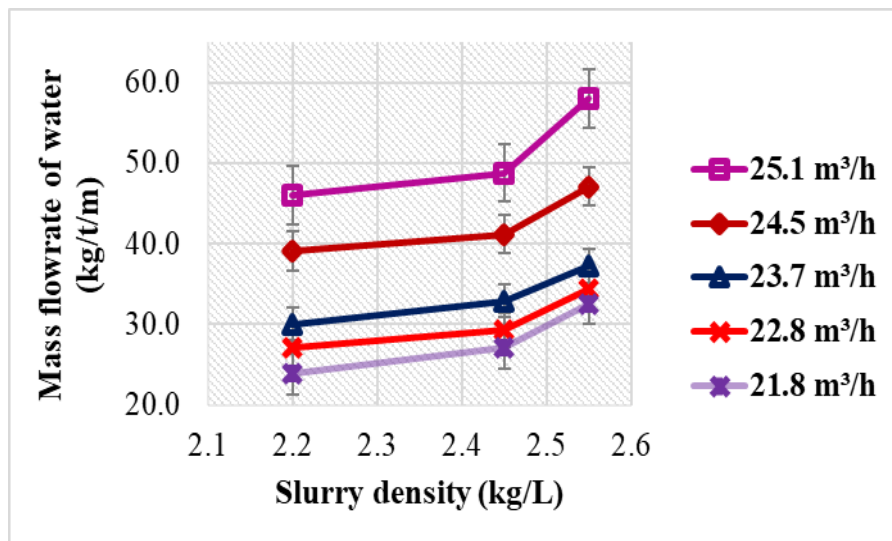
the screen surface, with a sharp increase observed between 2.2 – 2.45 kg/L. As the density increased beyond 2.45 kg/L, a significant increase in moisture bypass to the overflow stream was observed. The result was consistent with the drainage rate obtained on the same set of panels with a sharp drop in medium drainage rate observed between 2.2 – 2.45 kg/L, postulating a sharp increase in moisture and medium bypass to the overflow. Equivalent results obtained on the 0.63x8.8 mm screen panels in Figure 4-10 (b) and (c) show a positive linear relationship between slurry density and percent moisture (b), and mass flowrate of water (b) between 2.2 - 2.45 kg/L, and afterwards, a sharp rise in water bypass was observed. The result was consistent with the drainage rate obtained on the same set of panels with a marked drop in medium drainage rate observed beyond 2.45 kg/L slurry density.



(a)



(b)



(c)

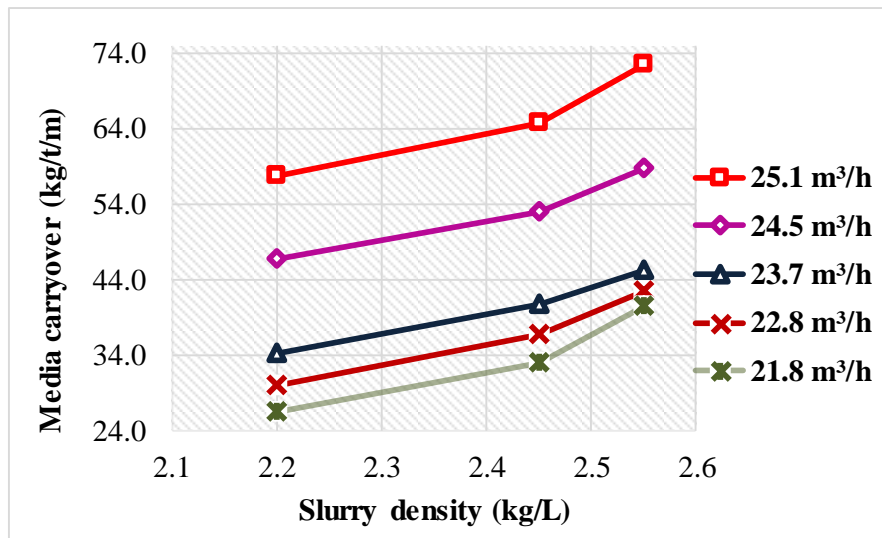
Figure 4-10: Effects of slurry density variation on moisture bypass for 1x13 mm (a) and 0.63x8.8 mm (b), and (c) polyurethane panels

From the observations made, it can be hypothesised that the fraction of water in the feed is proportional to the efficiency of a screen surface. As water permeates through the bed of material, it carries medium particles with it (Valine et al. 2009). Considering that water has comparatively the lowest viscosity, its passage rate is comparatively high. Thence, as the water percolates through the screen apertures carrying along medium particles, part of the medium is held up in the percolation trail, creating a thick bed of material. Hence, a higher water and medium bypass to the oversize stream with increase in slurry density.

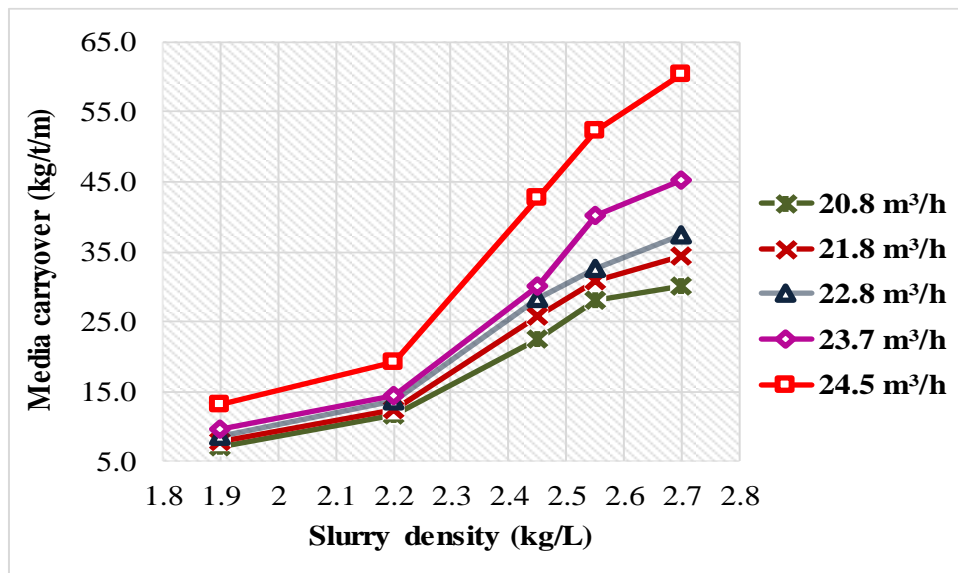
4.3.2.3 Effects of slurry density variation on medium carryover

Assessment of the consequences of slurry density variation on medium carryover is shown in Figure 4-11 (a) for 0.63x8.8 mm and (b) for 1x13 mm screen panels. As was the case with percent moisture, the amount of medium bypassing the separating surface increased gradually with slurry density up to 2.45 kg/L and further than that, there was a sharp increase in medium carryover and more pronounced at volumetric flowrate above 23.7 m³/h, as shown in Figure 4-11 (a) below for 0.63x8.8 mm screen panels. Comparable results obtained on 1x13 mm screen panels showed a gradual increase in medium carryover between 1.9 - 2.2 kg/L with a significant increase between 2.2 - 2.55 kg/L. However, a saturation point was reached between 2.55 - 2.7 kg/L such that any further increase in slurry density led to a gradual increase in medium carryover. It can be postulated that increase in slurry density reduces the porosity of the particle bed on the screen surface to the extent that only a small amount of water with fine particles can pass through the screen holes. This qualifies the sharp increase in medium loss to the oversize stream between 2.2 - 2.55 kg/L for 1x13 mm and between 2.45 -

2.55 kg/L for 0.63x8.8 mm. Past the screen critical point, most of the medium will sidestep to the overflow stream.



(a)



(b)

Figure 4-11: Effects of slurry density variation on fresh ferrosilicon carryover for 0.63x8.8 mm (a) and 1x13 mm (b) polyurethane panels

Furthermore, it can be suggested that as the slurry density increased, there was an increase in slurry viscosity due to a higher amount of medium coagulation onto iron ore particles. Thus, a point was reached where most of the medium particles were glued to the iron ore particles, and any further increase in slurry density led to more medium carryover. Hence, the graphs broadened at a slurry density above 2.2 kg/L for 1x13 mm screen panels. Bevilacqua & Ferrara (1994) observed that increase in slurry density leads to an increase in draining time. Thus, an increase in slurry density and volumetric flowrate leads to higher moisture and

medium carryover to the overflow stream due to a thick bed of material and reduced residence time for passage.

4.3.2.4 Section summary

Increase in slurry density from 1.9 to 2.7 kg/L led to a decrease in medium drainage rate and an increase in water and medium bypass to the overflow stream, with a significant decline in drainage rate observed between 2.2 – 2.45 kg/L, postulating a sharp increase in moisture and medium bypass to the oversize stream. This point could be assumed to be the critical slurry density the screen could handle, and any further increase in solid concentration led to a sharp drop in the recovery of ferrosilicon. However, a further sharp drop in medium drainage rate was observed between 2.45 – 2.55 kg/L and thereafter, a point was reached where a further increase in the slurry density had minimal further influence on medium drainage rate. Hence, a slight upward sagging in medium drainage rate and a gradual increase in moisture and medium carryover observed between 2.55 – 2.7 kg/L. This point could be due to the screen reaching its saturation point such that any further increase in slurry density led to minimal further medium loss even if the loss was still incurred. It can be postulated that the increase in slurry density reduces the porosity of the particle bed on the screen surface to the extent that only a small amount of water with medium particles can pass through the screen holes. Thus, a point was reached where most of the water had passed through the screen and any remaining medium particles were glued to the iron ore particles and bypassed to the oversize stream.

4.3.3 Effects of aperture size variation on ferrosilicon recovery

This subsection discusses the influence of aperture size variation on drainage rate, percent moisture and medium carryover. In this case, the 1x13 mm, 0.8x8.8 mm and 0.63x8.8 mm screen panels were used in the assessment at 2.2 kg/L slurry density.

4.3.3.1 Influence of aperture size variation on ferrosilicon drainage rate

The effects of aperture size variation on ferrosilicon drainage rate for fresh material shown in Figure 4-12 illustrates that as the aperture size increased from 0.63x8.8 mm to 1x13 mm, there was a corresponding volumetric increase in drainage rate of about 1.4 - 1.9 m³/m²/h. The increase in medium drainage rate with aperture size can be attributed to a reduction in material build up on the screen surface due to the increase in aperture size. Considering that the percent open area for 1x13 mm panels was lower than that of 0.63x8.8 mm panels by 3.26 %, higher drainage rate was expected on the 0.63x8.8 mm screen panels instead. Hence, from the results obtained, it can be settled that medium drainage rate is not entirely dictated by the percent open area of the screen panels.

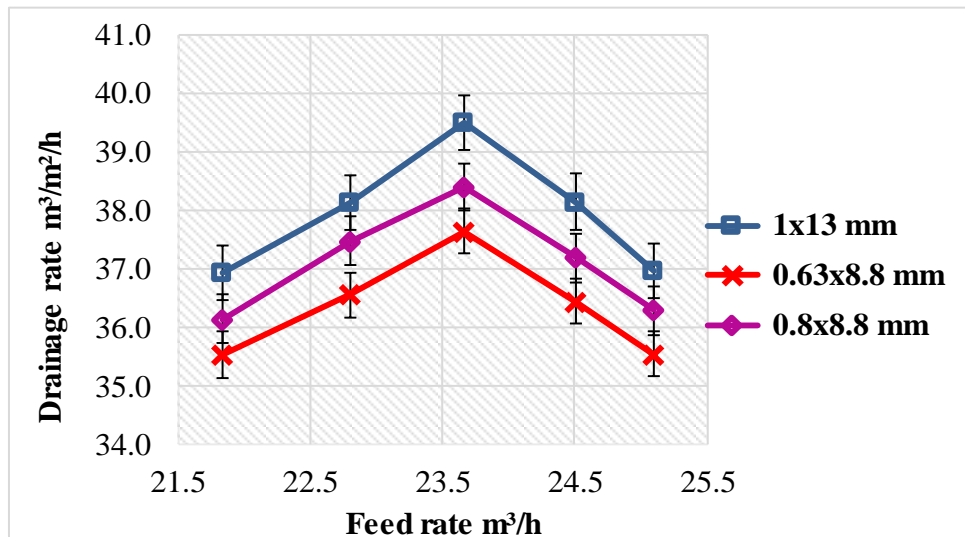


Figure 4-12: Influence of aperture size variation on fresh ferrosilicon drainage rate at 2.2 kg/L slurry density

4.3.3.2 Influence of aperture size variation on moisture and medium carryover

Water bypass to the overflow stream escalated sharply from 0.6 – 0.8 w/w% with decrease in slot size from 1x13 mm to 0.8x8.8 mm, and between 0.8x8.8 mm to 0.63x8.8 mm, a gradual increase of about 0.3 – 0.4 w/w% was seen, as shown in Figure 4-13 below. The increase in moisture bypass can be attributed to material build-up on the screen surface with decrease in aperture size to an extent that the effective aperture size is reduced, hence, more fines and moisture bypass to the overflow stream.

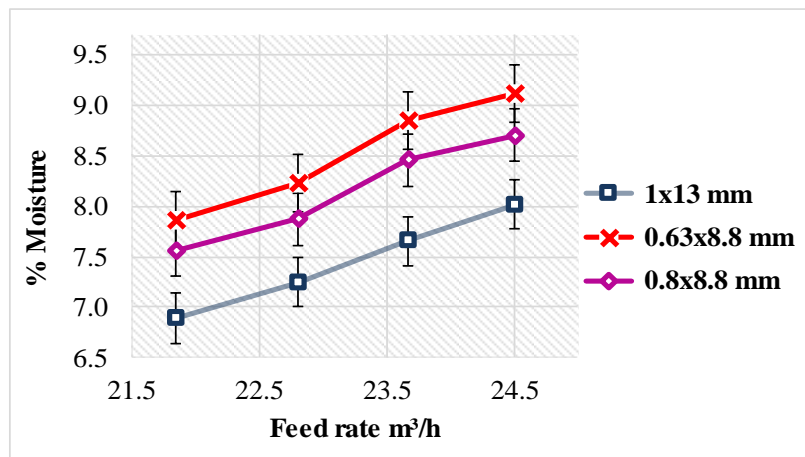


Figure 4-13: Influence of aperture size variation on moisture bypass for fresh ferrosilicon at 2.2 kg/L slurry density

Figure 4-14 shows the influence of aperture size variation on medium carryover to the overflow stream. As the aperture size increased from 0.63x8.8 to 0.8x8.8 mm, there was a gradual decrease in medium carryover of about 3.6 – 5.1 kg/t/m. However, a sharp decrease of about 10.4 – 15.4 kg/t/m in medium carryover to the overflow stream was seen between

0.8x8.8 mm and 1x13 mm and more pronounced at volumetric flowrate above 23.7 m³/h. The decline in medium carryover can be credited to the increase in screen handling capacity with aperture size, hence, able to recover more medium with bigger aperture sizes. Similar result was obtained by Aplan et al. (2003) who established that decrease in screen aperture size leads to a reduction in the screen's ability to handle a specific tonnage of feed material, thus, resulting in an increase in undersize carryover to the oversize stream.

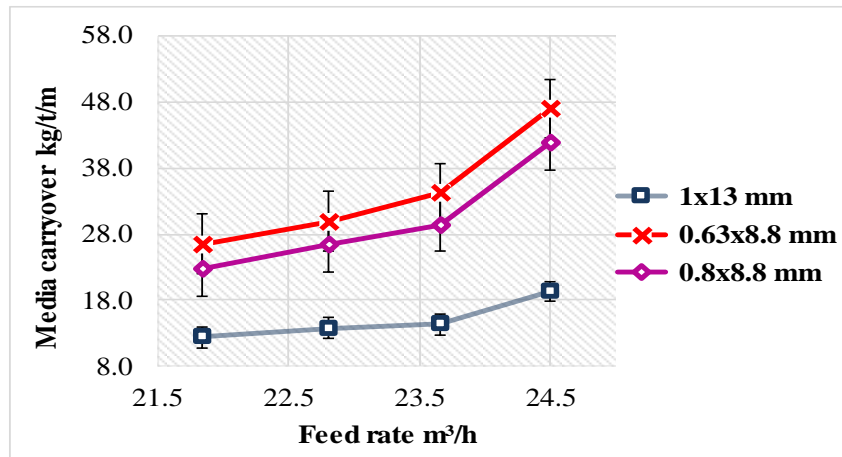


Figure 4-14: Influence of screen aperture size on medium carryover for fresh material at 2.2 kg/L slurry density

4.3.3.4 Section summary

Increase in aperture size from 0.63x8.8 mm to 1x13 mm led to an increase in medium drainage rate of about 1.4 - 1.9 m³/m²/h with a reduction in water and medium carryover of about 1.0 - 1.2 w/w% and 14.1 - 20.2 kg/t/m respectively, depending on the volumetric flowrate. The increase in medium drain rate with aperture size can be attributed to a reduction in material build up on the screen surface. Bearing in mind that the percent open area for 1x13 mm panels was lower than that of 0.63x8.8 mm panels by 3.26 %, higher medium drainage rate was expected on the 0.63x8.8 mm screen panels. However, the 1x13 mm screen panels drained more medium with increase in volumetric flowrate and slurry density. Hence, it can be concluded that open area does not entirely dictate medium drainage rate.

4.3.4 Influence of slot width on fresh ferrosilicon recovery

The shape of a slot aperture is defined by two key dimensions, the length and width. While both parameters play a vital role in the separation of medium particles, presented in this section is the assessment of the influence of slot width on drainage rate, percent moisture and medium carryover using the 0.63x8.8 mm and 0.8x8.8 mm screen panels. The slot apertures were oriented with the flow direction of the material on the screen surface.

4.3.4.1 Influence of slot width on medium drainage rate

Shown in Figure 4-15 below is the assessment of the influence of slot width on medium drainage rate. As the slot width increased from 0.63 to 0.8 mm, there was a corresponding increase in medium drainage rate of about 0.5 – 0.9 m³/m²/h with feed rate. Higher medium drainage rate can be attributed to the increase in the load handling capacity of the screen surface with slot width. The result obtained is consistent with Aplan et al. (2003) who established that increasing screen width of a wedge wire while maintaining its length leads to an increase in screen capacity and thus, higher fine particles screening rate.

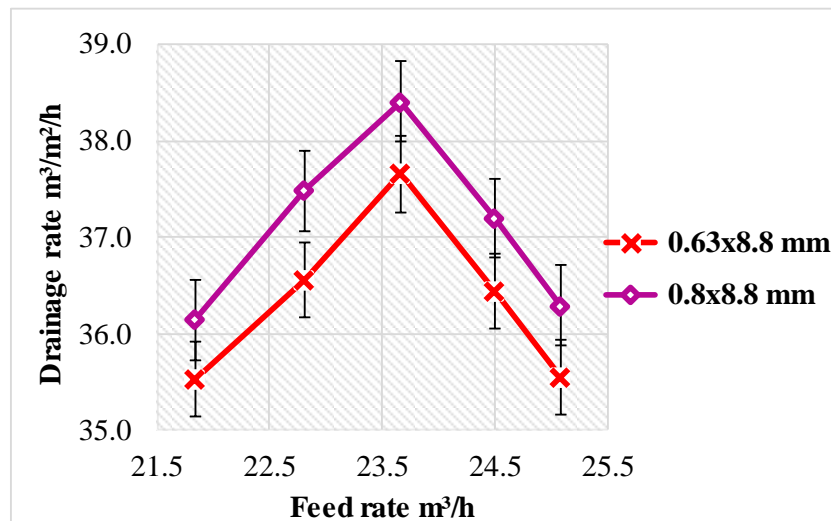


Figure 4-15: Influence of slot width on fresh ferrosilicon drainage rate at 2.2 kg/L slurry density

4.3.4.2 Influence of slot width on moisture bypass

Figure 4-16 shows the influence of slot width on moisture bypass to the overflow stream. It can be seen that as the slot width increased from 0.63 to 0.8 mm, there was a gradual decrease of about 0.2 – 0.5 w/w% in moisture bypass. However, the influence of slot width was more pronounced at volumetric flowrate higher than 22.8 m³/h. As the slot width increased, there was a formation of a thin material bed on the screen surface due to increased flow of water through the bed of material, thus, reduced moisture bypass.

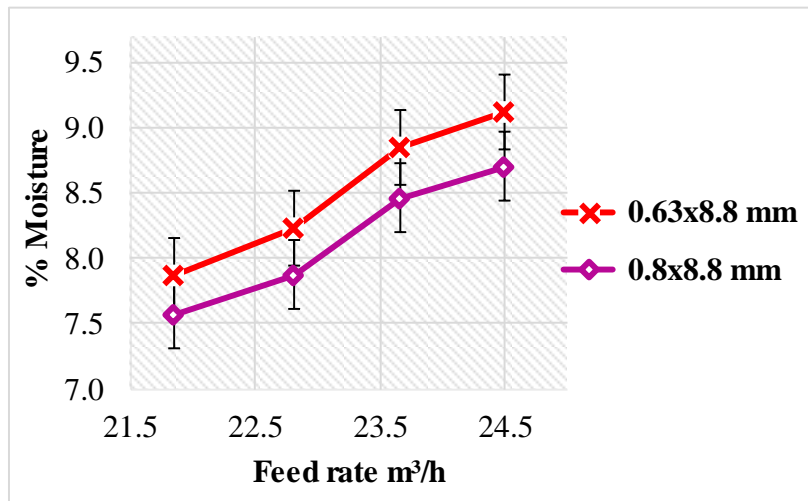


Figure 4-16: Influence of slot width on moisture bypass for fresh ferrosilicon at 2.2 kg/L slurry density

4.3.4.3 Influence of slot width on medium carryover

Increase in slot width from 0.63 to 0.8 mm led to a decrease in medium carryover of about 3.5 – 5.1 kg/t/m, as shown in Figure 4-17 below. At finer slot width, material bed depth tends to build up on the screen surface resulting in reduced effective slot size for separation. This led to more medium carryover to the overflow stream. However, the influence of slot width variation on medium carryover was more pronounced at volumetric flowrate above 23.7 m³/h. Thus, the smaller the slot width, the more fines and moisture carryover to the overflow stream. It should be noted that the moisture and medium carryover were seen to be more pronounced at different volumetric flowrates.

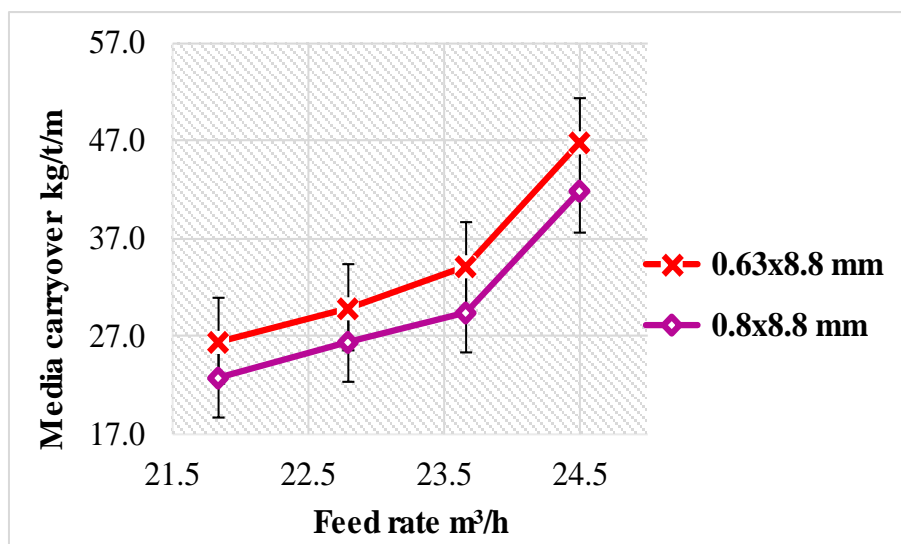


Figure 4-17: Influence of slot width on medium carryover at 2.2 kg/L slurry density

4.3.4.4 Section summary

Slot width increase from 0.63 – 0.8 mm led to an increase in medium drainage rate of about 0.5 – 0.9 m³/m²/h with a decrease in moisture and medium carryover of about 0.2 – 0.5 w/w% and 3.5 – 7 kg/t/m respectively, depending on the feed rate. Higher medium drain rate can be attributed to the increase in the load handling capacity of the screen surface with slot width. As the slot width increased, there was a formation of a thin bed of material on the screen surface due to the increase in water flow through the bed of material, thus, reduced moisture and medium bypass to the oversize stream. Therefore, it can be construed that the smaller the slot width, the more fines and moisture carryover to the overflow stream.

4.4 Ferrosilicon degradation

After one month of experimental runs on ferrosilicon and iron ore, a change in medium behaviour was observed on the screen surface as well as in the storage buckets. The medium became very viscous such that it could not be pumped easily on to the screen surface without adding iron ore particles, as the pump kept cavitating in the absence of iron ore. A rise in the material bed depth on the screen surface was also observed regardless of the volumetric flowrate, feed slurry density and slot size used, with the exception of rubber panels. On the other hand, air bubbles were seen on top of the material with a gradual rise in the slurry level whilst in the storage buckets. From literature, it has been observed that the change in ferrosilicon behaviour arise due to the presence of slimes from ore material, solid concentration, shear rate, oxidation of medium surface, particle size and shape of medium (Napier-Munn & Scott 1990; Poletto & Joseph. 1995; Alturki et al. 2013; Mangesana et al. 2008; Olhero & Ferreira 2004; Luckham & Ukeje 1999; Amiri et al. 2010). All these factors have been known to influence the medium viscosity and stability, thus, negatively affecting the separation process. Hence, experiments were conducted on this material to assess the effects of volumetric flowrate, slurry density and aperture size on the recovery of degraded material. An assessment was also done on the influence of degradation on medium recovery by comparing the results for the fresh and degraded material.

4.4.1 Possible causes of ferrosilicon degradation

Presented in this section are the possible causes of the change in medium behaviour on the screen surface.

4.4.1.1 Slime contamination

Slime contamination is a condition that arises due to the presence of ore slimes in the heavy medium. Slimes are basically fines of the ore material being separated and are usually finer

than 10 μm (Grobler et al. 2002). During the addition of ore material to a cyclone in a dense medium circuit, the adhered slimes go into suspension and alter the medium rheology properties (i.e. viscosity and stability). To minimise this effect, most plants use pre-washing screens to get rid of the fine particles. Nevertheless, during normal plant operations, it is unavoidable that some fraction of the fine material will still be present in the heavy medium. The presence of these slimes has been known to have a positive influence on medium stability and adverse effect on viscosity. One reason is that ore slimes have a lower density compared to that of ferrosilicon, hence, a slime contaminated medium will necessitate a higher concentration of solids to attain the same slurry density as the fresh medium (Napier-Munn & Scott 1990). This, in turn, leads to a higher medium resistance to flow in the cyclone and on the drain and rinse vibrating screen surface (Grobler et al. 2002). Considering that no pre-washing was done on the iron ore used due to the absence of a pre-washing screen, the change in ferrosilicon behaviour due to adhered slimes was probable with time. Table 4:1 below shows the chemical analysis comparison for fresh and slime contaminated ferrosilicon, and it can be seen that there was an increase in iron oxide of about 16.99 w/w% due to the presence of iron ore slimes.

Table 4:1: Elemental analysis of fresh and slime contaminated ferrosilicon

	Fe ₂ O ₃	Mn ₃ O ₄	TiO ₂	CaO	K ₂ O	P ₂ O ₅	SiO ₂	Al ₂ O ₃	MgO	Na ₂ O
Fresh (wt%)	72.97	0.97	0.06	bdl	bdl	0.04	30.90	0.73	0.02	bdl
Contaminated (wt%)	89.96	0.22	2.81	0.19	0.07	1.33	8.53	2.07	0.70	bdl
	16.99	-0.75	2.75	0.19	0.07	1.29	-22.37	1.35	0.68	

On the other hand, Bowman et al. (2000) established that cavities on ore particles act as particle disintegration points. Similar observations were made by Mikli et al. (2001). Hence, the cavities noticed on the iron ore particles contributed to slime accumulation. While measures were put in place to remove the minus 1 mm iron ore particles through sieving, the iron ore slimes that went into solution with the medium could not be removed. Thus, the presence of iron ore fines contributed to a change in medium behaviour due to their adverse effects on medium rheology properties.

Figure 4-18 shows the viscosity comparison between fresh and slime contaminated ferrosilicon at low shear rate. At slurry densities as low as 2.0 kg/L, slime contaminated ferrosilicon had a viscosity of about 3 - 5 times that of the fresh material. However, the discrepancy increased rapidly with further increase in slurry density and shear rate as shown in Appendix C, with a sharp rise in viscosity seen above 2.2 kg/L slurry density for the contaminated material. The difference in viscosity can be attributed to the formation of

aggregates within a slurry due to strong cohesive forces created by the presence of iron ore slimes, thus, resulting in a highly viscous slurry (Napier-Munn & Scott 1990).

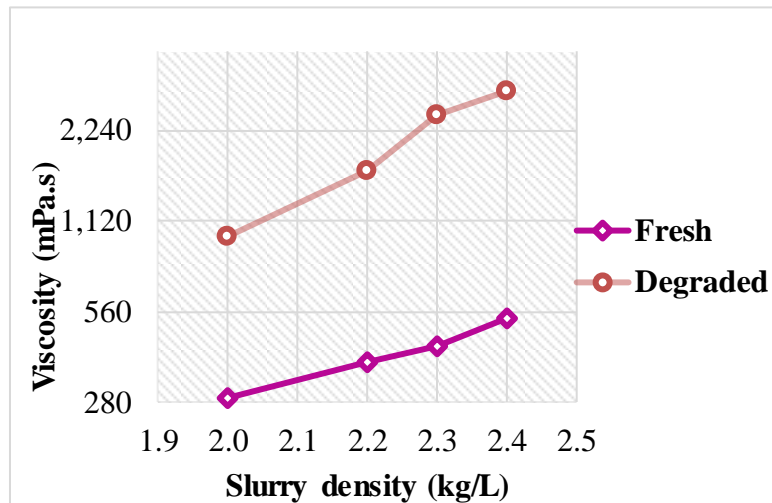


Figure 4-18: Viscosity comparison for fresh and contaminated ferrosilicon at 3.45 S^{-1} shear rate

It is worth noting that an ideal heavy medium has low apparent viscosity to maximise on pump and separation efficiencies (Shi & Napier-Munn 2002; Grobler et al. 2002; Luckham & Ukeje 1999). Overly viscous ferrosilicon is undesirable particularly on a screen surface due to a decrease in particle settling rate, thus, reducing the contact times that the medium makes with the screen surface for passage.

4.4.1.2 Solid concentration

Solid concentration represents the amount of solid particles in a slurry. Figure 4-19 shows the effect of solid concentration on apparent viscosity with shear rate for degraded ferrosilicon. It can be seen that as the solid concentration increased from 2.0 to 2.4 kg/L, there was a corresponding increase in the viscosity of the material. An initial rise was observed between 2.2 - 2.3 kg/L, and after that, the viscosity rose sharply with further increase in solid concentration. The accustomed rapid increase in the viscosity of the material with increase in slurry density, typically shown as an exponential function of percent solids, means that separation processes running at high slurry density are repeatedly affected by a minor upsurge in the viscosity (Napier-Munn & Scott 1990).

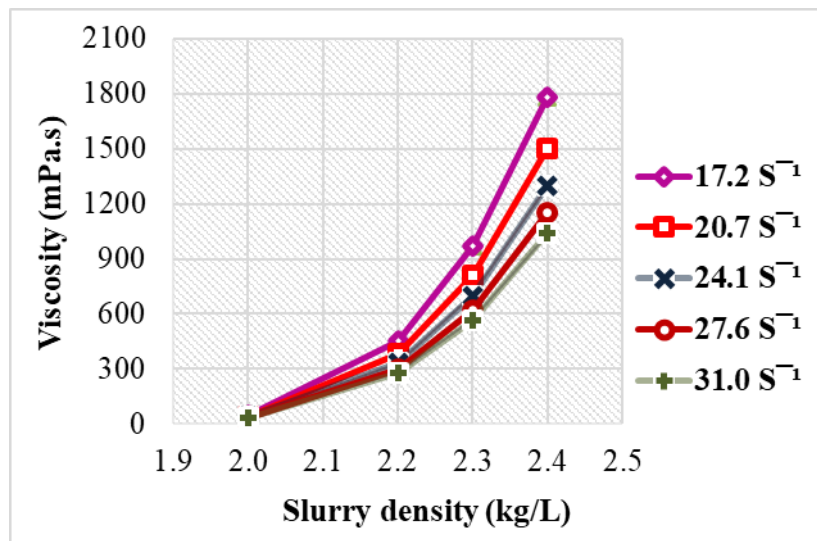


Figure 4-19: Viscosity variation with slurry density for degraded ferrosilicon

Figure 4-20 below shows the variation of viscosity with increase in slurry density from 2.0 to 2.5 kg/L for fresh ferrosilicon. An initial rise in viscosity was observed from 2.0 to 2.3 kg/L slurry density with some stability between 2.3 – 2.4 kg/L. However, the viscosity increased sharply with further increase in slurry density beyond 2.4 kg/L. The rise in viscosity beyond 2.4 kg/L can be attributed to the augmented interparticle interactions within a slurry (He & Laskowski 1994). The increase in interparticle interactions has been known to promote the formation of agglomerates within the fluid and more predominant at a high slurry density (Shi 2016). Hence, the amount of solid particles in the slurry contributed significantly towards the change in material behaviour and particularly at high slurry density.

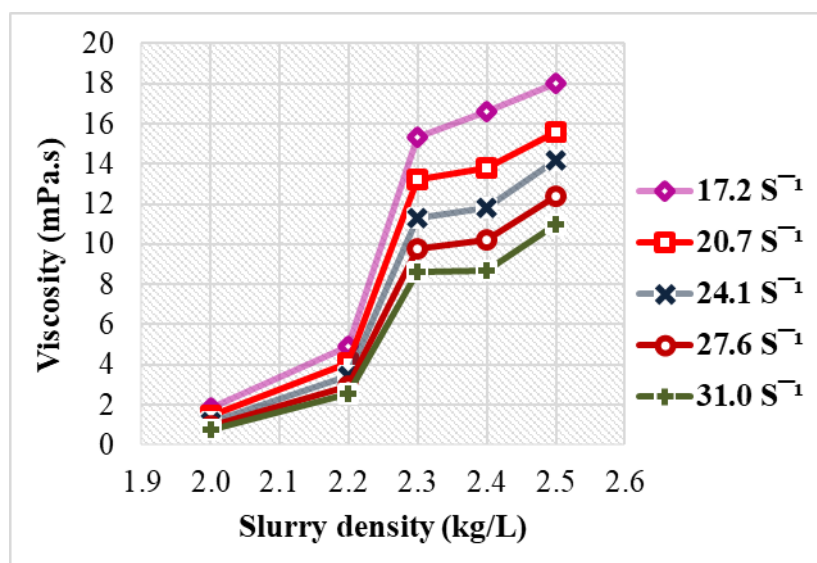
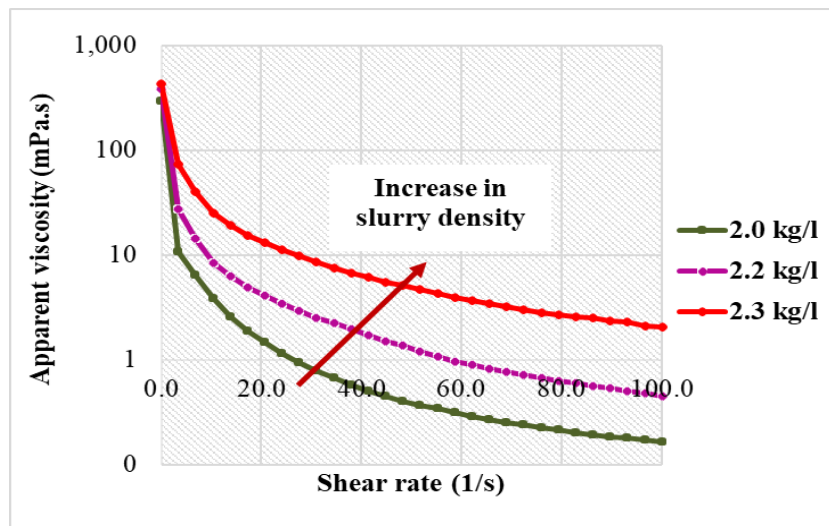


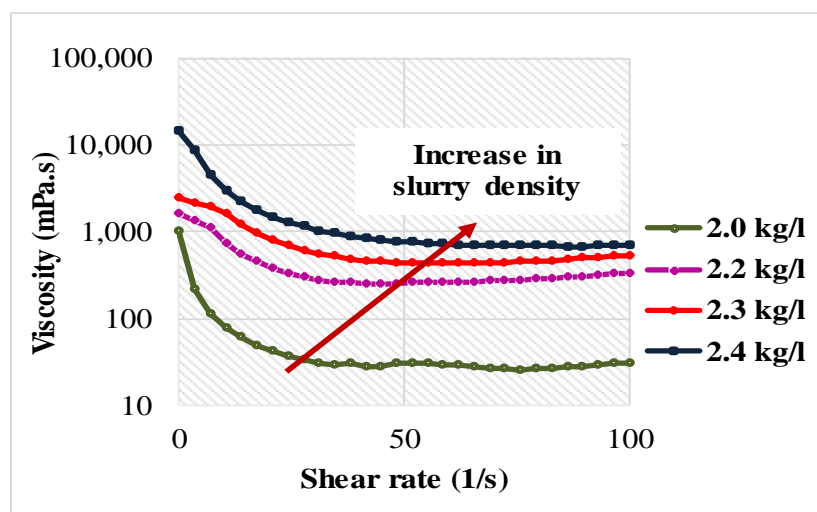
Figure 4-20: Viscosity variation with slurry density for fresh ferrosilicon

4.4.1.3 Shear rate

Figure 4-21 below depicts the variation of apparent viscosity for fresh (a) and degraded (b) ferrosilicon with shear rate and slurry density. From Figure 4-21 (a), it can be seen that medium viscosity showed a shear thinning effect (viscosity reduced with shear rate) with increase in the shear rate for fresh ferrosilicon. Amiri et al. (2010) attributed this drastic drop in slurry viscosity with increase in shear rate to the settling behaviour of ferrosilicon particles. Considering that there is a direct relationship between apparent viscosity and percent solids of a slurry at the time of measurement, a further increase in the shear rate will, therefore, lead to an overall decrease in viscosity. Collins et al. (1974) observed that viscosity measurement for this type of material is made difficult by the necessity to maintain the particles in a homogeneous state while measuring.



(a)



(b)

Figure 4-21: Viscosity variation with slurry density and shear rate for fresh (a) and degraded (b) ferrosilicon

However, in the case of degraded ferrosilicon, the shear thinning effect was only observed at shear rates below 50 s^{-1} , and after which, the curves seemed to have reached a Newtonian plateau before showing a slight shear thickening behaviour with a further increase in shear rate and slurry density, as shown in Figure 4-21 (b). Olhero & Ferreira (2004) attributed this transition in material behaviour to particle rearrangements and increase in middling distance between particle layers. Under such conditions, the capillary forces compete with the flow of the fluid, hence, the slurry thickens (Jiang et al. 2013). Once shear thickening is reached, it becomes challenging to recover medium particles through the screen apertures due to the high cohesive forces among the particles, hence, resulting in increased medium loss to the overflow stream.

Ferrosilicon is an iron alloy. Therefore, it is inherently magnetic (Collins et al. 1974). Hence, it can be assumed that the degree of magnetisation was enhanced by the continuous pumping of slurry and abrasion forces between particles and the screen surface, resulting in an increase in medium viscosity and change in behaviour with time. Thus, efficient recovery of the medium can be achieved by reducing medium residence time in the circuit, thereby, keeping the viscosity-shear rate curve on the shear thinning side.

4.4.1.4 Medium oxidation

Corrosion is an external phenomenon and arises from the electrochemical oxidation of medium surface. Williams & Kelsall (1992) observed that oxidation leads to a formation of a non-magnetic iron oxide layer around the medium particles. Under static conditions, an inactive coating is created on the medium surface that tend to prevent further corrosion. However, under dynamic plant conditions, the inert layer is continuously removed due to abrasion forces between particles and the screen surface, thus, accelerating the oxidation process (Collins et al. 1974). This, in turn, affects the viscosity and stability of the material. Collins et al. (1974) and later Williams & Kelsall (1992) established that irregularly shaped ferrosilicon particles with crevices and sharp points have a larger surface area and hence, more susceptible to corrosion during normal plant operations. Hence, medium oxidation was inevitable considering that crevices and sharp points characterised the ferrosilicon used in the experimental work. From the chemical analysis comparison shown in Table 4:2, it can be seen that there was an increase in oxide formation for all the elements present after running the experiments for more than a month, with the exception of silicon and manganese oxides. Hence it can be postulated that the bubbles observed on top of the material in storage buckets was due to oxidation reactions of the material.

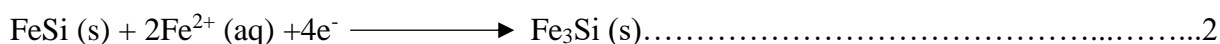
Table 4:2: Medium oxidation

	Fe2O3	Mn3O4	TiO2	CaO	K2O	P2O5	SiO2	Al2O3	MgO	Na2O
Fresh (wt%)	72.97	0.97	0.06	bdl	bdl	0.04	30.90	0.73	0.02	bdl
Contaminated (wt%)	89.96	0.22	2.81	0.19	0.07	1.33	8.53	2.07	0.70	bdl
	16.99	-0.75	2.75	0.19	0.07	1.29	-22.37	1.35	0.68	

Interestingly, the silicon oxide reduced by about 22.37 w/w%. Though the reduction in silica was unavoidable due to oxidation, but such a high reduction could be extrapolated. According to Collins et al. (1974), the phenomenon of hydrogen evolution and medium surface oxidation is often encountered on large scale plants, especially after a settled medium has stood for some time in a storage vessel. The result obtained is consistent with Williams & Kelsall (1992) who established that at low potentials, there is a preferential oxidation of the silicon content in the alloy by reactions such as;



And iron ore surface oxidation;



Therefore, medium surface oxidation largely contributed towards the change in ferrosilicon behaviour on the screen surface.

4.4.1.5 Ferrosilicon disintegration

While it has been well documented that the disintegration rate of ferrosilicon with silicon content between 14 - 16 % is moderate, in this thesis, ferrosilicon disintegration was significant. Sciarone (1976) noted that ferrosilicon particles with 14 - 16 % silica have ideal properties with abridged disintegration. If the silicon content is less than 14 %, there is enhanced magnetic properties with reduced disintegration resistance while above 16 %, there is an increase in friability resistance. However, friability of about 11.7 – 18.3 % was observed over time as shown in Figure 4-22. This can be attributed to probably the high reduction in silicon content of about 11.13 w/w%, as can be seen from Table 4-2. It is clear that recirculating the same medium led to more fine particles formation and in turn, increase in medium viscosity and reduced stability on the screen surface. Kawatra & Eisele (1988) observed that medium particle size reduction leads to an increase in viscosity due to an enlarged surface area, thereby, binding up the water and increasing the operative solid concentration of a slurry. Grobler et al. (2002) also established that increase in medium slimes leads to an increase in medium viscosity.

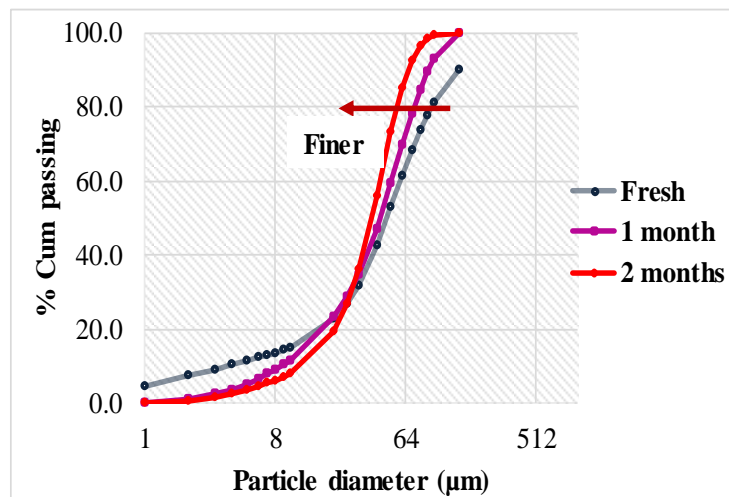


Figure 4-22: Particle size comparison for fresh and degraded ferrosilicon after two months of running experiments with the same material

4.4.1.6 Section summary

Ferrosilicon friability of about 11.7 – 18.3 % was observed after two (2) months of running the experiments on ferrosilicon and iron ore particles. Iron disintegration was also observed because of the presence of cavities on ore particles. While measures were put in place to remove the minus 1 mm iron ore particles through sieving on a vibrating swico screen, the iron ore slimes that went into solution with the medium could not be removed. Degraded ferrosilicon had a viscosity of about 3 - 5 times that of the fresh material at low shear rate and slurry density between 2.0 – 2.2 kg/L. The difference rose sharply with further increase in shear rate and slurry density above 2.2 kg/L. The accustomed rapid rise in medium viscosity, typically shown as an exponential function of percent solids, means that separation processes running at high slurry density are repeatedly affected by minor upsurge in the viscosity. Besides, fresh ferrosilicon showed a shear thinning effect (viscosity reducing with shear rate) with increase in shear rate and degraded ferrosilicon exhibited a shear thinning effect at shear rates below 50 s^{-1} , and thereafter, a slight shear thickening behaviour. On the other hand, ferrosilicon is an iron alloy. Therefore, it is inherently magnetic. Hence, it can be postulated that the degree of magnetisation was enhanced by the continuous pumping of slurry and abrasion forces between ore particles and the screen surface, resulting in an increase in medium viscosity and change in behaviour with time.

Considering the results presented, it can be concluded that the presence of fine particles as a result of ferrosilicon disintegration, slime contamination from iron ore, oxidised ferrosilicon surface and increased medium magnetisation due to shear rates from the pump and abrasion forces, had detrimental effects on the quality of medium and ultimately on the drainage rate. While it is necessary to control the viscosity of medium in a cyclone and on a screen surface,

in practice, this is not feasible due to the difficulties in online measurements and uncertainties in the interpretation of results. Conversely, it is very problematic to regulate the viscosity of a slurry directly through a fast response control action. Nevertheless, it is much easier to manage the effects of viscosity by choosing operating conditions that limit viscosity effects.

4.4.2 Influence of operating conditions on degraded ferrosilicon recovery rate

Medium degradation is a condition that is hardly noticed on a drain and rinse vibrating screen due to the treatment of high volumes of material and continuous addition of fresh medium to the cyclone. However, it has a considerable influence on the recovery of ferrosilicon on a vibrating screen. Hence, in line with the objectives of the study, this section discusses the influence of slurry density, volumetric flowrate and aperture size on degraded ferrosilicon recovery rate using the 1x13 mm and 0.8x8.8 mm polyurethane panels, 0.63 mm poly-wedge wire and 1x12 mm rubber panels. The subsection also discusses the influence of degradation on drainage rate, percent moisture and medium carryover by comparing the results for degraded material with that of the fresh material. No information was found in the open literature regarding the influence of medium degradation on medium recovery on a vibrating screen. Hence, the results presented in this subsection contribute to a better understanding of the effects of degradation on medium loss on a drain and rinse vibrating screen.

4.4.2.1 Influence of volumetric flowrate on degraded ferrosilicon recovery rate

Presented in this subsection is the influence of volumetric flowrate on drainage rate, moisture and medium carryover.

4.4.2.1.1 Influence of volumetric flowrate on deg ferrosilicon drainage rate

Figure 4-23 depicts the effects of feed rate on drainage rate of degraded ferrosilicon for 1x13 mm polyurethane panels. It can be seen that as the volumetric flowrate increased from 21.8 to 24.5 m³/h, there was a corresponding increase in the drainage rate of medium particles. However, a gradual drop in drainage rate was observed with further increase in feed rate beyond 24.5 m³/h. Related results obtained for 1x12 mm rubber panels, 0.8x8.8 mm polyurethane and 0.63 mm poly-wedge panels showed a gradual drop in drainage rate with increase in volumetric flowrate beyond 24.5 m³/h, as shown in Appendix D. It is worth noting that there was a shift in the critical volumetric flowrate from 23.7 m³/h for fresh material to 24.5 m³/h for degraded material. The shift can be attributed to the reduced stability of the material on the screen surface due to degradation, as explained in section 4.4.1. It can be deduced that regardless of the material type and quality, increase in volumetric flowrate leads to an increase in medium drainage rate but only up to a certain point, and thereafter, medium drainage rate reduces gradually.

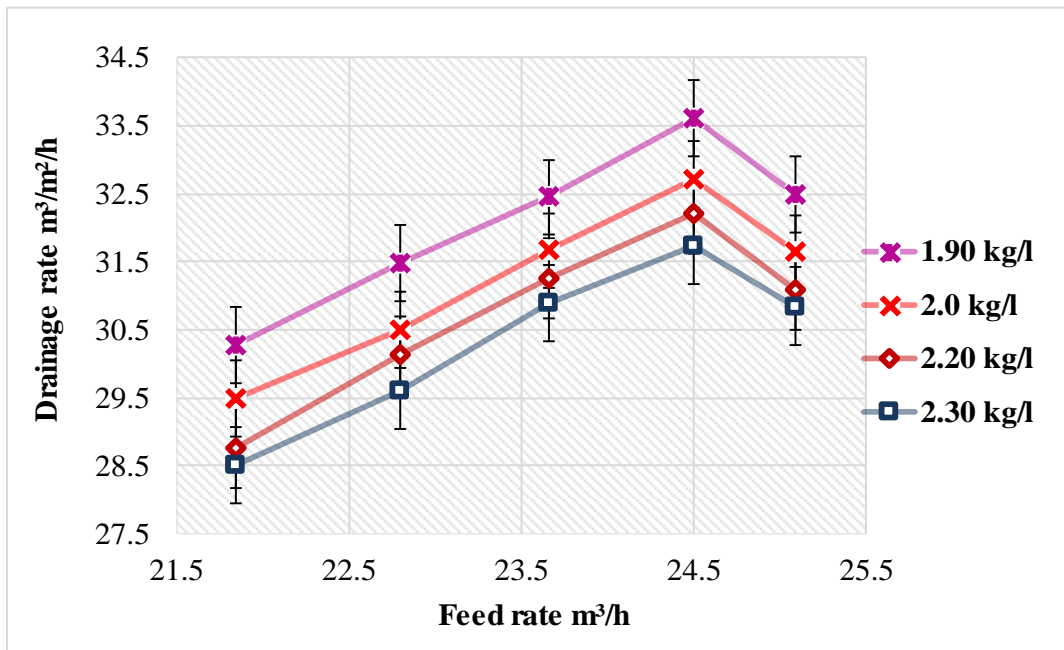


Figure 4-23: Effects of volumetric flowrate on degraded ferrosilicon drainage rate for 1x13 mm polyurethane panels

4.4.2.1.2 Influence of volumetric flowrate on moisture bypass

Figure 4-24 below for 1x13 mm screen panels shows the influence of volumetric flowrate on moisture bypass. As can be seen, increase in volumetric flowrate increased from 21.8 – 25.2 m³/h led to an increase in the moisture reporting to the overflow stream.

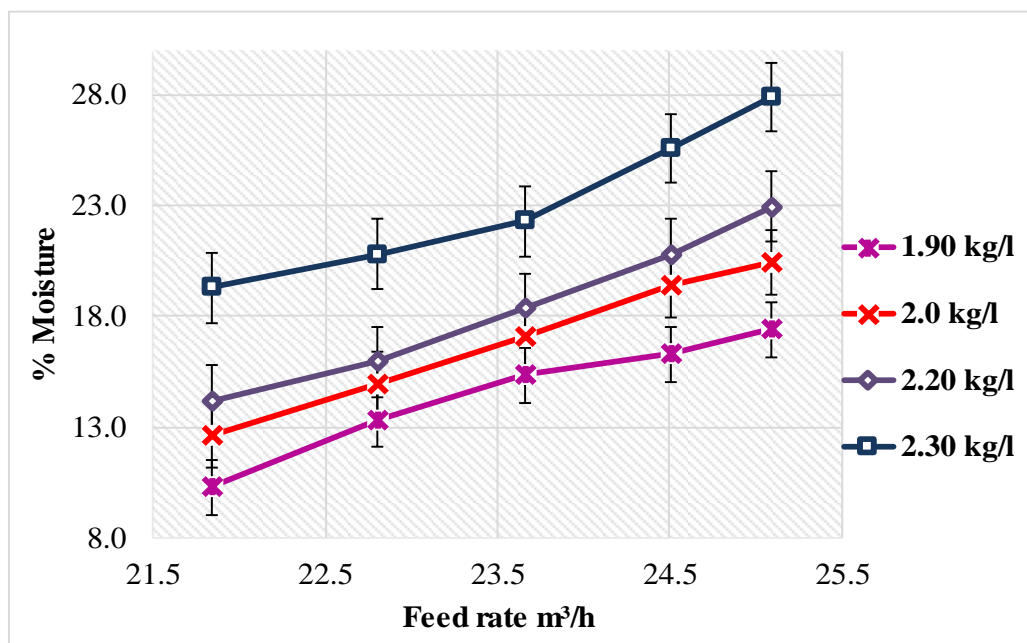


Figure 4-24: Effects of feed rate variation on moisture carryover for 1x13 mm polyurethane panels

However, a slight up-swing in the moisture bypass was observed at volumetric flowrate above 23.7 m³/h, with the exception of 1.9 kg/L curve. It can be hypothesised that once the critical screen capacity is exceeded, a further increase in material feed rate leads to further moisture and medium carryover to the oversize stream. A similar result was observed on 1x12 mm rubber panels, as shown in Appendix E.

4.4.2.1.3 Influence of volumetric flowrate on degraded ferrosilicon carryover

Figure 4-25 below for 1x13 mm screen panels for degraded ferrosilicon show a positive linear relationship between the volumetric flowrate of material and medium carryover up to a screen critical point of 24.5 m³/h, and thereafter, a sharp rise in medium carryover was observed. Due to reduced material residence time on the screen surface with increase in volumetric flowrate, there was a restraint of medium flow through a bed of material. Hence, any further increase in the volumetric flowrate led to an increase in medium carryover to the overflow stream. The result obtained was consistent with the drainage rate obtained on the same set of panels showing a reduction in medium recovery beyond 24.5 m³/h, representing a higher medium and water carryover to the oversize stream. The result obtained is consistent with Preti & Ferrara (1975) who established that increase in feed rate leads to a crowded particle separation owing to the augmented amount of particles on the screen surface. This, in turn, leads to a reduction in screen handling capacity and increase in undersize carryover. Comparable results obtained on 0.63 mm poly-wedge wire, 1x12 mm rubber and 0.8x8.8 mm polyurethane screen panels showed a sharp increase in medium carryover beyond 24.5 m³/h, as shown in Appendix F.

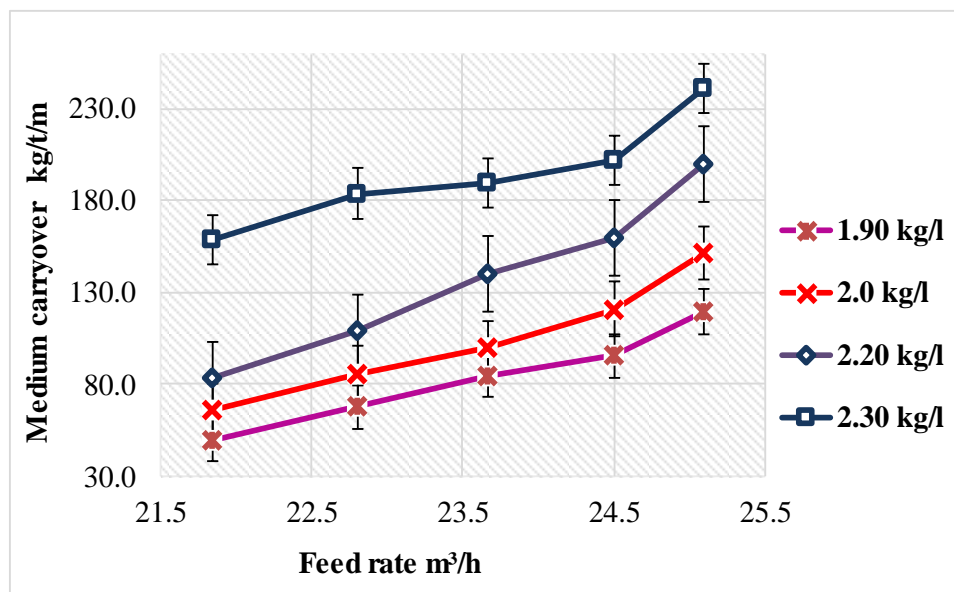


Figure 4-25: Effects of volumetric flowrate on medium carryover on 1x13 mm polyurethane panels for degraded ferrosilicon

4.4.2.1.4 Section summary

Increase in volumetric flowrate from 21.8 to 25.1 m³/h led to an increase in medium drainage rate up to the screen critical point and after which, a gradual drop in drainage rate was observed with further increase in feed rate. This was accompanied by an increase in moisture and medium carryover with a slight upswing observed above the screen critical point. The critical point was the same at 24.5 m³/h for all the panels tested on degraded ferrosilicon. It is worth noting that there was a shift in the critical volumetric flowrate from 23.7 m³/h for fresh material to 24.5 m³/h for degraded material.

4.4.2.2 Effects of slurry density on degraded ferrosilicon recovery rate

Discussed in this section are the effects of slurry density variation on drainage rate, moisture and medium carryover for degraded ferrosilicon.

4.4.2.2.1 Effects of slurry density on deg ferrosilicon drainage rate

Figure 4-26 shows the effect of slurry density on medium drainage rate for 1x13 mm screen panels. It can be seen that increase in slurry density from 1.9 to 2.3 kg/L led to a sharp reduction in the drainage rate between 1.9 – 2.0 and thereafter, a gradual reduction was observed between 2.0 – 2.3 kg/L. At higher slurry density, there was a fast build-up of a thick bed of material on the screen surface due to increased particle competition for passage, hence, leading to a reduction in drainage rate even at low volumetric flowrate. Napier-Munn et al. (1995) during their investigations on iron ore washing plants established that medium loss increases with screen loading and the effect was quite strong even on moderately loaded screens. This was attributed to the increase in operating relative density. It was further observed that a small increase in slurry density led to a large increase in viscosity and thus, poorer drainage rates. Hence, the result obtained is consistent with Napier-Munn et al. (1995).

Related results were obtained on 1x12 mm rubber panels shown in Figure 4-27. It can be seen that as the slurry density increased from 1.9 – 2.45 kg/L, there was a reduction in medium drainage rate with a sharp drop observed at slurry density above 2.20 kg/L regardless of the volumetric flowrate. From the viscosity plot for degraded ferrosilicon, as shown in Figure 4-19, an initial rise in viscosity was noticed between 2.2 – 2.3 kg/L with a sharp increase beyond 2.3 kg/L. Hence, the marked decrease in drainage rate beyond 2.2 kg/L can be attributed to the increase in slurry viscosity.

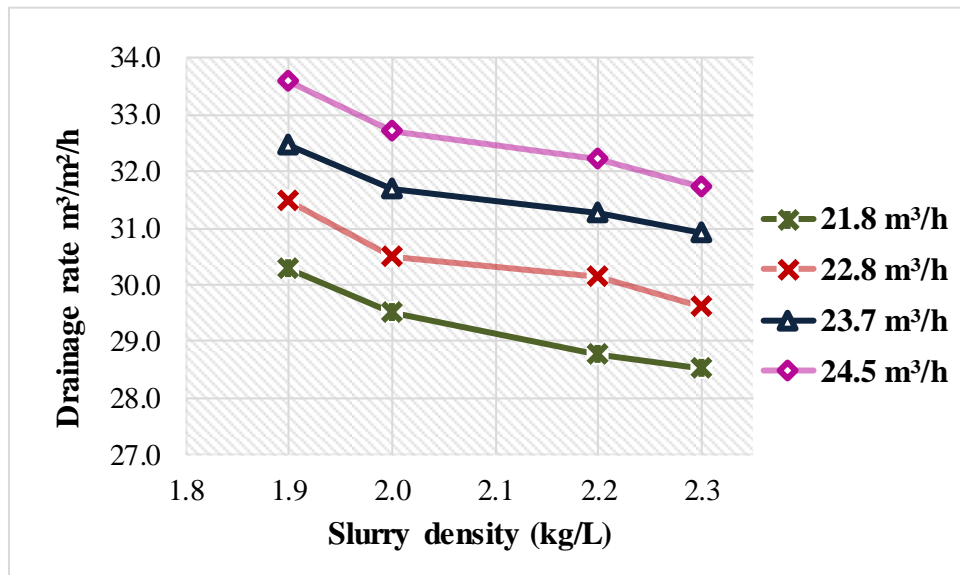


Figure 4-26: Effects of slurry density variation on degraded medium drainage rate for 1x13 mm polyurethane panels

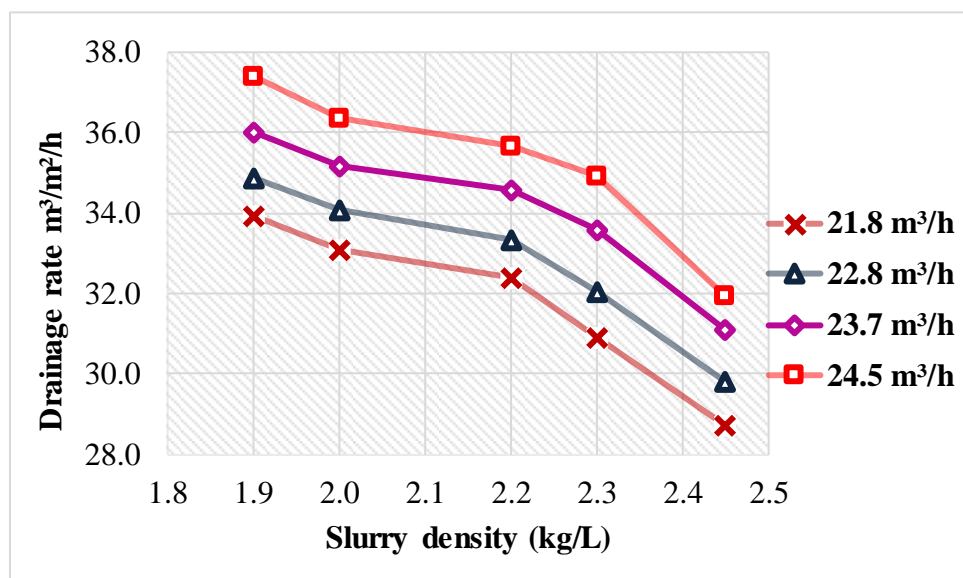


Figure 4-27: Effects of slurry density variation on degraded ferrosilicon drainage rate for 1x12 mm rubber panels

4.4.2.2.2 Effects of slurry density on moisture bypass

An analysis of the effects of slurry density on moisture bypass is shown in Figure 4-28 for 1x13 mm screen panels. It can be seen that increase in slurry density from 1.9 – 2.3 kg/L led to an increase in moisture bypass to the oversize stream with a sharp rise at a slurry density above 2.2 kg/L. The marked increase in moisture bypass beyond 2.2 kg/L can be attributed to the increase in material viscosity due to medium degradation. Comparable results obtained on the same set of panels showed a substantial decrease in medium drainage rate beyond 2.2 kg/L slurry density, thus, a sharp increase in water and medium carryover to the oversize

stream. At this point, any further increase in solid concentration led to more water reporting to the oversize stream.

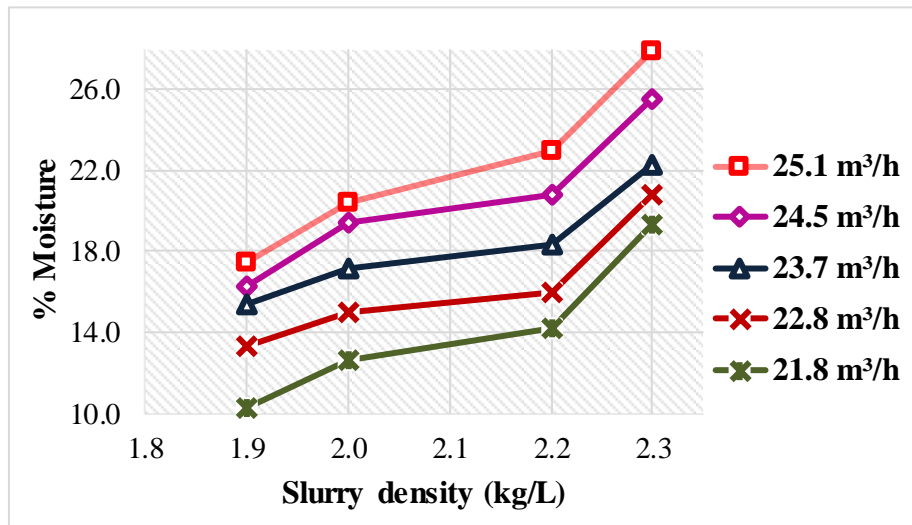


Figure 4-28: Effects of slurry density on moisture bypass for 1x13 mm polyurethane panels

Figure 4-29 below shows a related result obtained on 1x12 mm rubber panels with a marked increase in moisture bypass to the oversize stream at slurry density beyond 2.2 kg/L.

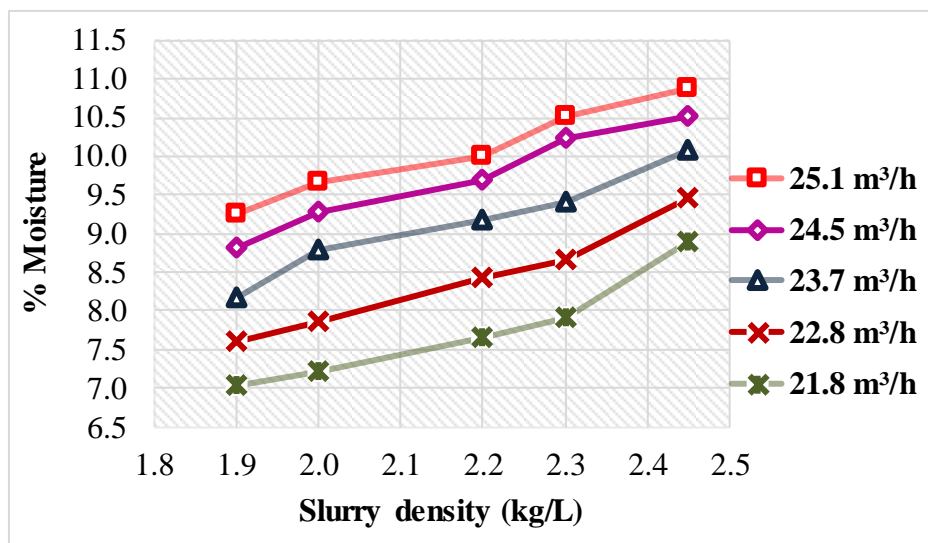
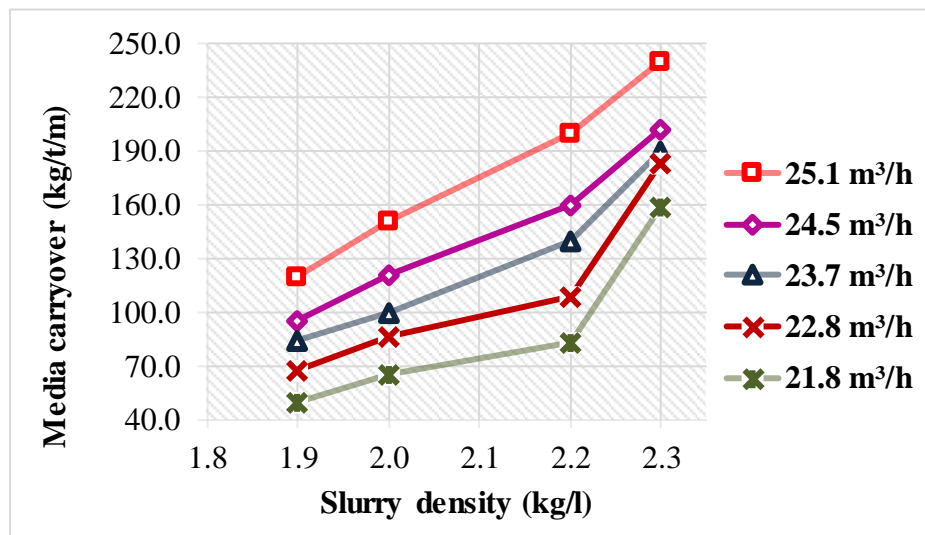


Figure 4-29: Effects of slurry density on moisture bypass for 1x12 mm rubber panels

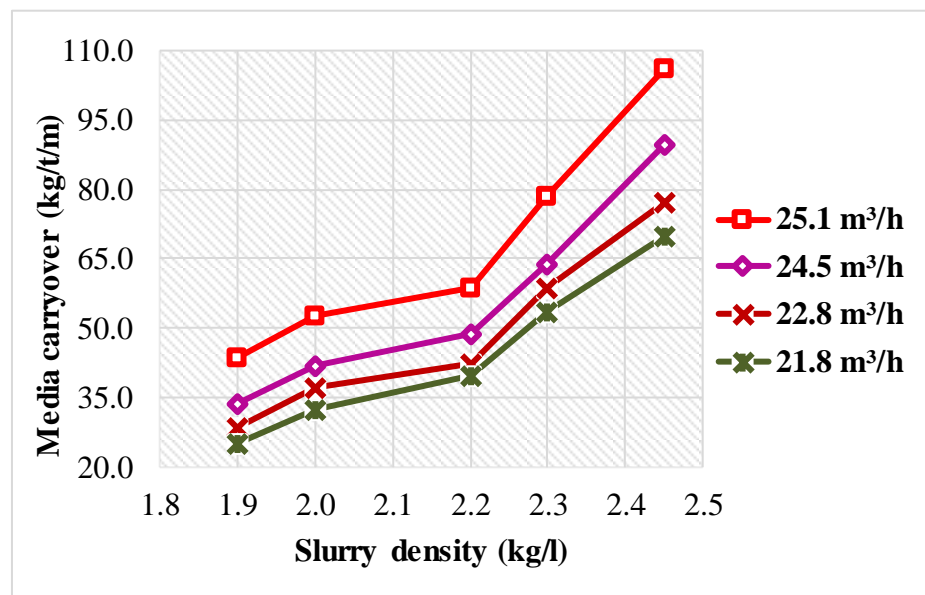
4.4.2.2.3 Effects of slurry density on degraded ferrosilicon carryover

An analysis of the consequences of slurry density variation on degraded medium carryover is shown in Figure 4-30 for 1x13 mm (a) and 1x12 mm (b) rubber panels. For both panels, a gradual increase in medium carryover was observed at slurry density between 1.9 - 2.2 kg/L with a sharp rise above 2.2 kg/L. Comparable results obtained for the same screen panels

showed a marked decrease in medium drainage rate beyond 2.2 kg/L, indicating a sharp rise in medium carryover to the oversize stream. The sharp rise in medium carryover can be attributed to the marked increase in slurry viscosity above 2.2 kg/L slurry density for the degraded material. Cheng (1984) and later He & Laskowski (1994) observed that as the relative density of the material increases, there is a corresponding increase in slurry viscosity due to a higher particle to particle interaction, thus, increasing medium carryover to the oversize stream.



(a)



(b)

Figure 4-30: Effects of slurry density variation on degraded medium carryover for 1x13 mm polyurethane panels (a) and 1x12 mm (b) rubber panels

4.4.2.2.4 Section summary

Increase in slurry density from 1.9 to 2.3 kg/L led to a reduction in medium drainage rate, with a sharp decline in drainage rate and a sharp rise in moisture and medium carryover observed at slurry density above 2.2 kg/L. The marked decrease in medium recovery rate beyond 2.2 kg/L can be attributed to the increase in material viscosity due to degradation. Further, at higher slurry density, there is a fast build-up of a thick bed of material on the screen surface due to the increase in particle competition for passage, hence, leading to a reduction in drainage rate and increase in material bypass even at low volumetric flowrate.

4.4.2.3 Influence of aperture size on degraded ferrosilicon recovery rate

The influence of aperture size on degraded ferrosilicon recovery is presented in this section. The 1x13 mm and 0.8x8.8 mm polyurethane panels were used for the analysis.

4.4.2.3.1 Influence of aperture size on deg ferrosilicon drainage rate

The influence of aperture size on medium drainage rate is presented in Figure 4-31 below. An increase in medium drainage rate of about 1.0 - 1.2 m³/m²/h with increase in screen hole size from 0.8x8.8 mm to 1x13 mm was observed. Tsakalakis (2001) deliberated on the effects of four dissimilar screen opening sizes i.e. 0.6, 1.0, 2.0 and 4 mm on screening efficiency using crushed quartz. The 0.6 mm and 1.0 mm screen panels produced screening efficiencies of about 45 - 50 % and 75 - 80 % respectively. The decrease in screening efficiency for the 0.6 mm screen panels was attributed to the aperture size reduction, as the efficiency of separation decreases with aperture size (Aplan et al. 2003). Therefore, the result obtained in this thesis regarding the increase in aperture size with drainage rate is consistent with the results obtained by Tsakalakis (2001) and Aplan et al. (2003).

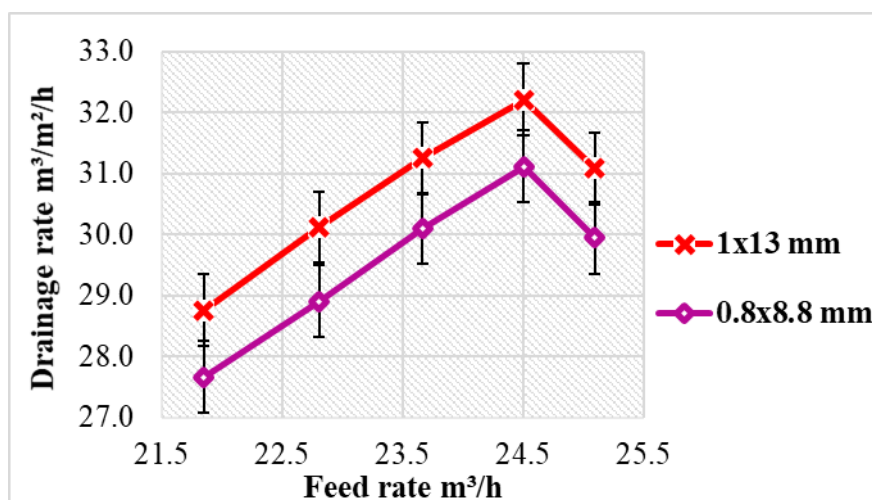
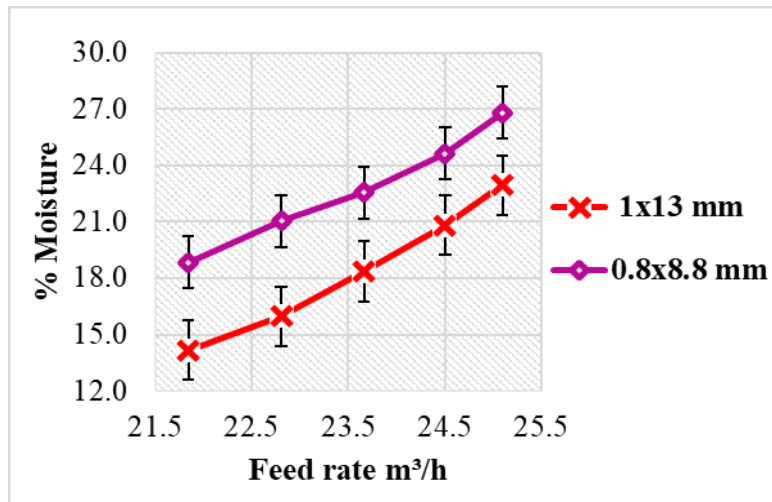


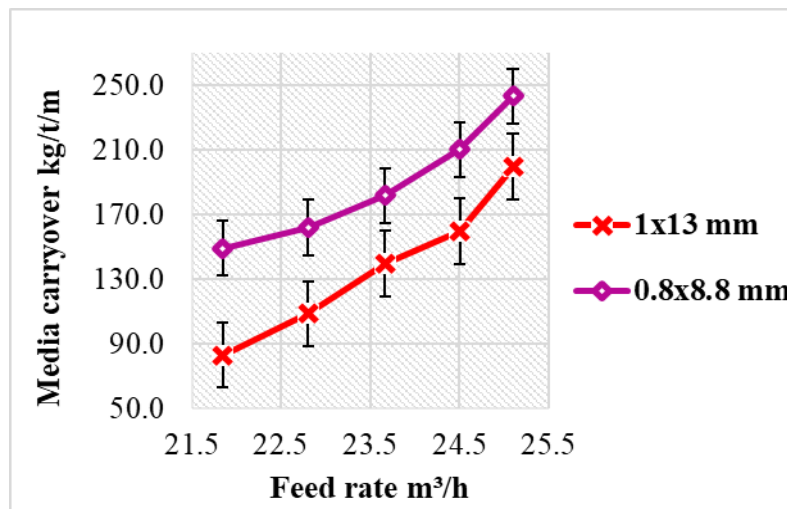
Figure 4-31: Influence of aperture size on degraded ferrosilicon drainage rate at 2.2 kg/L slurry density

4.4.2.3.2 Influence of aperture size on moisture and medium carryover

Figure 4-32 below shows the influence of aperture size on moisture (a) and medium carryover (b) to the oversize stream. As can be seen, there was a gradual increase in moisture and medium carryover of about 3.8 – 5.1 w/w% and 43 – 54 kg/t/m respectively with decrease in aperture size from 1x13 mm to 0.8x8.8 mm.



(a)



(b)

Figure 4-32: Effects of aperture size variation on moisture (a) and medium carryover (b) for degraded ferrosilicon at 2.2 kg/L slurry density

4.4.2.3.4 Section summary

An increase in screen hole size from 0.8x8.8 mm to 1x13 mm led to an increase in medium drainage rate of about 1.0 - 1.2 m³/m²/h with a decrease in moisture and medium carryover of

about 3.8 – 5.1 w/w% and 43 – 54 kg/t/m respectively. The increase in medium recovery with aperture size can be attributed to the increase in screen carrying capacity.

4.4.3 Influence of degradation on medium recovery

This section discusses the influence of medium degradation on drainage rate, percent moisture and medium carryover by comparing the results for degraded and fresh material using the 0.8x8.8 mm screen panels at 2.0 kg/L slurry density.

4.4.3.1 Influence of degradation on drainage rate

Figure 4-33 below for 0.8x8.8 mm screen panels depicts the influence of degradation on medium drainage rate. It can be seen that medium loss of about 9.0 - 9.3 m³/m²/h with increase in volumetric flowrate from 21.8 - 23.7 m³/h was accrued due to degradation. As the feed rate increased further than 23.7 m³/h, there was a slight reduction in medium drainage rate of about 9.0 – 6.8 m³/m²/h. As explained in section 4.4, ferrosilicon degradation leads to an increase in slurry viscosity. Highly viscous slurry is undesirable on a screen surface as it decreases the settling rate of medium, thus, reducing the contact times medium particles makes with the screen surface (Franck 1964; Cheng 1984; Mangesana et al. 2008). This, in turn, leads to a reduction in medium drainage rate.

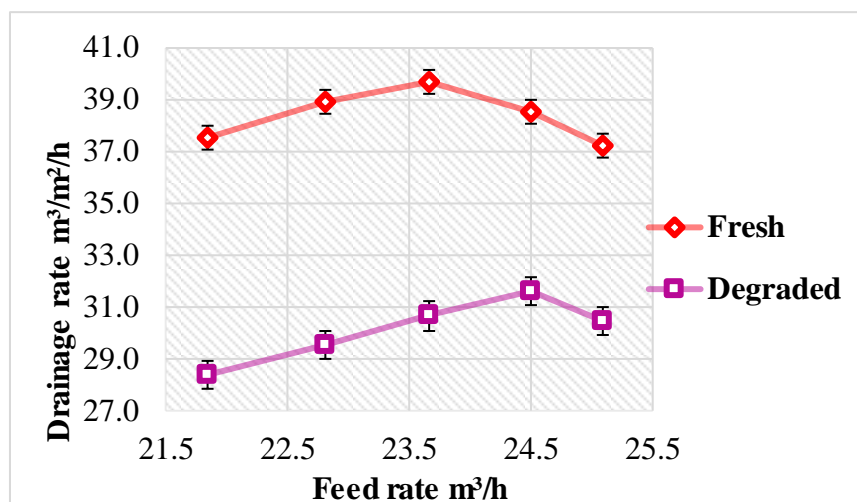


Figure 4-33: Influence of degradation on ferrosilicon drainage rate for 0.8x8.8 mm polyurethane panels at 2.0 kg/L slurry density

4.4.3.2 Influence of medium degradation on moisture bypass

Figure 4-34 shows an increase in moisture bypass of about 8.9 – 11.8 w/w% to the overflow stream due to medium degradation at low volumetric flowrate between 21.8 - 23.7 m³/h. However, the effect of degradation was noticeable at volumetric flowrate above 23.7 m³/h with a further increase in moisture bypass of about 11.8 – 14.5 w/w%. This can be attributed

to the increase in medium viscosity due to degradation, as explained in section 4.4. Increase in slurry viscosity accompanied by an increase in cohesive forces among medium particles tend to block the easy flow of water through a bed of material (Franck 1964; Cheng 1984; Mangesana et al. 2008; Kawatra & Eisele 1988). Hence, the material bed easily builds up with increase in slurry density and volumetric flowrate, resulting in an increase in moisture bypass to the oversize stream.

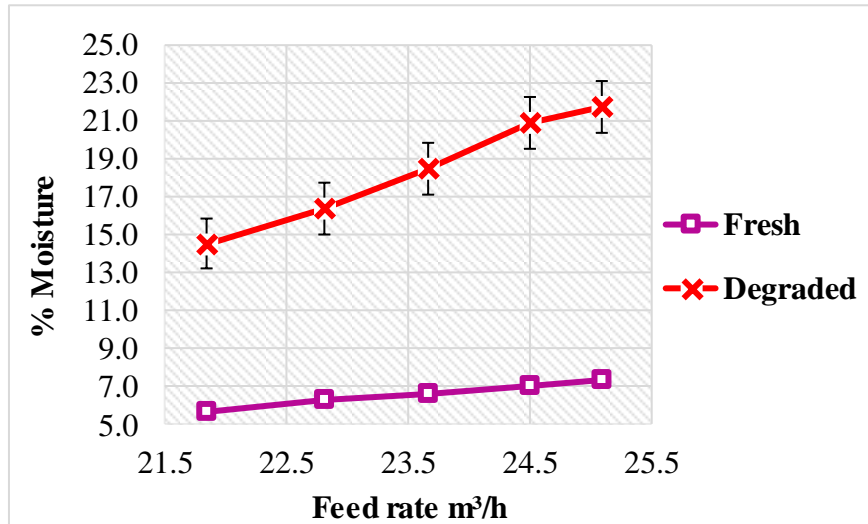


Figure 4-34: Influence of medium degradation on moisture bypass for 0.8x8.8 mm polyurethane panels at 2.0 kg/L slurry density

4.4.3.3 Influence of degradation on medium carryover

The influence of degradation on medium carryover is shown in Figure 4-35. Medium loss to the oversize stream of about 64.4 – 101 kg/t/m was ensued due to degradation at volumetric flowrate lower than 23.7 m³/h. A sharp rise in medium carryover was observed with further increase in volumetric flowrate beyond 23.7 m³/hr for fresh and 24.5 m³/h for degraded material. This was due to a high flocculation of medium particles onto iron ore particles due to degradation, hence, reducing the separation rate. Mangesana et al. (2008) established that high fine particulate matter aggregation leads to an increase in interparticle interactions, and more especially at high slurry density. Thus, high medium carryover was inevitable at high slurry density and volumetric flowrate. The result obtained was consistent with the drainage rate obtained for the same set of panels with a slight reduction in medium drainage rate beyond 23.7 m³/h for fresh material and 24.5 m³/h for degraded material, thus, increased medium carryover to the oversize stream.

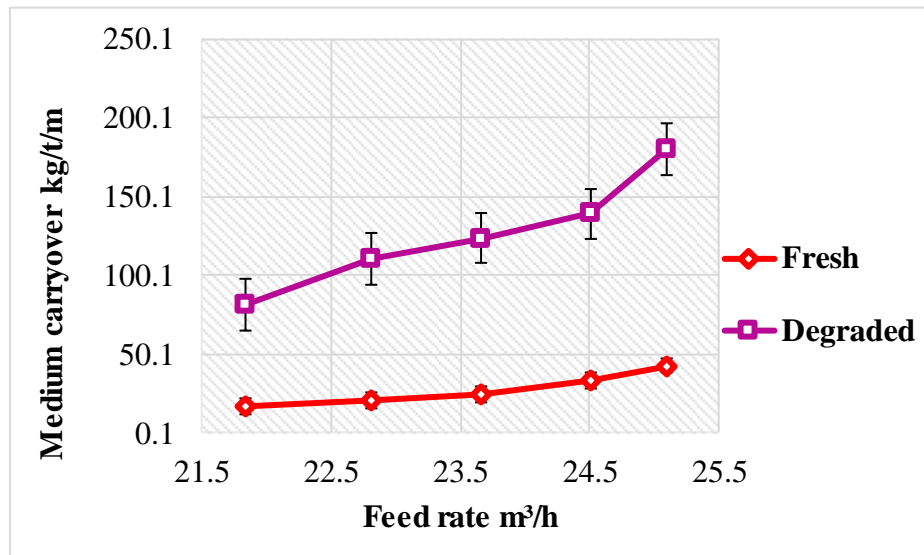


Figure 4-35: Influence of degradation on medium carryover for 0.8x8.8 mm screen panels at 2.0 kg/L slurry density

4.4.3.4 Section summary

The results presented shows a reduction in medium drainage rate and an increase in moisture and medium bypass of about 9.0 - 9.3 m³/m²/h, 8.9 – 11.8 w/w% and 64.4 – 101 kg/t/m respectively with an increase in volumetric flowrate from 21.8 - 23.7 m³/h due to degradation. However, the effect of degradation was noticeable at volumetric flowrate above 23.7 m³/h with a further increase in moisture and medium carryover.

4.4.4 Effects of screen panel material on degraded medium recovery

Presented in this section is the comparison of the performance of the 1x12 mm rubber panels and 1x13 mm polyurethane panels for degraded material.

4.4.4.1 Effects of screen panel material on degraded medium drainage rate

Figure 4-36 shows the assessment of the effects of using 1x12 mm rubber panels instead of 1x13 mm polyurethane panels on medium drainage rate. As can be seen, the 1x12 mm rubber panels drained more medium of about 3.3 – 3.6 m³/m²/h than the 1x13 mm polyurethane panels at volumetric flowrate between 21.8 – 25.1 m³/h. The increase in medium drainage rate can be attributed to the higher flexibility of rubber apertures. Wills (1985) established that rubber panels have a high elasticity and thus, able to separate even near-size particles with minimal aperture pegging. O'Brien & Firth (2015) compared the effects of using soft and hard polyurethane panels on magnetite drainage rate and established that soft polyurethane panels produced comparatively high drainage rate due to reduced aperture pegging. Hence, the result obtained in this thesis is supported by Wills (1985) and O'Brien & Firth (2015) results.

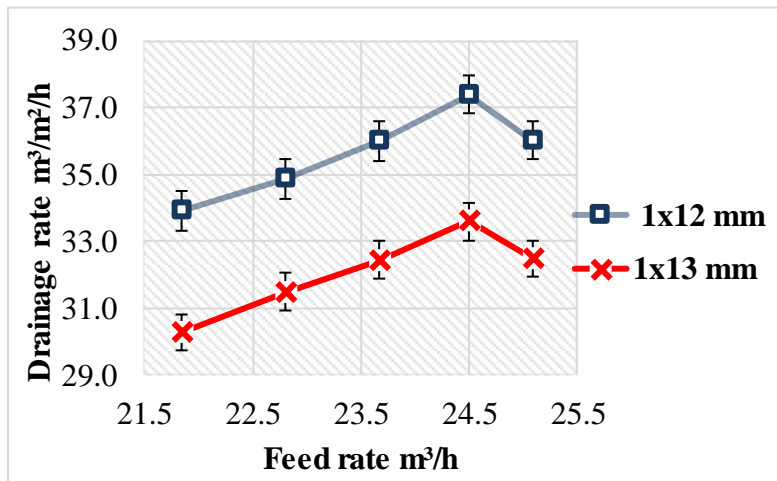


Figure 4-36: Effects of screen panel material on degraded ferrosilicon drainage rate at 1.9 kg/L slurry density

4.4.4.2 Effects of screen panel material on moisture bypass

The effects of screen panel material on moisture carryover is shown in Figure 4-37 below. The use of 1x12 mm rubber screen panels led to a reduction of about 5.7 – 7.2 w/w% in the percent moisture bypass at volumetric flowrate between 21.8 - 23.7 m³/h. However, the amount of moisture bypass to the overflow stream reduced even further by about 7.5 – 8.2 w/w% with increase in volumetric flowrate beyond 23.7 m³/h. While the rubber panels have flexible apertures compared to the polyurethane panels, it should be noted that the 1x12 mm rubber panels had an open area of about 3.72 % higher than the 1x13 mm screen panels, hence, offering medium particles a higher capacity for passage. At higher volumetric flowrate, high moisture bypass to the overflow stream was expected as the medium became too viscous for the 1x13 mm polyurethane screen panels to efficiently drain medium particles.

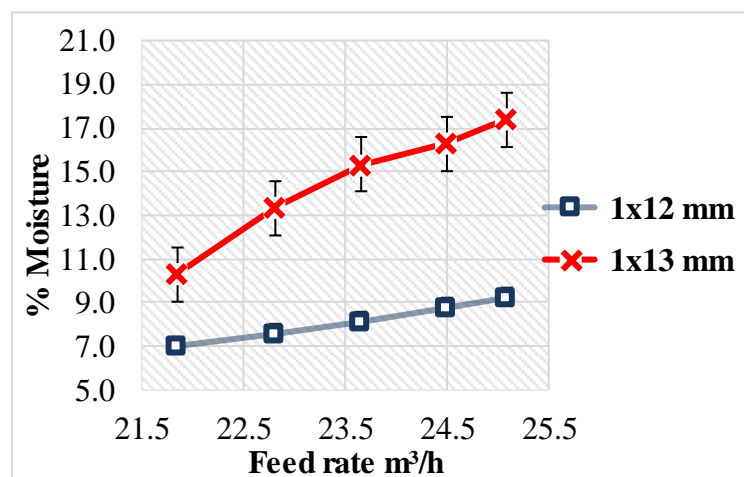


Figure 4-37: Effects of screen panel material on moisture bypass at 1.9 kg/L slurry density

4.4.4.3 Effects of screen panel material on degraded medium carryover

Figure 4-38 below illustrates the effects of screen panel material on medium carryover to the overflow stream. The use of 1x13 mm polyurethane panels led to an increase in medium carryover of about 24.4 - 54.1 kg/t/m with increase in volumetric flowrate up to 24.5 m³/h compared to using 1x12 mm rubber panels. However, the variance in medium carryover was more pronounced at higher slurry density and volumetric flowrate. This is due to the fact that rubber panels have a high elasticity, hence, able to absorb the impact of material weight at higher volumetric flowrate (Wills 1985). Thus, the screen capacity was not easily exceeded even with increase in slurry density and feed rate. Nonetheless, both panels showed an upswing in medium carryover at volumetric flowrate above 24.5 m³/h. This point could be assumed to be the critical point for the two panels and any further increase in material flow onto the screen led to further increase in medium and water bypass.

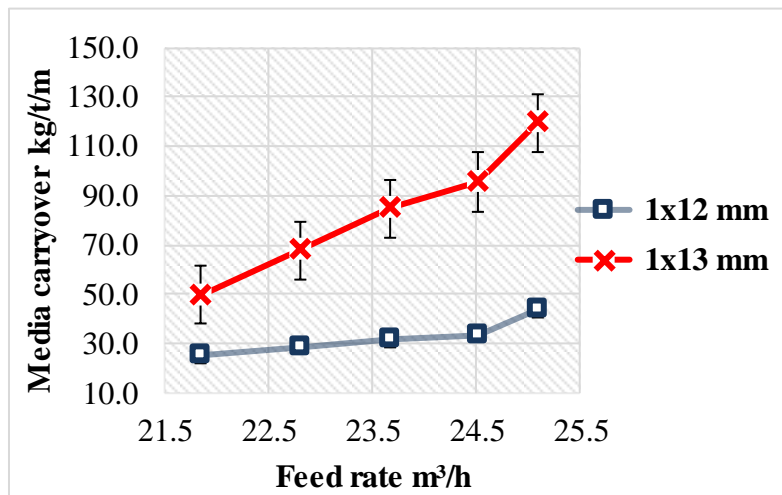


Figure 4-38: Effects of screen panel material on degraded medium carryover at 1.9 kg/L slurry density

4.4.4.4 Section summary

The 1x12 mm rubber panels drained more medium of about 3.3 – 3.6 m³/m²/h than the 1x13 mm polyurethane panels with a reduction of about 5.7 – 7.2 w/w% and 24.4 - 54.1 kg/t/m for moisture and medium bypass respectively at volumetric flowrate between 21.8 – 23.7 m³/h. However, the variance in water and medium bypass was more pronounced at higher slurry density and volumetric flowrate. At higher slurry density and volumetric flowrate, high moisture and medium bypass was expected as the medium became too viscous for the 1x13 mm polyurethane screen panels to efficiently drain medium particles. The increase in medium drainage rate with reduced bypass can be attributed to the higher flexibility of rubber apertures. While the rubber panels have flexible apertures compared to the polyurethane

panels, it should be noted that the 1x12 mm rubber panels had an open area of about 3.72 % higher than the 1x13 mm screen panels, hence, offering medium particles a higher capacity for passage.

4.5 Effects of operating conditions on magnetite recovery

Figure 4-39 below shows the performance of all the screen panels tested on magnetite at 1.64 kg/L slurry density with volumetric flowrate ranging from 18.3 to 22.8 m³/h. It can be seen that an increase in volumetric flowrate led to an increase in medium drain rate only up to a certain point and thereafter, drainage rate reduced gradually. This trend was observed on all the panels tested. The critical volumetric flowrate differed for different screen panels with 1x13 mm and 0.8x8.8 mm at 20.8 m³/h, 1x12 mm and 0.63 mm poly-wedge at 21.3 m³/h, and 0.63x12 mm and 0.63x8.8 mm at 20.4 m³/h. The difference in critical volumetric flowrates can be attributed to the difference in tonnage handling capacities for the different screen panels tested.

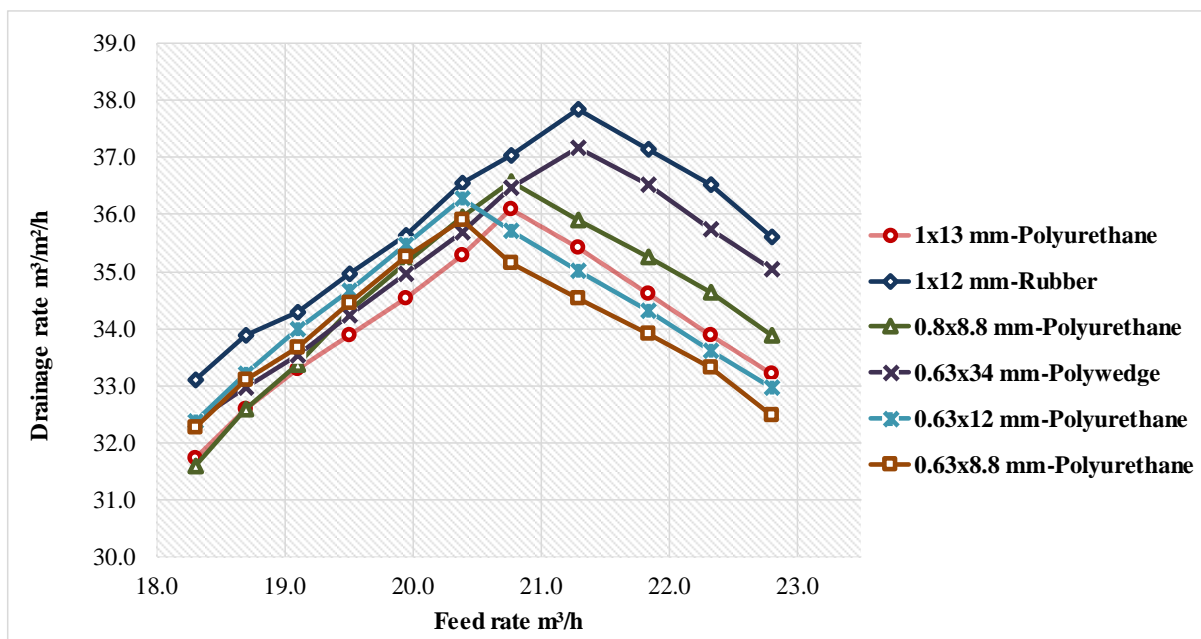


Figure 4-39: Magnetite drainage rates for various screen panels at 1.64 kg/L slurry density

4.5.1 Effects of feed rate variation on magnetite drainage rate

Figure 4-40 shows the effects of volumetric flowrate variation on magnetite drainage rate for 1x13 mm screen panels. Increasing volumetric flowrate onto a screen surface from 18.3 – 22.8 m³/h led to an increase in medium drainage rate. However, beyond the screen critical point of 20.8 m³/h, there was a reduction in medium drainage rate. Similar result was obtained by Valine & Wennen (2002) who established that material feed rate greater than the specified

capacity of a screen results in a decrease in fine particles screening rate. Comparable results were also obtained for fresh and degraded ferrosilicon, as explained in sections 4.3.1.1 and 4.4.2.1.1. At higher volumetric flowrate, there was an increase in material transport on the screen surface, resulting in a decrease in medium residence time for passage. This led to a reduction in medium drainage rate. Comparative results obtained for 1x12 mm rubber panels, 0.63 mm poly-wedge, 0.8x8.8 mm, 0.63x8.8 mm and 0.63x12 mm polyurethane panels showed a decline in medium drainage rate with further increase in volumetric flowrate beyond the screen critical point, as shown in Appendix G.

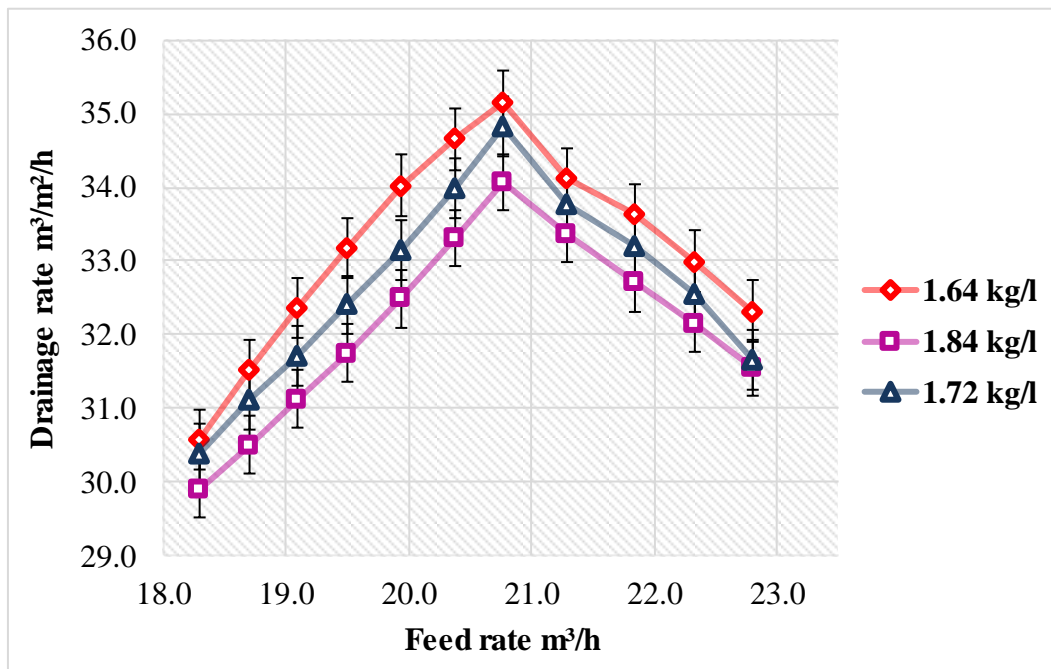


Figure 4-40: Effects of feed rate variation on magnetite drainage rate for 1x13 mm polyurethane panels

4.5.2 Effects of slurry density variation on magnetite drainage rate

The effect of slurry density variation on magnetite recovery presented in Figure 4-41 for 1x13 mm screen panels shows that as the slurry density increased from 1.64 to 1.84 kg/L, there was a gradual decrease in medium drainage rate. It can be hypothesised that as the slurry density increased, a thick bed of material was formed on the screen surface and thus, reducing the fine particles' contact times with the screen surface for passage. The probability of undersize particle passage reduced and any further increase in slurry density led to a further reduction in drainage rate. As the solid concentration increased in a slurry, the screen handling capacity was merely surpassed even at low volumetric flowrate. Dong & Yu (2012) observed that higher amount of water in a slurry leads to a reduction in cohesive forces between particles and the screen surface. Hence, it can be postulated that increase in slurry density leads to an

increase in cohesive forces between particles and the screen surface, thus, reducing the medium drainage rate. Guerreiro et al. (2015) investigated the effects of slurry density on screening rate at 1 - 3 v/v% solids and observed a decrease in recovery rate with increase in slurry density. Therefore, the result obtained is consistent with the results achieved by Guerreiro et al. (2015) and Dong & Yu (2012).

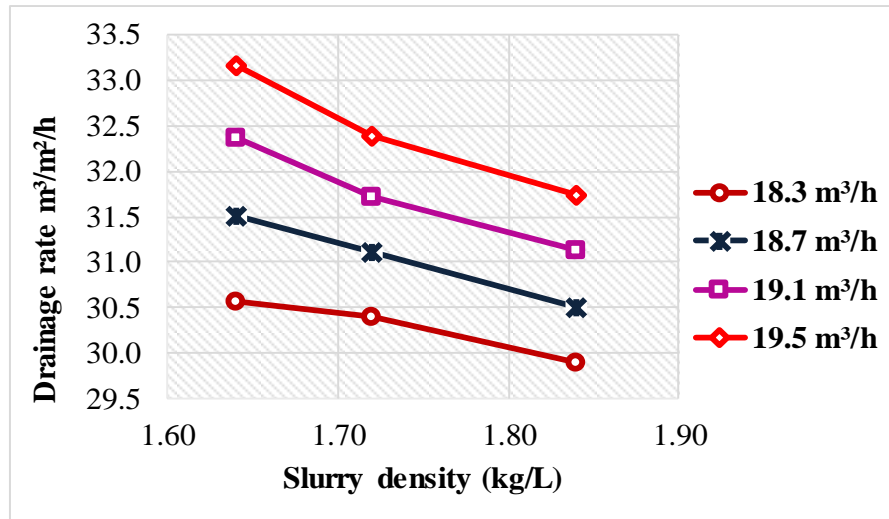


Figure 4-41: Effects of slurry density variation on magnetite drainage rate for 1x13 mm polyurethane panels

Comparable results obtained on 1x12 mm, 0.8x8.8 mm and 0.63 mm panels as shown in Appendix H indicated a decline in magnetite drainage rate with increase in slurry density. However, the 0.63x8.8 mm screen panels showed a slightly different response with a slight up-swing in drainage rate with increase in slurry density beyond 1.72 kg/L, as shown in Figure 4-42 below. This point could be thought as a saturation point for the two set of panels where a further increase in slurry density led to a steady decrease in medium drainage rate.

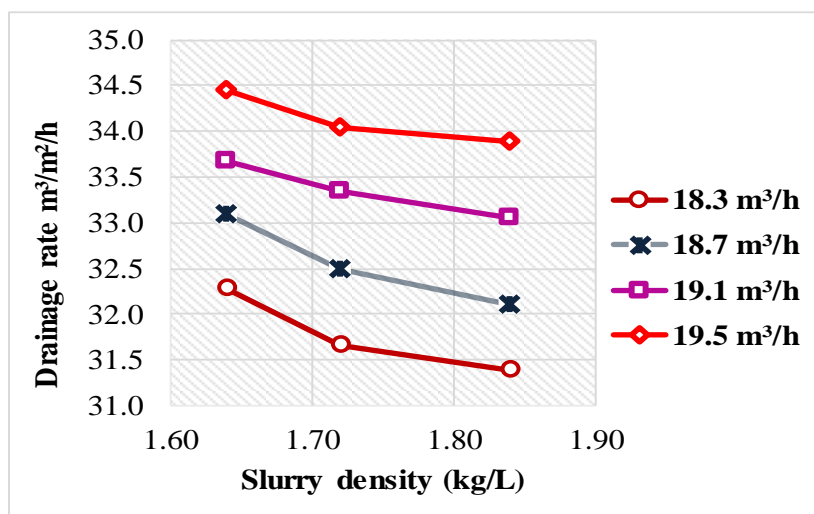


Figure 4-42: Effects of slurry density on magnetite drainage rate for 0.63x8.8 mm polyurethane panels

4.5.3 Influence of slot width on magnetite drainage rate

Figure 4-43 below shows the assessment of the influence of slot width increase from 0.63 to 0.8 mm on drainage rate using 0.8x8.8 mm and 0.63x8.8 mm screen panels at 1.64 kg/L slurry density. As the feed rate increased from 18.3 to 20.4 m³/h, there seemed to be very little to no difference in medium drainage rate from the two set of panels. Nonetheless, as the volumetric flowrate increased beyond 20.4 m³/h, there was an increase in the drainage rate of about 1.0 - 1.4 m³/m²/h with increase in slot width. Increase in slot width from 0.63 – 0.8 mm led to an increase in screen handling ability of about 0.39 m³/h. Comparable results obtained at 1.72 kg/L and 1.84 kg/L slurry density showed a similar trend, as shown in Appendix I. It can be hypothesised that the handling capacity of the two panels was the same at low volumetric flowrate below 20.4 m³/h. However, as the feed rate increased beyond the critical point, the increase in slot width played a significant role in medium drainage rate.

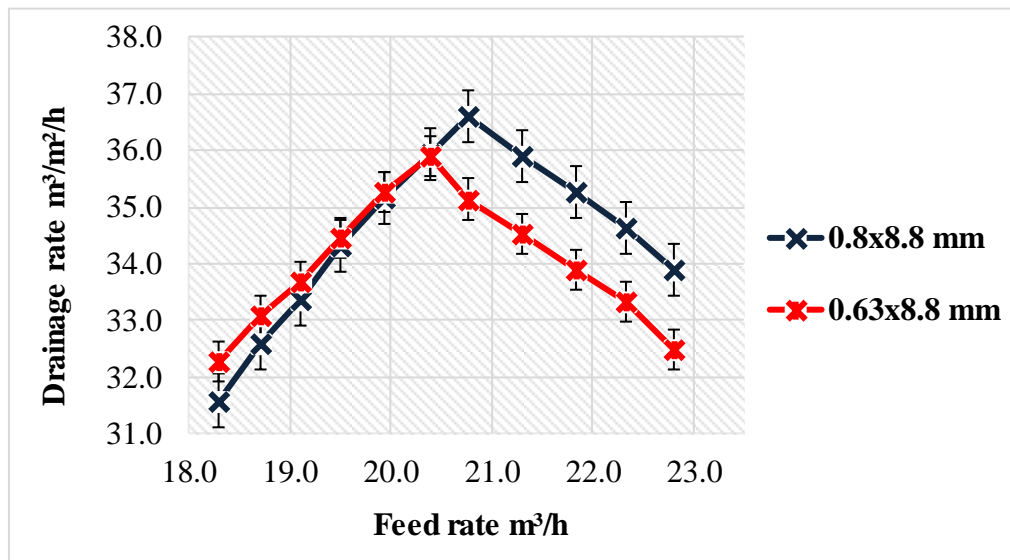


Figure 4-43: Influence of slot width on magnetite drainage rate at 1.64 kg/L slurry density

4.5.4 Influence of slot length on magnetite drainage rate

Figure 4-44 shows the assessment of the effects of slot length on medium drainage rate using 0.63x12 mm and 0.63x8.8 mm screen panels at 1.64 kg/L slurry density. It can be seen that increase in slot length from 8.8 to 12 mm had minimal influence on medium drain rate at a volumetric flowrate below 20.4 m³/h. However, the influence was significant at a flowrate above 20.4 m³/h with an increase in drainage rate of about 0.1 - 0.5 m³/m²/h. This could be due to a slight increase in screen handling capacity with slot length, hence, able to drain more medium.

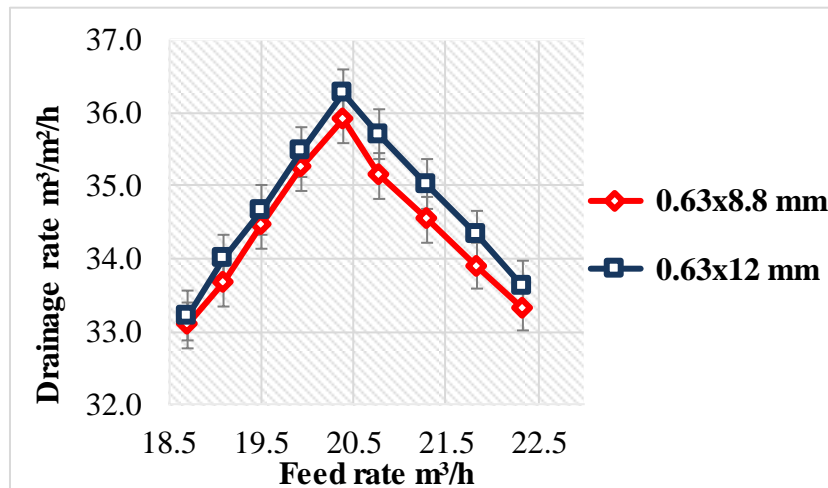


Figure 4-44: Influence of slot length on magnetite drainage rate at 1.64 kg/L slurry density

4.5.5 Effects of deflectors on magnetite drainage rate

Deflectors were installed in between the screen panels to assist in redirecting all the feed particles towards the middle of the screen surface for passage. These accessories are usually used on screen panels with low open area. While this was not part of the aims of the study, results were generated to establish the effects of these accessories on medium drainage rate. It is worth noting that no experimental works and results were found in the open literature regarding the influence of deflectors on medium drainage rate on a vibrating screen. Hence, the results discussed in this subsection contribute to an enhanced understanding of the influence of these accessories on drain rate on a drain and rinse vibrating screen.

Experiments were conducted with and without deflectors on the 1x13 mm screen panels and results obtained compared as shown in Figure 4-45. It can be seen that the use of deflectors led to an increase in drainage rate of about 0.73 – 0.93 m³/m²/h at volumetric flowrate below 20.8 m³/h. However, the influence of these accessories was more pronounced at volumetric flowrate above 20.8 m³/h with a considerable gain in drainage rate of about 0.90 – 1.35 m³/m²/h. The increase in drainage rate can be attributed to the channelling of all medium particles by the deflectors towards the screen holes, thereby, maximising the available screen apertures for passage. Similar trends obtained at 1.64 and 1.84 kg/L slurry densities showed an increase in medium drainage rate with the use of deflectors, as shown in Appendix J.

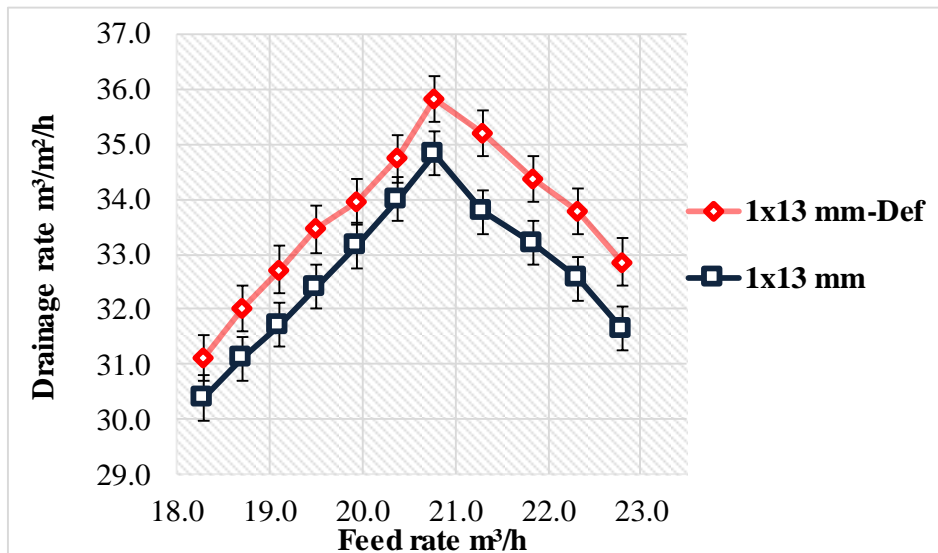


Figure 4-45: Effects of material deflectors on magnetite drainage rate for 1x13 mm screen panels at 1.72 kg/L slurry density

4.5.6 Effects of screen panel material on magnetite drainage rate

Figure 4-46 below shows a comparison of medium drainage rate for 1x12 mm rubber panels and 1x13 mm polyurethane panels. The 1x12 mm rubber panels showed a gain of about 0.91 – 1.70 m³/m²/h in drainage rate with increase in volumetric flowrate from 18.3 to 20.8 m³/h. The dominance in material recovery of this panel was noticed at volumetric flowrate above 20.8 m³/h with a further increase in drainage rate of up to 2.35 m³/m²/h. The 1x12 mm rubber panels also exhibited a higher handling capacity of about 0.5 m³/h than the 1x13 mm polyurethane panels. This can be attributed to high aperture flexibility, thence, able to recover more medium particles even at higher volumetric flowrate. Similar results were obtained at 1.64 and 1.84 kg/L slurry density as shown in Appendix K (a).

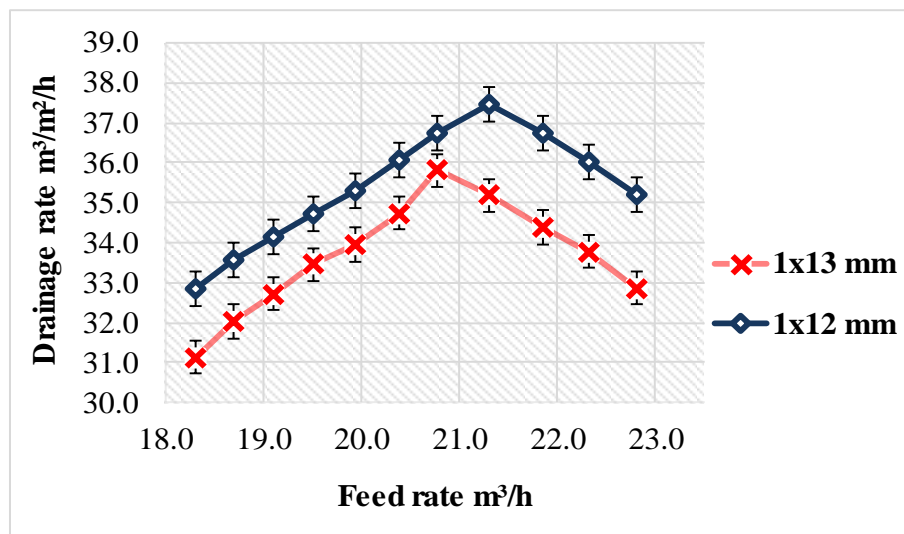


Figure 4-46: Effects of screen panel material on magnetite drainage rate at 1.72 kg/L

Figure 4-47 below shows a similar analysis done on the 0.63 mm poly-wedge wire and 0.63x12 mm polyurethane panels. Increase in medium recovery of about $0.35 - 0.54 \text{ m}^3/\text{m}^2/\text{h}$ was observed on polyurethane screen panels at volumetric flowrate between $18.3 - 20.4 \text{ m}^3/\text{h}$. This can be ascribed to the minimal friction created between the polyurethane panels and the slurry compared to the wedge wire (Drake 1988). However, above $20.4 \text{ m}^3/\text{h}$, the poly-wedge wire showed a higher material handling capacity of up to $0.9 \text{ m}^3/\text{h}$ than the 0.63x12 mm polyurethane panels, thus, able to sustain a higher feed rate with improved medium drainage rate of about $0.89 - 2.25 \text{ m}^3/\text{m}^2/\text{h}$. This can be attributed to the ability of the poly-wedge wire to withstand higher loads with higher precision in separating medium particles. On the other hand, the poly-wedge wire used had a continuous slot design, thus, offered particles more open space for separation. However, the 0.63 mm poly-wedge wire had an open area of about 0.79 % lower than the 0.63x12 mm panels. Hence, it can be deduced that open area does not entirely dictate the drain rate of magnetite on a vibrating screen. Related results were obtained at 1.64 and 1.72 kg/L slurry densities as shown in Appendix K (b).

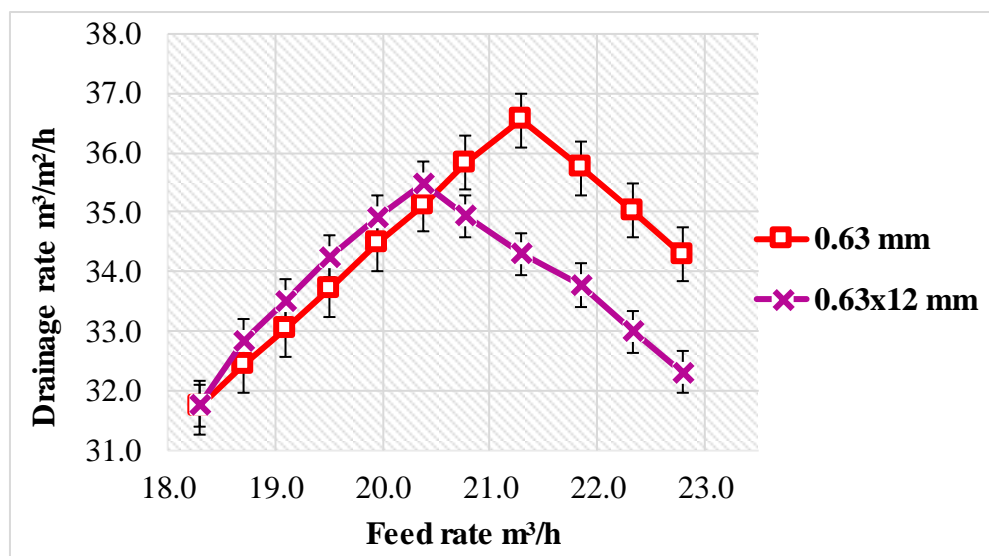


Figure 4-47: Effects of screen panel material on magnetite drainage rate at 1.84 kg/L slurry density

4.5.7 Influence of screening area on drainage rate

Figure 4-48 and Figure 4-49 shows a comparison of the current work screen set up using six panels with screen area of 0.511 m^2 and the work done by Combrick (2017) under Multotec using two panels with screen area of 0.186 m^2 . In both cases, magnetite was used for the experimental works with slot rubber panels, same flow direction of feed material and orientation of slot apertures with slurry density of 1.64 kg/L (current) and 1.6 kg/L (Multotec). Combrick (2017) showed that the Injection moulded 0.63x8.8 mm rubber panels

with a screen area of 0.186 m^2 provided an average drainage rate of $67.367 \text{ m}^3/\text{h}/\text{m}^2$ at 1.6 kg/L slurry density with a feed flow rate of $13.505 \text{ m}^3/\text{h}$. Further, a comparison of the drainage rate values for $1 \times 12 \text{ mm}$ rubber panels at 1.64 kg/L is presented for two panels (depicting Multotec's screening area) and six panels (for the current study), as shown in Table 4:3. It can be seen that the higher the available area for material separation, the lower the drainage rate value being reported in $\text{m}^3/\text{m}^2/\text{h}$. The screen area, therefore, has a considerable influence on drainage rate values being reported. While six panels were used for the current work, visual observation showed that most of the drainage occurred predominantly through the first two panels. Therefore, adjustment of the drainage rate values as per Tables 4:3 seems valid and shown in comparison to Combrick (2017). However, exact quantification of the percent draining occurring through the first set of panels compared to subsequent panels is recommended for future work.

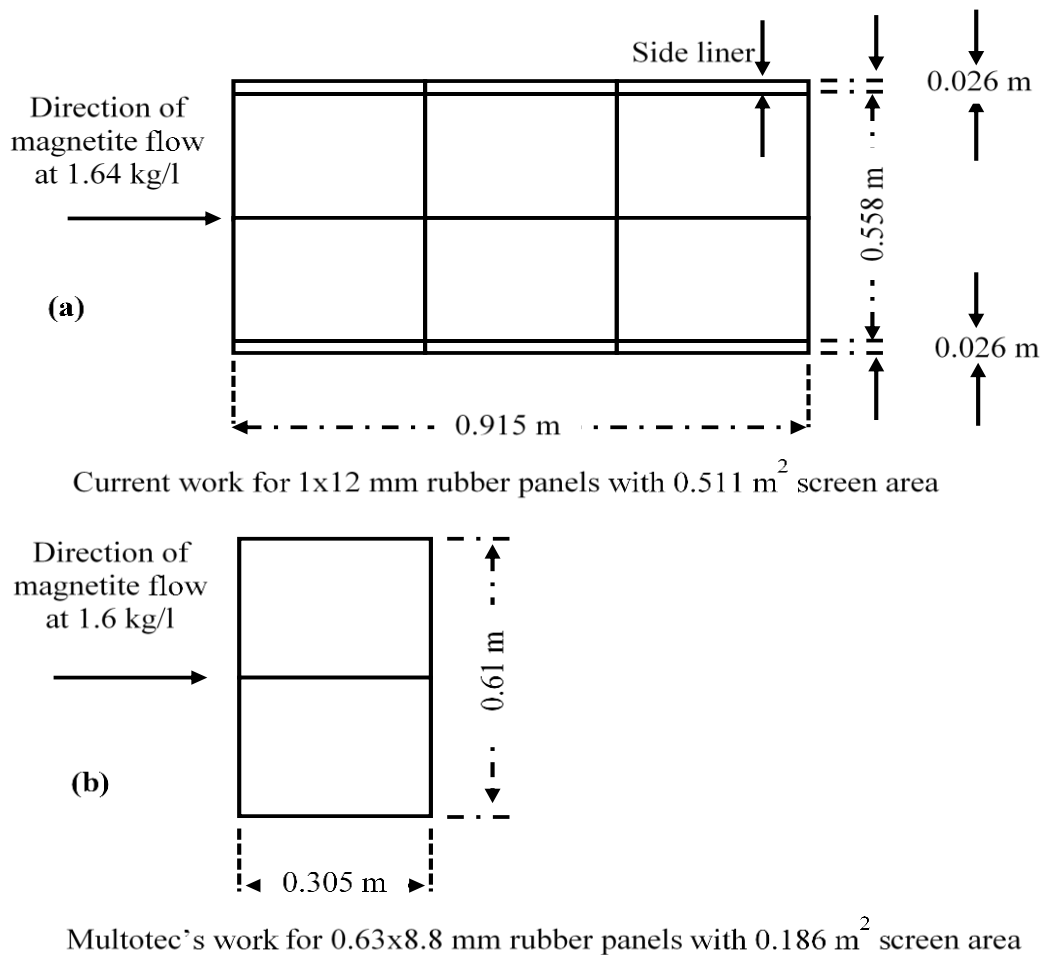


Figure 4-48: Comparison of the screen panel set up for multotec and current work

Table 4:3: Influence of screen area on drainage rate

1x12 mm rubber panels					
Density 1.64 kg/l		Screen area (m ²)			
Feed flowrate (m ³ /h)	Average drainage rate (m ³ /h)	0.511		0.186	
		Feed flowrate (m ³ /h/m ²)	Drainage rate (m ³ /m ² /h)	Feed flowrate (m ³ /h/m ²)	Drainage rate (m ³ /m ² /h)
18.3	16.9	35.8	33.1	98.4	91.0
18.7	17.3	36.6	33.9	100.5	93.1
19.1	17.5	37.4	34.3	102.7	94.2
19.5	17.9	38.2	35.0	104.8	96.0
19.9	18.2	39.0	35.6	107.2	97.9
20.4	18.7	39.9	36.6	109.6	100.4
20.8	18.9	40.7	37.0	111.7	101.8
21.3	19.3	41.7	37.8	114.5	104.0
21.8	19.0	42.7	37.1	117.4	102.0
22.3	18.7	43.7	36.5	120.1	100.4
22.8	18.2	44.6	35.6	122.6	97.9
23.3	17.8	45.6	34.9	125.2	95.9
23.7	17.4	46.3	34.1	127.2	93.7
24.1	17.0	47.2	33.4	129.6	91.6
24.5	16.5	48.0	32.2	131.7	88.6

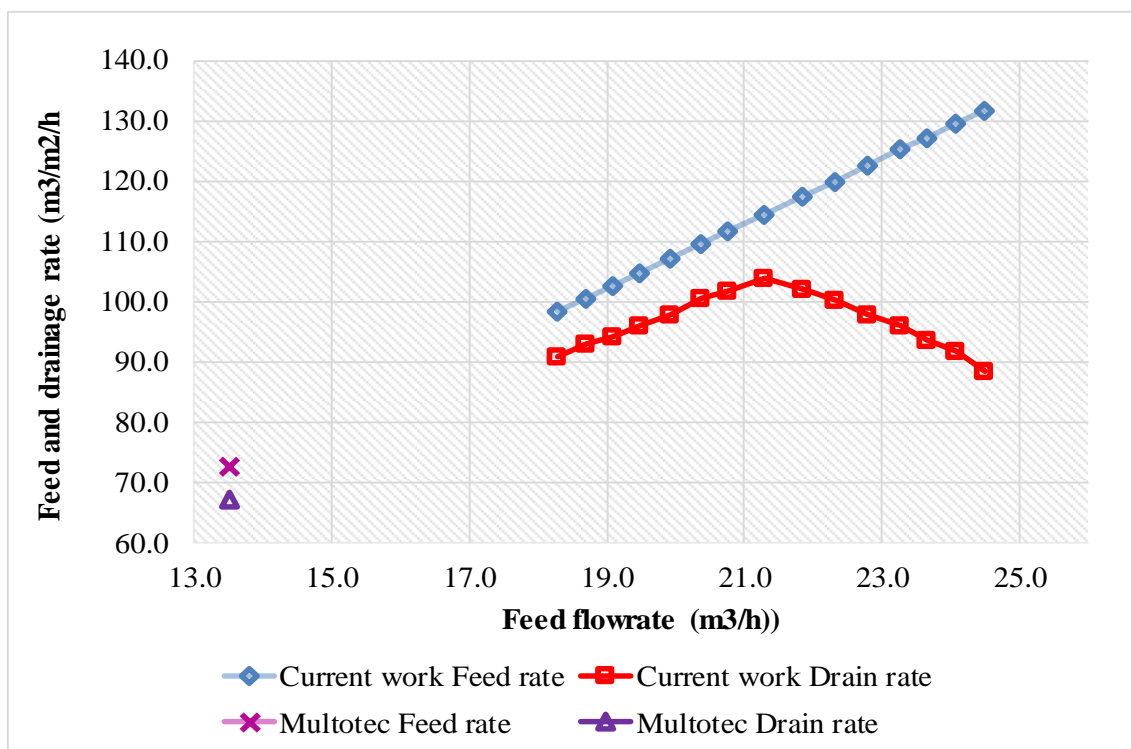


Figure 4-49: Drainage rate comparison between current and Multotec's work at 0.186 m² screen area for 0.63x8.8 mm (1.6 kg/L) and 1x12 mm (1.64 kg/L) rubber panels

4.5.8 Section summary

Increasing volumetric flowrate from 18.3 – 22.8 m³/h led to an increase in magnetite drainage rate up to a certain point and thereafter, a gradual drop in recovery was observed. The critical volumetric flowrates varied for different screen panels with 1x13 mm and 0.8x8.8 mm at 20.8 m³/h, 1x12 mm and 0.63 mm poly-wedge at 21.3 m³/h, and 0.63x12 mm and 0.63x8.8 mm at

20.4 m³/h. The difference in critical volumetric flowrates can be attributed to the difference in tonnage handling capacities for the different screen panels tested.

Increase in slot width from 0.63 to 0.8 mm had little to no influence on magnetite drainage rate at volumetric flowrate below 20.4 m³/h. However, an increase in the drainage rate of about 1.2 - 1.4 m³/m²/h was observed between 20.4 – 22.8 m³/h. On the other hand, increase in slot length from 8.8 to 12 mm had a minimal influence on magnetite drainage rate at volumetric flowrate below 19.94 m³/h. However, the effect was significant at flowrate between 19.94 – 22.8 m³/h with an increase in drainage rate of about 0.1 - 0.5 m³/m²/h. Increasing slurry density from 1.64 to 1.84 kg/L led to a gradual decrease in medium drainage rate for 1x12 mm, 1x13 mm, 0.63 mm and 0.8x8.8 mm panels. However, the 0.63x8.8 and 0.63x12 mm screen panels showed a sluggish reduction in drainage rate with increase in slurry density between 1.72 – 1.84 kg/L.

On the other hand, the 0.63x12 mm polyurethane screen panels showed an improvement in medium drainage rate of about 0.35 – 0.54 m³/m²/h at low volumetric flowrate between 18.3 - 20.4 m³/h over the 0.63 mm poly-wedge panels. However, 0.9 m³/h increase in material handling capacity was observed on the 0.63 mm poly-wedge wire at volumetric flowrate higher than 20.4 m³/h and hence, able to drain more medium particles of up to 2.25 m³/m²/h than the 0.63x12 mm panels. The 1x12 mm rubber panels showed a gain of about 0.91 – 1.70 m³/m²/h in drainage rate with increase in volumetric flowrate from 18.3 to 20.8 m³/h than the 1x13 mm panels with a further increase of up to 2.35 m³/m²/h accrued above 20.8 m³/h. In contrast, the 1x12 mm rubber panels exhibited a higher material handling capacity of about 0.5 m³/h than the 1x13 mm screen panels.

Inserting deflectors between screen panels led to an increase in drainage rate of about 0.73 – 0.93 m³/m²/h for volumetric flowrate between 18.3 - 20.8 m³/h. However, a considerable gain in drainage rate of about 0.90 – 1.35 m³/m²/h was observed beyond 20.8 m³/h feed rate. The increase in drainage rate can be attributed to the channelling of all medium particles by the deflectors towards the screen holes, thereby, maximising the available screen apertures for passage.

4.6 Partition curves

Efficiency curves are expediently used to demonstrate the separation efficiency of a separating surface on a size by size basis. They are basically used to represent a particular size fraction in the feed reporting either to the overflow or underflow stream (Svarovsky 1996). This is done by performing a mass balance of the material from feed, overflow and underflow

streams. Mass balancing is a technique mostly used in establishing a rational picture across a separator through data redundancy. This technique aims to assess the consistency and integrity of the experimental data collected and provide information on missing data. This was done using Microsoft Excel software, as shown Appendix T for 1x13 mm screen panels. To quantify the performance of each screen panel used in a manner that gave performance indicator values, a Whitten model was fitted to the balanced particle size distribution analysis for the feed, overflow, and underflow streams and partition curve parameters generated using excel solver to assess the influence of slurry density and volumetric flowrate on the recovery rate of medium. The three parameters extracted using the Whitten model in Equation 4.1 below included the cut size (D50), water split to the overflow stream (Rf) and sharpness of separation (α). However, partition curves were only generated for the experimental runs on ferrosilicon and iron, and results obtained compared. The Whitten model was used in the assessment of the screen performance as it offered a good representation of the partition curves for the current work. Besides, Hilden (2007) regarded this model as the most accurate mathematical screen model available in the literature compared to other physical separation models.

$$E_{oa} = 1 - C \left[\frac{(1 + \beta\beta^*X) * (e^\alpha - 1)}{e^{\alpha\beta^*X} + e^\alpha - 2} \right] \dots \dots \dots 4.1$$

Where;

E_{oa} = Actual separation efficiency of a particular size fraction to the oversize stream

R_f = Water split ratio to the overflow stream (1-C) and C = Water recovery to the overflow stream and $X = \frac{d_i}{D_{50c}}$

β = Parameter that corrects the initial rise in the curve (fish hook effect) and β^* = Fitting parameter introduced to preserve the D50c definition

An example of the efficiency curve from the experimental results is shown in Figure 4-50 for 1x13 mm screen panels at 1.9 kg/L slurry density. It can be seen that the experimental data fitted well with the predicted values using a Whitten model with no noticeable fish-hook behaviour exhibited. Authors who have premeditated on the fish-hook behaviour in physical separation have proposed dissimilar theories for its occurrence (Majumder et al. 2007; Nageswararao 2000; Hwang et al. 2008). However, Nageswararao (2000) noted that this phenomenon arises due to experimental errors. Whitten equation presented in Equation 4.1 uses β -parameter to define the fish-hook behaviour of a separating surface. High β -values

correspond to highly noticeable fish hook effect and a value of zero (0) as was the case with this thesis corresponds to a situation when there is no existence of fish hook behaviour.

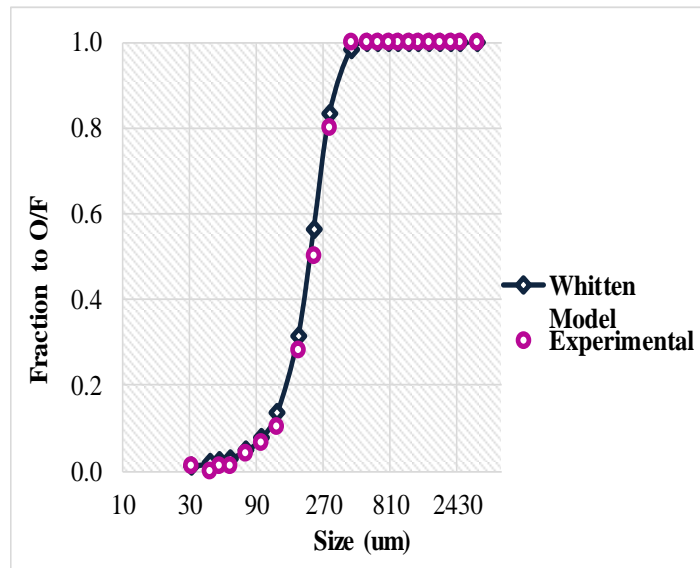


Figure 4-50: Actual efficiency curve vs Whitten model curve for 1x13 mm at 1.90 kg/L slurry density

Figure 4-51 below depicts an example of the efficiency curves obtained for 0.8x8.8 mm screen panels at different volumetric flowrates. As can be seen, an increase in volumetric flowrate from 21.8 – 25.1 m³/h led to a shift in the efficiency curve towards the finer side indicating an increase in medium carryover to the oversize stream with an increase in feed rate (Nageswararao 2000; Nageswararao 1999). The curve shifts to the left as the volumetric flowrate increases affects the cut size and the sharpness of separation of the screen panels.

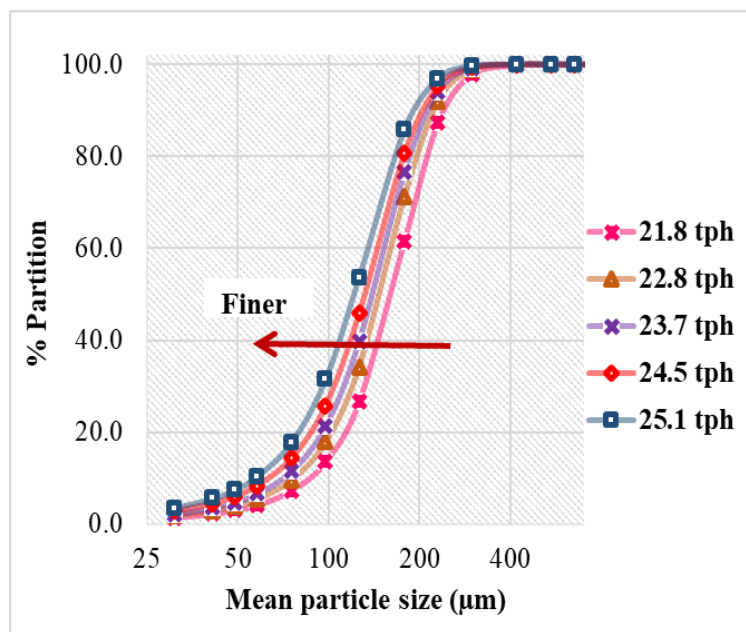


Figure 4-51: Effects of volumetric flowrate on partition curves for 0.8x8.8 mm polyurethane panels at 2.2 slurry density for degraded ferrosilicon

On the other hand, fine particles to the oversize stream increased with slurry density from 1.9 to 2.7 kg/L for 1x13 mm screen panels, as indicated in Figure 4-52 below. Regardless of the screen panel size used, higher slurry density and volumetric flowrate led to higher medium carryover to the overflow stream. High medium carryover to the overflow stream was expected under such extreme conditions of operation due to the formation of a thick closely packed bed of material on the screen surface (Mabote 2016). The formation of a thick bed of material led to a restriction in water flow due to reduced effective aperture size. Hence, a significant amount of medium bypassed to the overflow stream.

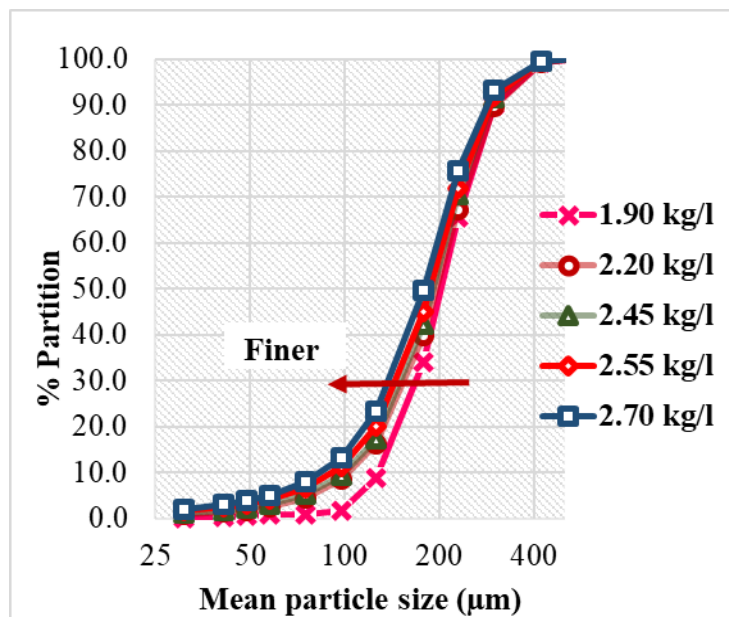


Figure 4-52: Effects of slurry density variation on efficiency curves for 1x13 mm polyurethane panels at 23.7 m³/hr volumetric flowrate for fresh ferrosilicon

However, the influence of aperture size variation on partition curve parameters was not considered in this analysis since the panel sizes used were bigger than the largest particle size of ferrosilicon. On the other hand, the change in material behaviour made it challenging to compare screen panel performance on PSD thoroughly. Besides, the excessive sieve blinding encountered during sieve analysis because of the presence of iron ore slimes made it difficult to adequately compare the effects of aperture size on partition curve parameters.

4.6.1 Effects of slurry density and volumetric flowrate on the efficiency curve parameters

Variations in solid concentration, aperture size and volumetric flowrate have been known to influence the efficient operation of a separating surface significantly. However, this subsection presents the effects of slurry density and feed rate on the partition curve parameters.

4.6.1.1 Effects of slurry density variation on the sharpness of separation (α)

The effect of varying slurry density on the sharpness of separation is provided in Figure 4-53 below for 1x13 mm polyurethane panels. It can be seen that as the slurry density increased from 1.9 to 2.7 kg/L, there was a gradual decrease in the sharpness of separation of the screen surface. However, a sharp reduction in alpha values was observed between 2.45 – 2.55 kg/L, after that, a gradual decrease in the efficiency of separation with increase in slurry density up to 2.7 kg/L was observed. Though with slight exceptions of 20.8 and 24.5 m³/h curves showing a sharp downward trend in alpha values beyond 2.55 kg/L. This indicates that the separation of medium particles at slurry density above 2.45 kg/L is poor regardless of the feed rate. At this point most of the material fed to the screen bypasses to the oversize without being separated. Hence, it can be deduced that reduced percent solids in the feed translates in improved screen performance and reduced medium carryover to the oversize stream.

The down ward trend in the efficiency of separation with an increase in slurry density can be attributed to increased restriction of medium flow through a bed of material. As the slurry density increased, there was a formation of a closely parked bed of material that restrained the presentation of medium particles onto the screen surface. Hence, high medium carryover to the overflow stream. The decline in the sharpness of separation with increase in slurry density was also observed by Mwale (2015) who did works on chromite ore.

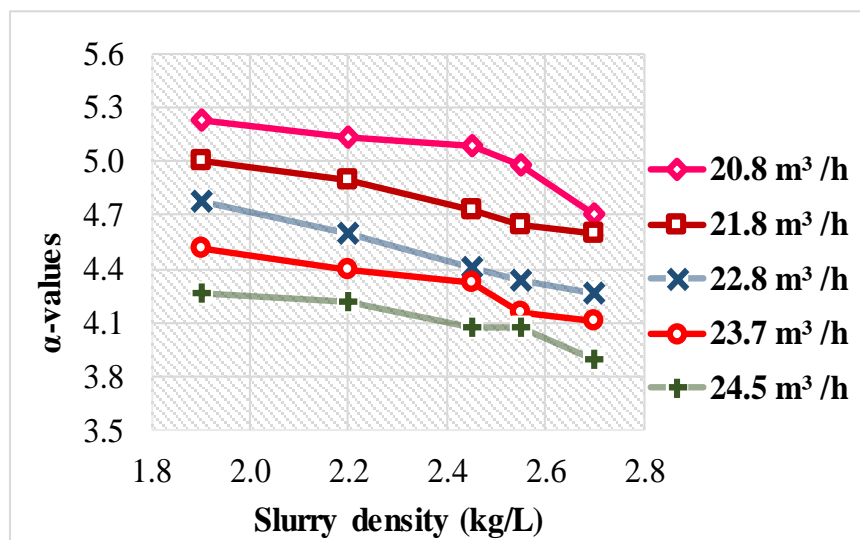


Figure 4-53: Effects of slurry density variation on the sharpness of separation for fresh ferrosilicon

4.6.1.2 Effect of slurry density variation on water split (Rf)

Using the water split ratio between the oversize stream and feed stream, an assessment of the effects of slurry density variation on water bypass to the oversize stream is shown in Figure

4-54 for 1x13 mm polyurethane panels. As the slurry density increased from 1.9 - 2.7 kg/L, there was a gradual increase in water bypass to the overflow stream with a sharp increase observed further than 2.45 kg/L. Valine et al. (2009) obtained a similar result and attributed this trend to the restricted flow of water as the bed of material thickens with increase in slurry density. An increase in slurry density reduced the porosity of the particle bed to the extent that only a small amount of water with the medium could pass through the screen holes. Hence, the sharp rise in water loss to the oversize stream beyond 2.45 kg/L (71 w/w% solids). A comparable result obtained for the same set of panels showed a sharp rise in moisture bypass above 2.45 kg/L slurry density, as discussed in section 4.3.2.2. The results obtained shows that regardless of the feed rate of material onto the screen surface, increase in slurry density leads to an increase in the amount of water reporting to the oversize stream and more pronounced above 2.45 kg/L.

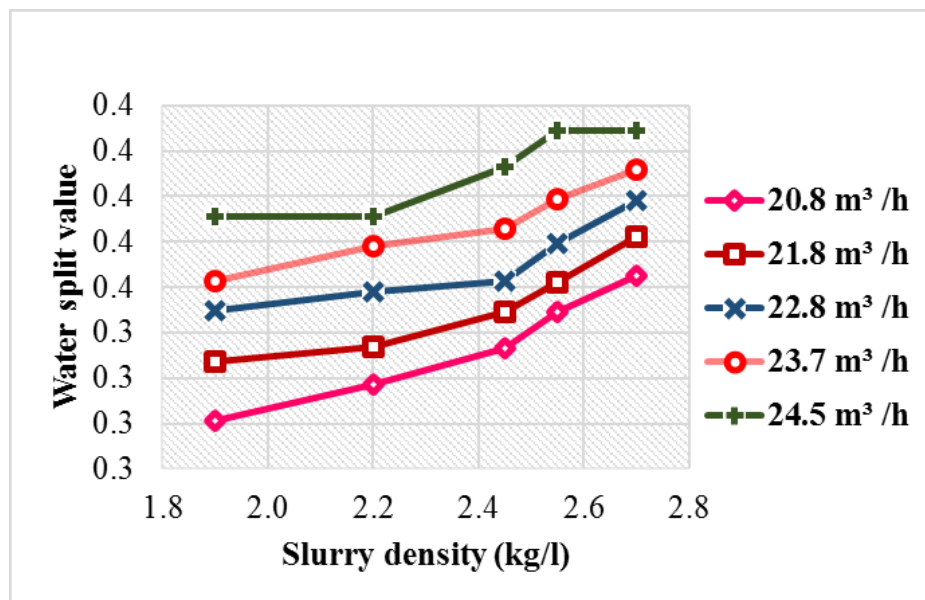


Figure 4-54: Effects of slurry density variation on water recovery to the oversize stream for fresh ferrosilicon

4.6.1.3 Effects of slurry density variation on cut size

Figure 4-55 shows the assessment of the effects of slurry density variation on cut sizes for 1x13 mm polyurethane panels. It can be seen that as the solid concentration increased from 1.9 – 2.45 kg/L, the cut size got finer postulating an increase in medium carryover to the oversize stream. The decrease in cut size can be accredited to the bed thickening with increase in slurry density and hence, dipping the effective aperture size (R.S. Rogers & Brame 1985). As can be seen that the cut size gets finer as the percent solids increases indicating poor screen performance. However, a sharp decrease in the cut size values was observed between

2.45 – 2.7 kg/L. This shows that the feed slurry density has a considerable influence on the performance of a separating surface and more pronounced at slurry density above 2.45 kg/L. This result is comparable with the moisture and medium carryover obtained on the same set of panels with a sharp increase beyond 2.45 kg/L for all the feed rates. It is worth noting that due to the PSD gap in iron ore and ferrosilicon, the cut sizes obtained using the Whitten model were not close to the screen aperture sizes used for the test work. However, this is not a good indication because each cut size is relative to the aperture size used.

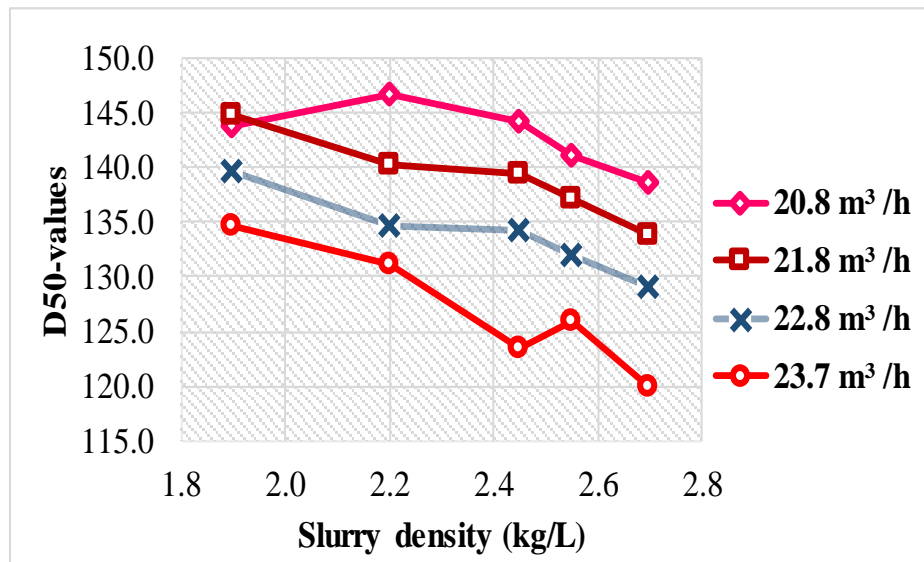


Figure 4-55: Effects of slurry density variation on cut size for fresh ferrosilicon

4.6.1.4 Effects of feed rate variation on the sharpness of separation (α)

Figure 4-56 shows the effects of volumetric flowrate variation on the sharpness of separation for 1x13 mm screen panels. Regardless of the slurry density, increase in feed rate from 21.2 – 24.1 m³/h led to a steady decrease in the sharpness of separation with a slight downward trend beyond 23.7 m³/h. At higher volumetric flowrate, the residence time of medium particles on the screen surface reduced, thus, limiting the probability of medium passage. This led to a higher amount of medium to the oversize and hence, a reduction in the sharpness of separation of the screen panels. The result obtained is similar with Valine & Wennen (2002) who established that increasing feed rate of material leads to an increase in fine particles misplacement and in turn decreasing the sharpness of separation. Hence it can be concluded that for an increase in volumetric flowrate below the screen critical point, there is a corresponding decrease in the efficiency of separation of medium particles even though an increase in drainage rate is observed. However, a poor separation of medium particles is observed beyond the screen critical point.

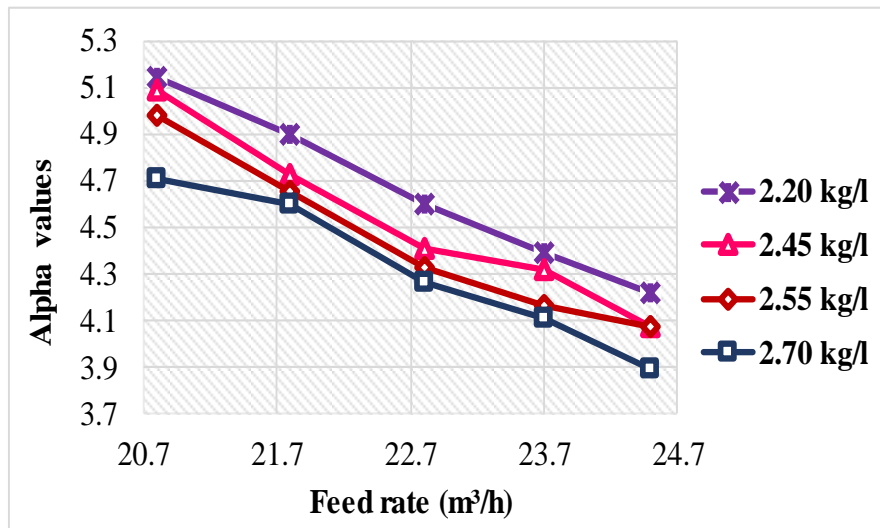


Figure 4-56: Effects of feed rate variation on the sharpness of separation for fresh ferrosilicon

4.6.1.5 Effects of feed rate variation on water bypass (Rf)

Owing to the influence of feed rate variation on the residence time of materials on the screen surface, higher water bypass was expected with increase in volumetric flowrate, as shown in Figure 4-57 below for 0.63x8.8 mm polyurethane panels. Increasing volumetric flow rate from 21.8 – 25.2 m³/h led to an increase in water bypass to the oversize stream. Similar result was obtained by Mabote (2016) who observed an increase in water bypass to oversize with increase in feed rate while working with UG2-chrome ore and attributed this trend to the reduction in material residence time. However, a sharp increase in water split was observed at volumetric flowrate between 22.8 – 25.1 m³/h. Hence, from the results presented, it can be deduced that feed rate of material onto the screen surface has a significant negative influence on the fraction of water that reports to the oversize stream regardless of the slurry density.

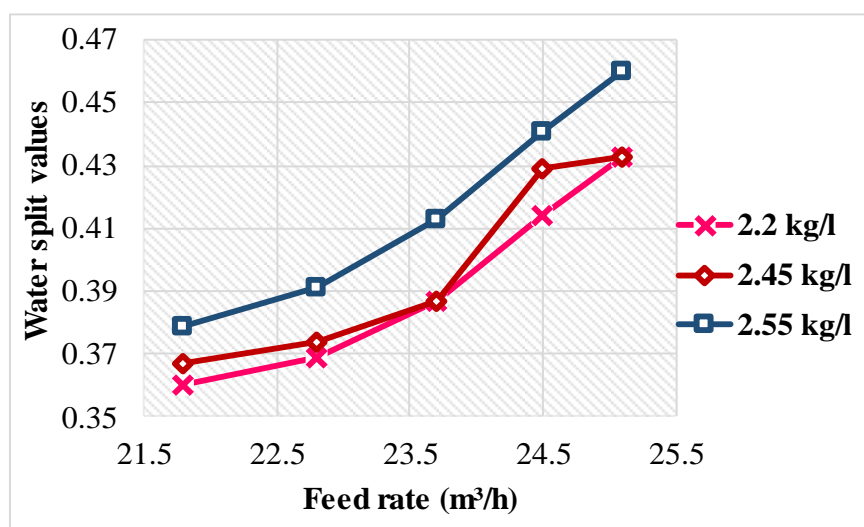


Figure 4-57: Effects of feed rate on water split for fresh ferrosilicon

4.6.1.6 Effects of feed rate variation on cut size

The influence of volumetric flowrate on the cut size is shown in Figure 4-58 below for 1x13 mm polyurethane panels. Increasing feed rate from 21.8 to 25.1 m³/h led to a decrease in the cut size, and more pronounced at feed rate beyond 23.7 m³/h. The reduction in the cut size values can be attributed to the increase in material load presented on to the screen surface with increase in feed rate. Higher feed rate coupled with higher slurry density leads to a formation of a thick bed of material on the screen surface that limits the percolation of fine particles through the pores created by coarse particles, thus, reducing the effective aperture size. At this point, most of the fine particles bypass to the overflow stream, hence, reducing medium cut size. Even though the results have shown decreasing cut size with increase in volumetric flowrate, the cut size decrease shown in Figure 4-55 is sharper with an increase in slurry density. Hence, it can be deduced that while there is a decrease in cut size with increase in feed rate indicating an increase in medium carryover to the oversize stream, the cut size is more sensitive to the slurry density than to the feed rate.

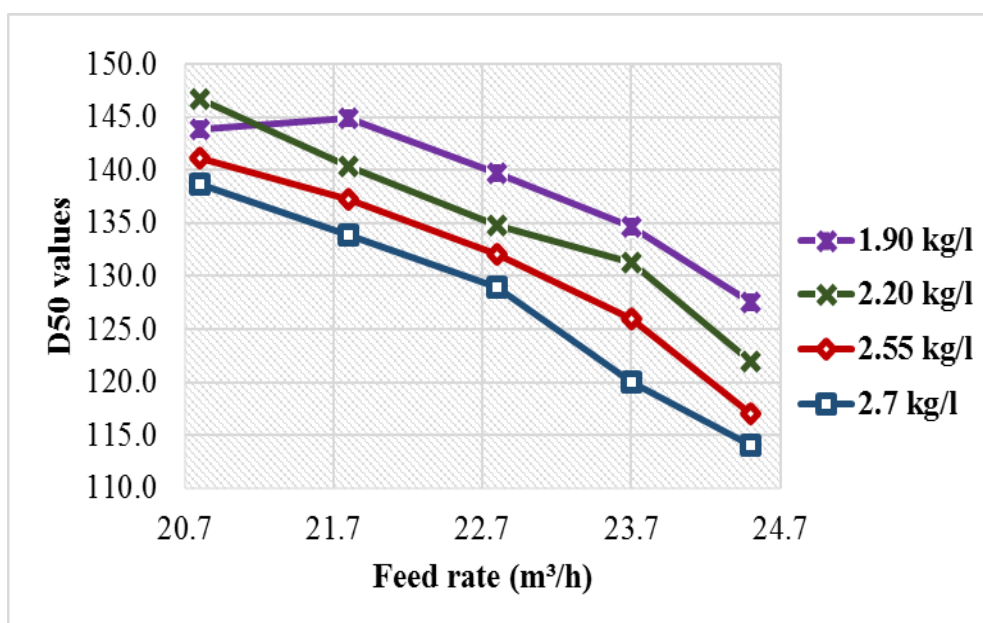


Figure 4-58: Effects of feed rate variation on cut size for fresh ferrosilicon

4.6.2 Section summary

Increase in slurry density from 1.90 to 2.45 kg/L led to a gradual decrease in the sharpness of separation and gradual increase in water bypass with cut sizes getting finer postulating a rise in medium carryover to the oversize. However, there was a slight sharp decline in the efficiency of separation and cut size values with a sharp increase in water bypass at slurry density between 2.45 – 2.7 kg/L. Increasing volumetric flowrate from 21.8 to 24.5 m³/h led to a gradual decrease in the sharpness of separation and cut size values with an increase in water

bypass to the oversize stream. From the results presented, it has been observed that increasing volumetric flowrate simultaneously reduces the cut size and the sharpness of separation of the screen panels while at the same time increasing the oversize water split ratio. This is a threefold negative effect on the performance of the screen panels.

4.7 Summary of results

The following observations were drawn from the results.

4.7.1 Ferrosilicon recovery

- 1) Increasing volumetric flowrate from 19.9 – 23.7 m³/h had a direct and positive impact on medium drainage rate. However, once a certain point was reached, a further increase led to a decrease in medium drainage rate. The critical volumetric flowrate was the same for all the panels tested on fresh ferrosilicon at 23.7 m³/h and 24.5 m³/h for degraded material. On the other hand, the increase in feed rate led to an increase in moisture and medium carryover to the overflow stream with a slight up-swing observed above 23.7 m³/h for fresh material and 24.5 m³/h for degraded material.
- 2) As the slurry density increased from 1.9 to 2.7 kg/L, there was a gradual decrease in medium recovery to the underflow stream up to 2.45 kg/L, and after that, a sharp drop in medium drainage rate was observed. This was accompanied by an increase in water and medium bypass, with a slight up-swing seen between 2.2 – 2.45 kg/L and after which, a sharp increase in moisture and medium carryover was observed. A comparable result obtained for the degraded material showed a marked decrease in medium drainage rate and an increase in the moisture and medium bypass to the oversize stream beyond 2.2 kg/L slurry density.
- 3) Aperture size increase from 0.63x8.8 to 1x13 mm led to a volumetric increase in drainage rate of about 1.4 - 1.9 m³/m²/h with a reduction in water and medium carryover of about 1.0 – 1.2 w/w% and 14.1 – 20.2 kg/t/m respectively.
- 4) Slot width increase from 0.63 – 0.8 mm led to an increase in medium drainage rate of about 0.5 – 0.9 m³/m²/h with a decrease in moisture and medium carryover of about 0.2 – 0.5 w/w% and 3.5 – 7 kg/t/m respectively.
- 5) 1x12 mm rubber panels drained more medium of about 3.3 – 3.8 m³/m²/h than the 1x13 mm polyurethane panels, resulting in a reduction in moisture and medium carryover of about 5.7 – 8.2 w/w% and 24.4 - 63.4 kg/t/m respectively, depending on the feed rate.
- 6) Medium degradation led to a decrease in drainage rate of about 6.8 - 9.3 m³/m²/h, resulting in an increase in moisture and medium carryover of about 8.9 – 13.9 w/w% and

64.4 – 108.1 kg/t/m respectively, with a sharp rise observed beyond the screen critical point.

- 7) The change in ferrosilicon behaviour on the screen surface was due to the presence of iron ore slimes, shear rate, oxidation of medium surface and ferrosilicon disintegration. According to Collins et al. (1974) the phenomenon of hydrogen evolution and medium surface oxidation is often encountered on large scale plants, especially after a settled medium has stood for some time in a storage vessel.
- 8) Ferrosilicon friability of about 11.7 – 18.3 % was seen after two (2) months of running the experiments. Iron disintegration was also observed owing to the presence of cavities on ore particles, thus, leading to aperture pegging on all the panels tested.
- 9) Degraded ferrosilicon had a viscosity of about 3 - 5 times that of the fresh material at low shear rate and slurry density between 2.0 – 2.2 kg/L. The difference rose sharply with further increase in shear rate and slurry density above 2.2 kg/L.
- 10) Fresh ferrosilicon showed a shear thinning effect (viscosity reducing with shear rate) with increase in shear rate. Degraded ferrosilicon, on the other hand, exhibited a shear thinning effect at shear rates below 50 s^{-1} , and after that, a slight shear thickening behaviour was observed.

4.7.2 Magnetite recovery

- 1) Increasing volumetric flowrate from 18.3 – 22.8 m^3/h led to an increase in medium drainage rate only upto the screen critical point and thereafter, a reduction in medium drainage rate was observed. Critical volumetric flowrates varied for different screen panels with 1x13 mm and 0.8x8.8 mm at 20.8 m^3/h , 1x12 mm rubber and 0.63 mm poly-wedge at 21.3 m^3/h , and 0.63x12 mm and 0.63x8.8 mm at 20.4 m^3/h .
- 2) Increase in slurry density from 1.64 to 1.84 kg/L led to a gradual decrease in medium drainage rate. The 0.63x8.8 and 0.63x12 mm screen panels, however, showed a sluggish reduction in drainage rate with increase in slurry density between 1.72 – 1.84 kg/L.
- 3) Increase in slot width from 0.63 to 0.8 mm had a minimal to no influence on drainage rate at volumetric flowrate between 18.3 - 20.4 m^3/h . However, an increase in the drainage rate of about 1.2 - 1.4 $\text{m}^3/\text{m}^2/\text{h}$ was seen between 20.4 – 22.8 m^3/h volumetric flowrate.
- 4) Increase in slot length from 8.8 to 12 mm had a minimal influence on medium recovery rate at volumetric flowrate below 19.94 m^3/h . However, the effect was significant at flowrate between 19.94 – 22.8 m^3/h with an increase in drainage rate of about 0.1 - 0.5 $\text{m}^3/\text{m}^2/\text{h}$.

- 5) Inserting deflectors between screen panels led to an increase in drainage rate of about $0.73 - 0.93 \text{ m}^3/\text{m}^2/\text{h}$ for volumetric flowrate between $18.3 - 20.8 \text{ m}^3/\text{h}$. However, a considerable gain in drainage rate of about $0.90 - 1.35 \text{ m}^3/\text{m}^2/\text{h}$ was observed beyond $20.8 \text{ m}^3/\text{h}$ feed rate.
- 6) The $1 \times 12 \text{ mm}$ rubber panels showed a gain of about $0.91 - 1.70 \text{ m}^3/\text{m}^2/\text{h}$ in drainage rate with increase in volumetric flowrate from 18.3 to $20.8 \text{ m}^3/\text{h}$. However, beyond a certain point ($20.8 \text{ m}^3/\text{h}$) for $1 \times 13 \text{ mm}$ screen panels, a further increase in drainage rate of up to $2.35 \text{ m}^3/\text{m}^2/\text{h}$ was accrued. On the other hand, the $1 \times 12 \text{ mm}$ rubber panels exhibited a higher material handling capacity of about $0.5 \text{ m}^3/\text{h}$ than the $1 \times 13 \text{ mm}$ screen panels.
- 7) The $0.63 \times 12 \text{ mm}$ polyurethane screen panels showed an improvement in medium drainage rate of about $0.35 - 0.54 \text{ m}^3/\text{m}^2/\text{h}$ at low volumetric flowrate between $18.3 - 20.4 \text{ m}^3/\text{h}$ over the 0.63 mm poly-wedge panels. However, $0.9 \text{ m}^3/\text{h}$ increase in material handling capacity was observed on the 0.63 mm poly-wedge wire at volumetric flowrate higher than $20.4 \text{ m}^3/\text{h}$ and hence, able to drain more medium of up to $2.25 \text{ m}^3/\text{m}^2/\text{h}$ than the $0.63 \times 12 \text{ mm}$ panels.

4.7.3 Partition curve parameters

- 1) Increase in slurry density from 1.90 to 2.45 kg/L led to a gradual decrease in the sharpness of separation with cut sizes getting finer postulating a rise in medium carryover to the oversize. However, there was a slight sharp decline in the efficiency of separation and cut size values at slurry density between $2.45 - 2.7 \text{ kg/L}$.
- 2) Slurry density increase from $1.9 - 2.45 \text{ kg/L}$ led to a gradual increase in water bypass with a sharp increase observed beyond 2.45 kg/L .
- 3) Increase in volumetric flowrate from 21.8 to $24.5 \text{ m}^3/\text{h}$ led to a gradual decrease in the sharpness of separation and cut size values with an increase in water bypass to the oversize stream

4 CONCLUSIONS AND RECOMMENDATIONS

The purpose of this thesis was to establish the effects of volumetric flowrate, slurry density and slot size on medium recovery in terms of drainage rate, percent moisture and medium carryover for ferrosilicon and iron, and drainage rate for magnetite. The thesis also incorporated the influence of ferrosilicon degradation and screen panel material on drainage rate, water, and medium carryover to the oversize stream. Furthermore, the influence of slurry density and volumetric flowrate on partition curve parameters i.e. sharpness of separation, cut size and water split ratio was also investigated. Thus, the section presents the conclusions and recommendations drawn from the experimental results.

5.1 Conclusions

In line with the objectives of the project, the following conclusions were drawn from the test results.

5.1.1 Effects of volumetric flowrate on medium recovery

An increase in volumetric flowrate leads to an increase in drainage rate up to the screen critical point, and after that, medium drainage rate reduces with an increase in medium and water bypass to the oversize stream. Hence, exceeding the capacity of a separating surface by overfeeding it leads to a reduction in medium drain rate. This is due to an increase in material transport on the screen surface, resulting in a decrease in medium residence time for passage and in turn, an increase in moisture and medium carryover, as part of the water and medium still trapped in the material bed bypass to the overflow stream with a slight up-swing beyond the screen critical point.

5.1.2 Effects of slurry density on medium recovery

During heavy medium separation, the amount of water in the fluid plays a significant role in the percolation path of fine particulate matter through a bed of material. Hence, the quantity of the fluid in the feed is critical in the efficient separation of medium particles. The results obtained showed that an increase in slurry density leads to a reduction in medium drainage rate with an increase in moisture and medium carryover, regardless of the feed rate and panel size. As the slurry density increases, there is a formation of a thick bed of material on the screen surface due to an increase in particle competition for passage and thus, reducing the fine particles' contact times with the screen surface. It is worth noting that as the solid concentration increases in a slurry, the particle bed of the material on a separating surface builds up faster and hence, easily exceeding the capacity of a screen even at low volumetric flowrate. Hence, any further increase in slurry density leads to a further reduction in medium drainage rate with an upswing in moisture and medium carryover to the oversize stream.

5.1.3 Combined effects of volumetric flowrate and slurry density on medium recovery

High volumetric flowrate and slurry density beyond the screen critical point leads to a decrease in medium drainage rate with an increase in percent moisture and medium carryover to the oversize stream. An increase in slurry density leads to an increase in the time needed for medium draining. Thus, coupled with a reduction in medium residence time due to higher volumetric flowrate, higher moisture and medium carryover to the overflow stream is probable. Whereas slurry density has a direct influence on screen capacity and feed rate on screen efficiency, improving the capacity of a screen without losing its efficiency is fundamental in heavy medium recovery.

5.1.4 Effects of aperture size on medium recovery

The increase in slot size i.e. length and width leads to higher drainage rate with a reduction in moisture and medium carryover to the oversize stream. The increase in medium recovery can be attributed to a reduction in material build up on the screen surface with increase in aperture size. Generally, the increase in screen aperture size leads to an increase in the screen's ability to handle a specific tonnage of feed material, thus, resulting in an increase in medium drain rate with a reduction in moisture and medium carryover to the oversize stream.

5.1.5 Effects of screen panel material on medium recovery

The influence of screen panel on medium recovery was investigated by comparing the performance of the 1x12 mm rubber panels with 1x13 mm polyurethane panels. It can be concluded that the use of rubber panels in comparison to polyurethane panels leads to an increase in medium drainage rate with a reduction in moisture and medium carryover to the overflow stream. The increase in medium drainage rate can be attributed to the higher aperture flexibility and elasticity of the rubber panels, thus, able to absorb the impact of material weight with a high precision in separating even near-size particles with minimal aperture pegging. At higher volumetric flowrate and slurry density, high moisture and medium carryover is expected as the medium becomes too viscous for the polyurethane panels to efficiently drain medium particles.

On the other hand, the performance of the 0.63 mm poly-wedge wire was compared to that of the 0.63x12 mm polyurethane panels. It can be concluded that the polyurethane panels drain more medium than the poly-wedge panels at volumetric flowrate below 20.4 m³/h due to the minimal friction created between the polyurethane panels and the medium particles. However, above the 20.4 m³/h feed rate, the 0.63 mm poly-wedge panels show a higher material handling capacity of up to 0.9 m³/h than the 0.63x12 mm polyurethane panels, thus, able to

sustain a higher feed rate with improved medium drainage rate. This is due to the ability of the poly-wedge wire to withstand higher loads with higher precision in separating medium particles.

5.1.6 Effects of particle curves on medium recovery

Increase in slurry density and volumetric flowrate leads to a reduction in the sharpness of separation and cut size, with an increase in moisture bypass to the oversize stream. A value higher than 4 for the sharpness of separation was obtained for most screen panels tested showing that separating devices tested were efficient in separating medium particles.

5.2 Recommendations

The following recommendations are drawn from the study for future work.

- 1) Based on the results presented, it is evident that medium degradation plays a significant role in the recovery of medium particles on the drain and rinse vibrating screen. Some of the causes were covered in this thesis, but more work is required so as to quantify the contribution of each variable on medium recovery and make recommendations of when replacement of medium should be done in an industrial plant.
- 2) Considering that excessive aperture pegging was observed across all the panels tested and more prominent at the feed end, an all-inclusive study on the effects of aperture pegging on medium recovery rate is recommended.
- 3) Considering that the screen critical points were the same for the panels tested on fresh and degraded ferrosilicon, further study is recommended to establish the fundamental principles behind the phenomenon.
- 4) Considering that only volumetric flowrate, aperture size and slurry density were investigated, additional tests works on screen performance using other feed and design conditions i.e. screen area, vibration intensity, angle of inclination of the screen and aperture shape are recommended to allow for enhanced understanding of medium recovery on a vibrating screen.

6 REFERENCES

- Albrecht, M.C., 1972. *Coal Preparation Processes*, Oakland, California. Available at: www.smartdogmining.com.
- Albrecht, M.C., 2013. *SDM Vibrating screens*, Available at: www.smartdogmining.com.
- Albuquerque, L.G., Wheeler, J. & Valine, S., 2008. Application of high frequency screens in closing grinding circuits. In *In International Mineral Processing Seminar– Gecamin*. United states of America, pp. 1–9.
- Alturki, A.A., Maini, B.B. & Gates, I.D., 2013. The effect of fracture aperture and flow rate ratios on two-phase flow in smooth-walled single fracture. *Journal of Petroleum Exploration and Production Technology*, 3(2), pp.119–132.
- Amiri, A., Nuland, S. & Johan, S., 2010. *Determining rheology for settling suspensions*, Ugelstad laboratory; department of chemical engineering, Trondheim, Norway.
- Anon, 1978. *VSMA-Screen calculation method: Selection of screen size and type*, Available at: [www.aggflow.com/help/en/content/vsma screen cal method.pdf](http://www.aggflow.com/help/en/content/vsma%20screen%20cal%20method.pdf).
- Aplan, F.F., Colijn, H. & Flintoff, B.C., 2003. *Principles of Mineral Processing* M. C. F. and K. N. Han, ed., Colorado, USA 80127: Society for Mining, Metallurgy, and Exploration, Inc.
- Barkhuysen, N.J., 2009. Implementing strategies to improve mill capacity and efficiency through classification by particle size only, with case studies. *The South African Institute of Mining and Metallurgy, Base Metal Conference*, pp.101–114.
- Beunder, E.M. & Rem, P.C., 1999. Screening kinetics of cylindrical particles. *International journal of mineral processing*, 57(June 1998), pp.73–81.
- Bevilacqua, P. & Ferrara, G., 1994. Technical note: Carry-over of water and suspension of fines by coarser particulate solids-Its influence on the design of DMS regeneration circuits. *Minerals Engineering*, 7(7), pp.943–949.
- Bosman, J., 2014. The art and science of dense medium selection. *Journal of the Southern African Institute of Mining and Metallurgy*, 114(November 2013), pp.529–536.
- Bowman, E.T., Saga, K. & Drummond, T.W., 2000. Particle shape characterisation using fourier analysis. *Geotechniques journal*, 51(6), pp.545–554.
- Boylu, F., Dincer, H. & Atesok, G., 2004. Effect of coal particle size distribution, volume fraction and rank on the rheology of coal – water slurries. *Fuel processing technology*, 85, pp.241–250. Available at: www.elsevier.com/locate/fuproc.

- Burke, T. & Craig, E., 2005. Getting the most out of your screening operations. *Minerals Engineering*, 1(5), pp.25–30.
- Carnes, B. & Olsen, L., 2001. *Screen capacity calculations* T-JCI-201st ed., JCI- an Astec company. Available at: www.vibfem.com.au/resources/vibrating_screens_and_screen_capacity.
- Chastont, I.R.M. & Napier-Munn, T., 1972. Design and operation of dense-medium cyclone plants for the recovery of diamonds in Africa. *Journal of the South African Institute of Mining & Metallurgy*, pp.120–133.
- Cheng, D.C., 1984. Further observation on the rheological behaviour of dense suspensions. *Powder Technology*, 37, pp.255–273.
- Christopher, B., 2013. *Modern american coal mining: Methods and applications*, Englewood, Colorado: Society for Mining, Metallurgy and Exploration inc, 2013.
- Cleary, P.W., Sinnott, M.D. & Morrison, R.D., 2009. Separation performance of double deck banana screens – Part 2 : Quantitative predictions. *Minerals Engineering*, 22(14), pp.1230–1244.
- Collins, B., Napier-Munn, T.J. & Sciarone, M., 1974. The production, properties and selection of ferrosilicon powders for heavy-medium separation. *Journal of the South African Institute of Mining & Metallurgy*, (December), pp.103–119.
- Combrick, B., 2017. *Multotec internal test work: drainage rate*, South Africa.
- DeCenso, A.J., 2000. *Dry Screening of Granular Solids*, Cincinnati: Rotex inc. Available at: www.che.com/dryscreeningofgranularsolids.
- Donaghy, S., 2016. *Pit and quarry lesson 8- Screening*, Available at: www.pitandquarry.com/lesson8.
- Dong, K.J. & Yu, A.B., 2012. Numerical simulation of the particle flow and sieving behaviour on sieve bend/low head screen combination. *Minerals Engineering*, 31, pp.2–9.
- Dong, K.J., Yu, A.B. & Brake, I., 2009. DEM simulation of particle flow on a multi-deck banana screen. *Minerals Engineering*, 22(11), pp.910–920.
- Drake, B., 1988. Screening out noise, dust problems. *An advanstar publication for Pit and quarry*, pp.1–3. Available at: www.pitandquarry.com/screeningoutnoisedustproblems.
- Drzymala, J., 2007. Mineral Processing-Foundations of theory and practice of minerallurgy. *Journal of Chemical Information and Modeling*, 53(9), pp.1689–1699.

- Drzymala, J. & Konopacka, Z., 2012. *Mining and Power Engineering Course : Screening and Sieving*, Development of potential and academic programmes of the Wroclaw University of technology.
- Fallon, N.E. & Gottfried, B.S., 1985. Statistical representation of generalized distribution data for float-sink coal-cleaning devices: Baum jigs, Batac jigs, Dynawhirlpools. *International Journal of Mineral Processing*, 15(3), pp.231–236.
- Feller, R., 1976. Screening duration and size distribution effects on sizing efficiency. *Journal of Agricultural Engineering Research*, 21(March), pp.347–353.
- Ferrara, G., Preti, U. & Schena, G.D., 1987. Computer-aided use of a screening process model. In *Proceeding of the Twentieth International Symposium on the Application of Computers and Mathematics in the Mineral Industries. Johannesburg: SAIMM*, pp. 153–166.
- Ferrara, G., Preti, U. & Schena, G.D., 1988. Modelling of Screening Operations. *International Journal of Mineral Processing*, 22, pp.193–222.
- Firth, B. & O'Brien, M., 2000. Some aspects of banana screen operations. In *International coal preparation congress 2010: conference proceedings: XVI ICPC*. pp. 231–241.
- Firth, B., Vince, A. & Lees, G., 2012. Prediction of the performance of dense medium cyclones in coal preparation. *Minerals Engineering*, 31, pp.59–70.
- Fourie, P.J., Walt, P., Van der & Falcon, L., 1980. The beneficiation of fine coal by dense-medium cyclone. *The South African Institute of Mining and Metallurgy*, (October), pp.357–361.
- Franck, A., 1964. *Understanding Rheology of Structured Fluids*, Available at: www.tainstruments.com/pdf/literature/AAN016_V1_U_Structfluid.pdf.
- Glastonbury, J.R. & Jansen, M., 1967. The size separation of particles by screening. *Powder Technology*, 1(6), pp.334–343.
- Govender, A. & Van Dyk, J.C., 2003. Effect of wet screening on particle size distribution and coal properties. *Fuel processing technology*, 82(18), pp.2231–2237.
- Grobler, J.D., Sandenbergh, R.F. & Pistorius, P.C., 2002. The stability of ferrosilicon dense medium suspensions. *The South African Institute of Mining and Metallurgy*, (March), pp.83–86.
- Grozubinsky, V., Sultanovitch, E. & Lin, I.J., 1998. Efficiency of solid particle screening as a function of screen slot size, particle size, and duration of screening: The theoretical approach.

International Journal of Mineral Processing, 52(4), pp.261–272.

Guerreiro, F.S., Gedraite, R. & Ataide, C.H., 2015. Residual moisture content and separation efficiency optimization in pilot-scale vibrating screen. *Powder Technology*, 287, pp.301–307.

Gupta, A. & Yan, D.S., 2006. Introduction to mineral processing design and operation. In *Mineral processing design and operation*. pp. 293–353.

Hailin, D., Chusheng, L. & Yuemin, Z., 2013. Influence of vibration mode on the screening process. *International Journal of Mining Science and Technology*, 23(1), pp.95–98.

He, Y.B. & Laskowski, J.S., 1994. Effect of dense medium properties on the separation performance of a dense medium cyclone. *Minerals Engineering*, 7(2-3), pp.209–221.

Hilden, M.M., 2007. *Dimensional analysis approach to the scale-up and modelling of industrial screens*. University of Queensland.

Holt, E.C., 1978. An engineering/economical analysis of the coal preparation plant operation and cost. In *Interagency energy/environment R&D program report*. Washington, D.C: Hoffman-Muntner Corp, Silver spring for U.S. Environmental protection agency-Office of energy, minerals and industryresearch and development, pp. 1–297.

Hudson, R., Jansen, M. & Linkson, P., 1969. Batch sieving of deep particulate beds on a vibratory sieve. *Powder Technology*, 2(4), pp.229–240.

Hwang, K.-J., Wu, W.-H. & Qian, S., 2008. CFD Study on the effect of hydrocyclone structure on the separation efficiency of fine particles. *Separation Science and Technology*, 43(March 2015), pp.3777–3797.

Jiang, J., Liu, Y. & Zhang, X., 2013. Shear thinning and shear thickening characteristics in electrorheological fluids. *Smart materials and structures*, (23), pp.1–9.

Kawatra, S. & Eisele, T., 1988. Rheological effects in grinding circuits. *Separation Science and Technology*, 22, pp.251–259.

Kindig, J.K., 1998. Coal cleaning process. *United states patent office-US 5,794,791*, 177(1939), pp.220–239.

King, R., 2000. *Technical Notes 4 - Vibrating Screens*, Available at: www.mineraltech.com/MODSIM/Modsimtraining/modules/vibratingscreen.pdf.

Korte, G.J. De, 2008. *Dry screening tests conducted with Bivi-tec screen*, South Africa: Coaltech (CSIR/NRE/MIN/ER/2008/0075/A).

Korte, G.J. De, 2000. *Literature review of dense-medium beneficiation of fine coal*, South

Africa: Coaltech 2020.

De Korte, G.J., 2008. The Influence of near-dense material on the separation efficiency of dense-medium processes. *International Journal of Coal Preparation and Utilization*, 28(2), pp.69–93.

Kwade, A., H.G, J. & T, M., 2012. *Mineral, renewable and secondary raw material processing-current engineering challenges*, Frankfurt, Germany: ProcessNet Subject division.

De Lange, T. & Venter, P.E., 1987. The use of simulation tromp partition curves in developing the flowsheet of plant extensions at grootegeluk coal mine. In *20th APCOM Symposium*. pp. 295–311.

Lawire, A.E. & Needham, L.W., 1949. Separation of solid materials of different specific gravities. *United states patent office-US 2,621,790 A*, pp.1–15.

Lawrence, L.R. & Beddow, J.K., 1969. Powder segregation during die filling. *Powder Technology*, 2(5), pp.253–259.

Levoguer, C., 2013. Using laser diffraction to measure particle size and distribution. *Powder Technology*, 68(3), pp.15–18.

Li, Z. & Tong, X., 2015. A study of particles penetration in sieving process on a linear vibration screen. *Coal science technology*, 18(2 (4)), pp.299–305.

Li, Z., Tong, X. & Wang, X., 2015. Modeling and parameter optimization for the design of vibrating screens. *Minerals Engineering*, 83, pp.149–155.

Liu, K., 2009. Some factors affecting sieving performance and efficiency. *Powder Technology*, 193(2), pp.208–213.

Luckham, P.F. & Ukeje, M.A., 1999. Effect of Particle Size Distribution on the Rheology of Dispersed Systems. *Colloid and interface science*, 356, pp.347–356.

Ma, Z., Merkus, H.G. & Smet, J., 2000. New developments in particle characterization by laser diffraction : size and shape. *Powder Technology*, pp.66–78.

Mabote, S., 2016. *Development of a wet fine screen model integrating the effect of operating and design variables on screening performance*. Department of Chemical engineering, Cape town university.

Majumder, A.K., Shukla, P. & Barnwal, J.P., 2007. Effect of operating variables on shape of ‘fish-hook’ curves in cyclones. *Minerals Engineering*, 20(2), pp.204–206.

Makinde, O.A., 2014. *Functionality assessment of a reconfigurable vibrating screen*.

Department of Industrial engineering, Tshwane university of technology.

Makinde, O.A., Ramatsetse, B.I. & Mporu, K., 2015. Review of vibrating screen development trends: Linking the past and the future in mining machinery industries. *International Journal of Mineral Processing*, 145, pp.17–22.

Mangesana, N., Chikuku, R.S. & Mainza, A.N., 2008. The effect of particle sizes and solids concentration on the rheology of silica sand based suspensions. *The South African Institute of Mining and Metallurgy*, (April), pp.237–243.

Mariki, D.J., 2000. *Laboratory Testing Manual*, Dar es Salaam: The republic of Tanzania, Ministry of works.

Marot, P., 1960. Process of separating mixtures of particles. *United states patent office- US 2,932,395 A*.

Marsh, C., 1945. Heavy media separation process for assorting solids. *United states patent office- US-2,496,590 A*, 1.

Mbuyi, N.M., Randigwane, A. & Mulaba, A.F., 2014. Technological assessment of product screens performance. *International journal of research in chemical, metallurgical and civil engineering (IJRCMCE)*, 1(1(2014)), pp.61–65.

Metso, 2008. *Operating green and efficient with vibrating screens*, Available at: www.metsominerals.com.

Mikli, V., Kaerdi, H. & Besterici, M., 2001. Characterisation of powder particle morphology. *Materials technology*, pp.22–34.

Mohanty, M.K., 2003. Fine coal screening performance enhancement using the Pansep screen. *International Journal of Mineral Processing*, 69(1-4), pp.205–220.

Mohanty, M.K., Palit, A. & Khanna, N., 2003. Models for predicting the performance of a linear screen. *Coal Preparation and utilisation*, 23(4), pp.213–235.

Mwale, A. ntaja, 2015. *A mathematical model for predicting classification performance in wet fine screens*. Department of Chemical engineering, University of cape town.

Nageswararao, K., 2000. Critical analysis of the fish hook effect in hydrocyclone classifiers. *Chemical engineering*, 80(1-3), pp.251–256.

Nageswararao, K., 1999. Reduced efficiency curves of industrial hydrocyclones - an analysis for plant practice. *Minerals Engineering*, 12(5), pp.517–544.

Napier-Munn, T.. & Scott, I., 1990. The effect of demagnetisation and ore contamination on

the viscosity of the medium in a dense medium cyclone plant. *Minerals Engineering*, 3(6), pp.607–613.

Napier-Munn, T.J., Kojovic, T. & Scott, I.A., 1995. Some causes of medium loss in dense medium plants. *Minerals Engineering*, 8(6), pp.659–678.

Noble, A. & Luttrell, G.H., 2015. A review of state-of-the-art processing operations in coal preparation. *International Journal of Mining Science and Technology*, 25(4), pp.511–521.

O'Brien, M. & Firth, B., 2005. *Factors influencing the drain and rinse operation of banana screens*, Wilmington: Australian coal research limited. Available at: www.coalage.com.

O'Brien, M. & Firth, B., 2015. *Improved Performance of Banana Screens in Drain and Rinse*, Australian coal research limited. Available at: <https://www.acarp.com.au/abstracts.aspx?repld=C8042>.

O'Brien, M., Firth, B. & Mardel, J., 2010. Predictive control of screen process efficiency. *Coal Preparation and Utilization*, 30(2-5), pp.83–99.

Olhero, S.M. & Ferreira, J.M.F., 2004. Influence of particle size distribution on rheology and particle packing of silica-based suspensions. *Powder Technology*, 139, pp.69–75.

Ondrias, L., 1990. *Solutions for dry fines screening*, Cincinnati, United states of America: Tema isenmann manufacturing plant. Available at: www.aggman.com/solutionsfordryfinesscreening.

Parlar, J., 2010. *Vibration analysis and vibrating screen: theory and practice-Phd*. Software engineering-Graduate studies, McMaster University.

Pieterse, D.P., 1992. Dry screening of fine coal. In *Beltcon 8 conference*. Sastech engineering services, mechanical engineering department, pp. 1–22.

Plitt, L.R., Conil, P. & Broussaud, A., 1990. An improved method of calculating the water-split in hydrocyclones. *Minerals Engineering*, 3(5), pp.533–535.

Poletto, M. & Joseph., D.D., 1995. The effect of density and viscosity of a suspension. *Journal of Rheology*, 39(2), pp.323–343.

Preti, G. & Ferrara, U., 1975. A contribution to screening kinetics. In *11th International Minerals Processing Congress*. pp. 1–35.

Rogers, R.S.. & Brame, K.A., 1985. An analysis of the high-frequency screening of fine slurries. *Powder Technology*, 42, pp.297–304.

Rogers, R.S.C., 1982. A classification function for vibrating screens. *Powder Technology*,

31(1), pp.135–137.

Roller, W.L. & Hazleton, P., 1952. Method and apparatus for gravity separation of coal and other minerals. *United states patent office- US-2,738,069*.

Satyenda, 2015. Screening of materials and types of screens. Available at: www.ispatguru.com/screening_of_materials_and_types_of_screens.

Sawant, A.G., Mohan, M. & Ashok, S.S., 2016. Study and analysis of deck inclination angle on efficiency of vibration Screen. *international journal of engineering development and research*, 4(1), pp.631–635. Available at: www.ijedr.org.

Schlemmer, G., 2010. *Principles of screening and sizing*, Quarry academy. Available at: https://www.911metallurgist.com/blog/wp/principles_of_screening_and_sizing.pdf.

Schlemmer, G., 2016. *Screening for maximum accuracy*, Quarry academy. Available at: https://www.911metallurgist.com/blog/crushing_by/screening_for_maximum_accuracy.pdf.

Schumacher, B.A., Shines, K.C. & Burton, J.V., 1990. *A comparison of soil sample homogenization techniques*, Lockheed Engineering and Sciences Company, Inc.

Sciarone, M., 1976. *The production of ferrosilicon powder for heavy-medium separation*, South Africa: Metallloys Limited. Available at: www.pyrometallurgy.co.za/infaconl/057-sciarone.pdf.

Shi, F., 2016. Determination of ferrosilicon medium rheology and stability. *Minerals Engineering*, 98, pp.60–70.

Shi, F.N. & Napier-Munn, T., 2002. Effects of slurry rheology on industrial grinding performance. *Mineral Processing*, 65, pp.125–140.

Soldinger, M., 2000. Influence of particle size and bed thickness on the screening process. *Minerals Engineering*, 13(3), pp.297–312.

Soldinger, M., 1999. Interrelation of stratification and passage in the screening process. *Minerals Engineering*, 12(5), pp.497–516.

Sripriya, R., Banerjee, P.K. & Rao, M.V.S., 2001. Critical evaluation of factors affecting the operation of dense medium cyclones treating medium coking coals. *Mineral Processing*, 63(4), pp.191–206.

Sripriya, R., Bapat, J.P. & Singh, N.P., 2003. Development of an alternative to magnetite for use as heavy media in coal washeries. *Mineral Processing*, 71(1-4), pp.55–71.

Sripriya, R., Dutta, A. & Narasimha, M., 2006. An analysis of medium losses in coal washing

plants. *Mineral Processing*, 80, pp.177–188.

Stairs, D., 2014. Screening 101-An introduction to the principles and importance of proper screening. Available at: www.aeisccreens.com.

Standish, N., Bharadwaj, A.K. & Hariri-Akbari, G., 1986. A study of the effect of operating variables on the efficiency of a vibrating screen. *Powder Technology*, 48(2), pp.161–172.

Subasinghe, G., Schaap, W. & Kelly, E.G., 1989. Modelling the screening process: A probabilistic approach. *Powder Technology*, 59, pp.37–44.

Subasinghe, G.K.N.S., Schaap, W. & Kelly, E.G., 1989. Modelling the screening process - an empirical approach. *Minerals Engineering*, 2(2), pp.235–244.

Sullivan, J. w., Hill, R.M. & Sullivan, J.F., 1990. The place of trommel in resource recovery. In *National waste processing conference*. Dallas, Texas, United States of America: Triple/S Dynamics, Inc, pp. 1–8.

Sullivan, J.F., 2013. *Screening theory and practice*, Dallas, Texas, United states of America: Triple/S dynamics services, inc.

Svarovsky, L., 1996. *Solid to liquid separation* 4th editio., FPS Institute, University of Pardubice, Czech Republic.

Trumic, M. & Magdalinovic, N., 2011. New model of screening kinetics. *Minerals Engineering*, 24(1), pp.42–49.

Tsakalakis, K., 2001. Some basic factors affecting screen performance in horizontal vibrating screens. *The European Journal of Mineral Processing and Environmental Protection*, 1, pp.42–54.

Valine, S.. & Wennen, J.E., 2002. Fine Screening in Mineral Processing operations. In *In A. L. Mular, D. N. Halbe, & D. J. Barret, eds. Mineral processing plant design, practice and control. Colorado: Sme/Aimme, pp. 917–928.*

Valine, S.B., Wheeler, J.E. & Albuquerque, G., 2009. Fine sizing with the derrick stack sizer screen. In *Recent Advances in Mineral Processing Plant Design. SME*, pp.433–443.

Vorster, W., Hinde, A. & Schiefer, F., 2002. Increased screening efficiency using a Kroosher unit coupled with a Sweco screen (Part 1). *Minerals Engineering*, 15(1-2), pp.107–110.

Walker, G.B., 1943. Heavy media separation process. *United states patent office- US-2,387,866*.

Wang, G. & Tong, X., 2011. Screening efficiency and screen length of a linear vibrating

screen using DEM 3D simulation. *Mining Science and Technology (China)*, 21(3), pp.451–455.

Williams, R.A. & Kelsall, G.H., 1992. Degradation of ferrosilicon media in dense medium separation circuits. *Minerals Engineering*, 5(I), pp.57–77.

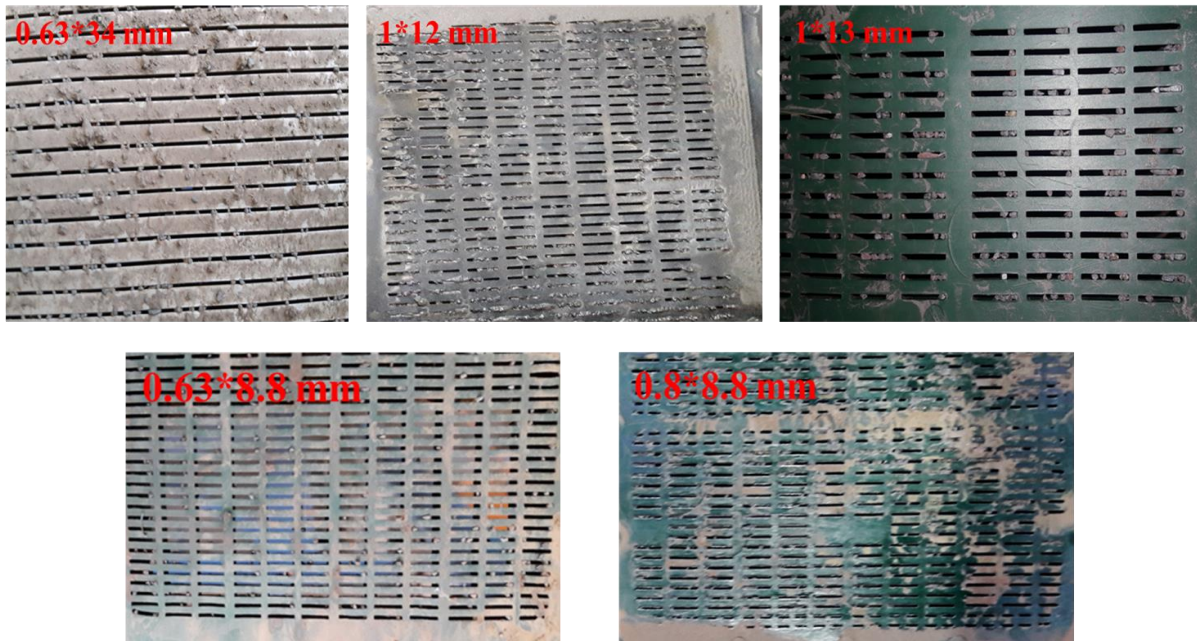
Wills, B.A., 1985. *Mineral processing technology* 3rd edition. D. W. HOPKINS, ed., Pergamon Press.

Wills, B.A. & Napier-Munn, T., 2006. *Mineral processing technology-An introduction to the practical aspects of ore treatment and mineral processing* 7th edition., Elsevier Science & Technology Books.

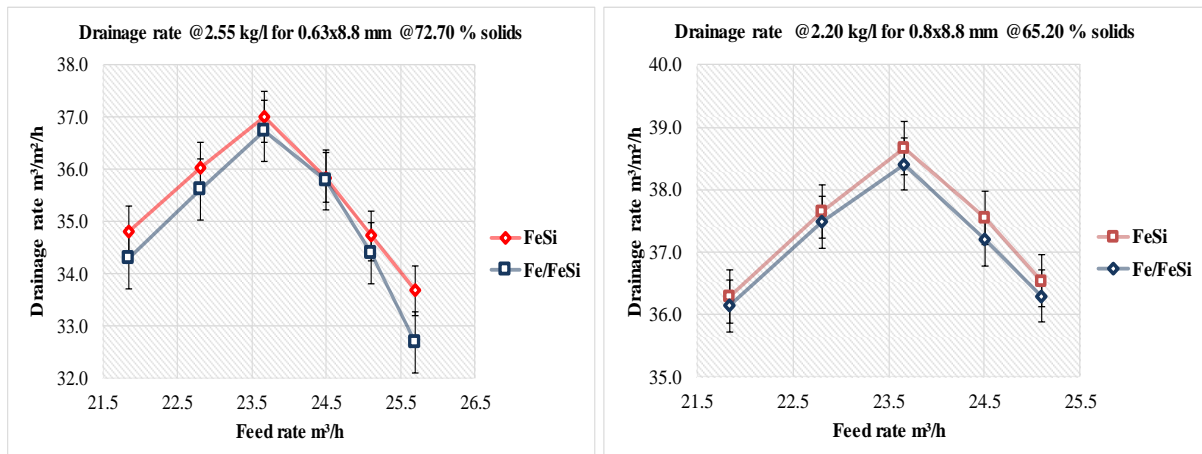
Wodzinski, P., 2003. Screening of fine granular material. *Coal Preparation and utilisation*, 23(4), pp.183–211.

7 APPENDICES

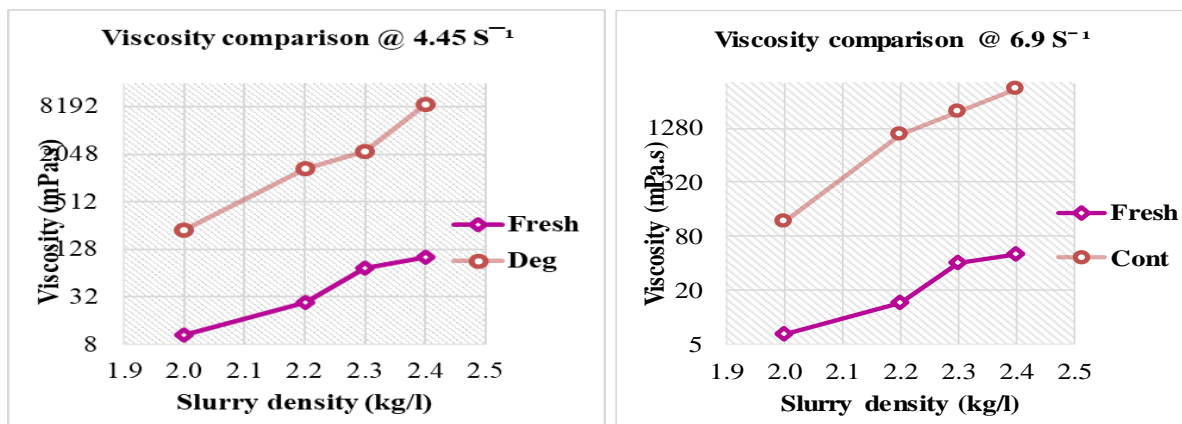
Appendix A: Aperture pegging



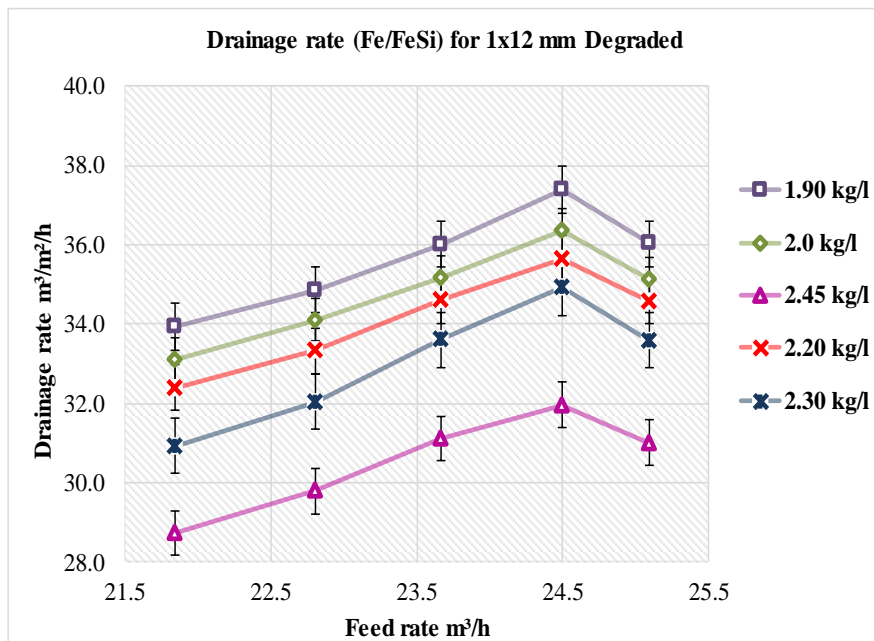
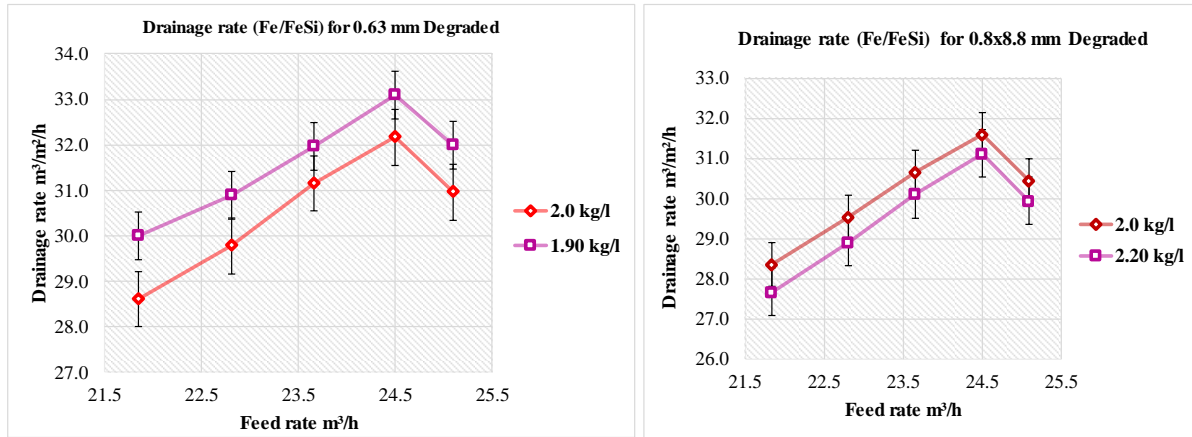
Appendix B: Influence of iron ore on medium drainage rate



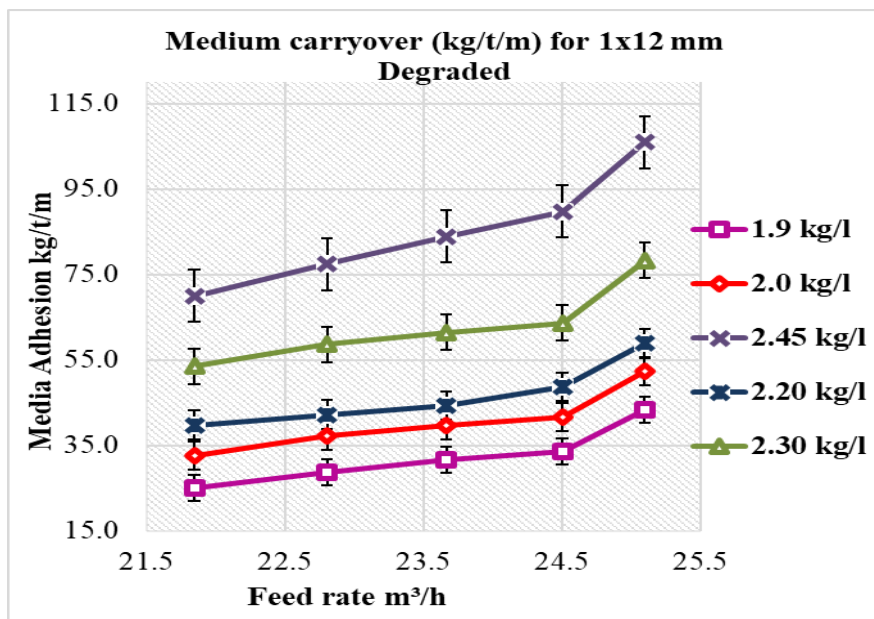
Appendix C: Effects of slimes contamination on medium viscosity



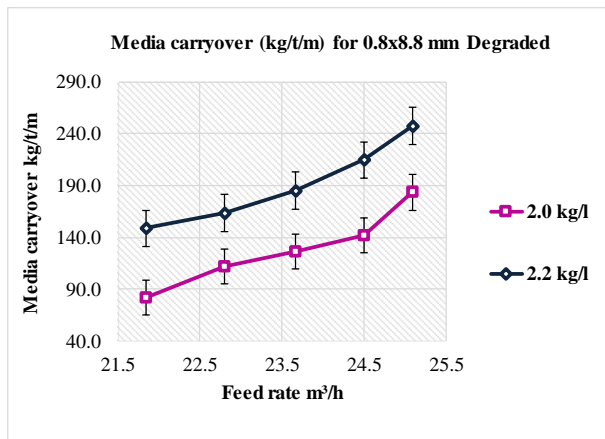
Appendix D: Effects of feed rate variation on degraded ferrosilicon drainage rate



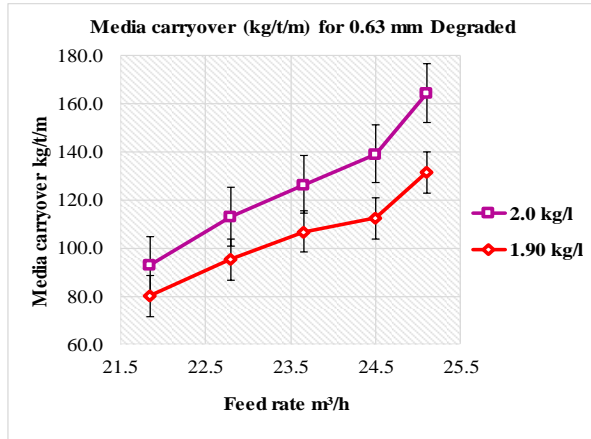
Appendix E: Moisture bypass for 1x12 mm rubber panel.



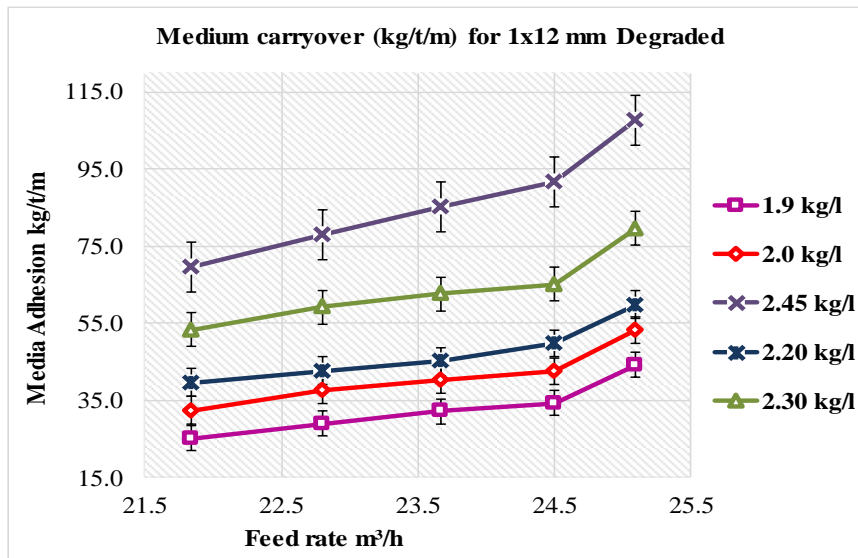
Appendix F: Media carryover for 0.8x8.8 mm (a), 0.63 mm (b) and 1x12 mm (c) screen panels



(a)

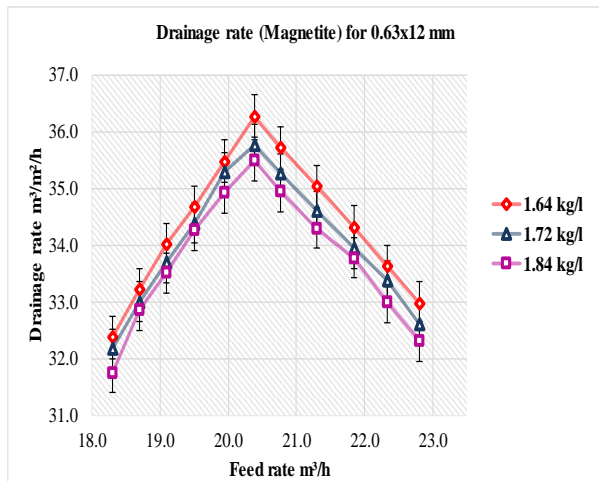
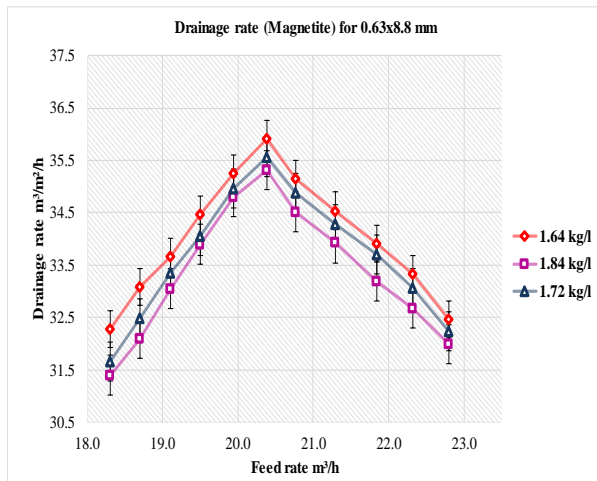


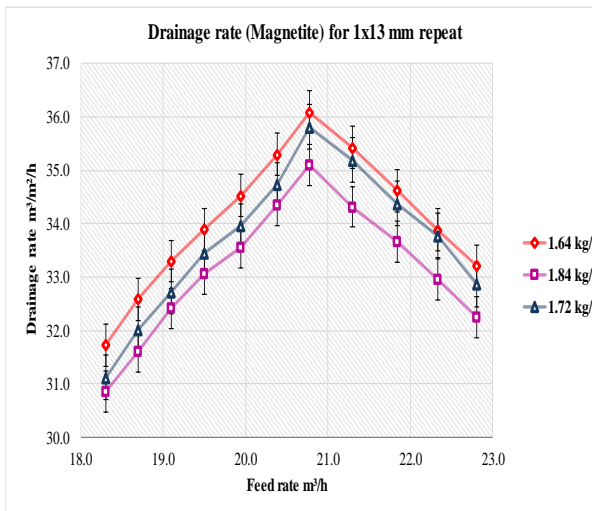
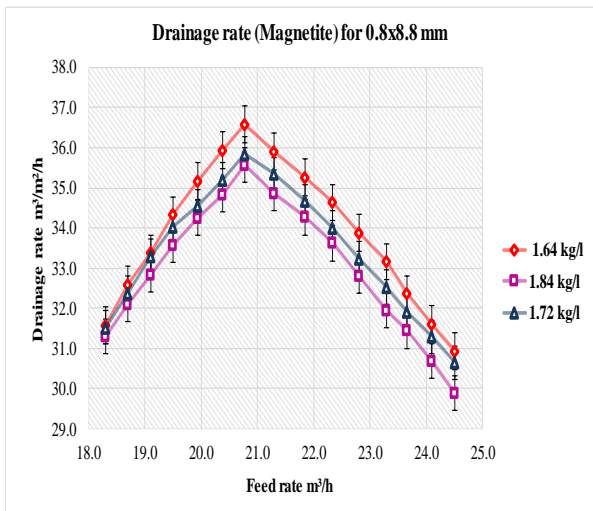
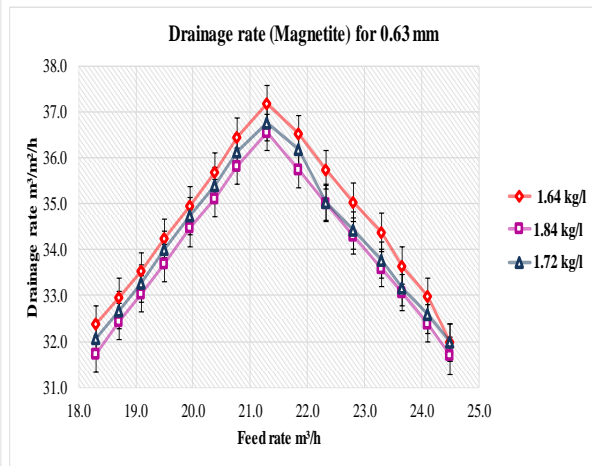
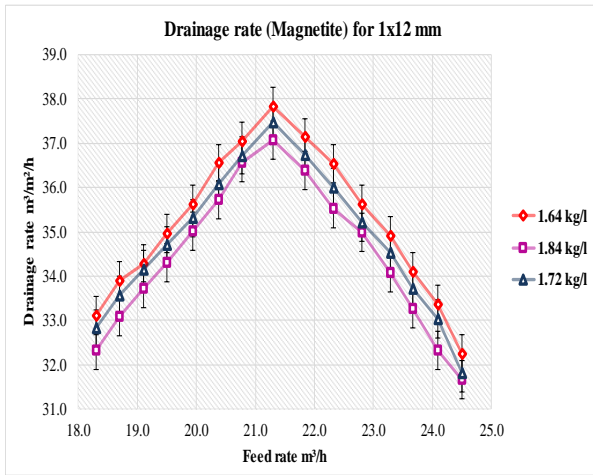
(b)



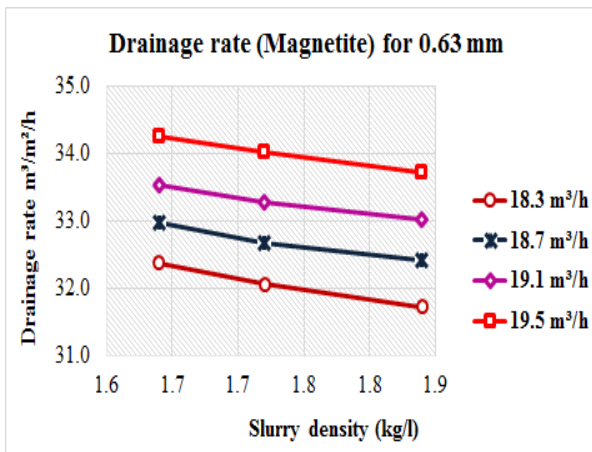
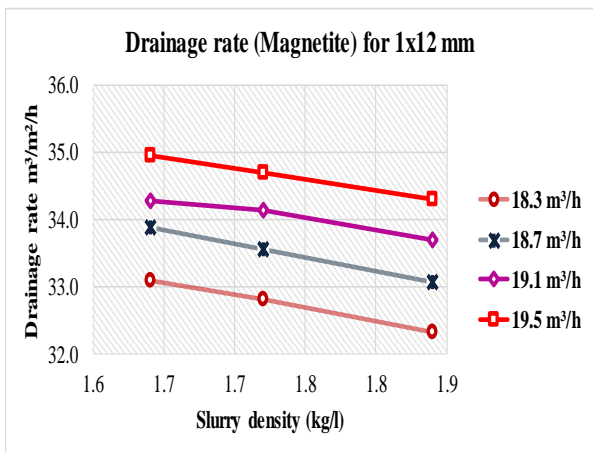
(c)

Appendix G: Effects of volumetric flowrate variation on magnetite drainage rate

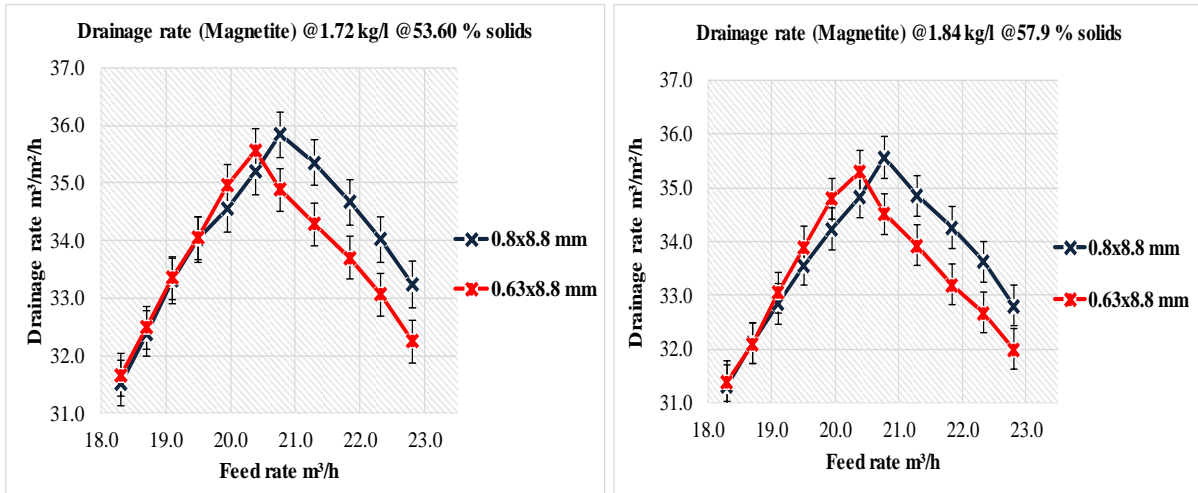




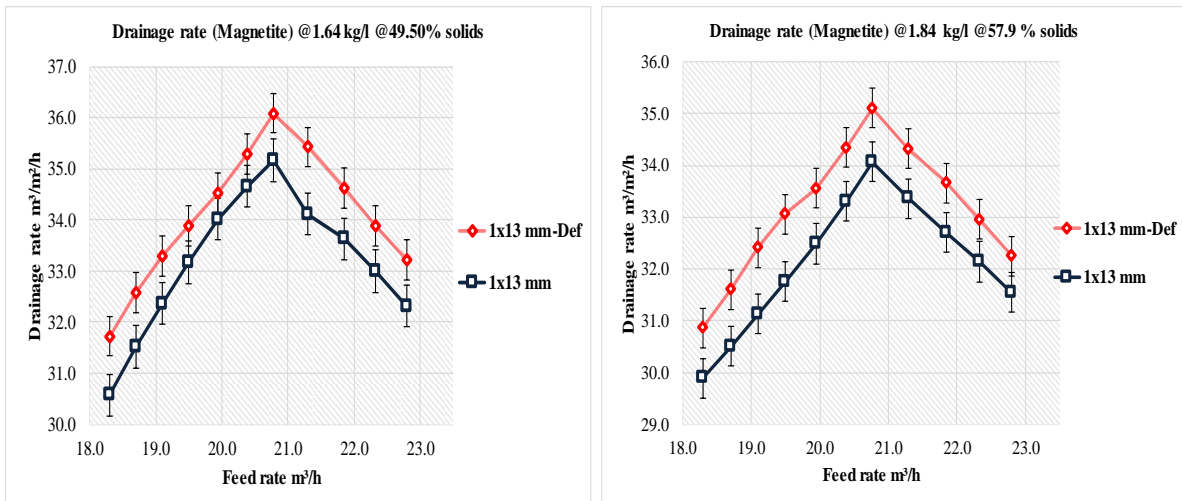
Appendix H: Effects of slurry density variation on magnetite drainage rate



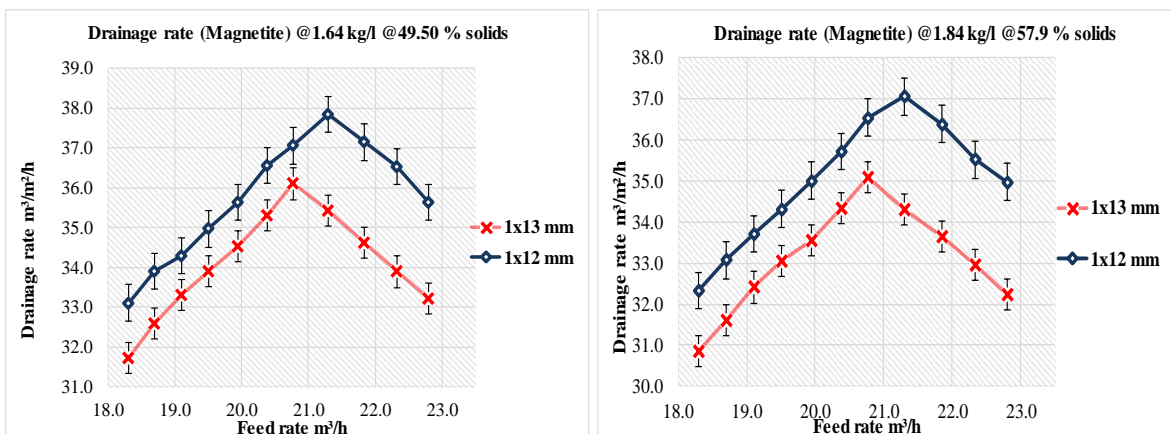
Appendix I: Effects of slot width on magnetite drainage rate



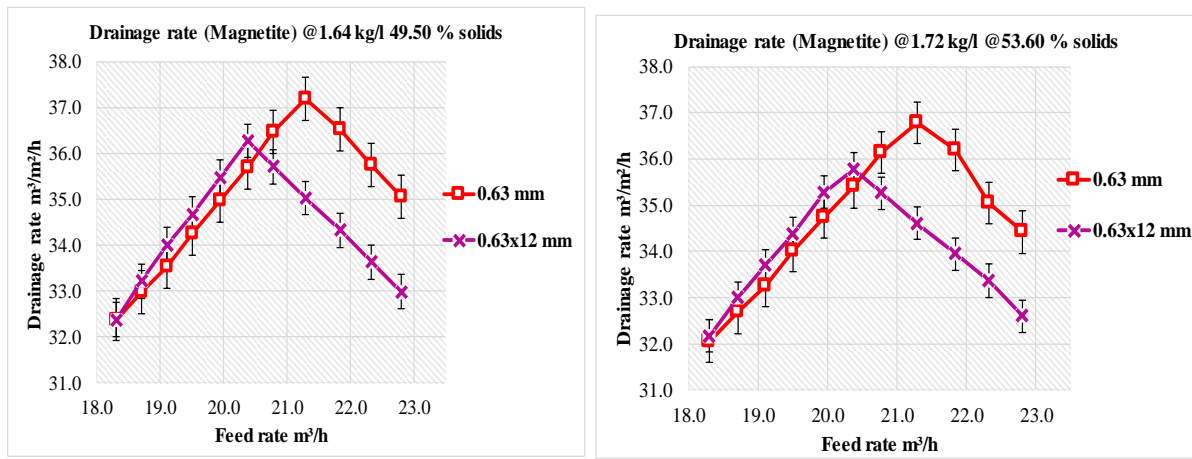
Appendix J: Effects of deflectors on magnetite drainage rate for 1x13 mm screen panels



Appendix K: Effects of screen panel material on magnetite drainage rate



(a)



(b)

Appendix L: Drainage rate for fresh ferrosilicon only

The tables below show the raw data for drainage rate calculations on fresh ferrosilicon only (appendix M), fresh ferrosilicon and iron (appendix N), degraded ferrosilicon and iron (appendix O), and magnetite (appendix P). The first column comprises of the volumetric flowrate of material onto the screen surface, the second column represents the time taken to fill the specific underflow tank volume, third column shows the volume of the material into the underflow tank just before overflow. The fourth column was calculated by dividing column 3 with column 2. The fifth column indicates the average of column 4 values, sixth column represents the conversion of column 5 to m³/h by multiplying with 3.6 m³/s/hl and column seven represents the drainage rate in m³/m²/h calculated by dividing column 6 with 0.511 m² (available area for material separation).

0.63x8.8mm aperture size with FeSi					Screen area(m ²)	0.511
Feed flowrate(m ³ /hr)	Time taken to fill underflow tank (S)	underflow tank Volume (L)	Drainage rate (L/S)	Drainage rate (m ³ /h)	Average drainage rate (m ³ /h)	Drainage rate (m ³ /m ² /h)
21.8	11.80	59.75	5.06	18.23	18.30	35.81
	11.74	59.75	5.09	18.32		
	11.72	59.75	5.10	18.35		
Average	11.75	59.75	5.08	18.30		
22.8	9.21	49.33	5.36	19.28	18.80	36.80
	9.22	47.65	5.17	18.61		
	9.26	47.65	5.15	18.52		
Average	9.23	48.21	5.22	18.80		
23.7	6.81	36.88	5.41	19.49	19.39	37.94
	6.84	36.88	5.39	19.41		
	6.89	36.88	5.35	19.27		
Average	6.85	36.88	5.39	19.39		
24.5	5.08	26.50	5.22	18.78	18.82	36.82
	5.10	26.50	5.20	18.71		
	5.03	26.50	5.27	18.97		
Average	5.07	26.50	5.23	18.82		
25.1	3.30	16.65	5.05	18.16	18.26	35.73
	3.26	16.65	5.11	18.39		
	3.29	16.65	5.06	18.22		
Average	3.28	16.65	5.07	18.26		
25.5	2.71	13.30	4.91	17.67	17.71	34.66
	2.70	13.30	4.93	17.73		
	2.70	13.30	4.93	17.73		
Average	2.70	13.30	4.92	17.71		
		Weight	Volume	Density		
	1	6.82	3.10	2.20		
	2	6.74	3.10	2.17		
	average	6.78	3.10	2.19		
		2.2 kg/l				

0.63x8.8mm aperture size with FeSi					Screen area(m2)	0.511
Feed flowrate(m3/hr)	Time taken to fill underflow tank (S)	underflow tank Volume (L)	Drainage rate (L/S)	Drainage rate (m3/h)	Average drainage rate (m3/h)	Drainage rate (m3/m2/h)
21.8	12.57	63.60	5.06	18.21	18.11	35.45
	12.55	63.60	5.07	18.24		
	12.54	62.30	4.97	17.89		
Average	12.55	63.17	5.03	18.11		
22.8	11.44	59.75	5.22	18.80	18.69	36.58
	11.41	59.75	5.24	18.85		
	11.43	58.50	5.12	18.43		
Average	11.43	59.33	5.19	18.69		
23.7	9.35	49.33	5.28	18.99	19.03	37.23
	9.31	49.33	5.30	19.07		
	9.34	49.33	5.28	19.01		
Average	9.33	49.33	5.28	19.03		
24.5	7.00	36.88	5.27	18.96	18.67	36.55
	7.04	36.88	5.24	18.86		
	7.07	35.75	5.06	18.20		
Average	7.04	36.50	5.19	18.67		
25.1	5.30	26.50	5.00	18.00	18.01	35.25
	5.27	26.50	5.03	18.10		
	5.32	26.50	4.98	17.93		
Average	5.30	26.50	5.00	18.01		
25.5	4.80	23.25	4.84	17.44	17.46	34.17
	4.80	23.25	4.84	17.44		
	4.78	23.25	4.86	17.51		
Average	4.79	23.25	4.85	17.46		
		Weight	Volume	Density		
	1	6.18	2.55	2.42		
	2	7.43	3.05	2.44		
	average	6.81	2.80	2.43		
	2.45 kg/l					

0.63x8.8mm aperture size with FeSi					Screen area(m2)	0.511
Feed flowrate(m3/hr)	Time taken to fill underflow tank (S)	underflow tank Volume (L)	Drainage rate (L/S)	Drainage rate (m3/h)	Average drainage rate (m3/h)	Drainage rate (m3/m2/h)
21.8	13.25	66.20	5.00	17.99	17.8	34.82
	13.47	66.20	4.91	17.69		
	13.47	66.20	4.91	17.69		
Average	13.40	66.20	4.94	17.79		
22.8	10.18	52.25	5.13	18.48	18.4	36.04
	10.25	52.25	5.10	18.35		
	10.21	52.25	5.12	18.42		
Average	10.21	52.25	5.12	18.42		
23.7	8.16	42.73	5.24	18.85	18.9	37.01
	8.11	42.73	5.27	18.97		
	8.13	42.73	5.26	18.92		
Average	8.13	42.73	5.25	18.91		
24.5	5.90	30.00	5.08	18.31	18.3	35.84
	5.91	30.00	5.08	18.27		
	5.88	30.00	5.10	18.37		
Average	5.90	30.00	5.09	18.32		
25.1	4.36	21.63	4.96	17.86	17.7	34.73
	4.44	21.63	4.87	17.53		
	4.36	21.63	4.96	17.86		
Average	4.39	21.63	4.93	17.75		
25.5	3.00	14.98	4.99	17.97	17.2	33.68
	3.01	14.98	4.98	17.91		
	3.04	13.30	4.38	15.75		
Average	3.02	14.42	4.78	17.21		
		Weight	Volume	Density		
	1	6.98	2.75	2.54		
	2	7.24	2.85	2.54		
	average	7.11	2.80	2.54		
	2.55 kg/l					

1x13mm aperture size with FeSi					Screen area(m2)	0.511
Feed flowrate(m3/hr)	Time taken to fill underflow tank (S)	underflow tank Volume (L)	Drainage rate (L/S)	Drainage rate (m3/h)	Average drainage rate (m3/h)	Drainage rate (m3/m2/h)
19.9	19.28	95.50	4.95	17.83	17.89	35.01
	19.19	95.50	4.98	17.92		
	19.18	95.50	4.98	17.92		
Average	19.22	95.50	4.97	17.89		
20.4	17.21	87.85	5.10	18.38	18.21	35.63
	17.22	87.85	5.10	18.37		
	17.31	86.00	4.97	17.89		
Average	17.25	87.23	5.06	18.21		
20.8	15.69	80.95	5.16	18.57	18.60	36.39
	15.69	80.95	5.16	18.57		
	15.63	80.95	5.18	18.64		
Average	15.67	80.95	5.17	18.60		
21.3	13.95	72.25	5.18	18.65	18.91	37.01
	13.97	74.00	5.30	19.07		
	14.01	74.00	5.28	19.01		
Average	13.98	73.42	5.25	18.91		
21.8	12.84	68.35	5.32	19.16	19.21	37.60
	12.78	68.35	5.35	19.25		
	12.80	68.35	5.34	19.22		
Average	12.81	68.35	5.34	19.21		
22.3	11.84	64.90	5.48	19.73	19.54	38.23
	11.80	63.60	5.39	19.40		
	11.76	63.60	5.41	19.47		
Average	11.80	64.03	5.43	19.54		
22.8	10.54	58.50	5.55	19.98	19.90	38.94
	10.60	58.50	5.52	19.87		
	10.61	58.50	5.51	19.85		
Average	10.58	58.50	5.53	19.90		
23.3	9.22	52.25	5.67	20.40	20.24	39.61
	9.19	52.25	5.69	20.47		
	9.25	51.00	5.51	19.85		
Average	9.22	51.83	5.62	20.24		
23.7	8.27	47.65	5.76	20.74	20.59	40.28
	8.34	47.65	5.71	20.57		
	8.39	47.65	5.68	20.45		
Average	8.33	47.65	5.72	20.59		
24.1	7.33	41.15	5.61	20.21	20.33	39.79
	7.25	41.15	5.68	20.43		
	7.28	41.15	5.65	20.35		
Average	7.29	41.15	5.65	20.33		
24.5	6.44	35.75	5.55	19.98	20.00	39.13
	6.41	35.75	5.58	20.08		
	6.46	35.75	5.53	19.92		
Average	6.44	35.75	5.55	20.00		
24.8	5.12	28.38	5.54	19.95	19.69	38.54
	5.12	28.38	5.54	19.95		
	5.14	27.38	5.33	19.17		
Average	5.13	28.04	5.47	19.69		
25.1	4.18	22.44	5.37	19.32	19.17	37.52
	4.25	22.44	5.28	19.01		
	4.21	22.44	5.33	19.19		
Average	4.21	22.44	5.33	19.17		
	Weight	Volume	Density			
1	4.84	2.6	1.86			
2	3.32	1.8	1.84			
average	4.08	2.20	1.85			

1x13mm aperture size with FeSi					Screen area(m ²)	0.511
Feed flowrate(m ³ /hr)	Time taken to fill underflow tank (S)	underflow tank Volume (L)	Drainage rate (L/S)	Drainage rate (m ³ /h)	Average drainage rate (m ³ /h)	Drainage rate (m ³ /m ² /h)
20.4	14.75	72.25	4.90	17.63	17.88	34.99
	14.41	72.25	5.01	18.05		
	14.48	72.25	4.99	17.96		
Average	14.55	72.25	4.97	17.88		
20.8	13.25	67.28	5.08	18.28	18.26	35.73
	13.28	67.28	5.07	18.24		
	13.27	67.28	5.07	18.25		
Average	13.27	67.28	5.07	18.26		
21.3	12.54	64.90	5.18	18.63	18.66	36.51
	12.54	64.90	5.18	18.63		
	12.49	64.90	5.20	18.71		
Average	12.52	64.90	5.18	18.66		
21.8	10.87	57.25	5.27	18.96	18.97	37.12
	10.88	57.25	5.26	18.94		
	10.85	57.25	5.28	19.00		
Average	10.87	57.25	5.27	18.97		
22.3	9.84	52.25	5.31	19.12	19.33	37.82
	9.57	52.25	5.46	19.66		
	9.56	51.00	5.33	19.21		
Average	9.66	51.83	5.37	19.33		
22.8	8.74	47.65	5.45	19.63	19.69	38.54
	8.67	47.65	5.50	19.79		
	8.72	47.65	5.46	19.67		
Average	8.71	47.65	5.47	19.69		
23.3	7.40	41.15	5.56	20.02	19.98	39.11
	7.38	41.15	5.58	20.07		
	7.46	41.15	5.52	19.86		
Average	7.41	41.15	5.55	19.98		
23.7	6.20	34.88	5.63	20.25	20.36	39.84
	6.18	34.88	5.64	20.32		
	6.12	34.88	5.70	20.51		
Average	6.17	34.88	5.66	20.36		
24.1	5.74	31.75	5.53	19.91	19.92	38.99
	5.75	31.75	5.52	19.88		
	5.72	31.75	5.55	19.98		
Average	5.74	31.75	5.53	19.92		
24.5	4.84	26.50	5.48	19.71	19.60	38.36
	4.88	26.50	5.43	19.55		
	4.88	26.50	5.43	19.55		
Average	4.87	26.50	5.45	19.60		
24.8	4.33	23.25	5.37	19.33	19.26	37.68
	4.36	23.25	5.33	19.20		
	4.35	23.25	5.34	19.24		
Average	4.35	23.25	5.35	19.26		
25.1	3.58	18.88	5.27	18.98	19.00	37.18
	3.55	18.88	5.32	19.14		
	3.60	18.88	5.24	18.88		
Average	3.58	18.88	5.28	19.00		
	Weight	Volume	Density			
1	5.17	2.40	2.15			
2	5.05	2.30	2.20			
average	5.11	2.35	2.17			

1x13mm aperture size with FeSi					Screen area(m2)	0.511
Feed flowrate(m3/hr)	Time taken to fill underflow tank (S)	underflow tank Volume (L)	Drainage rate (L/S)	Drainage rate (m3/h)	Average drainage rate (m3/h)	Drainage rate (m3/m2/h)
20.4	14.77	72.25	4.89	17.61	17.66	34.56
	14.72	72.25	4.91	17.67		
	14.70	72.25	4.91	17.69		
Average	14.73	72.25	4.90	17.66		
20.8	13.59	68.35	5.03	18.11	17.98	35.19
	13.63	68.35	5.01	18.05		
	13.61	67.28	4.94	17.80		
Average	13.61	67.99	5.00	17.98		
21.3	12.20	62.30	5.11	18.38	18.29	35.80
	12.30	62.30	5.07	18.23		
	12.28	62.30	5.07	18.26		
Average	12.26	62.30	5.08	18.29		
21.8	11.06	58.50	5.29	19.04	18.71	36.61
	11.14	57.25	5.14	18.50		
	11.09	57.25	5.16	18.58		
Average	11.10	57.67	5.20	18.71		
22.3	9.69	52.25	5.39	19.41	19.03	37.24
	9.77	51.00	5.22	18.79		
	9.72	51.00	5.25	18.89		
Average	9.73	51.42	5.29	19.03		
22.8	8.36	44.30	5.30	19.08	19.30	37.77
	8.35	45.98	5.51	19.82		
	8.39	44.30	5.28	19.01		
Average	8.37	44.86	5.36	19.30		
23.3	7.28	39.58	5.44	19.57	19.71	38.56
	7.22	39.58	5.48	19.73		
	7.19	39.58	5.50	19.82		
Average	7.23	39.58	5.47	19.71		
23.7	6.01	33.50	5.57	20.07	20.00	39.14
	6.04	33.50	5.55	19.97		
	6.04	33.50	5.55	19.97		
Average	6.03	33.50	5.56	20.00		
24.1	5.37	29.00	5.40	19.44	19.65	38.45
	5.28	29.00	5.49	19.77		
	5.29	29.00	5.48	19.74		
Average	5.31	29.00	5.46	19.65		
24.5	4.33	23.25	5.37	19.33	19.32	37.80
	4.29	23.25	5.42	19.51		
	4.38	23.25	5.31	19.11		
Average	4.33	23.25	5.37	19.32		
24.8	3.49	18.33	5.25	18.90	18.99	37.17
	3.48	18.33	5.27	18.96		
	3.45	18.33	5.31	19.12		
Average	3.47	18.33	5.28	18.99		
25.1	2.57	13.30	5.18	18.63	18.66	36.51
	2.59	13.30	5.14	18.49		
	2.54	13.30	5.24	18.85		
Average	2.57	13.30	5.18	18.66		
25.5	2.27	11.60	5.11	18.40	18.34	35.90
	2.29	11.60	5.07	18.24		
	2.27	11.60	5.11	18.40		
Average	2.28	11.60	5.10	18.34		
	Weight	Volume	Density			
1	7.22	3	2.41			
2	6.45	2.65	2.43			
average	6.84	2.83	2.42			

1x13mm aperture size with FeSi					Screen area(m ²)	0.511
Feed flowrate(m ³ /hr)	Time taken to fill underflow tank (S)	underflow tank Volume (L)	Drainage rate (L/S)	Drainage rate (m ³ /h)	Average drainage rate (m ³ /h)	Drainage rate (m ³ /m ² /h)
20.4	14.87	72.25	4.86	17.49	17.44	34.14
	14.90	72.25	4.85	17.46		
	14.96	72.25	4.83	17.39		
Average	14.91	72.25	4.85	17.44		
20.8	13.53	67.28	4.97	17.90	17.86	34.95
	13.56	67.28	4.96	17.86		
	13.59	67.28	4.95	17.82		
Average	13.56	67.28	4.96	17.86		
21.3	12.48	62.30	4.99	17.97	18.24	35.69
	12.46	63.60	5.10	18.38		
	12.47	63.60	5.10	18.36		
Average	12.47	63.17	5.07	18.24		
21.8	11.00	56.00	5.09	18.33	18.58	36.35
	11.01	57.25	5.20	18.72		
	11.03	57.25	5.19	18.69		
Average	11.01	56.83	5.16	18.58		
22.3	9.95	52.25	5.25	18.90	18.92	37.02
	9.98	52.25	5.24	18.85		
	9.90	52.25	5.28	19.00		
Average	9.94	52.25	5.25	18.92		
22.8	8.65	45.98	5.32	19.13	19.19	37.56
	8.60	45.98	5.35	19.25		
	8.62	45.98	5.33	19.20		
Average	8.62	45.98	5.33	19.19		
23.3	7.72	41.15	5.33	19.19	19.46	38.08
	7.73	41.15	5.32	19.16		
	7.68	42.73	5.56	20.03		
Average	7.71	41.68	5.41	19.46		
23.7	6.50	35.75	5.50	19.80	19.83	38.81
	6.47	35.75	5.53	19.89		
	6.50	35.75	5.50	19.80		
Average	6.49	35.75	5.51	19.83		
24.1	5.59	30.00	5.37	19.32	19.51	38.17
	5.52	30.00	5.43	19.57		
	5.50	30.00	5.45	19.64		
Average	5.54	30.00	5.42	19.51		
24.5	4.69	24.88	5.30	19.09	19.20	37.58
	4.66	24.88	5.34	19.22		
	4.64	24.88	5.36	19.30		
Average	4.66	24.88	5.33	19.20		
24.8	3.17	16.65	5.25	18.91	18.89	36.97
	3.20	16.65	5.20	18.73		
	3.15	16.65	5.29	19.03		
Average	3.17	16.65	5.25	18.89		
25.1	2.55	13.30	5.22	18.78	18.58	36.37
	2.58	13.30	5.16	18.56		
	2.60	13.30	5.12	18.42		
Average	2.58	13.30	5.16	18.58		
25.5	2.34	11.60	4.96	17.85	18.13	35.49
	2.27	11.60	5.11	18.40		
	2.30	11.60	5.04	18.16		
Average	2.30	11.60	5.04	18.13		
	Weight	Volume	Density			
1	5.35	2.15	2.49			
2	6.46	2.55	2.53			
average	5.91	2.35	2.51			

1x13mm aperture size with FeSi					Screen area(m ²)	0.511
Feed flowrate(m ³ /hr)	Time taken to fill underflow tank (S)	underflow tank Volume (L)	Drainage rate (L/S)	Drainage rate (m ³ /h)	Average drainage rate (m ³ /h)	Drainage rate (m ³ /m ² /h)
20.8	14.75	72.25	4.90	17.63	17.70	34.65
	14.81	72.25	4.88	17.56		
	14.87	74.00	4.98	17.92		
Average	14.81	72.83	4.92	17.70		
21.3	13.50	67.68	5.01	18.05	18.07	35.37
	13.50	67.68	5.01	18.05		
	13.44	67.68	5.04	18.13		
Average	13.48	67.68	5.02	18.07		
21.8	12.34	62.30	5.05	18.18	18.41	36.02
	12.37	63.60	5.14	18.51		
	12.35	63.60	5.15	18.54		
Average	12.35	63.17	5.11	18.41		
22.3	11.29	58.50	5.18	18.65	18.73	36.66
	11.19	58.50	5.23	18.82		
	11.25	58.50	5.20	18.72		
Average	11.24	58.50	5.20	18.73		
22.8	10.11	53.50	5.29	19.05	19.10	37.38
	10.07	53.50	5.31	19.13		
	10.07	53.50	5.31	19.13		
Average	10.08	53.50	5.31	19.10		
23.3	9.01	49.33	5.47	19.71	19.39	37.95
	9.05	47.65	5.27	18.95		
	9.10	49.33	5.42	19.51		
Average	9.05	48.77	5.39	19.39		
23.7	8.35	45.98	5.51	19.82	19.73	38.61
	8.31	45.98	5.53	19.92		
	8.20	44.30	5.40	19.45		
Average	8.29	45.42	5.48	19.73		
24.1	7.05	38.00	5.39	19.40	19.41	37.99
	7.03	38.00	5.41	19.46		
	7.06	38.00	5.38	19.38		
Average	7.05	38.00	5.39	19.41		
24.5	6.39	33.50	5.24	18.87	19.08	37.35
	6.38	33.50	5.25	18.90		
	6.40	34.63	5.41	19.48		
Average	6.39	33.88	5.30	19.08		
24.8	5.14	26.50	5.16	18.56	18.70	36.60
	5.12	26.50	5.18	18.63		
	5.21	27.38	5.25	18.92		
Average	5.16	26.79	5.20	18.70		
25.1	4.73	24.06	5.09	18.31	18.35	35.92
	4.73	24.06	5.09	18.31		
	4.70	24.06	5.12	18.43		
Average	4.72	24.06	5.10	18.35		
25.2	3.30	16.65	5.05	18.16	18.02	35.26
	3.34	16.65	4.99	17.95		
	3.34	16.65	4.99	17.95		
Average	3.33	16.65	5.01	18.02		
25.5	3.06	14.98	4.89	17.62	17.68	34.59
	3.05	14.98	4.91	17.68		
	3.04	14.98	4.93	17.73		
Average	3.05	14.98	4.91	17.68		
	Weight	Volume	Density			
1	5.47	2.05	2.67			
2	4.5	1.7	2.66			
average	4.99	1.87	2.67			

0.8x8.8mm aperture size with FeSi					Screen area(m ²)	0.511
Feed flowrate(m ³ /hr)	Time taken to fill underflow tank (S)	underflow tank Volume (L)	Drainage rate (L/S)	Drainage rate (m ³ /h)	Average drainage rate (m ³ /h)	Drainage rate (m ³ /m ² /h)
21.8	12.19	64.90	5.32	19.17	19.29	37.75
	12.26	66.20	5.40	19.44		
	12.13	64.90	5.35	19.26		
Average	12.19	65.33	5.36	19.29		
22.8	9.25	51.00	5.51	19.85	19.89	38.93
	9.22	51.00	5.53	19.91		
	9.22	51.00	5.53	19.91		
Average	9.23	51.00	5.53	19.89		
23.7	6.41	36.88	5.75	20.71	20.40	39.93
	6.34	35.75	5.64	20.30		
	6.37	35.75	5.61	20.20		
Average	6.37	36.13	5.67	20.40		
24.5	4.32	24.06	5.57	20.05	19.88	38.91
	4.36	24.06	5.52	19.87		
	4.39	24.06	5.48	19.73		
Average	4.36	24.06	5.52	19.88		
25.1	2.27	12.03	5.30	19.07	19.27	37.71
	2.22	12.03	5.42	19.50		
	2.25	12.03	5.34	19.24		
Average	2.25	12.03	5.35	19.27		
		Weight	Volume	Density		
	1	6.58	3.3	1.99		
	2	4.17	2.1	1.99		
	average	5.38	2.70	1.99		
	2.01 kg/l					

0.8x8.8mm aperture size with FeSi					Screen area(m ²)	0.511
Feed flowrate(m ³ /hr)	Time taken to fill underflow tank (S)	underflow tank Volume (L)	Drainage rate (L/S)	Drainage rate (m ³ /h)	Average drainage rate (m ³ /h)	Drainage rate (m ³ /m ² /h)
21.8	12.53	64.98	5.19	18.67	18.55	36.29
	12.56	64.98	5.17	18.62		
	12.51	63.75	5.10	18.35		
Average	12.53	64.57	5.15	18.55		
22.8	9.22	49.33	5.35	19.26	19.24	37.65
	9.25	49.33	5.33	19.20		
	9.22	49.33	5.35	19.26		
Average	9.23	49.33	5.34	19.24		
23.7	6.31	34.63	5.49	19.75	19.75	38.66
	6.32	34.63	5.48	19.72		
	6.30	34.63	5.50	19.79		
Average	6.31	34.63	5.49	19.75		
24.5	4.83	25.69	5.32	19.15	19.19	37.55
	4.82	25.69	5.33	19.19		
	4.81	25.69	5.34	19.23		
Average	4.82	25.69	5.33	19.19		
25.1	2.25	11.60	5.16	18.56	18.67	36.54
	2.24	11.60	5.18	18.64		
	2.22	11.60	5.23	18.81		
Average	2.24	11.60	5.19	18.67		
		Weight	Volume	Density		
	1	6.97	3.20	2.18		
	2	5.39	2.45	2.20		
	average	6.18	2.83	2.19		
	2.2 kg/l					

Appendix M: Drainage rate for fresh ferrosilicon and iron ore

0.63x8.8mm aperture size with FeSi/Fe					Screen area(m2)	0.511
Feed flowrate(m3/hr)	Time taken to fill underflow tank (S)	underflow tank Volume (L)	Drainage rate (L/S)	Drainage rate (m3/h)	Average drainage rate (m3/h)	Drainage rate (m3/m2/h)
21.8	16.72	84.50	5.05	18.19	18.16	35.53
	16.78	84.50	5.04	18.13		
	16.76	84.50	5.04	18.15		
Average	16.75	84.50	5.04	18.16		
22.8	14.22	74.00	5.20	18.73	18.68	36.56
	14.27	74.00	5.19	18.67		
	14.29	74.00	5.18	18.64		
Average	14.26	74.00	5.19	18.68		
23.7	12.11	64.90	5.36	19.29	19.24	37.65
	12.13	64.90	5.35	19.26		
	12.19	64.90	5.32	19.17		
Average	12.14	64.90	5.34	19.24		
24.5	11.06	57.25	5.18	18.63	18.62	36.45
	11.05	57.25	5.18	18.65		
	11.09	57.25	5.16	18.58		
Average	11.07	57.25	5.17	18.62		
25.1	10.86	54.75	5.04	18.15	18.17	35.55
	10.81	54.75	5.06	18.23		
	10.88	54.75	5.03	18.12		
Average	10.85	54.75	5.05	18.17		
25.5	10.47	51.00	4.87	17.54	17.56	34.36
	10.44	51.00	4.89	17.59		
	10.46	51.00	4.88	17.55		
Average	10.46	51.00	4.88	17.56		
		Weight	Volume	Density		
	1	4.84	2.20	2.20		
	2	6.10	2.70	2.26		
	3					
	average	5.47	2.45	2.23		
	2.2 kg/l					

0.63x8.8mm aperture size with FeSi/Fe					Screen area(m2)	0.511
Feed flowrate(m3/hr)	Time taken to fill underflow tank (S)	underflow tank Volume (L)	Drainage rate (L/S)	Drainage rate (m3/h)	Average drainage rate (m3/h)	Drainage rate (m3/m2/h)
21.8	16.66	83.75	5.03	18.10	17.95	35.12
	16.77	83.75	4.99	17.98		
	16.97	83.75	4.94	17.77		
Average	16.80	83.75	4.99	17.95		
22.8	14.22	73.13	5.14	18.51	18.45	36.10
	14.22	73.13	5.14	18.51		
	14.20	72.25	5.09	18.32		
Average	14.21	72.83	5.12	18.45		
23.7	12.57	66.20	5.27	18.96	18.96	37.10
	12.55	66.20	5.27	18.99		
	12.59	66.20	5.26	18.93		
Average	12.57	66.20	5.27	18.96		
24.5	10.97	56.00	5.10	18.38	18.49	36.18
	10.84	56.00	5.17	18.60		
	10.90	56.00	5.14	18.50		
Average	10.90	56.00	5.14	18.49		
25.1	9.35	45.98	4.92	17.70	17.94	35.11
	9.32	45.98	4.93	17.76		
	9.34	47.65	5.10	18.37		
Average	9.34	46.53	4.98	17.94		
25.5	8.30	39.58	4.77	17.17	17.44	34.14
	8.44	41.15	4.88	17.55		
	8.41	41.15	4.89	17.61		
Average	8.38	40.63	4.85	17.44		
		Weight	Volume	Density		
	1	6.62	2.70	2.45		
	2	6.80	2.75	2.47		
	average	6.71	2.73	2.46		
	2.45kg/l					

0.63x8.8mm aperture size with FeSi/Fe					Screen area(m2)	0.511
Feed flowrate(m3/hr)	Time taken to fill underflow tank (S)	underflow tank Volume (L)	Drainage rate (L/S)	Drainage rate (m3/h)	Average drainage rate (m3/h)	Drainage rate (m3/m2/h)
21.8	18.94	92.00	4.86	17.49	17.5	34.30
	18.84	92.00	4.88	17.58		
	18.91	92.00	4.87	17.51		
Average	18.90	92.00	4.87	17.53		
22.8	16.45	83.00	5.05	18.16	18.2	35.61
	16.43	83.00	5.05	18.19		
	16.38	83.00	5.07	18.24		
Average	16.42	83.00	5.05	18.20		
23.7	14.78	76.45	5.17	18.62	18.8	36.75
	14.53	76.45	5.26	18.94		
	14.66	76.45	5.21	18.77		
Average	14.66	76.45	5.22	18.78		
24.5	13.89	70.50	5.08	18.27	18.3	35.80
	13.85	70.50	5.09	18.32		
	13.88	70.50	5.08	18.29		
Average	13.87	70.50	5.08	18.29		
25.1	7.56	36.88	4.88	17.56	17.6	34.39
	7.59	36.88	4.86	17.49		
	7.51	36.88	4.91	17.68		
Average	7.55	36.88	4.88	17.58		
25.5	7.01	32.62	4.65	16.75	16.7	32.69
	7.05	32.62	4.63	16.66		
	7.03	32.62	4.64	16.70		
Average	7.03	32.62	4.64	16.70		
		Weight	Volume	Density		
	1	4.67	1.80	2.59		
	2	5.48	2.15	2.55		
	average	5.08	1.98	2.57		
	2.55 kg/l					

0.8x8.8mm aperture size with FeSi/Fe					Screen area(m2)	0.511
Feed flowrate(m3/hr)	Time taken to fill underflow tank (S)	underflow tank Volume (L)	Drainage rate (L/S)	Drainage rate (m3/h)	Average drainage rate (m3/h)	Drainage rate (m3/m2/h)
21.8	15.72	83.00	5.28	19.01	19.18	37.53
	15.81	84.50	5.34	19.24		
	15.78	84.50	5.35	19.28		
Average	15.77	84.00	5.33	19.18		
22.8	12.00	66.20	5.52	19.86	19.87	38.89
	12.00	66.20	5.52	19.86		
	11.98	66.20	5.53	19.89		
Average	11.99	66.20	5.52	19.87		
23.7	8.69	49.33	5.68	20.43	20.28	39.69
	8.84	49.33	5.58	20.09		
	8.74	49.33	5.64	20.32		
Average	8.76	49.33	5.63	20.28		
24.5	6.78	36.88	5.44	19.58	19.68	38.51
	6.70	36.88	5.50	19.81		
	6.76	36.88	5.45	19.64		
Average	6.75	36.88	5.47	19.68		
25.1	4.39	23.25	5.30	19.07	19.02	37.23
	4.41	23.25	5.27	18.98		
	4.40	23.25	5.28	19.02		
Average	4.40	23.25	5.28	19.02		
		Weight	Volume	Density		
	1	4.83	2.40	2.01		
	2	6.78	3.30	2.05		
	average	5.81	2.85	2.03		
	2.0kg/l					

0.8x8.8mm aperture size with FeSi/Fe					Screen area(m2)	0.511
Feed flowrate(m3/hr)	Time taken to fill underflow tank (S)	underflow tank Volume (L)	Drainage rate (L/S)	Drainage rate (m3/h)	Average drainage rate (m3/h)	Drainage rate (m3/m2/h)
21.8	13.30	68.50	5.15	18.54	18.47	36.14
	13.40	68.50	5.11	18.40		
	13.36	68.50	5.13	18.46		
Average	13.35	68.50	5.13	18.47		
22.8	10.50	56.00	5.33	19.20	19.15	37.48
	10.52	56.00	5.32	19.16		
	10.56	56.00	5.30	19.09		
Average	10.53	56.00	5.32	19.15		
23.7	8.11	44.30	5.46	19.66	19.62	38.40
	8.08	44.30	5.48	19.74		
	8.19	44.30	5.41	19.47		
Average	8.13	44.30	5.45	19.62		
24.5	6.00	31.75	5.29	19.05	19.01	37.20
	6.03	31.75	5.27	18.96		
	6.01	31.75	5.28	19.02		
Average	6.01	31.75	5.28	19.01		
25.1	4.53	23.25	5.13	18.48	18.55	36.29
	4.50	23.25	5.17	18.60		
	4.51	23.25	5.16	18.56		
Average	4.51	23.25	5.15	18.55		
		Weight	Volume	Density		
	1	6.00	2.70	2.22		
	2	5.47	2.45	2.23		
	3					
	average	5.74	2.58	2.23		
	2.2 kg/l					

1x13mm aperture size with FeSi/Fe					Screen area(m2)	0.511
Feed flowrate(m3/hr)	Time taken to fill underflow tank (S)	underflow tank Volume (L)	Drainage rate (L/S)	Drainage rate (m3/h)	Average drainage rate (m3/h)	Drainage rate (m3/m2/h)
19.9	20.61	101.00	4.90	17.64	17.64	34.52
	20.61	101.00	4.90	17.64		
	20.61	101.00	4.90	17.64		
Average	20.61	101.00	4.90	17.64		
20.4	20.04	101.00	5.04	18.14	18.09	35.41
	20.14	101.00	5.01	18.05		
	20.11	101.00	5.02	18.08		
Average	20.10	101.00	5.03	18.09		
20.8	18.34	94.00	5.13	18.45	18.48	36.17
	18.27	94.00	5.15	18.52		
	18.32	94.00	5.13	18.47		
Average	18.31	94.00	5.13	18.48		
21.3	16.47	86.00	5.22	18.80	18.80	36.79
	16.38	86.00	5.25	18.90		
	16.56	86.00	5.19	18.70		
Average	16.47	86.00	5.22	18.80		
21.8	17.68	94.00	5.32	19.14	19.24	37.65
	17.50	94.00	5.37	19.34		
	17.59	94.00	5.34	19.24		
Average	17.59	94.00	5.34	19.24		
22.3	16.41	89.70	5.47	19.68	19.44	38.04
	16.40	87.85	5.36	19.28		
	16.34	87.85	5.38	19.35		
Average	16.38	88.47	5.40	19.44		
22.8	14.72	80.95	5.50	19.80	19.82	38.80
	14.69	80.95	5.51	19.84		
	14.69	80.95	5.51	19.84		
Average	14.70	80.95	5.51	19.82		
23.3	13.68	76.45	5.59	20.12	20.16	39.46
	13.67	76.45	5.59	20.13		
	13.60	76.45	5.62	20.24		
Average	13.65	76.45	5.60	20.16		
23.7	10.66	61.00	5.72	20.60	20.50	40.11
	10.70	61.00	5.70	20.52		
	10.78	61.00	5.66	20.37		
Average	10.71	61.00	5.69	20.50		
24.1	9.34	52.25	5.59	20.14	20.28	39.68
	9.30	52.25	5.62	20.23		
	9.19	52.25	5.69	20.47		
Average	9.28	52.25	5.63	20.28		
24.5	8.22	45.98	5.59	20.14	19.92	38.99
	8.25	45.98	5.57	20.06		
	8.15	44.30	5.44	19.57		
Average	8.21	45.42	5.53	19.92		
24.8	7.02	38.00	5.41	19.49	19.51	38.17
	7.02	38.00	5.41	19.49		
	7.00	38.00	5.43	19.54		
Average	7.01	38.00	5.42	19.51		
25.1	5.97	31.75	5.32	19.15	19.09	37.36
	5.99	31.75	5.30	19.08		
	6.00	31.75	5.29	19.05		
Average	5.99	31.75	5.30	19.09		
	Weight	Volume	Density			
1	6.67	3.60	1.85			
2	6.59	3.50	1.88			
average	6.63	3.55	1.87			

1x13mm aperture size with FeSi/Fe					Screen area(m ²)	0.511
Feed flowrate(m ³ /hr)	Time taken to fill underflow tank (S)	underflow tank Volume (L)	Drainage rate (L/S)	Drainage rate (m ³ /h)	Average drainage rate (m ³ /h)	Drainage rate (m ³ /m ² /h)
20.4	20.61	101.00	4.90	17.64	17.70	34.64
	20.51	101.00	4.92	17.73		
	20.51	101.00	4.92	17.73		
Average	20.54	101.00	4.92	17.70		
20.8	18.44	93.00	5.04	18.16	18.14	35.49
	18.48	93.00	5.03	18.12		
	18.46	93.00	5.04	18.14		
Average	18.46	93.00	5.04	18.14		
21.3	17.44	89.70	5.14	18.52	18.49	36.19
	17.51	89.70	5.12	18.44		
	17.44	89.70	5.14	18.52		
Average	17.46	89.70	5.14	18.49		
21.8	16.16	84.50	5.23	18.82	18.87	36.94
	16.11	84.50	5.25	18.88		
	16.08	84.50	5.25	18.92		
Average	16.12	84.50	5.24	18.87		
22.3	14.62	77.68	5.31	19.13	19.17	37.52
	14.57	77.68	5.33	19.19		
	14.56	77.68	5.33	19.21		
Average	14.58	77.68	5.33	19.17		
22.8	13.40	72.25	5.39	19.41	19.49	38.15
	13.31	72.25	5.43	19.54		
	13.32	72.25	5.42	19.53		
Average	13.34	72.25	5.41	19.49		
23.3	11.30	62.30	5.51	19.85	19.78	38.70
	11.33	62.30	5.50	19.80		
	11.39	62.30	5.47	19.69		
Average	11.34	62.30	5.49	19.78		
23.7	9.97	56.00	5.62	20.22	20.19	39.50
	10.00	56.00	5.60	20.16		
	9.99	56.00	5.61	20.18		
Average	9.99	56.00	5.61	20.19		
24.1	8.98	49.33	5.49	19.77	19.80	38.75
	8.97	49.33	5.50	19.80		
	8.95	49.33	5.51	19.84		
Average	8.97	49.33	5.50	19.80		
24.5	7.84	42.73	5.45	19.62	19.49	38.15
	7.94	42.73	5.38	19.37		
	7.89	42.73	5.42	19.49		
Average	7.89	42.73	5.42	19.49		
24.8	6.90	36.88	5.34	19.24	19.18	37.54
	6.87	36.88	5.37	19.32		
	6.99	36.88	5.28	18.99		
Average	6.92	36.88	5.33	19.18		
25.1	6.18	32.62	5.28	19.00	18.89	36.97
	6.22	32.62	5.24	18.88		
	6.25	32.62	5.22	18.79		
Average	6.22	32.62	5.25	18.89		
	Weight	Volume	Density			
1	6.66	3.00	2.22			
2	5.27	2.40	2.20			
average	5.97	2.70	2.21			

1x13mm aperture size with FeSi/Fe					Screen area(m ²)	0.511
Feed flowrate(m ³ /hr)	Time taken to fill underflow tank (S)	underflow tank Volume (L)	Drainage rate (L/S)	Drainage rate (m ³ /h)	Average drainage rate (m ³ /h)	Drainage rate (m ³ /m ² /h)
20.4	19.60	95.50	4.87	17.54	17.58	34.41
	19.51	95.50	4.89	17.62		
	19.55	95.50	4.88	17.59		
Average	19.55	95.50	4.88	17.58		
20.8	19.15	95.50	4.99	17.95	17.90	35.03
	19.27	95.50	4.96	17.84		
	19.20	95.50	4.97	17.91		
Average	19.21	95.50	4.97	17.90		
21.3	18.23	92.00	5.05	18.17	18.21	35.63
	18.15	92.00	5.07	18.25		
	18.19	92.00	5.06	18.21		
Average	18.19	92.00	5.06	18.21		
21.8	16.85	86.00	5.10	18.37	18.58	36.36
	16.94	87.85	5.19	18.67		
	16.91	87.85	5.20	18.70		
Average	16.90	87.23	5.16	18.58		
22.3	16.13	84.50	5.24	18.86	18.86	36.90
	16.16	84.50	5.23	18.82		
	16.11	84.50	5.25	18.88		
Average	16.13	84.50	5.24	18.86		
22.8	14.90	79.00	5.30	19.09	19.19	37.55
	14.85	79.00	5.32	19.15		
	14.89	79.93	5.37	19.32		
Average	14.88	79.31	5.33	19.19		
23.3	13.59	74.00	5.45	19.60	19.63	38.41
	13.55	74.00	5.46	19.66		
	13.58	74.00	5.45	19.62		
Average	13.57	74.00	5.45	19.63		
23.7	12.12	67.28	5.55	19.98	19.91	38.97
	12.22	67.28	5.51	19.82		
	12.15	67.28	5.54	19.93		
Average	12.16	67.28	5.53	19.91		
24.1	11.48	62.30	5.43	19.54	19.58	38.31
	11.45	62.30	5.44	19.59		
	11.44	62.30	5.45	19.60		
Average	11.46	62.30	5.44	19.58		
24.5	10.35	56.00	5.41	19.48	19.25	37.66
	10.45	56.00	5.36	19.29		
	10.39	54.75	5.27	18.97		
Average	10.40	55.58	5.35	19.25		
24.8	9.25	49.33	5.33	19.20	18.89	36.96
	9.29	49.33	5.31	19.11		
	9.35	47.65	5.10	18.35		
Average	9.30	48.77	5.25	18.89		
25.1	8.29	42.73	5.15	18.55	18.58	36.35
	8.26	42.73	5.17	18.62		
	8.29	42.73	5.15	18.55		
Average	8.28	42.73	5.16	18.58		
25.5	7.05	35.75	5.07	18.26	18.26	35.74
	7.05	35.75	5.07	18.26		
	7.04	35.75	5.08	18.28		
Average	7.05	35.75	5.07	18.26		
	Weight	Volume	Density			
1	7.66	3.10	2.47			
2	5.86	2.40	2.44			
average	6.76	2.75	2.46			

1x13mm aperture size with FeSi/Fe					Screen area(m ²)	0.511
Feed flowrate(m ³ /hr)	Time taken to fill underflow tank (S)	underflow tank Volume (L)	Drainage rate (L/S)	Drainage rate (m ³ /h)	Average drainage rate (m ³ /h)	Drainage rate (m ³ /m ² /h)
20.4	21.01	101.00	4.81	17.31	17.27	33.79
	21.06	101.00	4.80	17.26		
	21.10	101.00	4.79	17.23		
Average	21.06	101.00	4.80	17.27		
20.8	20.59	101.00	4.91	17.66	17.64	34.53
	20.60	101.00	4.90	17.65		
	20.63	101.00	4.90	17.62		
Average	20.61	101.00	4.90	17.64		
21.3	19.06	95.50	5.01	18.04	18.10	35.42
	19.10	95.50	5.00	18.00		
	19.13	97.00	5.07	18.25		
Average	19.10	96.00	5.03	18.10		
21.8	17.84	90.85	5.09	18.33	18.47	36.14
	17.89	92.00	5.14	18.51		
	17.85	92.00	5.15	18.55		
Average	17.86	91.62	5.13	18.47		
22.3	16.25	84.50	5.20	18.72	18.74	36.67
	16.25	84.50	5.20	18.72		
	16.20	84.50	5.22	18.78		
Average	16.23	84.50	5.21	18.74		
22.8	15.21	80.95	5.32	19.16	19.11	37.39
	15.26	80.95	5.30	19.10		
	15.29	80.95	5.29	19.06		
Average	15.25	80.95	5.31	19.11		
23.3	13.94	75.23	5.40	19.43	19.41	37.98
	13.97	75.23	5.38	19.39		
	13.95	75.23	5.39	19.41		
Average	13.95	75.23	5.39	19.41		
23.7	12.40	68.35	5.51	19.84	19.79	38.73
	12.52	68.35	5.46	19.65		
	12.38	68.35	5.52	19.88		
Average	12.43	68.35	5.50	19.79		
24.1	10.50	56.00	5.33	19.20	19.41	37.98
	10.49	56.00	5.34	19.22		
	10.41	57.25	5.50	19.80		
Average	10.47	56.42	5.39	19.41		
24.5	9.41	49.33	5.24	18.87	19.05	37.28
	9.47	51.00	5.39	19.39		
	9.40	49.33	5.25	18.89		
Average	9.43	49.88	5.29	19.05		
24.8	8.34	43.51	5.22	18.78	18.71	36.61
	8.31	43.51	5.24	18.85		
	8.47	43.51	5.14	18.49		
Average	8.37	43.51	5.20	18.71		
25.1	7.39	38.00	5.14	18.51	18.40	36.02
	7.41	37.44	5.05	18.19		
	7.39	38.00	5.14	18.51		
Average	7.40	37.81	5.11	18.40		
25.5	6.03	30.00	4.98	17.91	17.92	35.07
	6.02	30.00	4.98	17.94		
	6.03	30.00	4.98	17.91		
Average	6.03	30.00	4.98	17.92		
	Weight	Volume	Density			
1	6.34	2.45	2.59			
2	5.51	2.15	2.56			
average	5.93	2.30	2.58			
2.55 kg/l						

1x13mm aperture size with FeSi/Fe					Screen area(m ²)	0.511
Feed flowrate(m ³ /hr)	Time taken to fill underflow tank (S)	underflow tank Volume (L)	Drainage rate (L/S)	Drainage rate (m ³ /h)	Average drainage rate (m ³ /h)	Drainage rate (m ³ /m ² /h)
20.8	20.28	99.00	4.88	17.57	17.58	34.40
	20.25	99.00	4.89	17.60		
	20.30	99.00	4.88	17.56		
Average	20.28	99.00	4.88	17.58		
21.3	19.12	95.50	4.99	17.98	17.98	35.19
	19.12	95.50	4.99	17.98		
	19.11	95.50	5.00	17.99		
Average	19.12	95.50	5.00	17.98		
21.8	17.94	90.85	5.06	18.23	18.20	35.62
	18.00	90.85	5.05	18.17		
	17.97	90.85	5.06	18.20		
Average	17.97	90.85	5.06	18.20		
22.3	16.53	86.00	5.20	18.73	18.70	36.59
	16.55	86.00	5.20	18.71		
	16.60	86.00	5.18	18.65		
Average	16.56	86.00	5.19	18.70		
22.8	15.46	81.98	5.30	19.09	19.01	37.20
	15.59	81.98	5.26	18.93		
	15.53	81.98	5.28	19.00		
Average	15.53	81.98	5.28	19.01		
23.3	14.44	77.68	5.38	19.36	19.32	37.82
	14.49	77.68	5.36	19.30		
	14.48	77.68	5.36	19.31		
Average	14.47	77.68	5.37	19.32		
23.7	12.59	68.35	5.43	19.54	19.65	38.45
	12.58	68.35	5.43	19.56		
	12.60	69.43	5.51	19.84		
Average	12.59	68.71	5.46	19.65		
24.1	12.09	64.90	5.37	19.33	19.29	37.76
	12.05	64.90	5.39	19.39		
	12.19	64.90	5.32	19.17		
Average	12.11	64.90	5.36	19.29		
24.5	10.77	56.00	5.20	18.72	18.97	37.12
	10.75	57.25	5.33	19.17		
	10.84	57.25	5.28	19.01		
Average	10.79	56.83	5.27	18.97		
24.8	9.95	51.00	5.13	18.45	18.62	36.43
	9.97	52.25	5.24	18.87		
	9.91	51.00	5.15	18.53		
Average	9.94	51.42	5.17	18.62		
25.1	8.93	45.14	5.05	18.20	18.27	35.75
	8.93	45.14	5.05	18.20		
	8.99	45.98	5.11	18.41		
Average	8.95	45.42	5.07	18.27		
25.2	8.15	40.36	4.95	17.83	17.90	35.02
	8.07	40.36	5.00	18.01		
	8.14	40.36	4.96	17.85		
Average	8.12	40.36	4.97	17.90		
25.5	7.61	38.00	4.99	17.98	17.58	34.41
	7.67	36.88	4.81	17.31		
	7.60	36.88	4.85	17.47		
Average	7.63	37.25	4.88	17.58		
	Weight	Volume	Density			
1	6.44	2.40	2.68			
2	7.10	2.60	2.73			
average	6.77	2.50	2.71			
2.7 kg/l						

Appendix N: Drainage rate for degraded ferrosilicon and iron ore

0.8x8.8mm aperture size with Deg FeSi/Fe					Screen area(m ²)	0.511
Feed flowrate(m ³ /hr)	Time taken to fill underflow tank (S)	underflow tank Volume (L)	Drainage rate (L/S)	Drainage rate (m ³ /h)	Average drainage rate (m ³ /h)	Drainage rate (m ³ /m ² /h)
21.8	20.64	83.00	4.02	14.48	14.5	28.34
	20.60	83.00	4.03	14.50		
	20.65	83.00	4.02	14.47		
Average	20.63	83.00	4.02	14.48		
22.8	16.95	70.50	4.16	14.97	15.1	29.54
	16.92	70.50	4.17	15.00		
	16.99	72.25	4.25	15.31		
Average	16.95	71.08	4.19	15.09		
23.7	13.98	61.00	4.36	15.71	15.7	30.65
	13.98	61.00	4.36	15.71		
	14.11	61.00	4.32	15.56		
Average	14.02	61.00	4.35	15.66		
24.5	11.97	53.50	4.47	16.09	16.1	31.58
	11.90	53.50	4.50	16.18		
	11.93	53.50	4.48	16.14		
Average	11.93	53.50	4.48	16.14		
25.1	10.29	44.30	4.31	15.50	15.5	30.43
	10.22	44.30	4.33	15.60		
	10.26	44.30	4.32	15.54		
Average	10.26	44.30	4.32	15.55		
		Weight	Volume	Density		
	1	3.18	1.60	1.99		
	2	2.62	1.30	2.02		
	average	2.90	1.45	2.00		
	2.0 kg/l					

0.8x8.8mm aperture size with Deg FeSi/Fe					Screen area(m ²)	0.511
Feed flowrate(m ³ /hr)	Time taken to fill underflow tank (S)	underflow tank Volume (L)	Drainage rate (L/S)	Drainage rate (m ³ /h)	Average drainage rate (m ³ /h)	Drainage rate (m ³ /m ² /h)
21.8	21.10	83.00	3.93	14.16	14.1	27.66
	21.12	83.00	3.93	14.15		
	21.20	83.00	3.92	14.09		
Average	21.14	83.00	3.93	14.13		
22.8	18.31	75.23	4.11	14.79	14.8	28.91
	18.34	75.23	4.10	14.77		
	18.35	75.23	4.10	14.76		
Average	18.33	75.23	4.10	14.77		
23.7	15.98	68.35	4.28	15.40	15.4	30.10
	16.06	68.35	4.26	15.32		
	15.95	68.35	4.29	15.43		
Average	16.00	68.35	4.27	15.38		
24.5	13.83	61.00	4.41	15.88	15.9	31.12
	13.81	61.00	4.42	15.90		
	13.79	61.00	4.42	15.92		
Average	13.81	61.00	4.42	15.90		
25.1	11.97	51.00	4.26	15.34	15.3	29.94
	12.00	51.00	4.25	15.30		
	12.03	51.00	4.24	15.26		
Average	12.00	51.00	4.25	15.30		
		Weight	Volume	Density		
	1	4.53	2	2.27		
	2	6.09	2.8	2.18		
	average	5.31	2.40	2.22		
	2.20 kg/l					

1x12 mm aperture size with Deg FeSi/Fe					Screen area(m ²)	0.511
Feed flowrate(m ³ /hr)	Time taken to fill underflow tank (S)	underflow tank Volume (L)	Drainage rate (L/S)	Drainage rate (m ³ /h)	Average drainage rate (m ³ /h)	Drainage rate (m ³ /m ² /h)
21.8	20.95	101.00	4.82	17.36	17.34	33.93
	20.97	101.00	4.82	17.34		
	21.00	101.00	4.81	17.31		
Average	20.97	101.00	4.82	17.34		
22.8	18.55	92.00	4.96	17.85	17.81	34.86
	18.50	92.00	4.97	17.90		
	18.50	90.85	4.91	17.68		
Average	18.52	91.62	4.95	17.81		
23.7	15.48	78.90	5.10	18.35	18.40	36.01
	15.43	78.90	5.11	18.41		
	15.40	78.90	5.12	18.44		
Average	15.44	78.90	5.11	18.40		
24.5	12.93	68.50	5.30	19.07	19.11	37.39
	12.91	68.50	5.31	19.10		
	12.88	68.50	5.32	19.15		
Average	12.91	68.50	5.31	19.11		
25.1	9.60	49.33	5.14	18.50	18.41	36.02
	9.69	49.33	5.09	18.33		
	9.65	49.33	5.11	18.40		
Average	9.65	49.33	5.11	18.41		
		Weight	Volume	Density		
	1	3.63	1.90	1.91		
	2	6.04	3.20	1.89		
	average	4.84	2.55	1.90		
	1.90 kg/l					

1x12 mm aperture size with Deg FeSi/Fe					Screen area(m ²)	0.511
Feed flowrate(m ³ /hr)	Time taken to fill underflow tank (S)	underflow tank Volume (L)	Drainage rate (L/S)	Drainage rate (m ³ /h)	Average drainage rate (m ³ /h)	Drainage rate (m ³ /m ² /h)
21.8	21.46	101.00	4.71	16.94	16.92	33.11
	21.50	101.00	4.70	16.91		
	21.52	101.00	4.69	16.90		
Average	21.49	101.00	4.70	16.92		
22.8	18.48	89.70	4.85	17.47	17.43	34.11
	18.36	89.70	4.89	17.59		
	18.75	89.70	4.78	17.22		
Average	18.53	89.70	4.84	17.43		
23.7	15.56	77.68	4.99	17.97	17.97	35.16
	15.57	77.68	4.99	17.96		
	15.56	77.68	4.99	17.97		
Average	15.56	77.68	4.99	17.97		
24.5	12.34	63.60	5.15	18.55	18.58	36.37
	12.32	63.60	5.16	18.58		
	12.30	63.60	5.17	18.61		
Average	12.32	63.60	5.16	18.58		
25.1	10.87	54.75	5.04	18.13	17.94	35.12
	10.78	53.50	4.96	17.87		
	10.80	53.50	4.95	17.83		
Average	10.82	53.92	4.98	17.94		
		Weight	Volume	Density		
	1	5.77	2.90	1.99		
	2	4.82	2.30	2.10		
	average	5.30	2.60	2.04		
	2.0 kg/l					

1x12 mm aperture size with Deg FeSi/Fe					Screen area(m ²)	0.511
Feed flowrate(m ³ /hr)	Time taken to fill underflow tank (S)	underflow tank Volume (L)	Drainage rate (L/S)	Drainage rate (m ³ /h)	Average drainage rate (m ³ /h)	Drainage rate (m ³ /m ² /h)
21.8	21.91	101.00	4.61	16.60	16.6	32.39
	21.98	101.00	4.60	16.54		
	22.01	101.00	4.59	16.52		
Average	21.97	101.00	4.60	16.55		
22.8	19.40	92.00	4.74	17.07	17.0	33.32
	19.46	92.00	4.73	17.02		
	19.50	92.00	4.72	16.98		
Average	19.45	92.00	4.73	17.03		
23.7	16.26	79.93	4.92	17.70	17.7	34.59
	16.30	79.93	4.90	17.65		
	16.28	79.93	4.91	17.67		
Average	16.28	79.93	4.91	17.67		
24.5	14.74	75.23	5.10	18.37	18.2	35.66
	15.03	75.23	5.00	18.02		
	14.82	75.23	5.08	18.27		
Average	14.86	75.23	5.06	18.22		
25.1	13.47	66.20	4.91	17.69	17.7	34.57
	13.52	66.20	4.90	17.63		
	13.48	66.20	4.91	17.68		
Average	13.49	66.20	4.91	17.67		
		Weight	Volume	Density		
		1	5.79	2.65	2.18	
		2	4.76	2.15	2.21	
		average	5.28	2.40	2.20	
		2.2 kg/l				

1x12 mm aperture size with Deg FeSi/Fe					Screen area(m ²)	0.511
Feed flowrate(m ³ /hr)	Time taken to fill underflow tank (S)	underflow tank Volume (L)	Drainage rate (L/S)	Drainage rate (m ³ /h)	Average drainage rate (m ³ /h)	Drainage rate (m ³ /m ² /h)
21.8	22.97	101.00	4.40	15.83	15.8	30.91
	23.01	101.00	4.39	15.80		
	23.07	101.00	4.38	15.76		
Average	23.02	101.00	4.39	15.80		
22.8	19.72	89.70	4.55	16.38	16.4	32.03
	19.76	89.70	4.54	16.34		
	19.70	89.70	4.55	16.39		
Average	19.73	89.70	4.55	16.37		
23.7	17.19	81.98	4.77	17.17	17.2	33.61
	17.20	81.98	4.77	17.16		
	17.16	81.98	4.78	17.20		
Average	17.18	81.98	4.77	17.17		
24.5	14.54	72.25	4.97	17.89	17.8	34.92
	14.61	72.25	4.95	17.80		
	14.58	72.25	4.96	17.84		
Average	14.58	72.25	4.96	17.84		
25.1	12.73	61.00	4.79	17.25	17.2	33.58
	12.81	61.00	4.76	17.14		
	12.85	61.00	4.75	17.09		
Average	12.80	61.00	4.77	17.16		
		Weight	Volume	Density		
		1	4.78	2.10	2.28	
		2	4.60	2.05	2.24	
		average	4.69	2.08	2.26	
		2.30 kg/l				

1x12 mm aperture size with Deg FeSi/Fe					Screen area(m2)	0.511
Feed flowrate(m3/hr)	Time taken to fill underflow tank (S)	underflow tank Volume (L)	Drainage rate (L/S)	Drainage rate (m3/h)	Average drainage rate (m3/h)	Drainage rate (m3/m2/h)
21.8	24.84	101.00	4.07	14.64	14.7	28.73
	24.84	101.00	4.07	14.64		
	24.61	101.00	4.10	14.77		
Average	24.76	101.00	4.08	14.68		
22.8	21.20	89.70	4.23	15.23	15.2	29.79
	21.19	89.70	4.23	15.24		
	21.25	89.70	4.22	15.20		
Average	21.21	89.70	4.23	15.22		
23.7	18.31	80.95	4.42	15.92	15.9	31.11
	18.32	80.95	4.42	15.91		
	18.37	80.95	4.41	15.86		
Average	18.33	80.95	4.42	15.90		
24.5	15.69	70.50	4.49	16.18	16.3	31.96
	15.50	70.50	4.55	16.37		
	15.43	70.50	4.57	16.45		
Average	15.54	70.50	4.54	16.33		
25.1	13.25	58.50	4.42	15.89	15.8	31.01
	13.29	58.50	4.40	15.85		
	13.33	58.50	4.39	15.80		
Average	13.29	58.50	4.40	15.85		
		Weight	Volume	Density		
	1	5.04	2.05	2.46		
	2	5.10	2.10	2.43		
	average	5.07	2.08	2.44		
	2.45 kg/l					

0.63 mm aperture size with Deg FeSi/Fe					Screen area(m2)	0.511
Feed flowrate(m3/hr)	Time taken to fill underflow tank (S)	underflow tank Volume (L)	Drainage rate (L/S)	Drainage rate (m3/h)	Average drainage rate (m3/h)	Drainage rate (m3/m2/h)
21.8	23.70	101.00	4.26	15.34	15.33	30.00
	23.72	101.00	4.26	15.33		
	23.73	101.00	4.26	15.32		
Average	23.72	101.00	4.26	15.33		
22.8	21.41	94.00	4.39	15.81	15.79	30.90
	21.43	94.00	4.39	15.79		
	21.46	94.00	4.38	15.77		
Average	21.43	94.00	4.39	15.79		
23.7	19.20	87.85	4.58	16.47	16.34	31.97
	19.25	86.00	4.47	16.08		
	19.22	87.85	4.57	16.45		
Average	19.22	87.23	4.54	16.34		
24.5	16.80	78.90	4.70	16.91	16.91	33.09
	16.82	78.90	4.69	16.89		
	16.78	78.90	4.70	16.93		
Average	16.80	78.90	4.70	16.91		
25.1	13.40	61.00	4.55	16.39	16.35	31.99
	13.44	61.00	4.54	16.34		
	13.46	61.00	4.53	16.32		
Average	13.43	61.00	4.54	16.35		
		Weight	Volume	Density		
	1	4.52	2.40	1.88		
	2	5.17	2.70	1.91		
	average	4.85	2.55	1.90		
	Density 1.90 kg/l					

0.63 mm aperture size with Deg FeSi/Fe					Screen area(m ²)	0.511
Feed flowrate(m ³ /hr)	Time taken to fill underflow tank (S)	underflow tank Volume (L)	Drainage rate (L/S)	Drainage rate (m ³ /h)	Average drainage rate (m ³ /h)	Drainage rate (m ³ /m ² /h)
21.8	24.90	101.00	4.06	14.60	14.62	28.61
	24.87	101.00	4.06	14.62		
	24.85	101.00	4.06	14.63		
Average	24.87	101.00	4.06	14.62		
22.8	22.27	94.00	4.22	15.20	15.22	29.78
	22.21	94.00	4.23	15.24		
	22.23	94.00	4.23	15.22		
Average	22.24	94.00	4.23	15.22		
23.7	20.34	89.70	4.41	15.88	15.92	31.16
	20.21	89.70	4.44	15.98		
	20.30	89.70	4.42	15.91		
Average	20.28	89.70	4.42	15.92		
24.5	19.69	89.70	4.56	16.40	16.44	32.17
	19.64	89.70	4.57	16.44		
	19.61	89.70	4.57	16.47		
Average	19.65	89.70	4.57	16.44		
25.1	18.56	81.98	4.42	15.90	15.82	30.96
	18.60	80.95	4.35	15.67		
	18.57	81.98	4.41	15.89		
Average	18.58	81.63	4.39	15.82		
		Weight	Volume	Density		
	1	4.71	2.30	2.05		
	2	4.76	2.40	1.98		
	average	4.74	2.35	2.02		
Density 2.0 kg/l						

1x13 mm mm aperture size with FeSi/Fe					Screen area(m ²)	0.511
Feed flowrate(m ³ /hr)	Time taken to fill underflow tank (S)	underflow tank Volume (L)	Drainage rate (L/S)	Drainage rate (m ³ /h)	Average drainage rate (m ³ /h)	Drainage rate (m ³ /m ² /h)
21.8	23.42	101.00	4.31	15.53	15.5	30.27
	23.52	101.00	4.29	15.46		
	23.57	101.00	4.29	15.43		
Average	23.50	101.00	4.30	15.47		
22.8	22.54	101.00	4.48	16.13	16.1	31.49
	22.63	101.00	4.46	16.07		
	22.61	101.00	4.47	16.08		
Average	22.59	101.00	4.47	16.09		
23.7	21.94	101.00	4.60	16.57	16.6	32.45
	21.94	101.00	4.60	16.57		
	21.90	101.00	4.61	16.60		
Average	21.93	101.00	4.61	16.58		
24.5	20.01	95.50	4.77	17.18	17.2	33.61
	20.05	95.50	4.76	17.15		
	20.00	95.50	4.78	17.19		
Average	20.02	95.50	4.77	17.17		
25.1	19.07	87.85	4.61	16.58	16.6	32.49
	19.02	87.85	4.62	16.63		
	19.06	87.85	4.61	16.59		
Average	19.05	87.85	4.61	16.60		
		Weight	Volume	Density		
	1	4.58	2.40	1.91		
	2	4.43	2.35	1.89		
	average	4.51	2.38	1.90		
Density 1.90 kg/l						

1x13 mm mm aperture size with Deg FeSi/Fe					Screen area(m2)	0.511
Feed flowrate(m3/hr)	Time taken to fill underflow tank (S)	underflow tank Volume (L)	Drainage rate (L/S)	Drainage rate (m3/h)	Average drainage rate (m3/h)	Drainage rate (m3/m2/h)
21.8	24.14	101.00	4.18	15.06	15.07	29.49
	24.10	101.00	4.19	15.09		
	24.15	101.00	4.18	15.06		
Average	24.13	101.00	4.19	15.07		
22.8	23.37	101.00	4.32	15.56	15.59	30.50
	23.29	101.00	4.34	15.61		
	23.33	101.00	4.33	15.59		
Average	23.33	101.00	4.33	15.59		
23.7	22.23	100.00	4.50	16.19	16.18	31.67
	22.20	100.00	4.50	16.22		
	22.30	100.00	4.48	16.14		
Average	22.24	100.00	4.50	16.18		
24.5	20.23	94.00	4.65	16.73	16.72	32.71
	20.26	94.00	4.64	16.70		
	20.24	94.00	4.64	16.72		
Average	20.24	94.00	4.64	16.72		
25.1	18.61	83.00	4.46	16.06	16.17	31.64
	18.51	83.00	4.48	16.14		
	18.65	84.50	4.53	16.31		
Average	18.59	83.50	4.49	16.17		
		Weight	Volume	Density		
	1	6.47	3.2	2.02		
	2	4.27	2.10	2.03		
	average	5.37	2.65	2.03		
	Density 2.0 kg/l					

1x13 mm mm aperture size with FeSi/Fe					Screen area(m2)	0.511
Feed flowrate(m3/hr)	Time taken to fill underflow tank (S)	underflow tank Volume (L)	Drainage rate (L/S)	Drainage rate (m3/h)	Average drainage rate (m3/h)	Drainage rate (m3/m2/h)
21.8	24.68	101.00	4.09	14.73	14.69	28.76
	24.80	101.00	4.07	14.66		
	24.75	101.00	4.08	14.69		
Average	24.74	101.00	4.08	14.69		
22.8	23.61	101.00	4.28	15.40	15.39	30.12
	23.65	101.00	4.27	15.37		
	23.60	101.00	4.28	15.41		
Average	23.62	101.00	4.28	15.39		
23.7	22.78	101.00	4.43	15.96	15.97	31.25
	22.75	101.00	4.44	15.98		
	22.78	101.00	4.43	15.96		
Average	22.77	101.00	4.44	15.97		
24.5	20.61	94.00	4.56	16.42	16.46	32.22
	20.55	94.00	4.57	16.47		
	20.51	94.00	4.58	16.50		
Average	20.56	94.00	4.57	16.46		
25.1	19.21	84.50	4.40	15.84	15.88	31.08
	19.15	84.50	4.41	15.89		
	19.10	84.50	4.42	15.93		
Average	19.15	84.50	4.41	15.88		
		Weight	Volume	Density		
	1	5.35	2.40	2.23		
	2	4.55	2.05	2.22		
	average	4.95	2.23	2.22		
	Density 2.2kg/l					

1x13 mm mm aperture size with FeSi/Fe					Screen area(m2)	0.511	
Feed flowrate(m3/hr)	Time taken to fill underflow tank (S)	underflow tank Volume (L)	Drainage rate (L/S)	Drainage rate (m3/h)	Average drainage rate (m3/h)	Drainage rate (m3/m2/h)	
21.8	24.93	101.00	4.05	14.58	14.6	28.51	
	24.99	101.00	4.04	14.55			
	24.95	101.00	4.05	14.57			
Average	24.96	101.00	4.05	14.57			
22.8	23.99	101.00	4.21	15.16	15.1	29.61	
	24.10	101.00	4.19	15.09			
	24.01	101.00	4.21	15.14			
Average	24.03	101.00	4.20	15.13			
23.7	22.96	101.00	4.40	15.84	15.8	30.90	
	23.01	101.00	4.39	15.80			
	23.11	101.00	4.37	15.73			
Average	23.03	101.00	4.39	15.79			
24.5	21.54	97.00	4.50	16.21	16.2	31.74	
	21.50	97.00	4.51	16.24			
	21.55	97.00	4.50	16.20			
Average	21.53	97.00	4.51	16.22			
25.1	20.35	87.85	4.32	15.54	15.8	30.85	
	20.32	89.70	4.41	15.89			
	20.36	89.70	4.41	15.86			
Average	20.34	89.08	4.38	15.76			
		Weight	Volume	Density			
		1	4.44	1.90	2.34		
		2	5.20	2.30	2.26		
		average	4.82	2.10	2.30		
		Density 2.3 kg/l					

Appendix O: Drainage rate for magnetite only

0.63x12 aperture size with magnetite (panels)					Screen area(m2)	0.511			
flowrate(m3/h)	underflow tank (S)	underflow tank Volume (L)	Drainage rate (L/S)	Drainage rate (m3/h)	Average drainage rate (m3/h)	Drainage rate (m3/m2/h)			
18.3	20.47	94.00	4.59	16.53	16.54	32.37			
	20.48	94.00	4.59	16.52					
	20.43	94.00	4.60	16.56					
Average	20.46	94.00	4.59	16.54					
18.7	19.06	89.70	4.71	16.94	16.97	33.21			
	19.01	89.70	4.72	16.99					
	19.01	89.70	4.72	16.99					
Average	19.03	89.70	4.71	16.97					
19.1	17.05	80.50	4.72	17.00	17.38	34.00			
	17.01	83.00	4.88	17.57					
	17.01	83.00	4.88	17.57					
Average	17.02	82.17	4.83	17.38					
19.5	15.70	76.45	4.87	17.53	17.72	34.67			
	15.80	78.90	4.99	17.98					
	16.10	78.90	4.90	17.64					
Average	15.87	78.08	4.92	17.72					
19.9	14.62	73.13	5.00	18.01	18.13	35.47			
	14.52	73.13	5.04	18.13					
	14.43	73.13	5.07	18.24					
Average	14.52	73.13	5.04	18.13					
20.4	13.03	67.28	5.16	18.59	18.54	36.27			
	13.08	67.28	5.14	18.52					
	13.09	67.28	5.14	18.50					
Average	13.07	67.28	5.15	18.54					
20.8	12.37	61.00	4.93	17.75	18.25	35.71			
	12.31	63.60	5.17	18.60					
	12.45	63.60	5.11	18.39					
Average	12.38	62.73	5.07	18.25					
21.3	11.28	56.00	4.96	17.87	17.90	35.03			
	11.28	56.00	4.96	17.87					
	11.23	56.00	4.99	17.95					
Average	11.26	56.00	4.97	17.90					
21.8	10.53	51.00	4.84	17.44	17.54	34.32			
	10.38	51.00	4.91	17.69					
	10.50	51.00	4.86	17.49					
Average	10.47	51.00	4.87	17.54					
22.3	9.10	42.73	4.70	16.90	17.18	33.62			
	8.88	42.73	4.81	17.32					
	8.88	42.73	4.81	17.32					
Average	8.95	42.73	4.77	17.18					
22.8	7.11	33.50	4.71	16.96	16.85	32.98			
	7.15	33.50	4.69	16.87					
	7.21	33.50	4.65	16.73					
Average	7.16	33.50	4.68	16.85					
		Weight	Volume	Density	Dried mass	%Moisture	%Solids	Cal Density	
		1	4.42	2.75	1.61	2.26	48.9	51.1	1.63
		2	5.70	3.45	1.65				
		average	5.06	3.10	1.63				
		Density 1.64 kg/l							

0.63x12 aperture size with magnetite (panels)					Screen	0.511	
Feed flowrate(m ³ /h)	underflow tank (S)	underflow tank Volume (L)	Drainage rate (L/S)	Drainage rate (m ³ /h)	Average drainage rate (m ³ /h)	Drainage rate (m ³ /m ² /h)	
18.3	18.88	86.00	4.56	16.40	16.44	32.16	
	18.80	86.00	4.57	16.47			
	18.83	86.00	4.57	16.44			
Average	18.84	86.00	4.57	16.44			
18.7	16.69	77.68	4.65	16.75	16.86	32.99	
	16.57	77.68	4.69	16.88			
	16.50	77.68	4.71	16.95			
Average	16.59	77.68	4.68	16.86			
19.1	14.97	72.25	4.83	17.37	17.22	33.70	
	15.16	72.25	4.77	17.16			
	15.19	72.25	4.76	17.12			
Average	15.11	72.25	4.78	17.22			
19.5	13.71	66.20	4.83	17.38	17.57	34.38	
	13.75	66.20	4.81	17.33			
	13.73	68.60	5.00	17.99			
Average	13.73	67.00	4.88	17.57			
19.9	12.58	61.00	4.85	17.46	18.03	35.28	
	12.60	63.60	5.05	18.17			
	12.41	63.60	5.12	18.45			
Average	12.53	62.73	5.01	18.03			
20.4	11.31	56.00	4.95	17.82	18.28	35.77	
	11.41	58.50	5.13	18.46			
	11.35	58.50	5.15	18.56			
Average	11.36	57.67	5.08	18.28			
20.8	10.46	53.50	5.11	18.41	18.02	35.26	
	10.59	53.50	5.05	18.19			
	10.52	51.00	4.85	17.45			
Average	10.52	52.67	5.00	18.02			
21.3	9.56	47.65	4.98	17.94	17.68	34.60	
	9.87	47.65	4.83	17.38			
	9.68	47.65	4.92	17.72			
Average	9.70	47.65	4.91	17.68			
21.8	8.28	38.00	4.59	16.52	17.34	33.94	
	7.60	38.00	5.00	18.00			
	7.35	35.75	4.86	17.51			
Average	7.74	37.25	4.82	17.34			
22.3	7.09	33.50	4.72	17.01	17.05	33.37	
	7.05	33.50	4.75	17.11			
	7.08	33.50	4.73	17.03			
Average	7.07	33.50	4.74	17.05			
22.8	5.71	26.50	4.64	16.71	16.66	32.60	
	5.72	26.50	4.63	16.68			
	5.75	26.50	4.61	16.59			
Average	5.73	26.50	4.63	16.66			
	Weight	Volume	Density	Dried mass	%Moisture	%Solids	Cal Density
1	3.84	2.2	1.75	2.13	44.5	55.5	1.722
2	5.3	3.1	1.71				
3	3.59	2.1	1.71				
4	5.6	3.3	1.70				
average	4.58	2.68	1.72				
Density 1.72 kg/l							

0.63x12 aperture size with magnetite (panels)					Screen	0.511	
Feed flowrate(m ³ /h)	fill underflow tank (S)	tank Volume (L)	Drainage rate (L/S)	Drainage rate (m ³ /h)	drainage rate (m ³ /h)	Drainage rate (m ³ /m ² /h)	
18.3	20.37	92.00	4.52	16.26	16.22	31.75	
	20.41	92.00	4.51	16.23			
	20.47	92.00	4.49	16.18			
Average	20.42	92.00	4.51	16.22			
18.7	18.41	86.00	4.67	16.82	16.78	32.84	
	18.51	86.00	4.65	16.73			
	18.42	86.00	4.67	16.81			
Average	18.45	86.00	4.66	16.78			
19.1	17.19	80.95	4.71	16.95	17.12	33.51	
	17.44	83.00	4.76	17.13			
	17.29	83.00	4.80	17.28			
Average	17.31	82.32	4.76	17.12			
19.5	14.81	72.25	4.88	17.56	17.50	34.25	
	14.92	72.25	4.84	17.43			
	14.85	72.25	4.87	17.52			
Average	14.86	72.25	4.86	17.50			
19.9	13.60	68.50	5.04	18.13	17.84	34.91	
	14.19	68.50	4.83	17.38			
	14.09	70.50	5.00	18.01			
Average	13.96	69.17	4.96	17.84			
20.4	12.44	61.00	4.90	17.65	18.13	35.49	
	12.50	63.75	5.10	18.36			
	12.48	63.75	5.11	18.39			
Average	12.47	62.83	5.04	18.13			
20.8	11.31	56.00	4.95	17.82	17.85	34.93	
	11.22	56.00	4.99	17.97			
	11.35	56.00	4.93	17.76			
Average	11.29	56.00	4.96	17.85			
21.3	10.31	51.00	4.95	17.81	17.52	34.30	
	10.22	49.33	4.83	17.37			
	10.21	49.33	4.83	17.39			
Average	10.25	49.88	4.87	17.52			
21.8	8.81	44.30	5.03	18.10	17.26	33.77	
	8.69	41.15	4.74	17.05			
	8.91	41.15	4.62	16.63			
Average	8.80	42.20	4.79	17.26			
22.3	6.36	30.00	4.72	16.98	16.86	32.99	
	6.37	30.00	4.71	16.95			
	6.49	30.00	4.62	16.64			
Average	6.41	30.00	4.68	16.86			
22.8	4.71	21.63	4.59	16.53	16.51	32.30	
	4.70	21.63	4.60	16.56			
	4.74	21.63	4.56	16.42			
Average	4.72	21.63	4.58	16.51			
	Weight	Volume	Density	Dried mass	%Moisture	%Solids	Cal Density
1	6.36	3.45	1.84	3.87	39.2	60.8	1.85
2	5.22	2.80	1.86				
average	5.79	3.13	1.85				
Density 1.84kg/l							

0.63x8.8 aperture size with magnetite (panels)					Screen area(m2)	0.511	
Feed flowrate(m3/h)	Time taken to fill underflow tank (S)	underflow tank Volume (L)	Drainage rate (L/S)	Drainage rate (m3/h)	Average drainage rate (m3/h)	Drainage rate (m3/m2/h)	
18.3	20.09	92.00	4.58	16.49	16.49	32.28	
	20.12	92.00	4.57	16.46			
	20.03	92.00	4.59	16.54			
Average	20.08	92.00	4.58	16.49			
18.7	18.22	85.80	4.71	16.95	16.91	33.09	
	18.31	85.80	4.69	16.87			
	18.27	85.80	4.70	16.91			
Average	18.27	85.80	4.70	16.91			
19.1	16.53	78.90	4.77	17.18	17.20	33.67	
	16.75	78.90	4.71	16.96			
	16.68	80.95	4.85	17.47			
Average	16.65	79.58	4.78	17.20			
19.5	15.40	74.00	4.81	17.30	17.61	34.46	
	15.12	74.00	4.89	17.62			
	15.37	76.45	4.97	17.91			
Average	15.30	74.82	4.89	17.61			
19.9	13.70	68.35	4.99	17.96	18.01	35.25	
	13.69	68.35	4.99	17.97			
	13.59	68.35	5.03	18.11			
Average	13.66	68.35	5.00	18.01			
20.4	12.50	63.60	5.09	18.32	18.35	35.91	
	12.49	63.60	5.09	18.33			
	12.44	63.60	5.11	18.41			
Average	12.48	63.60	5.10	18.35			
20.8	11.40	58.50	5.13	18.47	17.96	35.14	
	11.41	56.00	4.91	17.67			
	11.37	56.00	4.93	17.73			
Average	11.39	56.83	4.99	17.96			
21.3	10.30	51.00	4.95	17.83	17.65	34.54	
	10.40	51.00	4.90	17.65			
	10.51	51.00	4.85	17.47			
Average	10.40	51.00	4.90	17.65			
21.8	8.92	44.30	4.97	17.88	17.32	33.90	
	8.71	41.15	4.72	17.01			
	8.67	41.15	4.75	17.09			
Average	8.77	42.20	4.81	17.32			
22.3	6.95	33.50	4.82	17.35	17.03	33.32	
	7.15	33.50	4.69	16.87			
	7.15	33.50	4.69	16.87			
Average	7.08	33.50	4.73	17.03			
22.8	5.77	26.50	4.59	16.53	16.59	32.47	
	5.80	26.50	4.57	16.45			
	5.68	26.50	4.67	16.80			
Average	5.75	26.50	4.61	16.59			
	Weight	Volume	Density	Dried weight	%Moisture	%Solids	Cal Density
1	3.93	2.40	1.64				
2	3.61	2.20	1.64	1.85	48.8	51.2	1.63
average	3.77	2.30	1.64				
Density 1.64 kg/l							

0.63x8.8 aperture size with magnetite (panels)					Screen area(m ²)	0.511	
Feed flowrate(m ³ /h)	Time taken to fill underflow tank (S)	underflow tank Volume (L)	Drainage rate (L/S)	Drainage rate (m ³ /h)	Average drainage rate (m ³ /h)	Drainage rate (m ³ /m ² /h)	
18.3	20.56	92.00	4.47	16.11	16.18	31.66	
	20.44	92.00	4.50	16.20			
	20.41	92.00	4.51	16.23			
Average	20.47	92.00	4.49	16.18			
18.7	18.41	83.00	4.51	16.23	16.60	32.48	
	18.42	85.80	4.66	16.77			
	18.39	85.80	4.67	16.80			
Average	18.41	84.87	4.61	16.60			
19.1	17.28	80.95	4.68	16.86	17.04	33.35	
	17.50	83.00	4.74	17.07			
	17.38	83.00	4.78	17.19			
Average	17.39	82.32	4.73	17.04			
19.5	15.87	76.45	4.82	17.34	17.40	34.05	
	15.78	76.45	4.84	17.44			
	15.81	76.45	4.84	17.41			
Average	15.82	76.45	4.83	17.40			
19.9	14.28	70.50	4.94	17.77	17.87	34.96	
	14.22	70.50	4.96	17.85			
	14.12	70.50	4.99	17.97			
Average	14.21	70.50	4.96	17.87			
20.4	13.00	66.20	5.09	18.33	18.17	35.57	
	13.15	66.20	5.03	18.12			
	13.19	66.20	5.02	18.07			
Average	13.11	66.20	5.05	18.17			
20.8	11.98	61.00	5.09	18.33	17.83	34.89	
	11.84	58.50	4.94	17.79			
	12.13	58.50	4.82	17.36			
Average	11.98	59.33	4.95	17.83			
21.3	10.94	53.50	4.89	17.61	17.52	34.28	
	10.72	53.50	4.99	17.97			
	10.81	51.00	4.72	16.98			
Average	10.82	52.67	4.87	17.52			
21.8	9.97	47.65	4.78	17.21	17.22	33.69	
	9.99	47.65	4.77	17.17			
	9.93	47.65	4.80	17.27			
Average	9.96	47.65	4.78	17.22			
22.3	8.10	38.00	4.69	16.89	16.90	33.06	
	8.06	38.00	4.71	16.97			
	8.13	38.00	4.67	16.83			
Average	8.10	38.00	4.69	16.90			
22.8	6.93	31.75	4.58	16.49	16.48	32.25	
	6.97	31.75	4.56	16.40			
	6.91	31.75	4.59	16.54			
Average	6.94	31.75	4.58	16.48			
23.3	6.02	26.50	4.40	15.85	16.02	31.35	
	5.87	26.50	4.51	16.25			
	5.98	26.50	4.43	15.95			
Average	5.96	26.50	4.45	16.02			
	Weight	Volume	Density	Dried weight	%Moisture	%Solids	Cal Density
1	4.36	2.50	1.74	2.41	44.7	55.3	1.72
2	3.72	2.20	1.69				
3	4.54	2.60	1.75				
average	4.21	2.43	1.73				
Density 1.72 kg/l							

1x13mm aperture size with magnetite without deflectors					Screen area(m ²)	0.511	
Feed flowrate(m ³ /h)	underflow tank (S)	underflow tank Volume (L)	Drainage rate (L/S)	Drainage rate (m ³ /h)	Average drainage rate (m ³ /h)	Drainage rate (m ³ /m ² /h)	
18.3	21.53	94.00	4.37	15.72	15.62	30.57	
	21.79	94.00	4.31	15.53			
	21.67	94.00	4.34	15.62			
Average	21.66	94.00	4.34	15.62			
18.7	20.08	89.70	4.47	16.08	16.11	31.52	
	20.02	89.70	4.48	16.13			
	20.04	89.70	4.48	16.11			
Average	20.05	89.70	4.47	16.11			
19.1	18.71	86.00	4.60	16.55	16.54	32.36	
	18.71	86.00	4.60	16.55			
	18.74	86.00	4.59	16.52			
Average	18.72	86.00	4.59	16.54			
19.5	16.71	78.90	4.72	17.00	16.95	33.18	
	16.74	78.90	4.71	16.97			
	16.81	78.90	4.69	16.90			
Average	16.75	78.90	4.71	16.95			
19.9	15.36	74.00	4.82	17.34	17.39	34.02	
	15.27	74.00	4.85	17.45			
	15.34	74.00	4.82	17.37			
Average	15.32	74.00	4.83	17.39			
20.4	14.32	70.50	4.92	17.72	17.71	34.66	
	14.36	70.50	4.91	17.67			
	14.31	70.50	4.93	17.74			
Average	14.33	70.50	4.92	17.71			
20.8	13.03	66.20	5.08	18.29	17.97	35.16	
	13.10	66.20	5.05	18.19			
	13.14	63.60	4.84	17.42			
Average	13.09	65.33	4.99	17.97			
21.3	11.66	56.00	4.80	17.29	17.44	34.12	
	11.53	56.00	4.86	17.48			
	11.50	56.00	4.87	17.53			
Average	11.56	56.00	4.84	17.44			
21.8	10.19	51.00	5.00	18.02	17.18	33.63	
	10.25	47.65	4.65	16.74			
	10.21	47.65	4.67	16.80			
Average	10.22	48.77	4.77	17.18			
22.3	9.00	41.15	4.57	16.46	16.86	33.00	
	9.03	41.15	4.56	16.41			
	9.00	44.30	4.92	17.72			
Average	9.01	42.20	4.68	16.86			
22.8	7.80	35.75	4.58	16.50	16.51	32.32	
	7.77	35.75	4.60	16.56			
	7.81	35.75	4.58	16.48			
Average	7.79	35.75	4.59	16.51			
	Weight	Volume	Density	Dried weights	%Moisture	%Solids	Cal Density
1	5.39	3.3	1.63		100.0	0.0	1.00
2	3.08	1.85	1.66	1.59	48.4	51.6	1.64
average	4.24	2.58	1.65				
Density 1.64 kg/l							

1x13mm aperture size with magnetite without deflectors					Screen area(m ²)	0.511	
Feed flowrate(m ³ /h)	to fill underflow	underflow tank Volume (L)	Drainage rate (L/S)	Drainage rate (m ³ /h)	Average drainage rate (m ³ /h)	Drainage rate (m ³ /m ² /h)	
18.3	22.15	95.50	4.31	15.52	15.53	30.39	
	22.15	95.50	4.31	15.52			
	22.11	95.50	4.32	15.55			
Average	22.14	95.50	4.31	15.53			
18.7	20.84	92.00	4.41	15.89	15.90	31.11	
	20.88	92.00	4.41	15.86			
	20.79	92.00	4.43	15.93			
Average	20.84	92.00	4.42	15.90			
19.1	19.15	86.00	4.49	16.17	16.21	31.72	
	19.10	86.00	4.50	16.21			
	19.06	86.00	4.51	16.24			
Average	19.10	86.00	4.50	16.21			
19.5	17.32	79.93	4.61	16.61	16.56	32.40	
	17.41	79.93	4.59	16.53			
	17.40	79.93	4.59	16.54			
Average	17.38	79.93	4.60	16.56			
19.9	15.60	74.00	4.74	17.08	16.94	33.16	
	15.79	74.00	4.69	16.87			
	15.78	74.00	4.69	16.88			
Average	15.72	74.00	4.71	16.94			
20.4	14.61	70.50	4.83	17.37	17.37	34.00	
	14.69	70.50	4.80	17.28			
	14.53	70.50	4.85	17.47			
Average	14.61	70.50	4.83	17.37			
20.8	13.25	66.20	5.00	17.99	17.80	34.83	
	13.41	66.20	4.94	17.77			
	13.51	66.20	4.90	17.64			
Average	13.39	66.20	4.94	17.80			
21.3	12.09	58.50	4.84	17.42	17.26	33.77	
	11.97	58.50	4.89	17.59			
	12.03	56.00	4.66	16.76			
Average	12.03	57.67	4.79	17.26			
21.8	10.31	47.65	4.62	16.64	16.97	33.21	
	10.38	47.65	4.59	16.53			
	10.35	51.00	4.93	17.74			
Average	10.35	48.77	4.71	16.97			
22.3	8.87	41.15	4.64	16.70	16.64	32.56	
	8.91	41.15	4.62	16.63			
	8.93	41.15	4.61	16.59			
Average	8.90	41.15	4.62	16.64			
22.8	7.75	34.63	4.47	16.08	16.17	31.65	
	7.68	34.63	4.51	16.23			
	7.69	34.63	4.50	16.21			
Average	7.71	34.63	4.49	16.17			
23.3	6.38	28.25	4.43	15.94	15.83	30.99	
	6.41	28.25	4.41	15.87			
	6.48	28.25	4.36	15.69			
Average	6.42	28.25	4.40	15.83			
	Weight	Volume	Density	Dried weights	%Moisture	%Solids	Cal Density
1	5.62	3.30	1.70	3.08	44.4	55.6	1.73
2	5.54	3.20	1.73				
average	5.58	3.25	1.72				
Density 1.72 kg/l							

1x13mm aperture size with magnetite without deflectors					Screen area(m ²)	0.511	
flowrate(m ³ /h)	underflow tank (S)	underflow tank Volume (L)	Drainage rate (L/S)	Drainage rate (m ³ /h)	Average drainage rate (m ³ /h)	Drainage rate (m ³ /m ² /h)	
18.3	23.21	99.00	4.27	15.36	15.28	29.89	
	23.14	99.00	4.28	15.40			
	23.17	97.00	4.19	15.07			
Average	23.17	98.33	4.24	15.28			
18.7	21.25	92.00	4.33	15.59	15.59	30.51	
	21.24	92.00	4.33	15.59			
	21.25	92.00	4.33	15.59			
Average	21.25	92.00	4.33	15.59			
19.1	18.91	83.75	4.43	15.94	15.91	31.13	
	18.98	83.75	4.41	15.89			
	18.97	83.75	4.41	15.89			
Average	18.95	83.75	4.42	15.91			
19.5	17.48	78.90	4.51	16.25	16.22	31.75	
	17.58	78.90	4.49	16.16			
	17.46	78.90	4.52	16.27			
Average	17.51	78.90	4.51	16.22			
19.9	16.07	74.00	4.60	16.58	16.60	32.49	
	16.06	74.00	4.61	16.59			
	16.01	74.00	4.62	16.64			
Average	16.05	74.00	4.61	16.60			
20.4	14.96	70.50	4.71	16.97	17.02	33.30	
	14.86	70.50	4.74	17.08			
	14.92	70.50	4.73	17.01			
Average	14.91	70.50	4.73	17.02			
20.8	13.61	66.20	4.86	17.51	17.41	34.07	
	13.78	66.20	4.80	17.29			
	13.68	66.20	4.84	17.42			
Average	13.69	66.20	4.84	17.41			
21.3	12.93	61.00	4.72	16.98	17.05	33.36	
	12.87	61.00	4.74	17.06			
	12.85	61.00	4.75	17.09			
Average	12.88	61.00	4.73	17.05			
21.8	11.00	51.00	4.64	16.69	16.71	32.70	
	11.00	51.00	4.64	16.69			
	10.96	51.00	4.65	16.75			
Average	10.99	51.00	4.64	16.71			
22.3	9.66	44.30	4.59	16.51	16.42	32.14	
	9.78	44.30	4.53	16.31			
	9.69	44.30	4.57	16.46			
Average	9.71	44.30	4.56	16.42			
22.8	7.93	35.75	4.51	16.23	16.12	31.55	
	7.88	35.75	4.54	16.33			
	7.89	34.63	4.39	15.80			
Average	7.90	35.38	4.48	16.12			
23.3	6.50	28.25	4.35	15.65	15.74	30.81	
	6.47	28.25	4.37	15.72			
	6.41	28.25	4.41	15.87			
Average	6.46	28.25	4.37	15.74			
0.0	4.85	20.81	4.29	15.45	15.45	30.23	
	4.81	20.81	4.33	15.58			
	4.89	20.81	4.26	15.32			
Average	4.85	20.81	4.29	15.45			
	Weight	Volume	Density	Dried weights	%Moisture	%Solids	Cal Density
1	4.88	2.60	1.88	2.94	39.8	60.2	1.84
2	3.49	1.90	1.84				
average	4.19	2.25	1.86				
Density 1.84 kg/l							

1x12mm aperture size with magnetite					Screen area(m ²)	0.511	
Feed flowrate(m ³ /h)	Time taken to fill underflow tank (S)	underflow tank Volume (L)	Drainage rate (L/S)	Drainage rate (m ³ /h)	Average drainage rate (m ³ /h)	Drainage rate (m ³ /m ² /h)	
18.3	21.47	101.00	4.70	16.94	16.92	33.11	
	21.50	101.00	4.70	16.91			
	21.51	101.00	4.70	16.90			
Average	21.49	101.00	4.70	16.92			
18.7	20.12	97.00	4.82	17.36	17.32	33.90	
	20.17	97.00	4.81	17.31			
	20.19	97.00	4.80	17.30			
Average	20.16	97.00	4.81	17.32			
19.1	18.40	89.70	4.88	17.55	17.52	34.29	
	18.46	89.70	4.86	17.49			
	18.43	89.70	4.87	17.52			
Average	18.43	89.70	4.87	17.52			
19.5	17.32	86.00	4.97	17.88	17.86	34.96	
	17.32	86.00	4.97	17.88			
	17.35	86.00	4.96	17.84			
Average	17.33	86.00	4.96	17.86			
19.9	16.40	83.00	5.06	18.22	18.20	35.63	
	16.43	83.00	5.05	18.19			
	16.41	83.00	5.06	18.21			
Average	16.41	83.00	5.06	18.20			
20.4	15.18	78.90	5.20	18.71	18.68	36.55	
	15.25	78.90	5.17	18.63			
	15.19	78.90	5.19	18.70			
Average	15.21	78.90	5.19	18.68			
20.8	14.03	74.00	5.27	18.99	18.93	37.05	
	13.94	73.13	5.25	18.88			
	13.91	73.13	5.26	18.93			
Average	13.96	73.42	5.26	18.93			
21.3	12.90	70.50	5.47	19.67	19.34	37.85	
	12.82	68.35	5.33	19.19			
	12.85	68.35	5.32	19.15			
Average	12.86	69.07	5.37	19.34			
21.8	11.84	62.30	5.26	18.94	18.98	37.14	
	11.97	63.60	5.31	19.13			
	11.89	62.30	5.24	18.86			
Average	11.90	62.73	5.27	18.98			
22.3	10.38	53.50	5.15	18.55	18.67	36.53	
	10.32	53.50	5.18	18.66			
	10.25	53.50	5.22	18.79			
Average	10.32	53.50	5.19	18.67			
22.8	9.19	45.98	5.00	18.01	18.20	35.62	
	9.06	45.98	5.07	18.27			
	9.03	45.98	5.09	18.33			
Average	9.09	45.98	5.06	18.20			
23.3	8.66	42.73	4.93	17.76	17.84	34.91	
	8.61	42.73	4.96	17.86			
	8.60	42.73	4.97	17.88			
Average	8.62	42.73	4.95	17.84			
23.7	7.62	36.88	4.84	17.42	17.42	34.09	
	7.64	36.88	4.83	17.38			
	7.60	36.88	4.85	17.47			
Average	7.62	36.88	4.84	17.42			
24.1	6.37	30.00	4.71	16.95	17.04	33.35	
	6.30	30.00	4.76	17.14			
	6.34	30.00	4.73	17.03			
Average	6.34	30.00	4.73	17.04			
24.5	5.31	23.25	4.38	15.76	16.48	32.24	
	5.34	24.88	4.66	16.77			
	5.30	24.88	4.69	16.90			
Average	5.32	24.33	4.58	16.48			
	Weight	Volume	Density	Dried weights	%Moisture	%Solids	Cal Density
1	4.04	2.4	1.68	2.11	47.8	52.2	1.65
2	3.44	2.1	1.64				
average	3.74	2.25	1.66				
Density 1.64 kg/l							

1x12mm aperture size with magnetite					Screen area(m ²)	0.511	
Feed flowrate(m ³ /h)	Time taken to fill underflow tank (S)	underflow tank Volume (L)	Drainage rate (L/S)	Drainage rate (m ³ /h)	Average drainage rate (m ³ /h)	Drainage rate (m ³ /m ² /h)	
18.3	21.67	101.00	4.66	16.78	16.77	32.83	
	21.71	101.00	4.65	16.75			
	21.65	101.00	4.67	16.79			
Average	21.68	101.00	4.66	16.77			
18.7	20.15	96.50	4.79	17.24	17.15	33.57	
	20.18	96.50	4.78	17.22			
	20.17	95.25	4.72	17.00			
Average	20.17	96.08	4.76	17.15			
19.1	18.51	89.70	4.85	17.45	17.45	34.15	
	18.53	89.70	4.84	17.43			
	18.47	89.70	4.86	17.48			
Average	18.50	89.70	4.85	17.45			
19.5	17.23	84.50	4.90	17.66	17.73	34.70	
	17.29	85.25	4.93	17.75			
	17.25	85.25	4.94	17.79			
Average	17.26	85.00	4.93	17.73			
19.9	15.70	78.90	5.03	18.09	18.05	35.31	
	15.78	78.90	5.00	18.00			
	15.74	78.90	5.01	18.05			
Average	15.74	78.90	5.01	18.05			
20.4	14.45	74.00	5.12	18.44	18.44	36.08	
	14.41	74.00	5.14	18.49			
	14.49	74.00	5.11	18.39			
Average	14.45	74.00	5.12	18.44			
20.8	13.49	70.50	5.23	18.81	18.77	36.73	
	13.55	70.50	5.20	18.73			
	13.53	70.50	5.21	18.76			
Average	13.52	70.50	5.21	18.77			
21.3	12.43	66.20	5.33	19.17	19.15	37.47	
	12.44	66.20	5.32	19.16			
	12.47	66.20	5.31	19.11			
Average	12.45	66.20	5.32	19.15			
21.8	11.56	59.75	5.17	18.61	18.78	36.75	
	11.49	61.00	5.31	19.11			
	11.55	59.75	5.17	18.62			
Average	11.53	60.17	5.22	18.78			
22.3	10.25	52.25	5.10	18.35	18.40	36.01	
	10.19	52.25	5.13	18.46			
	10.23	52.25	5.11	18.39			
Average	10.22	52.25	5.11	18.40			
22.8	9.25	45.98	4.97	17.89	17.99	35.21	
	9.16	45.98	5.02	18.07			
	9.19	45.98	5.00	18.01			
Average	9.20	45.98	5.00	17.99			
23.3	7.77	38.00	4.89	17.61	17.64	34.53	
	7.74	38.00	4.91	17.67			
	7.75	38.00	4.90	17.65			
Average	7.75	38.00	4.90	17.64			
23.7	6.81	31.75	4.66	16.78	17.23	33.72	
	6.93	33.50	4.83	17.40			
	6.89	33.50	4.86	17.50			
Average	6.88	32.92	4.79	17.23			
24.1	5.31	24.88	4.68	16.86	16.88	33.03	
	5.60	26.50	4.73	17.04			
	5.35	24.88	4.65	16.74			
Average	5.42	25.42	4.69	16.88			
24.5	4.00	18.33	4.58	16.49	16.25	31.80	
	4.05	18.33	4.52	16.29			
	4.13	18.33	4.44	15.97			
Average	4.06	18.33	4.51	16.25			
	Weight	Volume	Density	Dried weights	%Moisture	%Solids	Cal Density
1	5.25	3.00	1.75	2.89	45.0	55.0	1.71
2	4.17	2.45	1.70				
average	4.71	2.73	1.73				
Density 1.72 kg/l							

0.8x8.8mm aperture size with magnetite					Screen area(m2)	0.511	
Feed flowrate(m3/h)	Time taken to fill underflow tank (S)	underflow tank Volume (L)	Drainage rate (L/S)	Drainage rate (m3/h)	Average drainage rate (m3/h)	Drainage rate (m3/m2/h)	
18.3	22.55	101.00	4.48	16.12	16.14	31.58	
	22.50	101.00	4.49	16.16			
	22.54	101.00	4.48	16.13			
Average	22.53	101.00	4.48	16.14			
18.7	20.31	94.00	4.63	16.66	16.66	32.60	
	20.29	94.00	4.63	16.68			
	20.35	94.00	4.62	16.63			
Average	20.32	94.00	4.63	16.66			
19.1	19.42	92.00	4.74	17.05	17.05	33.37	
	19.45	92.00	4.73	17.03			
	19.39	92.00	4.74	17.08			
Average	19.42	92.00	4.74	17.05			
19.5	17.65	86.00	4.87	17.54	17.54	34.33	
	17.71	86.00	4.86	17.48			
	17.59	86.00	4.89	17.60			
Average	17.65	86.00	4.87	17.54			
19.9	16.64	83.00	4.99	17.96	17.97	35.16	
	16.60	83.00	5.00	18.00			
	16.65	83.00	4.98	17.95			
Average	16.63	83.00	4.99	17.97			
20.4	15.22	77.68	5.10	18.37	18.37	35.95	
	15.20	77.68	5.11	18.40			
	15.25	77.68	5.09	18.34			
Average	15.22	77.68	5.10	18.37			
20.8	13.58	70.50	5.19	18.69	18.70	36.59	
	13.59	70.50	5.19	18.68			
	13.55	70.50	5.20	18.73			
Average	13.57	70.50	5.19	18.70			
21.3	12.69	64.90	5.11	18.41	18.35	35.91	
	12.66	64.90	5.13	18.45			
	12.59	63.60	5.05	18.19			
Average	12.65	64.47	5.10	18.35			
21.8	11.94	59.75	5.00	18.02	18.02	35.26	
	11.90	59.75	5.02	18.08			
	11.97	59.75	4.99	17.97			
Average	11.94	59.75	5.01	18.02			
22.3	10.71	52.25	4.88	17.56	17.70	34.64	
	10.77	53.25	4.94	17.80			
	10.81	53.25	4.93	17.73			
Average	10.76	52.92	4.92	17.70			
22.8	9.20	44.30	4.82	17.33	17.32	33.89	
	9.22	44.30	4.80	17.30			
	9.21	44.30	4.81	17.32			
Average	9.21	44.30	4.81	17.32			
23.3	8.00	38.00	4.75	17.10	16.95	33.16	
	8.12	38.00	4.68	16.85			
	8.10	38.00	4.69	16.89			
Average	8.07	38.00	4.71	16.95			
23.7	6.14	28.25	4.60	16.56	16.54	32.36	
	6.11	28.25	4.62	16.64			
	6.20	28.25	4.56	16.40			
Average	6.15	28.25	4.59	16.54			
24.1	5.18	23.25	4.49	16.16	16.15	31.60	
	5.15	23.25	4.51	16.25			
	5.22	23.25	4.45	16.03			
Average	5.18	23.25	4.49	16.15			
24.5	3.80	16.65	4.38	15.77	15.80	30.92	
	3.81	16.65	4.37	15.73			
	3.77	16.65	4.42	15.90			
Average	3.79	16.65	4.39	15.80			
	Weight	Volume	Density	Dried weights	%Moisture	%Solids	Cal Density
1	5.01	3.1	1.62	2.59	48.3	51.7	1.64
2	3.41	2.05	1.66				
average	4.21	2.58	1.64				
Density 1.64 kg/l							

0.8x8.8mm aperture size with magnetite					Screen area(m ²)	0.511	
Feed flowrate(m ³ /h)	Time taken to fill underflow tank (S)	underflow tank Volume (L)	Drainage rate (L/S)	Drainage rate (m ³ /h)	Average drainage rate (m ³ /h)	Drainage rate (m ³ /m ² /h)	
18.3	22.53	101.00	4.48	16.14	16.11	31.52	
	22.60	101.00	4.47	16.09			
	22.59	101.00	4.47	16.10			
Average	22.57	101.00	4.47	16.11			
18.7	20.80	95.50	4.59	16.53	16.55	32.38	
	20.75	95.50	4.60	16.57			
	20.78	95.50	4.60	16.54			
Average	20.78	95.50	4.60	16.55			
19.1	18.56	87.85	4.73	17.04	17.02	33.30	
	18.61	87.85	4.72	16.99			
	18.59	87.85	4.73	17.01			
Average	18.59	87.85	4.73	17.02			
19.5	17.21	83.00	4.82	17.36	17.39	34.02	
	17.19	83.00	4.83	17.38			
	17.16	83.00	4.84	17.41			
Average	17.19	83.00	4.83	17.39			
19.9	16.10	78.90	4.90	17.64	17.66	34.55	
	16.05	78.90	4.92	17.70			
	16.11	78.90	4.90	17.63			
Average	16.09	78.90	4.90	17.66			
20.4	14.74	74.00	5.02	18.07	17.99	35.20	
	14.80	74.00	5.00	18.00			
	14.89	74.00	4.97	17.89			
Average	14.81	74.00	5.00	17.99			
20.8	13.65	69.43	5.09	18.31	18.32	35.85	
	13.63	69.43	5.09	18.34			
	13.65	69.43	5.09	18.31			
Average	13.64	69.43	5.09	18.32			
21.3	12.89	64.90	5.03	18.13	18.07	35.35	
	12.80	63.60	4.97	17.89			
	12.85	64.90	5.05	18.18			
Average	12.85	64.47	5.02	18.07			
21.8	12.11	59.75	4.93	17.76	17.72	34.67	
	12.15	59.75	4.92	17.70			
	12.16	59.75	4.91	17.69			
Average	12.14	59.75	4.92	17.72			
22.3	11.11	53.50	4.82	17.34	17.38	34.02	
	11.01	53.50	4.86	17.49			
	11.12	53.50	4.81	17.32			
Average	11.08	53.50	4.83	17.38			
22.8	9.45	44.30	4.69	16.88	16.98	33.24	
	9.38	44.30	4.72	17.00			
	9.34	44.30	4.74	17.07			
Average	9.39	44.30	4.72	16.98			
23.3	8.21	38.00	4.63	16.66	16.62	32.53	
	8.25	38.00	4.61	16.58			
	8.23	38.00	4.62	16.62			
Average	8.23	38.00	4.62	16.62			
23.7	6.56	30.00	4.57	16.46	16.32	31.93	
	6.69	30.00	4.48	16.14			
	6.61	30.00	4.54	16.34			
Average	6.62	30.00	4.53	16.32			
24.1	5.22	23.20	4.44	16.00	15.99	31.29	
	5.25	23.20	4.42	15.91			
	5.20	23.20	4.46	16.06			
Average	5.22	23.20	4.44	15.99			
24.5	4.03	17.49	4.34	15.62	15.66	30.65	
	4.03	17.49	4.34	15.62			
	4.00	17.49	4.37	15.74			
Average	4.02	17.49	4.35	15.66			
	Weight	Volume	Density	Dried weights	%Moisture	%Solids	Cal Density
1	5.34	3.10	1.72				
2	5.01	2.90	1.73	2.78	44.5	55.5	1.72
average	5.18	3.00	1.73				
Density 1.72 kg/l							

0.8x8.8mm aperture size with magnetite					Screen area(m2)	0.511	
Feed flowrate(m3/h)	Time taken to fill underflow tank (S)	underflow tank Volume (L)	Drainage rate (L/S)	Drainage rate (m3/h)	Average drainage rate (m3/h)	Drainage rate (m3/m2/h)	
18.3	21.87	97.00	4.44	15.97	16.00	31.31	
	21.81	97.00	4.45	16.01			
	21.80	97.00	4.45	16.02			
Average	21.83	97.00	4.44	16.00			
18.7	20.22	92.00	4.55	16.38	16.41	32.11	
	20.19	92.00	4.56	16.40			
	20.15	92.00	4.57	16.44			
Average	20.19	92.00	4.56	16.41			
19.1	18.67	86.93	4.66	16.76	16.78	32.84	
	18.70	86.93	4.65	16.73			
	18.77	87.85	4.68	16.85			
Average	18.71	87.23	4.66	16.78			
19.5	17.08	80.95	4.74	17.06	17.15	33.56	
	17.10	80.95	4.73	17.04			
	17.01	81.98	4.82	17.35			
Average	17.06	81.29	4.76	17.15			
19.9	15.74	76.45	4.86	17.49	17.50	34.24	
	15.68	76.45	4.88	17.55			
	15.77	76.45	4.85	17.45			
Average	15.73	76.45	4.86	17.50			
20.4	14.22	70.50	4.96	17.85	17.80	34.84	
	14.31	70.50	4.93	17.74			
	14.24	70.50	4.95	17.82			
Average	14.26	70.50	4.95	17.80			
20.8	13.15	66.20	5.03	18.12	18.17	35.57	
	13.10	66.20	5.05	18.19			
	13.09	66.20	5.06	18.21			
Average	13.11	66.20	5.05	18.17			
21.3	12.28	61.00	4.97	17.88	17.81	34.85	
	12.22	59.75	4.89	17.60			
	12.24	61.00	4.98	17.94			
Average	12.25	60.58	4.95	17.81			
21.8	11.54	56.00	4.85	17.47	17.51	34.27	
	11.51	56.00	4.87	17.52			
	11.49	56.00	4.87	17.55			
Average	11.51	56.00	4.86	17.51			
22.3	10.67	51.00	4.78	17.21	17.18	33.62	
	10.71	51.00	4.76	17.14			
	10.68	51.00	4.78	17.19			
Average	10.69	51.00	4.77	17.18			
22.8	9.55	44.30	4.64	16.70	16.76	32.81	
	9.50	44.30	4.66	16.79			
	9.49	44.30	4.67	16.81			
Average	9.51	44.30	4.66	16.76			
23.3	7.84	35.75	4.56	16.42	16.33	31.95	
	7.95	35.75	4.50	16.19			
	7.86	35.75	4.55	16.37			
Average	7.88	35.75	4.54	16.33			
23.7	6.34	28.25	4.46	16.04	16.07	31.44	
	6.30	28.25	4.48	16.14			
	6.35	28.25	4.45	16.02			
Average	6.33	28.25	4.46	16.07			
24.1	5.20	22.44	4.31	15.53	15.69	30.70	
	5.16	22.44	4.35	15.65			
	5.09	22.44	4.41	15.87			
Average	5.15	22.44	4.36	15.69			
24.5	3.90	16.65	4.27	15.36	15.27	29.89	
	3.93	16.65	4.24	15.25			
	3.94	16.65	4.22	15.21			
Average	3.92	16.65	4.24	15.27			
	Weight	Volume	Density	Dried weights	%Moisture	%Solids	Cal Density
1	5.12	2.80	1.83	3.09	39.6	60.4	1.84
2	4.29	2.35	1.83				
average	4.71	2.58	1.83				
Density 1.84 kg/l							

0.63x34mm aperture size with magnetite					Screen area(m ²)	0.511	
Feed flowrate(m ³ /h)	Time taken to fill underflow tank (S)	underflow tank Volume (L)	Drainage rate (L/S)	Drainage rate (m ³ /h)	Average drainage rate (m ³ /h)	Drainage rate (m ³ /m ² /h)	
18.3	21.10	97.00	4.60	16.55	16.54	32.37	
	21.14	97.00	4.59	16.52			
	21.09	97.00	4.60	16.56			
Average	21.11	97.00	4.59	16.54			
18.7	19.41	90.85	4.68	16.85	16.84	32.96	
	19.39	90.85	4.69	16.87			
	19.45	90.85	4.67	16.82			
Average	19.42	90.85	4.68	16.84			
19.1	18.82	89.70	4.77	17.16	17.13	33.53	
	18.87	89.70	4.75	17.11			
	18.85	89.70	4.76	17.13			
Average	18.85	89.70	4.76	17.13			
19.5	17.10	83.00	4.85	17.47	17.50	34.24	
	17.07	83.00	4.86	17.50			
	17.06	83.00	4.87	17.51			
Average	17.08	83.00	4.86	17.50			
19.9	15.93	78.90	4.95	17.83	17.87	34.97	
	15.86	78.90	4.97	17.91			
	15.90	78.90	4.96	17.86			
Average	15.90	78.90	4.96	17.87			
20.4	14.58	74.00	5.08	18.27	18.24	35.69	
	14.61	74.00	5.07	18.23			
	14.63	74.00	5.06	18.21			
Average	14.61	74.00	5.07	18.24			
20.8	13.53	69.43	5.13	18.47	18.63	36.46	
	13.41	70.50	5.26	18.93			
	13.51	69.43	5.14	18.50			
Average	13.48	69.78	5.18	18.63			
21.3	12.30	64.90	5.28	19.00	19.00	37.18	
	12.30	64.90	5.28	19.00			
	12.29	64.90	5.28	19.01			
Average	12.30	64.90	5.28	19.00			
21.8	11.25	58.50	5.20	18.72	18.66	36.53	
	11.31	58.50	5.17	18.62			
	11.29	58.50	5.18	18.65			
Average	11.28	58.50	5.18	18.66			
22.3	9.06	45.98	5.07	18.27	18.27	35.75	
	9.02	45.98	5.10	18.35			
	9.10	45.98	5.05	18.19			
Average	9.06	45.98	5.07	18.27			
22.8	8.22	41.15	5.01	18.02	17.91	35.04	
	8.09	39.58	4.89	17.61			
	8.19	41.15	5.02	18.09			
Average	8.17	40.63	4.97	17.91			
23.3	7.35	35.75	4.86	17.51	17.57	34.38	
	7.35	35.75	4.86	17.51			
	7.28	35.75	4.91	17.68			
Average	7.33	35.75	4.88	17.57			
23.7	6.27	30.00	4.78	17.22	17.20	33.66	
	6.33	30.00	4.74	17.06			
	6.24	30.00	4.81	17.31			
Average	6.28	30.00	4.78	17.20			
24.1	5.38	24.88	4.62	16.64	16.85	32.97	
	5.46	25.69	4.70	16.94			
	5.45	25.69	4.71	16.97			
Average	5.43	25.42	4.68	16.85			
24.5	4.43	20.00	4.51	16.25	16.34	31.97	
	4.40	20.00	4.55	16.36			
	4.39	20.00	4.56	16.40			
Average	4.41	20.00	4.54	16.34			
	Weight	Volume	Density	Dried weights	%Moisture	%Solids	Cal Density
1	4.41	2.7	1.63	2.26	48.8	51.2	1.63
2	4.81	2.95	1.63				
average	4.61	2.83	1.63				
Density 1.64 kg/l							

0.63x34mm aperture size with magnetite					Screen area(m ²)	0.511	
Feed flowrate(m ³ /h)	Time taken to fill underflow tank (S)	underflow tank Volume (L)	Drainage rate (L/S)	Drainage rate (m ³ /h)	Average drainage rate (m ³ /h)	Drainage rate (m ³ /m ² /h)	
18.3	21.75	99.00	4.55	16.39	16.38	32.06	
	21.81	99.00	4.54	16.34			
	21.71	99.00	4.56	16.42			
Average	21.76	99.00	4.55	16.38			
18.7	19.84	92.00	4.64	16.69	16.70	32.68	
	19.79	92.00	4.65	16.74			
	19.87	92.00	4.63	16.67			
Average	19.83	92.00	4.64	16.70			
19.1	18.20	86.00	4.73	17.01	17.00	33.27	
	18.21	86.00	4.72	17.00			
	18.23	86.00	4.72	16.98			
Average	18.21	86.00	4.72	17.00			
19.5	17.15	83.00	4.84	17.42	17.38	34.01	
	17.23	83.00	4.82	17.34			
	17.20	83.00	4.83	17.37			
Average	17.19	83.00	4.83	17.38			
19.9	15.56	76.45	4.91	17.69	17.75	34.74	
	15.61	77.68	4.98	17.91			
	15.59	76.45	4.90	17.65			
Average	15.59	76.86	4.93	17.75			
20.4	14.41	72.25	5.01	18.05	18.09	35.40	
	14.40	72.25	5.02	18.06			
	14.33	72.25	5.04	18.15			
Average	14.38	72.25	5.02	18.09			
20.8	13.32	68.35	5.13	18.47	18.46	36.13	
	13.35	68.35	5.12	18.43			
	13.31	68.35	5.14	18.49			
Average	13.33	68.35	5.13	18.46			
21.3	12.19	63.60	5.22	18.78	18.79	36.78	
	12.15	63.60	5.23	18.84			
	12.21	63.60	5.21	18.75			
Average	12.18	63.60	5.22	18.79			
21.8	10.38	53.50	5.15	18.55	18.50	36.20	
	10.41	53.50	5.14	18.50			
	10.45	53.50	5.12	18.43			
Average	10.41	53.50	5.14	18.50			
22.3	9.21	45.98	4.99	17.97	17.91	35.04	
	9.29	45.98	4.95	17.82			
	9.23	45.98	4.98	17.93			
Average	9.24	45.98	4.97	17.91			
22.8	8.12	39.58	4.87	17.55	17.59	34.42	
	8.09	39.58	4.89	17.61			
	8.09	39.58	4.89	17.61			
Average	8.10	39.58	4.89	17.59			
23.3	7.22	34.63	4.80	17.26	17.26	33.77	
	7.25	34.63	4.78	17.19			
	7.20	34.63	4.81	17.31			
Average	7.22	34.63	4.79	17.26			
23.7	6.38	30.00	4.70	16.93	16.95	33.16	
	6.33	30.00	4.74	17.06			
	6.41	30.00	4.68	16.85			
Average	6.37	30.00	4.71	16.95			
24.1	5.37	24.85	4.63	16.66	16.65	32.58	
	5.35	24.85	4.64	16.72			
	5.40	24.85	4.60	16.57			
Average	5.37	24.85	4.62	16.65			
24.5	4.42	20.00	4.52	16.29	16.34	31.97	
	4.40	20.00	4.55	16.36			
	4.40	20.00	4.55	16.36			
Average	4.41	20.00	4.54	16.34			
	Weight	Volume	Density	Dried weights	%Moisture	%Solids	Cal Density
1	5.32	3.10	1.72	2.96	44.4	55.6	1.73
2	5.93	3.40	1.74				
average	5.63	3.25	1.73				
Density 1.72 kg/l							

0.63x34mm aperture size with magnetite					Screen area(m2)	0.511	
Feed flowrate(m3/h)	underflow tank (S)	(L)	(L/S)	Drainage rate (m3/h)	(m3/h)	(m3/m2/h)	
18.3	20.85	94.00	4.51	16.23	16.21	31.72	
	20.90	94.00	4.50	16.19			
	20.88	94.00	4.50	16.21			
Average	20.88	94.00	4.50	16.21			
18.7	19.44	89.70	4.61	16.61	16.57	32.42	
	19.53	89.70	4.59	16.53			
	19.50	89.70	4.60	16.56			
Average	19.49	89.70	4.60	16.57			
19.1	17.72	83.00	4.68	16.86	16.88	33.03	
	17.80	83.75	4.71	16.94			
	17.75	83.00	4.68	16.83			
Average	17.76	83.25	4.69	16.88			
19.5	16.44	78.90	4.80	17.28	17.23	33.71	
	16.56	78.90	4.76	17.15			
	16.47	78.90	4.79	17.25			
Average	16.49	78.90	4.78	17.23			
19.9	15.12	74.00	4.89	17.62	17.62	34.47	
	15.10	74.00	4.90	17.64			
	15.15	74.00	4.88	17.58			
Average	15.12	74.00	4.89	17.62			
20.4	14.03	69.43	4.95	17.81	17.95	35.13	
	14.10	70.50	5.00	18.00			
	14.07	70.50	5.01	18.04			
Average	14.07	70.14	4.99	17.95			
20.8	13.01	66.20	5.09	18.32	18.31	35.83	
	13.01	66.20	5.09	18.32			
	13.03	66.20	5.08	18.29			
Average	13.02	66.20	5.09	18.31			
21.3	11.75	61.00	5.19	18.69	18.68	36.55	
	11.73	61.00	5.20	18.72			
	11.79	61.00	5.17	18.63			
Average	11.76	61.00	5.19	18.68			
21.8	9.70	49.33	5.09	18.31	18.27	35.75	
	9.71	49.33	5.08	18.29			
	9.75	49.33	5.06	18.21			
Average	9.72	49.33	5.07	18.27			
22.3	8.75	43.51	4.97	17.90	17.90	35.02	
	8.80	43.51	4.94	17.80			
	8.71	43.51	5.00	17.98			
Average	8.75	43.51	4.97	17.90			
22.8	7.85	38.00	4.84	17.43	17.52	34.29	
	7.80	38.00	4.87	17.54			
	7.77	38.00	4.89	17.61			
Average	7.81	38.00	4.87	17.52			
23.3	7.03	33.50	4.77	17.16	17.17	33.60	
	7.03	33.50	4.77	17.16			
	7.01	33.50	4.78	17.20			
Average	7.02	33.50	4.77	17.17			
23.7	5.62	26.50	4.72	16.98	16.90	33.06	
	5.68	26.50	4.67	16.80			
	5.64	26.50	4.70	16.91			
Average	5.65	26.50	4.69	16.90			
24.1	5.42	24.88	4.59	16.52	16.55	32.39	
	5.40	24.88	4.61	16.58			
	5.41	24.88	4.60	16.55			
Average	5.41	24.88	4.60	16.55			
24.5	4.47	20.00	4.47	16.11	16.19	31.69	
	4.44	20.00	4.50	16.22			
	4.43	20.00	4.51	16.25			
Average	4.45	20.00	4.50	16.19			
	Weight	Volume	Density	Dried weights	%Moisture	%Solids	Cal Density
1	4.15	2.25	1.84	2.51	39.5	60.5	1.84
2	4.20	2.30	1.83				
average	4.18	2.28	1.84				
Density 1.84 kg/l							

Appendix P: Percent moisture and medium carryover for fresh ferrosilicon and iron ore

The tables below show the moisture and medium carryover calculations for fresh (appendix Q) and degraded (appendix R) material. Columns one and three shows the density calculation using the mass and volume of the slurry. Columns two and four for the feed and underflow streams show the density confirmation using weight percent solids. Columns five and six indicate the weights for the wet and dry overflow samples used for percent moisture calculation indicated in column six. Columns seven and eight show the weight of unwashed and, washed and dried material used for calculating the percent media adhesion in column nine. Column ten indicate the media carryover calculation in kg of medium per tonne of feed per screen width (0.561 m).

0.8x8.8 mm at 2.0 kg/l										
25.1 m ³ /hr										
	Feed (wet)	Feed (dry)	Underflow (wet)	Underflow (dry)	Overflow (wet1)	Overflow (Dry1)	Overflow (before washing)	Overflow (after washing2)	O/F rate (kg/h)	25.1 t/h
Mass (kg)	4.83	2.97	6.59	3.98	2.19	2.03	2.05	1.70	6059.11	606.59 kg/h
Litres (L)	2.40		3.20							24.17 kg/t
Density (kg/L)	2.01	2.06	2.06	2.02					0.36	43.08 kg/t/m
Time					1.25		1.27		0.03	
%Moisture		38.51		39.61	1.75	7.31	1.61	17.32	0.33	
%Solids by Wt		61.49		60.39		92.69		%Media adhesion	10.01	
24.5 m ³ /h										
	Feed (wet)	Feed (dry)	Underflow (wet)	Underflow (dry)	Overflow (wet1)	Overflow (Dry1)	Overflow (before washing)	Overflow (after washing2)	O/F rate (kg/h)	24.5 t/h
Mass (kg)	6.78	4.14	6.41	3.86	1.85	1.72	1.81	1.51	4815.69	459.78 kg/h
Litres (L)	3.30		3.20							18.77 kg/t
Density (kg/L)	2.05	2.04	2.00	2.01					0.30	33.45 kg/t/m
Time					1.43		1.31		0.02	
%Moisture /rate		38.94		39.78	1.29	7.03	1.38	16.57	0.28	
%Solids by Wt		61.06		60.22		92.97		%Media adhesion	9.55	
23.7 m ³ /h										
	Feed (wet)	Feed (dry)	Underflow (wet)	Underflow (dry)	Overflow (wet1)	Overflow (Dry1)	Overflow (before washing)	Overflow (after washing2)	O/F rate (kg/h)	23.7 t/h
Mass (kg)	4.83	2.97	6.59	3.98	1.89	1.77	1.67	1.41	3680.07	329.55 kg/h
Litres (L)	2.40		3.20							13.91 kg/t
Density (kg/L)	2.01	2.06	2.06	2.02					0.26	24.79 kg/t/m
Time					1.82		1.66		0.02	
%Moisture/Rate		38.51		39.61	1.04	6.61	1.01	15.57	0.24	
%Solids by Wt		61.49		60.39		93.39		%Media adhesion	8.96	
22.8 m ³ /h										
	Feed (wet)	Feed (dry)	Underflow (wet)	Underflow (dry)	Overflow (wet1)	Overflow (Dry1)	Overflow (before washing)	Overflow (after washing2)	O/F rate (kg/h)	22.8 t/h
Mass (kg)	6.78	4.14	6.41	3.86	1.68	1.58	1.60	1.36	3134.02	266.39 kg/h
Litres (L)	3.30		3.20							11.68 kg/t
Density (kg/L)	2.05	2.04	2.00	2.01					0.24	20.83 kg/t/m
Time					1.96		1.81		0.01	
%Moisture /Rate		38.94		39.78	0.86	6.25	0.88	14.75	0.22	
%Solids by Wt		61.06		60.22		93.75		%Media adhesion	8.50	
21.8 m ³ /h										
	Feed (wet)	Feed (dry)	Underflow (wet)	Underflow (dry)	Overflow (wet1)	Overflow (Dry1)	Overflow (before washing)	Overflow (after washing2)	O/F rate (kg/h)	21.8 t/h
Mass (kg)	4.83	2.97	6.59	3.98	1.77	1.67	1.65	1.43	2772.37	207.98 kg/h
Litres (L)	2.40		3.20							9.54 kg/t
Density (kg/L)	2.01	2.06	2.06	2.02					0.22	17.01 kg/t/m
Time					2.28		2.16		0.01	
%Moisture /rate		38.51		39.61	0.78	5.65	0.76	13.15	0.20	
%Solids by Wt		61.49		60.39		94.35		%Media adhesion	7.50	
							Pump speed (m ³ /h)	%Moisture	Media adhesion (kg/t/m)	%Media Adhesion
							25.1	7.3	43.1	10.0
							24.5	7.0	33.5	9.5
							23.8	6.6	24.8	9.0
							22.8	6.3	20.8	8.5
							21.8	5.6	17.0	7.5

0.8x8.8 mm at 2.2 kg/l											
25.1 m ³ /hr											
	Feed (wet)	Feed (dry)	Underflow (wet)	Underflow (dry)	Overflow (wet1)	Overflow (Dry1)	Overflow (before washing)	Overflow (after washing2)	O/F rate (kg/h)	25.1	t/h
Mass (kg)	6.00	3.91	6.97	4.49	2.14	1.95	2.25	1.80	6589.57	717.46	kg/h
Litres (L)	2.70		3.20							28.58	kg/t
Density (kg/L)	2.22	2.20	2.18	2.17					0.45	50.95	kg/t/m
Time					1.15		1.25		0.04		
%Moisture		34.83		35.58	1.86	9.11	1.80	20.00	0.41		
%Solids by Wt		65.17		64.42		90.89		%Media adhesion	10.89		
24.5 m ³ /h											
	Feed (wet)	Feed (dry)	Underflow (wet)	Underflow (dry)	Overflow (wet1)	Overflow (Dry1)	Overflow (before washing)	Overflow (after washing2)	O/F rate (kg/h)	24.5	t/h
Mass (kg)	5.47	3.61	5.39	3.46	1.93	1.76	1.96	1.59	5515.42	575.15	kg/h
Litres (L)	2.45		2.45							23.48	kg/t
Density (kg/L)	2.23	2.23	2.20	2.16					0.38	41.85	kg/t/m
Time					1.29		1.25		0.03		
%Moisture		34.00		35.81	1.50	8.70	1.57	19.13	0.34		
%Solids by Wt		66.00		64.19		91.30		%Media adhesion	10.43		
23.7 m ³ /h											
	Feed (wet)	Feed (dry)	Underflow (wet)	Underflow (dry)	Overflow (wet1)	Overflow (Dry1)	Overflow (before washing)	Overflow (after washing2)	O/F rate (kg/h)	23.7	t/h
Mass (kg)	6.00	3.91	6.97	4.49	2.08	1.90	1.91	1.57	4080.22	391.75	kg/h
Litres (L)	2.70		3.20							16.53	kg/t
Density (kg/L)	2.22	2.20	2.18	2.17					0.35	29.46	kg/t/m
Time					1.83		1.69		0.03		
%Moisture		34.83		35.58	1.14	8.46	1.13	18.06	0.32		
%Solids by Wt		65.17		64.42		91.54		%Media adhesion	9.60		
22.8 m ³ /h											
	Feed (wet)	Feed (dry)	Underflow (wet)	Underflow (dry)	Overflow (wet1)	Overflow (Dry1)	Overflow (before washing)	Overflow (after washing2)	O/F rate (kg/h)	22.8	t/h
Mass (kg)	5.47	3.61	5.39	3.46	1.41	1.30	1.67	1.39	3791.08	337.18	kg/h
Litres (L)	2.45		2.45							14.79	kg/t
Density (kg/L)	2.23	2.23	2.20	2.16					0.28	26.36	kg/t/m
Time					1.38		1.54		0.02		
%Moisture		34.00		35.81	1.02	7.87	1.08	16.77	0.26		
%Solids by Wt		66.00		64.19		92.13		%Media adhesion	8.89		
21.8 m ³ /h											
	Feed (wet)	Feed (dry)	Underflow (wet)	Underflow (dry)	Overflow (wet1)	Overflow (Dry1)	Overflow (before washing)	Overflow (after washing2)	O/F rate (kg/h)	21.8	t/h
Mass (kg)	6.00	3.91	6.97	4.49	1.52	1.4	1.63	1.38	3458.18	279.365148	kg/h
Litres (L)	2.70		3.20							12.8149151	kg/t
Density (kg/L)	2.22	2.20	2.18	2.17					0.26	22.84	kg/t/m
Time					1.65		1.63		0.02		
%Moisture		34.83		35.58	0.92	7.57	1.00	15.64	0.24		
%Solids by Wt		65.17		64.42		92.43		%Media adhesion	8.08		
							Pump speed (m ³ /h)	%Moisture	Media adhesion (kg/t/m)	%Media Adhesion	
							25.1	9.1	51.0	10.9	
							24.5	8.7	41.8	10.4	
							23.8	8.5	29.5	9.6	
							22.8	7.9	26.4	8.9	
							21.8	7.6	22.8	8.1	

1x13 mm at 1.9 kg/l										
24.5 m3/hr										
	Feed (wet)	Feed (dry)	Underflow (wet)	Underflow (dry)	Overflow (wet1)	Overflow (Dry1)	Overflow (before washing)	Overflow (after washing2)	O/F rate(kg/h)	24.5 t/h
Mass (kg)	6.67	3.77	6.51	3.53	1.37	1.27	1.21	1.07	4641.20	181.29 kg/h
Litres (L)	3.6		3.55							7.40 kg/t
Density (kg/L)	1.85	1.90	1.83	1.83					0.14	13.19 kg/t/m
Time					1.05			0.95		0.01
%Moisture		43.48		45.78	1.30	7.66		11.57		0.13
%Solids by Wt		56.52		54.22		92.34		%Media adhesion	3.91	
23.7 m3/h										
	Feed (wet)	Feed (dry)	Underflow (wet)	Underflow (dry)	Overflow (wet1)	Overflow (Dry1)	Overflow (before washing)	Overflow (after washing2)	O/F rate(kg/h)	23.7 t/h
Mass (kg)	6.59	3.69	5.52	2.98	1.24	1.15	1.04	0.93	3562.06	128.49 kg/h
Litres (L)	3.5		3							5.42 kg/t
Density (kg/L)	1.88	1.88	1.84	1.82					0.11	9.66 kg/t/m
Time					1.21		1.09			0.01
%Moisture /rate		44.01		46.01	1.02	7.26		0.95	10.87	0.10
%Solids by Wt		55.99		53.99		92.74		%Media adhesion	3.61	
22.8 m3/h										
	Feed (wet)	Feed (dry)	Underflow (wet)	Underflow (dry)	Overflow (wet1)	Overflow (Dry1)	Overflow (before washing)	Overflow (after washing2)	O/F rate(kg/h)	22.8 t/h
Mass (kg)	6.67	3.77	6.51	3.53	1.34	1.25	1.13	1.02	3302.20	111.35 kg/h
Litres (L)	3.6		3.55							4.88 kg/t
Density (kg/L)	1.85	1.90	1.83	1.83					0.11	8.71 kg/t/m
Time					1.44		1.25			0.01
%Moisture/Rate		43.48		45.78	0.93	6.72		0.90	10.09	0.11
%Solids by Wt		56.52		54.22		93.28		%Media adhesion	3.37	
21.8 m3/h										
	Feed (wet)	Feed (dry)	Underflow (wet)	Underflow (dry)	Overflow (wet1)	Overflow (Dry1)	Overflow (before washing)	Overflow (after washing2)	O/F rate(kg/h)	21.8 t/h
Mass (kg)	6.59	3.69	5.52	2.98	1.57	1.47	1.62	1.47	3022.95	96.69 kg/h
Litres (L)	3.5		3							4.44 kg/t
Density (kg/L)	1.88	1.88	1.84	1.82					0.16	7.91 kg/t/m
Time					1.85		1.95			0.01
%Moisture /Rate		44.01		46.01	0.85	6.37		0.83	9.568	0.15
%Solids by Wt		55.99		53.99		93.63		%Media adhesion	3.20	
20.8 m3/h										
	Feed (wet)	Feed (dry)	Underflow (wet)	Underflow (dry)	Overflow (wet1)	Overflow (Dry1)	Overflow (before washing)	Overflow (after washing2)	O/F rate(kg/h)	20.8 t/h
Mass (kg)	6.67	3.77	6.51	3.53	1.13	1.06	1.33	1.21	2657.20	82.20 kg/h
Litres (L)	3.6		3.55							3.95 kg/t
Density (kg/L)	1.85	1.90	1.83	1.83					0.12	7.04 kg/t/m
Time					1.55		1.78			0.01
%Moisture /rate		43.48		45.78	0.73	5.93		0.75	9.02	0.11
%Solids by Wt		56.52		54.22		94.07		%Media adhesion	3.09	
20.4 m3/h										
	(wet)	(dry)	(wet)	(dry)	(wet1)	(Dry1)	washing)	washing2)	O/F rate(kg/h)	20.4 t/h
Mass (kg)	6.59	3.69	5.52	2.98	1.54	1.46	1.3	1.19	2425.13	71.35 kg/h
Litres (L)	3.5		3							3.50 kg/t
Density (kg/L)	1.88	1.88	1.84	1.82					0.11	6.23 kg/t/m
Time					2.31		1.91			0.01
%Moisture /rate		44.01		46.01	0.67	5.52		0.68	8.46	0.10
%Solids by Wt		55.99		53.99		94.48		%Media adhesion	2.94	
							Pump speed (m3/h)	%Moisture	(kg/t/m)	Adhesion
							24.5	7.7	13.2	3.9
							23.7	7.3	9.7	3.6
							22.8	6.7	8.7	3.4
							21.8	6.4	7.9	3.2
							20.8	5.9	7.0	3.1
							20.4	5.5	6.2	2.9

1x13 mm at 2.2 kg/l											
24.5 m ³ /h											
	Feed (wet)	Feed (dry)	Underflow (wet)	Underflow (dry)	Overflow (wet1)	Overflow (Dry1)	Overflow (before washing)	Overflow (after washing2)	O/F rate(kg/h)	24.5 t/h	
Mass (kg)	6.66	4.31	7.28	4.59	1.87	1.72	1.27	1.1	4950.57	265.57	kg/h
Litres (L)	3		3.35							10.84	kg/t
Density (kg/L)	2.22	2.18	2.17	2.11					0.17	19.32	kg/t/m
Time					1.51		0.84		0.01		
%Moisture		35.29		36.95	1.24	8.02	1.51	13.39	0.16		
%Solids by Wt		64.71		63.05		91.98		%Media adhesion	5.36		
23.7 m ³ /h											
	(wet)	(dry)	(wet)	(dry)	(wet1)	(Dry1)	washing)	washing2)	O/F rate(kg/h)	23.7 t/h	
Mass (kg)	5.27	3.42	5.31	3.39	0.98	0.91	1.47	1.28	3613.34	190.50	kg/h
Litres (L)	2.4		2.45							8.04	kg/t
Density (kg/L)	2.20	2.19	2.17	2.14					0.19	14.33	kg/t/m
Time					0.96		1.49		0.01		
%Moisture		35.10		36.16	1.02	7.65	0.99	12.93	0.18		
%Solids by Wt		64.90		63.84		92.35		%Media adhesion	5.27		
22.8 m ³ /h											
	(wet)	(dry)	(wet)	(dry)	(wet1)	(Dry1)	washing)	washing2)	O/F rate(kg/h)	22.8 t/h	
Mass (kg)	6.66	4.31	7.28	4.59	1.38	1.28	1.09	0.96	3496.45	176.47	kg/h
Litres (L)	3		3.35							7.74	kg/t
Density (kg/L)	2.22	2.18	2.17	2.11					0.13	13.80	kg/t/m
Time					1.64		0.99		0.01		
%Moisture		35.29		36.95	0.84	7.25	1.10	12.29	0.12		
%Solids by Wt		64.71		63.05		92.75		%Media adhesion	5.05		
21.8 m ³ /h											
	(wet)	(dry)	(wet)	(dry)	(wet1)	(Dry1)	washing)	washing2)	O/F rate(kg/h)	21.8 t/h	
Mass (kg)	5.27	3.42	5.31	3.39	0.9	0.838	1.28	1.13	3135.77	151.45	kg/h
Litres (L)	2.4		2.45							6.95	kg/t
Density (kg/L)	2.20	2.19	2.17	2.14					0.15	12.38	kg/t/m
Time					1.04		1.46		0.01		
%Moisture		35.10		36.16	0.87	6.89	0.88	11.72	0.14		
%Solids by Wt		64.90		63.84		93.11		%Media adhesion	4.83		
20.8 m ³ /h											
	Feed (wet)	Feed (dry)	Underflow (wet)	Underflow (dry)	Overflow (wet1)	Overflow (Dry1)	Overflow (before washing)	Overflow (after washing2)	O/F rate(kg/h)	20.8 t/h	
Mass (kg)	6.66	4.31	7.28	4.59	0.95	0.89	1.26	1.12	2921.88	137.04	kg/h
Litres (L)	3		3.35							6.59	kg/t
Density (kg/L)	2.22	2.18	2.17	2.11					0.14	11.74	kg/t/m
Time					1.18		1.54		0.01		
%Moisture		35.29		36.95	0.81	6.42	0.82	11.11	0.13		
%Solids by Wt		64.71		63.05		93.58		%Media adhesion	4.69		
20.4 m ³ /h											
	Feed (wet)	Feed (dry)	Underflow (wet)	Underflow (dry)	Overflow (wet1)	Overflow (Dry1)	Overflow (before washing)	Overflow (after washing2)	O/F rate(kg/h)	20.4 t/h	
Mass (kg)	5.27	3.42	5.31	3.39	1.29	1.22	0.9	0.81	2859.95	130.80	kg/h
Litres (L)	2.4		2.45							6.41	kg/t
Density (kg/L)	2.20	2.19	2.17	2.14					0.09	11.43	kg/t/m
Time					1.6		1.15		0.00		
%Moisture		35.10		36.16	0.81	5.43	0.78	10.00	0.09		
%Solids by Wt		64.90		63.84		94.57		%Media adhesion	4.57		
							Pump speed (m ³ /h)	%Moisture	Media adhesion	%Media	
							24.5	8.0	19.3	5.4	
							23.7	7.7	14.3	5.3	
							22.8	7.2	13.8	5.0	
							21.8	6.9	12.4	4.8	
							20.8	6.4	11.7	4.7	
							20.4	5.4	11.4	4.6	

1x13 mm at 2.45 kg/l										
24.5 m3/h										
	Feed (wet)	Feed (dry)	Underflow (wet)	Underflow (dry)	Overflow (wet1)	Overflow (Dry1)	Overflow (before washing)	Overflow (after washing2)	O/F rate(kg/h)	24.5 t/h
Mass (kg)	7.66	5.37	7.22	5.02	1.79	1.64	1.19	0.96	5489.38	588.70
Litres (L)	3.1		3							24.03
Density (kg/L)	2.47	2.42	2.41	2.39					0.23	42.83
Time					1.19		0.77			0.02
%Moisture		29.90		30.47	1.50	8.60	1.55	19.33	0.21	
%Solids by Wt		70.10		69.53		91.40		%Media adhesion	10.72	
23.7 m3/h										
	(wet)	(dry)	(wet)	(dry)	(wet1)	(Dry1)	washing)	washing2)	O/F rate(kg/h)	23.7 t/h
Mass (kg)	5.86	4.11	6.76	4.69	1.52	1.39	1.61	1.31	3980.85	401.60
Litres (L)	2.4		2.8							16.95
Density (kg/L)	2.44	2.42	2.41	2.38					0.30	30.21
Time					1.39		1.44			0.03
%Moisture		29.86		30.62	1.09	8.42	1.12	18.51	0.27	
%Solids by Wt		70.14		69.38		91.58		%Media adhesion	10.09	
22.8 m3/h										
	(wet)	(dry)	(wet)	(dry)	(wet1)	(Dry1)	washing)	washing2)	O/F rate(kg/h)	22.8 t/h
Mass (kg)	7.66	5.37	7.22	5.02	1.19	1.09	1.11	0.91	3715.41	363.47
Litres (L)	3.1		3							15.94
Density (kg/L)	2.47	2.42	2.41	2.39					0.20	28.42
Time					1.1		1.13			0.02
%Moisture		29.90		30.47	1.08	8.24	0.98	18.02	0.18	
%Solids by Wt		70.10		69.53		91.76		%Media adhesion	9.78	
21.8 m3/h										
	Feed	Feed	Underflow	Underflow	Overflow	Overflow	Overflow (before	Overflow (after	O/F rate(kg/h)	21.8 t/h
Mass (kg)	5.86	4.11	6.76	4.69	1.48	1.36	1.31	1.08	3344.94	316.07
Litres (L)	2.4		2.8							14.50
Density (kg/L)	2.44	2.42	2.41	2.38					0.23	25.84
Time					1.54		1.46			0.02
%Moisture		29.86		30.62	0.96	8.11	0.90	17.56	0.21	
%Solids by Wt		70.14		69.38		91.89		%Media adhesion	9.45	
20.8 m3/h										
	(wet)	(dry)	(wet)	(dry)	(wet1)	(Dry1)	washing)	washing2)	O/F rate(kg/h)	20.8 t/h
Mass (kg)	7.66	5.37	7.22	5.02	1.44	1.33	1.45	1.21	2989.69	262.31
Litres (L)	3.1		3							12.61
Density (kg/L)	2.47	2.42	2.41	2.39					0.24	22.48
Time					1.73		1.75			0.02
%Moisture		29.90		30.47	0.83	7.78	0.83	16.55	0.22	
%Solids by Wt		70.10		69.53		92.22		%Media adhesion	8.77	
20.4 m3/h										
	(wet)	(dry)	(wet)	(dry)	(wet1)	(Dry1)	washing)	washing2)	O/F rate(kg/h)	20.4 t/h
Mass (kg)	5.86	4.11	6.76	4.69	1.36	1.26	0.96	0.81	2909.08	240.64
Litres (L)	2.4		2.8							11.80
Density (kg/L)	2.44	2.42	2.41	2.38					0.15	21.03
Time					1.64		1.22			0.01
%Moisture		29.86		30.62	0.83	7.35	0.79	15.63	0.14	
%Solids by Wt		70.14		69.38		92.65		%Media adhesion	8.27	
							Pump speed (m3/h)	%Moisture	(kg/t/m)	Adhesion
							24.5	8.6	42.8	10.7
							23.7	8.4	30.2	10.1
							22.8	8.2	28.4	9.8
							21.8	8.1	25.8	9.4
							20.8	7.8	22.5	8.8
							20.4	7.4	21.0	8.3

1x13 mm at 2.55 kg/l											
24.5 m3/h											
	Feed (wet)	Feed (dry)	Underflow (wet)	Underflow (dry)	Overflow (wet1)	Overflow (Dry1)	Overflow (before washing)	Overflow (after washing2)	O/F rate(kg/h)	24.5	t/h
Mass (kg)	6.34	4.57	7.2	5.13	1.72	1.56	1.81	1.43	5572.87	661.31	kg/h
Litres (L)	2.45		2.8							26.99	kg/t
Density (kg/L)	2.59	2.52	2.57	2.47					0.38	48.11	kg/t/m
Time					1.13		1.15			0.03	
%Moisture		27.92		28.75	1.52	9.13	1.57	20.99		0.35	
%Solids by Wt		72.08		71.25		90.87		%Media adhesion		11.87	
23.7 m3/h											
	Feed (wet)	Feed (dry)	Underflow (wet)	Underflow (dry)	Overflow (wet1)	Overflow (Dry1)	Overflow (before washing)	Overflow (after washing2)	O/F rate(kg/h)	23.7	t/h
Mass (kg)	5.51	3.98	5.37	3.81	2.63	2.40	2.12	1.69	4371.38	496.05	kg/h
Litres (L)	2.15		2.1							20.93	kg/t
Density (kg/L)	2.56	2.52	2.56	2.46					0.43	37.31	kg/t/m
Time					2.24		1.69			0.04	
%Moisture /rate		27.77		29.05	1.17	8.94	1.25	20.28		0.39	
%Solids by Wt		72.23		70.95		91.06		%Media adhesion		11.35	
22.8 m3/h											
	Feed (wet)	Feed (dry)	Underflow (wet)	Underflow (dry)	Overflow (wet1)	Overflow (Dry1)	Overflow (before washing)	Overflow (after washing2)	O/F rate(kg/h)	22.8	t/h
Mass (kg)	6.34	4.57	7.2	5.13	1.85	1.69	2.15	1.73	3835.90	417.59	kg/h
Litres (L)	2.45		2.8							18.32	kg/t
Density (kg/L)	2.59	2.52	2.57	2.47					0.42	32.65	kg/t/m
Time					1.77		1.98			0.04	
%Moisture/Rate		27.92		28.75	1.05	8.65	1.09	19.53		0.38	
%Solids by Wt		72.08		71.25		91.35		%Media adhesion		10.89	
21.8 m3/h											
	Feed (wet)	Feed (dry)	Underflow (wet)	Underflow (dry)	Overflow (wet1)	Overflow (Dry1)	Overflow (before washing)	Overflow (after washing2)	O/F rate(kg/h)	21.80	t/h
Mass (kg)	5.51	3.98	5.37	3.81	1.86	1.70	1.05	0.85	3554.45	378.92	kg/h
Litres (L)	2.15		2.1							17.38	kg/t
Density (kg/L)	2.56	2.52	2.56	2.46					0.20	30.98	kg/t/m
Time					1.89		1.06			0.02	
%Moisture /Rate		27.77		29.05	0.98	8.39	0.99	19.05		0.18	
%Solids by Wt		72.23		70.95		91.61		%Media adhesion		10.66	
20.8 m3/h											
	(wet)	(dry)	(wet)	(dry)	(wet1)	(Dry1)	washing)	washing2)	O/F rate(kg/h)	20.8	t/h
Mass (kg)	6.34	4.57	7.2	5.13	1.87	1.72	1.81	1.48	3263.27	327.97	kg/h
Litres (L)	2.45		2.8							15.77	kg/t
Density (kg/L)	2.59	2.52	2.57	2.47					0.33	28.11	kg/t/m
Time					2.07		1.99			0.03	
%Moisture /rate		27.92		28.75	0.90	8.18	0.91	18.23		0.30	
%Solids by Wt		72.08		71.25		91.82		%Media adhesion		10.05	
20.4 m3/h											
	(wet)	(dry)	(wet)	(dry)	(wet1)	(Dry1)	washing)	washing2)	O/F rate(kg/h)	20.4	t/h
Mass (kg)	5.51	3.98	5.37	3.81	1.96	1.806	1.72	1.42	3155.69	302.46	kg/h
Litres (L)	2.15		2.1							14.83	kg/t
Density (kg/L)	2.56	2.52	2.56	2.46					0.30	26.43	kg/t/m
Time					2.25		1.95			0.02	
%Moisture /rate		27.77		29.05	0.87	7.86	0.88	17.44		0.28	
%Solids by Wt		72.23		70.95		92.14		%Media adhesion		9.58	
							Pump speed (m3/h)	%Moisture	(kg/t/m)	Adhesion	
							24.5	9.1	48.1	11.9	
							23.7	8.9	37.3	11.3	
							22.8	8.6	32.6	10.9	
							21.8	8.4	31.0	10.7	
							20.8	8.2	28.1	10.1	
							20.4	7.9	26.4	9.6	

1x13 mm at 2.7 kg/l										
24.5 m3/h										
	Feed (wet)	Feed (dry)	Underflow (wet)	Underflow (dry)	Overflow (wet1)	Overflow (Dry1)	Overflow (before washing)	Overflow (after washing2)	O/F rate(kg/h)	24.5 t/h
Mass (kg)	6.44	4.82	6.42	4.76	1.81	1.63	1.91	1.47	5746.60	765.04 kg/h
Litres (L)	2.4		2.4							31.23 kg/t
Density (kg/L)	2.68	2.67	2.68	2.63					0.44	55.66 kg/t/m
Time					1.15			1.18		0.04
%Moisture		25.16		25.86	1.57	9.72	1.62	23.04		0.40
%Solids by Wt		74.84		74.14		90.28		%Media adhesion		13.31
23.7 m3/h										
	Feed (wet)	Feed (dry)	Underflow (wet)	Underflow (dry)	Overflow (wet1)	Overflow (Dry1)	Overflow (before washing)	Overflow (after washing2)	O/F rate(kg/h)	23.7 t/h
Mass (kg)	7.1	5.35	6.78	5.06	1.53	1.39	1.55	1.21	4249.15	543.08 kg/h
Litres (L)	2.6		2.5							22.91 kg/t
Density (kg/L)	2.73	2.70	2.71	2.66					0.35	40.85 kg/t/m
Time					1.32			1.29		0.03
%Moisture		24.65		25.37	1.16	9.48	1.20	22.26		0.31
%Solids by Wt		75.35		74.63		90.52		%Media adhesion		12.78
22.8 m3/h										
	Feed (wet)	Feed (dry)	Underflow (wet)	Underflow (dry)	Overflow (wet1)	Overflow (Dry1)	Overflow (before washing)	Overflow (after washing2)	O/F rate(kg/h)	22.8 t/h
Mass (kg)	6.44	4.82	6.42	4.76	2.16	1.96	1.81	1.43	3986.50	478.84 kg/h
Litres (L)	2.4		2.4							21.00 kg/t
Density (kg/L)	2.68	2.67	2.68	2.63					0.39	37.44 kg/t/m
Time					1.91			1.67		0.04
%Moisture		25.16		25.86	1.13	9.26	1.08	21.27		0.35
%Solids by Wt		74.84		74.14		90.74		%Media adhesion		12.01
21.8 m3/h										
	(wet)	(dry)	(wet)	(dry)	(wet1)	(Dry1)	washing)	washing2)	O/F rate(kg/h)	21.8 t/h
Mass (kg)	7.1	5.35	6.78	5.06	1.62	1.475	1.93	1.54	3723.41	419.13 kg/h
Litres (L)	2.6		2.5							19.23 kg/t
Density (kg/L)	2.73	2.70	2.71	2.66					0.39	34.27 kg/t/m
Time					1.58			1.85		0.03
%Moisture		24.65		25.37	1.03	8.95	1.04	20.21		0.36
%Solids by Wt		75.35		74.63		91.05		%Media adhesion		11.26
20.8 m3/h										
	Feed (wet)	Feed (dry)	Underflow (wet)	Underflow (dry)	Overflow (wet1)	Overflow (Dry1)	Overflow (before washing)	Overflow (after washing2)	O/F rate(kg/h)	20.8 t/h
Mass (kg)	6.44	4.82	6.42	4.76	1.88	1.72	1.69	1.37	3371.39	351.44 kg/h
Litres (L)	2.4		2.4							16.90 kg/t
Density (kg/L)	2.68	2.67	2.68	2.63					0.32	30.12 kg/t/m
Time					1.98			1.83		0.03
%Moisture		25.16		25.86	0.95	8.51	0.92	18.93		0.29
%Solids by Wt		74.84		74.14		91.49		%Media adhesion		10.42
20.4 m3/h										
	Feed (wet)	Feed (dry)	Underflow (wet)	Underflow (dry)	Overflow (wet1)	Overflow (Dry1)	Overflow (before washing)	Overflow (after washing2)	O/F rate(kg/h)	20.4 t/h
Mass (kg)	7.1	5.35	6.78	5.06	1.72	1.59	1.86	1.53	3175.98	323.43 kg/h
Litres (L)	2.6		2.5							15.85 kg/t
Density (kg/L)	2.73	2.70	2.71	2.66					0.33	28.26 kg/t/m
Time					1.93			2.13		0.02
%Moisture		24.65		25.37	0.89	7.56	0.87	17.74		0.31
%Solids by Wt		75.35		74.63		92.44		%Media adhesion		10.18
							Pump speed (m3/h)	%Moisture	%media adhesion (kg/t/m)	%media Adhesion
							24.5	9.7	55.7	13.3
							23.7	9.5	40.8	12.8
							22.8	9.3	37.4	12.0
							21.8	9.0	34.3	11.3
							20.8	8.5	30.1	10.4
							20.4	7.6	28.3	10.2

0.63x8.8 mm at 2.45 kg/l										
25.1 m ³ /hr										
	Feed (wet)	Feed (dry)	Underflow (wet)	Underflow (dry)	Overflow (wet1)	Overflow (Dry1)	Overflow (before washing)	Overflow (after washing2)	O/F rate(kg/h)	25.1 t/h
Mass (kg)	6.62	4.67	6.18	4.3	2.3	2.08	2.11	1.64	7180.83	912.66 kg/h
Litres (L)	2.7		2.55							36.36 kg/t
Density (kg/L)	2.45	2.44	2.42	2.39					0.47	64.81 kg/t/m
Time					1.12		1.09		0.04	
%Moisture		29.46		30.42	2.05	9.57	1.94	22.27	0.43	
%Solids by Wt		70.54		69.58		90.43		%Media adhesion	12.71	
24.5 m ³ /h										
	Feed (wet)	Feed (dry)	Underflow (wet)	Underflow (dry)	Overflow (wet1)	Overflow (Dry1)	Overflow (before washing)	Overflow (after washing2)	O/F rate(kg/h)	24.5 t/h
Mass (kg)	6.8	4.86	7.33	5.15	2.35	2.13	2.15	1.69	6047.12	727.69 kg/h
Litres (L)	2.75		3							29.70 kg/t
Density (kg/L)	2.47	2.48	2.44	2.42					0.46	52.94 kg/t/m
Time					1.33		1.35		0.04	
%Moisture /rate		28.53		29.74	1.77	9.36	1.59	21.40	0.42	
%Solids by Wt		71.47		70.26		90.64		%Media adhesion	12.03	
23.8 m ³ /h										
	Feed (wet)	Feed (dry)	Underflow (wet)	Underflow (dry)	Overflow (wet1)	Overflow (Dry1)	Overflow (before washing)	Overflow (after washing2)	O/F rate(kg/h)	23.8 t/h
Mass (kg)	6.62	4.67	6.18	4.3	1.64	1.49	1.71	1.36	4786.05	541.85 kg/h
Litres (L)	2.7		2.55							22.77 kg/t
Density (kg/L)	2.45	2.44	2.42	2.39					0.35	40.58 kg/t/m
Time					1.23		1.29		0.03	
%Moisture/Rate		29.46		30.42	1.33	9.15	1.33	20.47	0.32	
%Solids by Wt		70.54		69.58		90.85		%Media adhesion	11.32	
22.8 m ³ /h										
	Feed (wet)	Feed (dry)	Underflow (wet)	Underflow (dry)	Overflow (wet1)	Overflow (Dry1)	Overflow (before washing)	Overflow (after washing2)	O/F rate(kg/h)	22.8 t/h
Mass (kg)	6.8	4.86	7.33	5.15	1.63	1.49	1.63	1.31	4298.96	469.46 kg/h
Litres (L)	2.75		3							20.59 kg/t
Density (kg/L)	2.47	2.48	2.44	2.42					0.32	36.70 kg/t/m
Time					1.37		1.36		0.03	
%Moisture /Rate		28.53		29.74	1.19	8.71	1.20	19.63	0.29	
%Solids by Wt		71.47		70.26		91.29		%Media adhesion	10.92	
21.8 m ³ /h										
	Feed (wet)	Feed (dry)	Underflow (wet)	Underflow (dry)	Overflow (wet1)	Overflow (Dry1)	Overflow (before washing)	Overflow (after washing2)	O/F rate(kg/h)	21.8 t/h
Mass (kg)	6.62	4.67	6.18	4.3	1.53	1.40	1.38	1.12	3891.84	402.57 kg/h
Litres (L)	2.7		2.55							18.47 kg/t
Density (kg/L)	2.45	2.44	2.42	2.39					0.26	32.92 kg/t/m
Time					1.38		1.31		0.02	
%Moisture /rate		29.46		30.42	1.11	8.50	1.05	18.84	0.24	
%Solids by Wt		70.54		69.58		91.50		%Media adhesion	10.34	
							Pump speed (m ³ /h)	%Moisture	Media adhesion (kg/t/m)	%Media Adhesion
							25.1	9.6	64.8	12.7
							24.5	9.4	52.9	12.0
							23.8	9.1	40.6	11.3
							22.8	8.7	36.7	10.9
							21.8	8.5	32.9	10.3

Appendix Q: Percent moisture and medium carryover for degraded ferrosilicon and iron ore

0.8x8.8 mm at 2.0 kg/l											
25.1 m ³ /hr											
	Feed (wet)	Feed (dry)	Underflow (wet)	Underflow (dry)	Overflow (wet1)	Overflow (Dry1)	Overflow (before washing)	Overflow (after washing2)	O/F rate (kg/h)	25.1	t/h
Mass (kg)	3.18	1.88	3.48	2.05	1.70	1.33	1.30	0.67	9461.25	2540.41	kg/h
Litres (L)	1.60		1.70							101.21	kg/t
Density (kg/L)	1.99	1.98	2.05	1.97					0.63	180.41	kg/t/m
Time					0.64		0.50		0.14		
%Moisture		40.88		41.09	2.66	21.76	2.60	48.62	0.49		
%Solids by Wt		59.12		58.91		78.24		%Media adhesion	26.85		
24.5 m ³ /hr											
	Feed (wet)	Feed (dry)	Underflow (wet)	Underflow (dry)	Overflow (wet1)	Overflow (Dry1)	Overflow (before washing)	Overflow (after washing2)	O/F rate (kg/h)	24.5	t/h
Mass (kg)	2.62	1.56	2.60	1.53	1.60	1.27	1.23	0.69	8341.18	1915.55	kg/h
Litres (L)	1.30		1.30							78.19	kg/t
Density (kg/L)	2.02	1.99	2.00	1.97					0.54	139.37	kg/t/m
Time					0.72		0.51		0.11		
%Moisture		40.46		41.15	2.22	20.94	2.41	43.90	0.43		
%Solids by Wt		59.54		58.85		79.06		%Media adhesion	22.96		
23.7 m ³ /hr											
	Feed (wet)	Feed (dry)	Underflow (wet)	Underflow (dry)	Overflow (wet1)	Overflow (Dry1)	Overflow (before washing)	Overflow (after washing2)	O/F rate (kg/h)	23.7	t/h
Mass (kg)	3.18	1.88	3.48	2.05	1.30	1.06	1.62	0.99	8074.43	1649.39	kg/h
Litres (L)	1.60		1.70							69.59	kg/t
Density (kg/L)	1.99	1.98	2.05	1.97					0.63	124.05	kg/t/m
Time					0.64		0.66		0.12		
%Moisture		40.88		41.09	2.03	18.46	2.45	38.89	0.51		
%Solids by Wt		59.12		58.91		81.54		%Media adhesion	20.43		
22.8 m ³ /hr											
	Feed (wet)	Feed (dry)	Underflow (wet)	Underflow (dry)	Overflow (wet1)	Overflow (Dry1)	Overflow (before washing)	Overflow (after washing2)	O/F rate (kg/h)	22.8	t/h
Mass (kg)	2.62	1.56	2.60	1.53	1.10	0.92	1.20	0.78	7593.94	1415.23	kg/h
Litres (L)	1.30		1.30							62.07	kg/t
Density (kg/L)	2.02	1.99	2.00	1.97					0.42	110.64	kg/t/m
Time					0.54		0.55		0.07		
%Moisture		40.46		41.15	2.04	16.36	2.18	35.00	0.35		
%Solids by Wt		59.54		58.85		83.64		%Media adhesion	18.64		
21.8 m ³ /hr											
	Feed (wet)	Feed (dry)	Underflow (wet)	Underflow (dry)	Overflow (wet1)	Overflow (Dry1)	Overflow (before washing)	Overflow (after washing2)	O/F rate (kg/h)	21.8	t/h
Mass (kg)	3.18	1.88	3.48	2.05	1.10	0.94	0.98	0.70	7125.49	999.42	kg/h
Litres (L)	1.60		1.70							45.84	kg/t
Density (kg/L)	1.99	1.98	2.05	1.97					0.28	81.72	kg/t/m
Time					0.54		0.51		0.04		
%Moisture		40.88		41.09	2.04	14.55	1.92	28.57	0.24		
%Solids by Wt		59.12		58.91		85.45		%Media adhesion	14.03		
							Pump speed (m ³ /h)	%Moisture	Media adhesion (kg/t/m)	%Media Adhesion	
							25.1	21.8	180.4	26.9	
							24.5	20.9	139.4	23.0	
							23.8	18.5	124.1	20.4	
							22.8	16.4	110.6	18.6	
							21.8	14.5	81.7	14.0	

0.8x8.8 mm at 2.2 kg/l											
25.1 m ³ /hr											
	Feed (wet)	Feed (dry)	Underflow (wet)	Underflow (dry)	Overflow (wet1)	Overflow (Dry1)	Overflow (before washing)	Overflow (after washing2)	O/F rate (kg/h)	25.1	t/h
Mass (kg)	4.53	2.94	6.09	3.91	1.53	1.12	1.24	0.48	9945.16	3430.38	kg/h
Litres (L)	2.00		2.80							136.67	kg/t
Density (kg/L)	2.27	2.19	2.18	2.16	#DIV/0!				0.76	243.62	kg/t/m
Time					0.53		0.47		0.20		
%Moisture		35.10		35.80	2.89	26.80	2.64	61.29	0.56		
%Solids by Wt		64.90		64.20		73.20		%Media adhesion	34.49		
24.5 m ³ /h											
	Feed (wet)	Feed (dry)	Underflow (wet)	Underflow (dry)	Overflow (wet1)	Overflow (Dry1)	Overflow (before washing)	Overflow (after washing2)	O/F rate (kg/h)	24.5	t/h
Mass (kg)	4.53	2.94	6.09	3.91	1.42	1.07	1.46	0.62	8792.41	2891.50	kg/h
Litres (L)	2.00		2.80							118.02	kg/t
Density (kg/L)	2.27	2.19	2.18	2.16					0.84	210.38	kg/t/m
Time					0.57		0.61		0.21		
%Moisture		35.10		35.80	2.49	24.65	2.39	57.53	0.63		
%Solids by Wt		64.90		64.20		75.35		%Media adhesion	32.89		
23.7 m ³ /h											
	Feed (wet)	Feed (dry)	Underflow (wet)	Underflow (dry)	Overflow (wet1)	Overflow (Dry1)	Overflow (before washing)	Overflow (after washing2)	O/F rate (kg/h)	23.7	t/h
Mass (kg)	4.53	2.94	6.09	3.91	1.73	1.34	1.53	0.74	8318.56	2419.92	kg/h
Litres (L)	2.00		2.80							102.11	kg/t
Density (kg/L)	2.27	2.19	2.18	2.16					0.79	182.01	kg/t/m
Time					0.74		0.67		0.18		
%Moisture		35.10		35.80	2.34	22.54	2.28	51.63	0.61		
%Solids by Wt		64.90		64.20		77.46		%Media adhesion	29.09		
22.8 m ³ /h											
	Feed (wet)	Feed (dry)	Underflow (wet)	Underflow (dry)	Overflow (wet1)	Overflow (Dry1)	Overflow (before washing)	Overflow (after washing2)	O/F rate (kg/h)	22.8	t/h
Mass (kg)	4.53	2.94	6.09	3.91	1.52	1.20	1.59	0.84	7944.08	2074.77	kg/h
Litres (L)	2.00		2.80							91.00	kg/t
Density (kg/L)	2.27	2.19	2.18	2.16					0.75	162.21	kg/t/m
Time					0.68		0.73		0.16		
%Moisture		35.10		35.80	2.24	21.05	2.18	47.17	0.59		
%Solids by Wt		64.90		64.20		78.95		%Media adhesion	26.12		
21.8 m ³ /h											
	Feed (wet)	Feed (dry)	Underflow (wet)	Underflow (dry)	Overflow (wet1)	Overflow (Dry1)	Overflow (before washing)	Overflow (after washing2)	O/F rate (kg/h)	21.8	t/h
Mass (kg)	4.53	2.94	6.09	3.91	1.38	1.12	1.30	0.74	7537.50	1826.81	kg/h
Litres (L)	2.00		2.80							83.80	kg/t
Density (kg/L)	2.27	2.19	2.18	2.16					0.56	149.37	kg/t/m
Time					0.64		0.64		0.11		
%Moisture		35.10		35.80	2.16	18.84	2.03	43.08	0.45		
%Solids by Wt		64.90		64.20		81.16		%Media adhesion	24.24		
							Pump speed (m ³ /h)	%Moisture	Media adhesion (kg/t/m)	%Media Adhesion	
							25.1	26.8	243.6	34.493	
							24.5	24.6	210.4	32.886	
							23.8	22.5	182.0	29.091	
							22.8	21.1	162.2	26.117	
							21.8	18.8	149.4	24.236	

1x13 mm at 1.9 kg/l											
25.1 m ³ /hr											
	Feed (wet)	Feed (dry)	Underflow (wet)	Underflow (dry)	Overflow (wet1)	Overflow (Dry1)	Overflow (before washing)	Overflow (after washing2)	O/F rate (kg/h)	25.1	t/h
Mass (kg)	4.43	2.49	4.55	2.60	2.01	1.66	1.72	1.08	8506.96	1684.07	kg/h
Litres (L)	2.35		2.40							67.09	kg/t
Density (kg/L)	1.89	1.89	1.90	1.91					0.64	119.60	kg/t/m
Time						0.90	0.69			0.11	
%Moisture		43.79		42.86	2.23	17.41	2.49	37.21		0.53	
%Solids by Wt		56.21		57.14		82.59		%Media adhesion	19.80		
24.5 m ³ /h											
	Feed (wet)	Feed (dry)	Underflow (wet)	Underflow (dry)	Overflow (wet1)	Overflow (Dry1)	Overflow (before washing)	Overflow (after washing2)	O/F rate (kg/h)	24.5	t/h
Mass (kg)	4.58	2.58	4.55	2.60	1.84	1.54	1.92	1.26	7277.46	1315.08	kg/h
Litres (L)	2.40		2.40							53.68	kg/t
Density (kg/L)	1.91	1.89	1.90	1.91					0.66	95.68	kg/t/m
Time						0.91	0.95			0.11	
%Moisture /rate		43.67		42.86	2.02	16.30	2.02	34.38		0.55	
%Solids by Wt		56.33		57.14		83.70		%Media adhesion	18.07		
23.7 m ³ /h											
	Feed (wet)	Feed (dry)	Underflow (wet)	Underflow (dry)	Overflow (wet1)	Overflow (Dry1)	Overflow (before washing)	Overflow (after washing2)	O/F rate (kg/h)	23.7	t/h
Mass (kg)	4.43	2.49	4.55	2.60	1.89	1.60	2.20	1.51	7035.03	1126.99	kg/h
Litres (L)	2.35		2.40							47.55	kg/t
Density (kg/L)	1.89	1.89	1.90	1.91					0.69	84.76	kg/t/m
Time						1.00	1.09			0.11	
%Moisture/Rate		43.79		42.86	1.89	15.34	2.02	31.36		0.58	
%Solids by Wt		56.21		57.14		84.66		%Media adhesion	16.02		
22.8 m ³ /h											
	Feed (wet)	Feed (dry)	Underflow (wet)	Underflow (dry)	Overflow (wet1)	Overflow (Dry1)	Overflow (before washing)	Overflow (after washing2)	O/F rate (kg/h)	22.8	t/h
Mass (kg)	4.58	2.58	4.55	2.60	1.65	1.43	1.69	1.25	6833.49	868.00	kg/h
Litres (L)	2.40		2.40							38.07	kg/t
Density (kg/L)	1.91	1.89	1.90	1.91					0.44	67.86	kg/t/m
Time						0.86	0.90			0.06	
%Moisture /Rate		43.67		42.86	1.92	13.33	1.88	26.04		0.38	
%Solids by Wt		56.33		57.14		86.67		%Media adhesion	12.70		
21.8 m ³ /h											
	Feed (wet)	Feed (dry)	Underflow (wet)	Underflow (dry)	Overflow (wet1)	Overflow (Dry1)	Overflow (before washing)	Overflow (after washing2)	O/F rate (kg/h)	21.8	t/h
Mass (kg)	4.43	2.49	4.55	2.60	1.36	1.22	1.25	1.00	6263.46	607.92	kg/h
Litres (L)	2.35		2.40							27.89	kg/t
Density (kg/L)	1.89	1.89	1.90	1.91					0.25	49.71	kg/t/m
Time						0.78	0.72			0.03	
%Moisture /rate		43.79		42.86	1.74	10.29	1.74	20.00		0.22	
%Solids by Wt		56.21		57.14		89.71		%Media adhesion	9.71		
								Pump speed (m ³ /h)	%Moisture	Media adhesion (kg/t/m)	%Media Adhesion
								25.1	17.4	119.6	19.8
								24.5	16.3	95.7	18.1
								23.8	15.3	84.8	16.0
								22.8	13.3	67.9	12.7
								21.8	10.3	49.7	9.7

Appendix R: Particle size distribution calculation

SIEVE ANALYSIS FOR 1x13 mm at 1.90 kg/l																		
Sieve Size	20.8			21.8			22.8			23.7			24.5			25.1		
	Feed	Overflow	Underflow	Feed	Overflow	Underflow	Feed	Overflow	Underflow	Feed	Overflow	Underflow	Feed	Overflow	Underflow	Feed	Overflow	Underflow
4.00	4.44	11.86	0	2.2	2.73	0	2.2	13.2	0	2.2	5.65	0	2.2	12.45	0	2.2	17.23	0
2.80	10.54	59.42	0	15.52	72.19	0	15.52	73.37	0	15.52	70.71	0	15.52	88.87	0	15.52	72.9	0
2.360	18.04	70.73	0	23.91	76.85	0	23.91	85.22	0	23.91	78.2	0	23.91	92.63	0	23.91	88.84	0
2.000	28.75	103.32	0	34.73	107.82	0	34.73	103.71	0	34.73	111.94	0	34.73	106.6	0	34.73	110.17	0
1.700	32.16	105.43	0	28.58	114.34	0	28.58	103.74	0	28.58	102.14	0	28.58	105.59	0	28.58	103.29	0
1.400	28.96	91.64	0	24.68	81.01	0	24.68	72.36	0	24.68	81.87	0	24.68	63.21	0	24.68	65.35	0
1.180	6.29	19.35	0	4.37	15.97	0	4.37	13.3	0	4.37	16.31	0	4.37	13.24	0	4.37	10.38	0
1.000	0.68	1.77	0	0.34	1.6	0	0.34	1.33	0	0.34	1.59	0	0.34	1.14	0	0.34	0.99	0
0.850	0.75	0	8.01	7.51	0	0	7.51	1	7.64	7.51	0	0	7.51	0.43	8.01	7.51	0.8	0
0.710	0.34	0	2.42	0.64	0	0	0.64	0	0.54	0.64	0	0	0.64	0	2.42	0.64	0	0
0.600	0	0	0	0	0	0	0	0	0	0	0	0	0	0	0	0	0	0
0.500	0	0	0	0	0	0	0	0	0	0	0	0	0	0	0	0	0	0
0.355	0	0	0	0	0	0	0	0	0	0	0	0	0	0	0	0	0	0
0.250	0.87	0	0	0	0	0	0	0	0	0	0	0	0	0	0	0	0	0
0.212	0	0	0	0	0	0	0	0	0	0	0	0	0	0	0	0	0	0
0.150	1.12	1.21	11.67	1.21	1.09	5.14	1.21	0.61	13.53	1.21	1.1	5.14	1.21	0	11.67	1.21	0.46	5.14
0.106	6.36	0.44	12.58	5.27	0.11	8.09	5.27	0.73	21.13	5.27	0.16	8.09	5.27	0.1	12.58	5.27	0.25	8.09
0.090	7.19	5.37	11.92	14.48	0.1	6.35	14.48	1.64	73.82	14.48	0.25	6.35	14.48	0.19	11.92	14.48	0.59	6.35
0.063	41.31	11.3	126.99	122.48	2.89	129.210	122.48	10.46	208.32	122.48	6.67	129.210	122.48	3.48	126.99	122.48	4.48	129.210
0.053	103	5.13	144.47	114.83	8.39	160.11	114.83	4.19	110.01	114.83	5.35	160.11	114.83	0.83	144.47	114.83	6.58	160.11
0.045	117.32	2.69	96.63	55.94	2.32	112.05	55.94	0.54	38.65	55.94	5.1	112.05	55.94	1.57	96.63	55.94	0.62	112.05
0.038	56.15	2.77	47.75	17.65	4.49	38.68	17.65	5.08	10.43	17.65	4.57	38.68	17.65	2.93	47.75	17.65	6.67	38.68
0.025	27.48	4.54	32.9	16.13	7.22	36.92	16.13	8.35	12.98	16.13	6.83	36.92	16.13	5.83	32.9	16.13	9.84	36.92
Sum	491.75	496.97	495.34	490.47	499.12	496.55	490.47	498.83	497.05	490.47	498.44	496.55	490.47	499.09	495.34	490.47	499.44	496.55

Sieve Size	20.8						21.8						22.8						23.7						24.5						25.1					
	Feed			Overflow			Underflow			Feed			Overflow			Underflow			Feed			Overflow			Underflow			Feed			Overflow			Underflow		
%Retained	%Cum pass	%Retained	%Cum pass	%Retained	%Cum pass	%Retained	%Cum pass	%Retained	%Cum pass	%Retained	%Cum pass	%Retained	%Cum pass	%Retained	%Cum pass	%Retained	%Cum pass	%Retained	%Cum pass	%Retained	%Cum pass	%Retained	%Cum pass	%Retained	%Cum pass	%Retained	%Cum pass	%Retained	%Cum pass	%Retained	%Cum pass					
4.00	0.9	99.1	2.4	97.6	0.0	100.0	0.4	99.6	0.5	99.5	0.0	100.0	0.4	99.6	2.6	97.4	0.0	100.0	0.4	99.6	1.1	98.9	0.0	100.0	0.4	99.6	2.5	97.5	0.0	100.0	0.4	99.6	3.4	96.6	0.0	100.0
2.80	2.1	97.0	12.0	85.7	0.0	100.0	3.2	96.4	14.5	85.0	0.0	100.0	3.2	96.4	14.7	82.6	0.0	100.0	3.2	96.4	14.2	84.7	0.0	100.0	3.2	96.4	17.8	79.7	0.0	100.0	3.2	96.4	14.6	82.0	0.0	100.0
2.360	3.7	93.3	14.2	71.4	0.0	100.0	4.9	91.5	15.4	69.6	0.0	100.0	4.9	91.5	17.1	65.6	0.0	100.0	4.9	91.5	15.7	69.0	0.0	100.0	4.9	91.5	18.6	61.1	0.0	100.0	4.9	91.5	17.8	64.2	0.0	100.0
2.000	5.8	87.4	20.8	50.6	0.0	100.0	7.1	84.4	21.6	48.0	0.0	100.0	7.1	84.4	20.8	44.8	0.0	100.0	7.1	84.4	22.5	46.5	0.0	100.0	7.1	84.4	21.4	39.8	0.0	100.0	7.1	84.4	22.1	42.1	0.0	100.0
1.700	6.5	80.9	21.2	29.4	0.0	100.0	5.8	78.6	22.9	25.1	0.0	100.0	5.8	78.6	20.8	24.0	0.0	100.0	5.8	78.6	20.5	26.0	0.0	100.0	5.8	78.6	21.2	18.6	0.0	100.0	5.8	78.6	20.7	21.4	0.0	100.0
1.400	5.9	75.0	18.4	11.0	0.0	100.0	5.0	73.6	16.2	8.9	0.0	100.0	5.0	73.6	14.5	9.5	0.0	100.0	5.0	73.6	16.4	9.6	0.0	100.0	5.0	73.6	12.7	6.0	0.0	100.0	5.0	73.6	13.1	8.3	0.0	100.0
1.180	1.3	73.7	3.9	7.1	0.0	100.0	0.9	72.7	3.2	5.7	0.0	100.0	0.9	72.7	2.7	6.8	0.0	100.0	0.9	72.7	3.3	6.3	0.0	100.0	0.9	72.7	2.7	3.3	0.0	100.0	0.9	72.7	2.1	6.3	0.0	100.0
1.000	0.1	73.6	0.4	6.7	0.0	100.0	0.1	72.6	0.3	5.3	0.0	100.0	0.1	72.6	0.3	6.5	0.0	100.0	0.1	72.6	0.3	6.0	0.0	100.0	0.1	72.6	0.2	3.1	0.0	100.0	0.1	72.6	0.2	6.1	0.0	100.0
0.850	0.2	73.4	0.0	6.7	1.6	98.4	1.5	71.1	0.0	5.3	0.0	100.0	1.5	71.1	0.2	6.3	1.5	98.5	1.5	71.1	0.1	6.0	0.0	100.0	1.5	71.1	0.1	3.0	1.6	98.4	1.5	71.1	0.2	5.9	0.0	100.0
0.710	0.1	73.4	0.0	6.7	0.5	97.9	0.1	71.0	0.0	5.3	0.0	100.0	0.1	71.0	0.0	6.3	0.1	98.4	0.1	71.0	0.0	6.0	0.0	100.0	0.1	71.0	0.0	3.0	0.5	97.9	0.1	71.0	0.0	5.9	0.0	100.0
0.600	0.0	73.4	0.0	6.7	0.0	97.9	0.0	71.0	0.0	5.3	0.0	100.0	0.0	71.0	0.0	6.3	0.0	98.4	0.0	71.0	0.0	6.0	0.0	100.0	0.0	71.0	0.0	3.0	0.0	97.9	0.0	71.0	0.0	5.9	0.0	100.0
0.500	0.0	73.4	0.0	6.7	0.0	97.9	0.0	71.0	0.0	5.3	0.0	100.0	0.0	71.0	0.0	6.3	0.0	98.4	0.0	71.0	0.0	6.0	0.0	100.0	0.0	71.0	0.0	3.0	0.0	97.9	0.0	71.0	0.0	5.9	0.0	100.0
0.355	0.0	73.4	0.0	6.7	0.0	97.9	0.0	71.0	0.0	5.3	0.0	100.0	0.0	71.0	0.0	6.3	0.0	98.4	0.0	71.0	0.0	6.0	0.0	100.0	0.0	71.0	0.0	3.0	0.0	97.9	0.0	71.0	0.0	5.9	0.0	100.0
0.250	0.2	73.2	0.0	6.7	0.0	97.9	0.0	71.0	0.0	5.3	0.0	100.0	0.0	71.0	0.0	6.3	0.0	98.4	0.0	71.0	0.0	6.0	0.0	100.0	0.0	71.0	0.0	3.0	0.0	97.9	0.0	71.0	0.0	5.9	0.0	100.0
0.212	0.0	73.2	0.0	6.7	0.0	97.9	0.0	71.0	0.0	5.3	0.0	100.0	0.0	71.0	0.0	6.3	0.0	98.4	0.0	71.0	0.0	6.0	0.0	100.0	0.0	71.0	0.0	3.0	0.0	97.9	0.0	71.0	0.0	5.9	0.0	100.0
0.150	0.2	73.0	0.2	6.5	2.4	95.5	0.2	70.7	0.2	5.1	1.0	99.0	0.2	70.7	0.1	6.2	2.7	95.6	0.2	70.7	0.2	5.8	1.0	99.0	0.2	70.7	0.0	3.0	2.4	95.5	0.2	70.7	0.1	5.8	1.0	99.0
0.106	1.3	71.7	0.1	6.4	2.5	93.0	1.1	69.6	0.0	5.1	1.6	97.3	1.1	69.6	0.1	6.1	4.3	91.4	1.1	69.6	0.0	5.8	1.6	97.3	1.1	69.6	0.0	3.0	2.5	93.0	1.1	69.6	0.1	5.8	1.6	97.3
0.090	1.5	70.2	1.1	5.3	2.4	90.6	3.0	66.7	0.0	5.1	1.3	96.1	3.0	66.7	0.3	5.7	14.9	76.5	3.0	66.7	0.1	5.7	1.3	96.1	3.0	66.7	0.0	2.9	2.4	90.6	3.0	66.7	0.1	5.6	1.3	96.1
0.063	8.4	61.8	2.3	3.0	25.6	65.0	25.0	41.7	0.6	4.5	26.0	70.0	25.0	41.7	2.1	3.6	41.9	34.6	25.0	41.7	1.3	4.4	26.0	70.0	25.0	41.7	0.7	2.2	25.6	65.0	25.0	41.7	0.9	4.7	26.0	70.0
0.053	20.9	40.9	1.0	2.0	29.2	35.8	23.4	18.3	1.7	2.8	32.2	37.8	23.4	18.3	0.8	2.8	22.1	12.5	23.4	18.3	1.1	3.3	32.2	37.8	23.4	18.3	0.2	2.1	29.2	35.8	23.4	18.3	1.3	3.4	32.2	37.8
0.045	23.9	17.0	0.5	1.5	19.5	16.3	11.4	6.9	0.5	2.3	22.6	15.2	11.4	6.9	0.1	2.7	7.8	4.7	11.4	6.9	1.0	2.3	22.6	15.2	11.4	6.9	0.3	1.8	19.5	16.3	11.4	6.9	0.1	2.3	22.6	15.2
0.038	11.4	5.6	0.6	0.9	9.6	6.6	3.6	3.3	0.9	1.4	7.8	7.4	3.6	3.3	1.0	1.7	2.1	2.6	3.6	3.3	0.9	1.4	7.8	7.4	3.6	3.3	0.6	1.2	9.6	6.6	3.6	3.3	1.3	2.0	7.8	7.4
0.025	5.6	0.0	0.9	0.0	6.6	0.0	3.3	0.0	1.4	0.0	7.4	0.0	3.3	0.0	1.7	0.0	2.6	0.0	3.3	0.0	1.4	0.0	7.4	0.0	3.3	0.0	1.2	0.0	6.6	0.0	3.3	0.0	2.0	0.0	7.4	0.0

SIEVE ANALYSIS FOR 1x13 mm at 2.2 kg/l																			
Sieve Size	20.8			21.8			22.8			23.7			24.5			25.1			
	Feed	Overflow	Underflow	Feed	Overflow	Underflow	Feed	Overflow	Underflow	Feed	Overflow	Underflow	Feed	Overflow	Underflow	Feed	Overflow	Underflow	
4.00	4.91	13.1	0	10.06	12.16	0	4.91	11.7	0	4.91	12.51	0	10.06	13.62	0	10.06	17.84	0	
2.80	16.78	56.43	0	26.62	46.71	0	16.78	54.14	0	16.78	46.89	0	26.62	62.49	0	26.62	58.49	0	
2.360	21.61	65.02	0	26.34	67.30	0	21.61	65.64	0	21.61	66.39	0	26.34	71.61	0	26.34	66.67	0	
2.000	26.65	105.52	0	34.45	96.9	0	26.65	103.78	0	26.65	99.25	0	34.45	108.79	0	34.45	89.95	0	
1.700	32.94	103.48	0	25.94	107.33	0	32.94	112.69	0	32.94	101.03	0	25.94	109.84	0	25.94	91.97	0	
1.400	33.18	90.92	0	17.36	104.62	0	33.18	92.02	0	33.18	92.26	0	17.36	75.42	0	17.36	79.16	0	
1.180	7.99	19.21	0	3.08	23.28	0	7.99	19.5	0	7.99	21.57	0	3.08	12.6	0	3.08	16.89	0	
1.000	1	1.79	0	0.31	1.02	0	1	2.01	0	1	2.12	0	0.31	1.6	0	0.31	1.49	0	
0.850	0.71	0.47	1.62	0.91	0.65	1.62	0.71	0.6	1.34	0.71	0.78	1.34	0.91	0.64	1.34	0.91	0.7	1.34	
0.710	0.59	0	0.84	0.48	0.36	0.84	0.59	0	0.91	0.59	0.31	0.91	0.48	0.36	0.91	0.48	0.51	0.91	
0.600	0	0	0	0	0	0	0	0	0	0	0	0	0	0	0	0	0	0	
0.500	0	0	0	0	0	0	0	0	0	0	0	0	0	0	0	0	0	0	
0.355	0	0	0	0	0	0	0	0	0	0	0	0	0	0	0	0	0	0	
0.250	0	0	0	0	0	0	0	0	0	0	0	0	0	0	0	0	0	0	
0.212	0	0	0	0	0	0	0	0	0	0	0	0	0	0	0	0	0	0	
0.150	3.56	0.8	27.83	7	0.62	27.83	3.56	0.04	33.3	3.56	0.7	33.3	7	0.46	33.3	7	0.58	33.3	
0.106	22.43	3.94	20.41	20.65	1.54	20.41	22.43	3.13	31.93	22.43	4.66	31.93	20.65	1.48	31.93	20.65	27.15	31.93	
0.090	34.64	6.16	35.37	67.97	3.67	35.37	34.64	5.21	48.39	34.64	16.31	48.39	67.97	5.42	48.39	67.97	16.42	48.39	
0.063	124.71	15.45	164.42	167.19	10.48	164.42	124.71	10.76	148.82	124.71	19.25	148.82	167.19	15.51	148.82	167.19	18.28	148.82	
0.053	108.42	3.04	171.62	60.1	9.16	171.62	108.42	7.2	165.49	108.42	5.26	165.49	60.1	8.26	165.49	60.1	4.58	165.49	
0.045	33.44	2.08	40.01	14.4	2.15	40.01	33.44	2.24	44.66	33.44	0.8	44.66	14.4	2.47	44.66	14.4	2.26	44.66	
0.038	12.38	3.09	14.87	4.92	4.84	14.87	12.38	4.54	8.76	12.38	4.49	8.76	4.92	3.63	8.76	4.92	2.62	8.76	
0.025	7.76	4.43	18.84	9.91	5.16	7.87	7.76	2.81	14.24	7.76	4.13	14.24	9.91	3.57	14.24	9.91	3.62	14.24	
Sum	493.70	494.93	495.83	497.69	497.95	484.86	493.70	498.01	497.84	493.70	498.71	497.84	497.69	497.77	497.84	497.69	499.18	497.84	

Sieve Size	20.8			21.8			22.8			23.7			24.5			25.1		
	Feed	Overflow	Underflow	Feed	Overflow	Underflow	Feed	Overflow	Underflow	Feed	Overflow	Underflow	Feed	Overflow	Underflow	Feed	Overflow	Underflow
4.00	1.0	99.0	2.6	97.4	0.0	100.0	2.0	98.0	2.4	97.6	0.0	100.0	1.0	99.0	2.5	97.5	0.0	100.0
2.80	3.4	95.6	11.4	86.0	0.0	100.0	5.3	92.6	9.4	88.2	0.0	100.0	3.4	95.6	9.4	88.1	0.0	100.0
2.360	4.4	91.2	13.1	72.8	0.0	100.0	5.3	87.3	13.5	74.7	0.0	100.0	4.4	91.2	13.3	74.8	0.0	100.0
2.000	5.4	85.8	21.3	51.5	0.0	100.0	6.9	80.4	19.5	55.2	0.0	100.0	5.4	85.8	19.9	54.9	0.0	100.0
1.700	6.7	79.2	20.9	30.6	0.0	100.0	5.2	75.2	21.6	33.6	0.0	100.0	6.7	79.2	20.3	34.6	0.0	100.0
1.400	6.7	72.4	18.4	12.2	0.0	100.0	3.5	71.7	21.0	12.6	0.0	100.0	6.7	72.4	18.5	16.1	0.0	100.0
1.180	1.6	70.8	3.9	8.3	0.0	100.0	0.6	71.1	4.7	8.0	0.0	100.0	1.6	70.8	4.3	11.8	0.0	100.0
1.000	0.2	70.6	0.4	8.0	0.0	100.0	0.1	71.0	0.2	7.8	0.0	100.0	0.2	70.6	0.4	11.1	0.0	100.0
0.850	0.1	70.5	0.1	7.9	0.3	99.7	0.2	70.9	0.1	7.6	0.3	99.7	0.1	70.5	0.2	11.2	0.3	99.7
0.710	0.1	70.4	0.0	7.9	0.2	99.5	0.1	70.8	0.1	7.6	0.2	99.5	0.1	70.4	0.1	11.1	0.2	99.5
0.600	0.0	70.4	0.0	7.9	0.0	99.5	0.0	70.8	0.0	7.6	0.0	99.5	0.0	70.4	0.0	11.1	0.0	99.5
0.500	0.0	70.4	0.0	7.9	0.0	99.5	0.0	70.8	0.0	7.6	0.0	99.5	0.0	70.4	0.0	11.1	0.0	99.5
0.355	0.0	70.4	0.0	7.9	0.0	99.5	0.0	70.8	0.0	7.6	0.0	99.5	0.0	70.4	0.0	11.1	0.0	99.5
0.250	0.0	70.4	0.0	7.9	0.0	99.5	0.0	70.8	0.0	7.6	0.0	99.5	0.0	70.4	0.0	11.1	0.0	99.5
0.212	0.0	70.4	0.0	7.9	0.0	99.5	0.0	70.8	0.0	7.6	0.0	99.5	0.0	70.4	0.0	11.1	0.0	99.5
0.150	0.7	69.6	0.2	7.7	5.6	93.9	1.4	69.3	0.1	7.4	5.7	93.8	0.7	69.6	0.1	11.0	6.7	92.9
0.106	4.5	65.1	0.8	6.9	4.1	89.8	4.1	65.2	0.3	7.1	4.2	89.5	4.5	65.1	0.6	6.6	6.4	86.4
0.090	7.0	58.1	1.2	5.7	7.1	82.6	13.7	51.5	0.7	6.4	7.3	82.2	7.0	58.1	1.0	5.5	9.7	76.7
0.063	24.3	32.8	3.1	2.6	33.2	49.5	33.6	17.9	2.1	4.3	33.9	48.3	25.3	32.8	2.2	3.4	29.9	46.8
0.053	22.0	10.9	0.6	1.9	34.6	14.9	12.1	5.9	1.8	2.4	35.4	12.9	22.0	10.9	1.4	1.9	33.2	13.6
0.045	6.8	4.1	0.4	1.5	8.1	6.8	2.9	3.0	0.4	2.0	8.3	4.7	6.8	4.1	0.4	1.5	9.0	4.6
0.038	2.5	1.6	0.6	0.9	3.0	3.8	1.0	2.0	1.0	1.0	3.1	1.6	2.5	1.6	0.9	0.6	1.8	2.9
0.025	1.6	0.0	0.9	0.0	3.8	0.0	2.0	0.0	1.0	0.0	1.6	0.0	1.6	0.0	0.6	0.0	2.9	0.0

SIEVE ANALYSIS FOR 1x13 mm at 2.45 kg/l																			
Sieve Size	FeSi	20.8			21.8			22.8			23.7			24.5			25.1		
		Feed	Overflow	Underflow	Feed	Overflow	Underflow	Feed	Overflow	Underflow	Feed	Overflow	Underflow	Feed	Overflow	Underflow	Feed	Overflow	Underflow
4.00	0	1.36	8.35	0	0.68	16.54	0	1.36	13.45	0	1.36	16.88	0	0.68	11.91	0	0.68	12.03	0
2.80	0	8.8	39.49	0	4.99	44.92	0	8.8	39.58	0	8.8	50.85	0	4.99	45.69	0	4.99	56.06	0
2.360	0	13.98	50.27	0	10.89	56.25	0	13.98	57.04	0	13.98	67.04	0	10.89	52	0	10.89	61.11	0
2.000	0	20.19	79.51	0	12.1	81.79	0	20.19	78.56	0	20.19	80.14	0	12.1	84.73	0	12.1	47.85	0
1.700	0	25.32	97.15	0	21.6	84.7	0	25.32	86.74	0	25.32	91.69	0	21.6	83.35	0	21.6	105.62	0
1.400	0	22.4	94.38	0	19.99	82.87	0	22.4	84.72	0	22.4	74.67	0	19.99	79.67	0	19.99	72.59	0
1.180	0	5.98	26.07	0	6.22	20.92	0	5.98	20.62	0	5.98	17.27	0	6.22	18.84	0	6.22	16.24	0
1.000	0	0.94	3.72	0	2.59	2.75	0	0.94	3.17	0	0.94	1.98	0	2.59	2.23	0	2.59	1.74	0
0.850	0	0.54	0.85	0.13	1.88	0.62	0.13	0.54	0.69	0.13	0.54	0.34	0.13	1.88	0.43	0.13	1.88	0.39	0.13
0.710	0	0	0	0	0	0	0	0	0	0	0	0	0	0	0	0	0	0	0
0.600	0	0	0	0	0	0	0	0	0	0	0	0	0	0	0	0	0	0	0
0.500	0	0	0	0	0	0	0	0	0	0	0	0	0	0	0	0	0	0	0
0.355	0	0	0	0	0	0	0	0	0	0	0	0	0	0	0	0	0	0	0
0.250	0	0	0	0	0	0	0	0	0	0	0	0	0	0	0	0	0	0	0
0.212	0	0	0	0	0	0	0	0	0	0	0	0	0	0	0	0	0	0	0
0.150	86.87	71.58	9.79	97.95	71.2	7.96	97.95	71.58	13.03	97.95	71.58	5.69	97.95	71.2	9.83	97.95	71.2	10.98	97.95
0.106	107.6	28.54	11.35	67.63	29.75	7.52	67.63	28.54	19.12	67.63	28.54	21.21	67.63	29.75	20.71	67.63	29.75	28.42	67.63
0.090	104.84	73.9	22	94.82	58.84	26.41	94.82	73.9	19.98	94.82	73.9	14.54	94.82	58.84	20.57	94.82	58.84	38.03	94.82
0.063	123.15	131.21	28.47	136.66	135.84	32.95	136.66	131.21	32.01	136.66	131.21	31.97	136.66	135.84	35.87	136.66	135.84	28.87	136.66
0.053	47.22	81.58	12.78	44.58	88.26	19.79	44.58	81.58	12.02	44.58	81.58	17.6	44.58	88.26	18.17	44.58	88.26	10.49	44.58
0.045	11.73	4.52	1.09	7.5	12.67	2.81	7.5	4.52	8.89	7.5	4.52	1.34	7.5	12.67	7.85	7.5	12.67	5.4	7.5
0.038	1.85	4.1	6.17	2.3	11.06	2.07	2.3	4.1	1.71	2.3	4.1	3.14	2.3	11.06	3.3	2.3	11.06	2.39	2.3
0.025	5.95	3.04	3.56	3.24	5.78	3.49	3.24	3.04	3.19	3.24	3.04	2.18	3.24	5.78	3.6	3.24	5.78	5.62	3.24
Sum	489.21	497.98	495.00	454.81	494.34	494.36	454.81	497.98	494.52	454.81	497.98	498.53	454.81	494.34	498.75	454.81	494.34	503.83	454.81

Sieve Size	FeSi	20.8						21.8						22.8						23.7						24.5						25.1						
		Feed			Overflow			Underflow			Feed			Overflow			Underflow			Feed			Overflow			Underflow			Feed			Overflow			Underflow			
%Retained	%Can pass	%Retained	%Can pass	%Retained	%Can pass	%Retained	%Can pass	%Retained	%Can pass	%Retained	%Can pass	%Retained	%Can pass	%Retained	%Can pass	%Retained	%Can pass	%Retained	%Can pass	%Retained	%Can pass	%Retained	%Can pass	%Retained	%Can pass	%Retained	%Can pass	%Retained	%Can pass	%Retained	%Can pass	%Retained	%Can pass					
4.00	0.0	100.0	0.3	99.7	1.7	98.3	0.0	100.0	0.1	99.9	3.3	96.7	0.0	100.0	0.3	99.7	2.7	97.3	0.0	100.0	0.3	99.7	3.4	96.6	0.0	100.0	0.1	99.9	2.4	97.6	0.0	100.0	0.1	99.9	2.4	97.6	0.0	100.0
2.80	0.0	100.0	1.8	98.0	8.0	90.3	0.0	100.0	1.0	98.9	9.1	87.6	0.0	100.0	1.8	98.0	8.0	89.3	0.0	100.0	1.8	98.0	10.2	86.4	0.0	100.0	1.0	98.9	9.2	88.5	0.0	100.0	1.0	98.9	11.1	86.5	0.0	100.0
2.360	0.0	100.0	2.8	94.2	10.2	80.2	0.0	100.0	2.2	96.7	11.4	76.2	0.0	100.0	2.8	95.2	11.5	77.7	0.0	100.0	2.8	96.2	13.4	73.0	0.0	100.0	2.2	96.7	10.4	78.0	0.0	100.0	2.2	96.7	12.1	74.4	0.0	100.0
2.000	0.0	100.0	4.1	91.1	16.1	64.1	0.0	100.0	2.4	94.2	16.5	59.6	0.0	100.0	4.1	91.1	15.9	61.9	0.0	100.0	4.1	91.1	16.1	56.9	0.0	100.0	2.4	94.2	17.0	61.0	0.0	100.0	2.4	94.2	9.5	64.9	0.0	100.0
1.700	0.0	100.0	5.1	86.0	19.6	44.5	0.0	100.0	4.4	89.8	17.1	42.5	0.0	100.0	5.1	86.0	17.5	44.3	0.0	100.0	4.4	89.8	16.7	44.3	0.0	100.0	4.4	89.8	16.7	44.3	0.0	100.0	4.4	89.8	21.0	43.9	0.0	100.0
1.400	0.0	100.0	4.5	81.5	19.1	25.4	0.0	100.0	4.0	85.8	16.8	25.7	0.0	100.0	4.5	81.5	17.1	27.2	0.0	100.0	4.5	81.5	15.0	23.5	0.0	100.0	4.0	85.8	16.0	28.4	0.0	100.0	4.0	85.8	14.4	29.5	0.0	100.0
1.180	0.0	100.0	1.2	80.3	5.3	20.2	0.0	100.0	1.3	84.5	4.2	21.5	0.0	100.0	1.2	80.3	4.2	23.0	0.0	100.0	1.2	80.3	3.5	20.1	0.0	100.0	1.3	84.5	3.8	24.6	0.0	100.0	1.3	84.5	3.2	26.3	0.0	100.0
1.000	0.0	100.0	0.2	80.1	0.8	19.4	0.0	100.0	0.5	84.0	0.6	21.0	0.0	100.0	0.2	80.1	0.6	22.4	0.0	100.0	0.2	80.1	0.4	19.7	0.0	100.0	0.5	84.0	0.4	24.1	0.0	100.0	0.5	84.0	0.3	25.9	0.0	100.0
0.850	0.0	100.0	0.1	80.0	0.2	19.2	0.0	100.0	0.4	83.6	0.1	20.8	0.0	100.0	0.1	80.0	0.1	22.2	0.0	100.0	0.1	80.0	0.1	19.6	0.0	100.0	0.4	83.6	0.1	24.0	0.0	100.0	0.4	83.6	0.1	25.8	0.0	100.0
0.710	0.0	100.0	0.0	80.0	0.0	19.2	0.0	100.0	0.0	83.6	0.0	20.8	0.0	100.0	0.0	80.0	0.0	22.2	0.0	100.0	0.0	80.0	0.0	19.6	0.0	100.0	0.0	83.6	0.0	24.0	0.0	100.0	0.0	83.6	0.0	25.8	0.0	100.0
0.600	0.0	100.0	0.0	80.0	0.0	19.2	0.0	100.0	0.0	83.6	0.0	20.8	0.0	100.0	0.0	80.0	0.0	22.2	0.0	100.0	0.0	80.0	0.0	19.6	0.0	100.0	0.0	83.6	0.0	24.0	0.0	100.0	0.0	83.6	0.0	25.8	0.0	100.0
0.500	0.0	100.0	0.0	80.0	0.0	19.2	0.0	100.0	0.0	83.6	0.0	20.8	0.0	100.0	0.0	80.0	0.0	22.2	0.0	100.0	0.0	80.0	0.0	19.6	0.0	100.0	0.0	83.6	0.0	24.0	0.0	100.0	0.0	83.6	0.0	25.8	0.0	100.0
0.355	0.0	100.0	0.0	80.0	0.0	19.2	0.0	100.0	0.0	83.6	0.0	20.8	0.0	100.0	0.0	80.0	0.0	22.2	0.0	100.0	0.0	80.0	0.0	19.6	0.0	100.0	0.0	83.6	0.0	24.0	0.0	100.0	0.0	83.6	0.0	25.8	0.0	100.0
0.250	0.0	100.0	0.0	80.0	0.0	19.2	0.0	100.0	0.0	83.6	0.0	20.8	0.0	100.0	0.0	80.0	0.0	22.2	0.0	100.0	0.0	80.0	0.0	19.6	0.0	100.0	0.0	83.6	0.0	24.0	0.0	100.0	0.0	83.6	0.0	25.8	0.0	100.0
0.212	0.0	100.0	0.0	80.0	0.0	19.2	0.0	100.0	0.0	83.6	0.0	20.8	0.0	100.0	0.0	80.0	0.0	22.2	0.0	100.0	0.0	80.0	0.0	19.6	0.0	100.0	0.0	83.6	0.0	24.0	0.0	100.0	0.0	83.6	0.0	25.8	0.0	100.0
0.150	17.8	82.2	14.4	65.6	2.0	17.3	21.5	78.4	14.4	69.2	1.6	19.2	21.5	78.4	14.4	65.6	2.6	19.6	21.5	78.4	14.4	65.6	1.1	18.5	21.5	78.4	14.4	69.2	2.0	22.1	21.5	78.4	14.4	69.2	2.2	23.7	21.5	78.4
0.106	22.0	60.2	5.7	59.9	2.3	15.0	14.9	63.6	6.0	63.2	1.5	17.7	14.9	63.6	5.7	59.9	3.9	15.7	14.9	63.6	5.7	59.9	4.3	14.2	14.9	63.6	6.0	63.2	4.2	17.9	14.9	63.6	6.0	63.2	5.6	18.0	14.9	63.6
0.090	21.4	38.8	14.8	45.1	4.4	10.5	20.8	42.7	11.9	51.3	5.3	12.4	20.8	42.7	14.8	45.1	4.0	1																				

SIEVE ANALYSIS FOR 1x13 mm at 2.55 kg/l																				
Sieve Size	FeSi	20.8			21.8			22.8			23.7			24.5			25.1			
		Feed	Overflow	Underflow	Feed	Overflow	Underflow	Feed	Overflow	Underflow	Feed	Overflow	Underflow	Feed	Overflow	Underflow	Feed	Overflow	Underflow	
4.00	0	0.14	8.35	0	0.3	16.54	0	0.14	13.45	0	0.14	16.88	0	0.3	11.91	0	0.3	9.16	0	
2.80	0	4.72	39.49	0	6.35	44.92	0	4.72	39.58	0	4.72	50.85	0	6.35	45.69	0	6.35	41.51	0	
2.360	0	7.49	50.27	0	9.61	56.25	0	7.49	57.04	0	7.49	67.04	0	9.61	52	0	9.61	57.89	0	
2.000	0	15.05	79.51	0	17.14	81.79	0	15.05	78.56	0	15.05	80.14	0	17.14	84.73	0	17.14	85.25	0	
1.700	0	19.16	97.15	0	22.92	84.7	0	19.16	86.74	0	19.16	91.69	0	22.92	83.35	0	22.92	100.27	0	
1.400	0	23.66	94.38	0	26.59	82.87	0	23.66	84.72	0	23.66	74.67	0	26.59	79.67	0	26.59	106.32	0	
1.180	0	9.29	26.07	0	8.64	20.92	0	9.29	20.62	0	9.29	17.27	0	8.64	18.84	0	8.64	30.69	0	
1.000	0	3.02	3.72	0	2.79	2.75	0	3.02	3.17	0	3.02	1.98	0	2.79	2.23	0	2.79	5.13	0	
0.850	0	2.62	0.85	0	1.24	0.62	0	2.62	0.69	0	2.62	0.34	0	1.24	0.43	0	1.24	1.05	0	
0.710	0	0	0	0	0	0	0	0	0	0	0	0	0	0	0	0	0	0	0	
0.600	0	0	0	0	0	0	0	0	0	0	0	0	0	0	0	0	0	0	0	
0.500	0	0	0	0	0	0	0	0	0	0	0	0	0	0	0	0	0	0	0	
0.355	0	0	0	0	0	0	0	0	0	0	0	0	0	0	0	0	0	0	0	
0.250	0	0	0	0	0	0	0	0	0	0	0	0	0	0	0	0	0	0	0	
0.212	0	0	0	0	0	0	0	0	0	0	0	0	0	0	0	0	0	0	0	
0.150	91.27	73.35	9.79	108.4	65.28	7.96	119.69	73.35	13.03	91.27	73.35	5.69	108.4	65.28	9.83	119.69	65.28	5.11	91.27	
0.106	124.9	27.16	11.35	42.77	27.53	7.52	31.45	27.16	19.12	124.9	27.16	21.21	42.77	27.53	20.71	31.45	27.53	8.5	124.9	
0.090	117.68	44.52	22	92.06	57.01	26.41	46.08	44.52	19.98	117.68	44.52	14.54	92.06	57.01	20.57	46.08	57.01	22.31	117.68	
0.063	116.29	162.98	28.47	130.91	128.53	32.95	139.550	162.98	32.01	116.29	162.98	31.97	130.91	128.53	35.87	139.550	128.53	24.12	116.29	
0.053	28.81	81.64	12.78	45.42	83.01	19.79	72.2	81.64	12.02	28.81	81.64	17.6	45.42	83.01	18.17	72.2	83.01	7.93	28.81	
0.045	1.71	7.36	1.09	2.81	25.24	2.81	13.62	7.36	8.89	1.71	7.36	1.34	2.81	25.24	7.85	13.62	25.24	0.21	1.71	
0.038	3.15	4.7	6.17	2.59	5.93	2.07	9.98	4.7	1.71	3.15	4.7	3.14	2.59	5.93	3.3	9.98	5.93	0.52	3.15	
0.025	4.01	4.81	3.56	3.09	3.01	3.49	3.77	4.81	3.19	4.01	4.81	2.18	3.09	3.01	3.6	3.77	3.01	2.15	4.01	
Sum	487.82	491.67	495.00	428.05	491.12	494.36	436.34	491.67	494.52	487.82	491.67	498.53	428.05	491.12	498.75	436.34	491.12	508.12	487.82	

Sieve Size	FeSi	20.8			21.8			22.8			23.7			24.5			25.1																					
		%Retained	%Cum pass	%Retained	%Cum pass	%Retained	%Cum pass	%Retained	%Cum pass	%Retained	%Cum pass	%Retained	%Cum pass	%Retained	%Cum pass	%Retained	%Cum pass	%Retained	%Cum pass																			
4.00	0.0	100.0	0.0	100.0	1.7	98.3	0.0	100.0	0.1	99.9	3.3	96.7	0.0	100.0	0.0	100.0	3.4	96.6	0.0	100.0	0.1	99.9	2.4	97.6	0.0	100.0	0.1	99.9	1.8	98.2	0.0	100.0						
2.80	0.0	100.0	1.0	99.0	8.0	90.3	0.0	100.0	1.3	98.6	9.1	87.6	0.0	100.0	1.0	99.0	10.2	86.4	0.0	100.0	1.3	98.6	9.2	88.5	0.0	100.0	1.3	98.6	8.2	90.0	0.0	100.0						
2.360	0.0	100.0	1.5	97.5	10.2	80.2	0.0	100.0	2.0	96.7	11.4	76.2	0.0	100.0	1.5	97.5	11.5	77.7	0.0	100.0	1.5	97.5	13.4	73.0	0.0	100.0	2.0	96.7	11.4	76.6	0.0	100.0						
2.000	0.0	100.0	3.1	94.4	16.1	64.1	0.0	100.0	3.5	93.2	16.5	59.6	0.0	100.0	3.1	94.4	16.1	56.9	0.0	100.0	3.5	93.2	17.0	61.0	0.0	100.0	3.5	93.2	16.8	61.9	0.0	100.0						
1.700	0.0	100.0	3.9	90.5	19.6	44.5	0.0	100.0	4.7	88.5	17.1	42.4	0.0	100.0	3.9	90.5	18.4	38.5	0.0	100.0	4.7	88.5	16.7	44.3	0.0	100.0	4.7	88.5	19.7	42.1	0.0	100.0						
1.400	0.0	100.0	4.8	85.7	19.1	25.4	0.0	100.0	5.4	83.1	16.8	25.7	0.0	100.0	4.8	85.7	17.1	27.2	0.0	100.0	5.4	83.1	16.0	28.4	0.0	100.0	5.4	83.1	20.9	21.2	0.0	100.0						
1.180	0.0	100.0	1.9	83.8	5.3	20.2	0.0	100.0	1.8	81.4	4.2	21.5	0.0	100.0	1.9	83.8	4.2	23.0	0.0	100.0	1.8	81.4	3.8	24.6	0.0	100.0	1.8	81.4	6.0	15.2	0.0	100.0						
1.000	0.0	100.0	0.6	83.2	0.8	19.4	0.0	100.0	0.6	80.8	0.6	21.0	0.0	100.0	0.6	83.2	0.6	22.4	0.0	100.0	0.6	83.2	0.4	19.7	0.0	100.0	0.6	80.8	1.0	14.2	0.0	100.0						
0.850	0.0	100.0	0.5	82.7	0.2	19.2	0.0	100.0	0.3	80.5	0.1	20.8	0.0	100.0	0.5	82.7	0.1	22.2	0.0	100.0	0.5	82.7	0.1	24.0	0.0	100.0	0.5	80.5	0.2	13.9	0.0	100.0						
0.710	0.0	100.0	0.0	82.7	0.0	19.2	0.0	100.0	0.0	80.5	0.0	20.8	0.0	100.0	0.0	82.7	0.0	22.2	0.0	100.0	0.0	82.7	0.0	19.6	0.0	100.0	0.0	80.5	0.0	13.9	0.0	100.0						
0.600	0.0	100.0	0.0	82.7	0.0	19.2	0.0	100.0	0.0	80.5	0.0	20.8	0.0	100.0	0.0	82.7	0.0	22.2	0.0	100.0	0.0	82.7	0.0	19.6	0.0	100.0	0.0	80.5	0.0	13.9	0.0	100.0						
0.500	0.0	100.0	0.0	82.7	0.0	19.2	0.0	100.0	0.0	80.5	0.0	20.8	0.0	100.0	0.0	82.7	0.0	22.2	0.0	100.0	0.0	82.7	0.0	19.6	0.0	100.0	0.0	80.5	0.0	13.9	0.0	100.0						
0.355	0.0	100.0	0.0	82.7	0.0	19.2	0.0	100.0	0.0	80.5	0.0	20.8	0.0	100.0	0.0	82.7	0.0	22.2	0.0	100.0	0.0	82.7	0.0	19.6	0.0	100.0	0.0	80.5	0.0	13.9	0.0	100.0						
0.250	0.0	100.0	0.0	82.7	0.0	19.2	0.0	100.0	0.0	80.5	0.0	20.8	0.0	100.0	0.0	82.7	0.0	22.2	0.0	100.0	0.0	82.7	0.0	19.6	0.0	100.0	0.0	80.5	0.0	13.9	0.0	100.0						
0.212	0.0	100.0	0.0	82.7	0.0	19.2	0.0	100.0	0.0	80.5	0.0	20.8	0.0	100.0	0.0	82.7	0.0	22.2	0.0	100.0	0.0	82.7	0.0	19.6	0.0	100.0	0.0	80.5	0.0	13.9	0.0	100.0						
0.150	18.7	81.3	14.9	67.8	2.0	17.3	25.3	74.7	13.3	67.2	1.6	19.2	27.4	72.6	14.9	67.8	2.6	19.6	18.7	81.3	14.9	67.8	1.1	18.5	25.3	74.7	13.3	67.2	2.0	17.3	27.4	72.6	13.3	67.2	1.0	12.9	18.7	81.3
0.106	25.6	55.7	5.5	62.2	2.3	15.0	10.0	64.7	5.6	61.6	1.5	17.7	7.2	65.4	5.5	62.2	3.9	15.7	25.6	55.7	5.5	62.2	4.3	14.2	10.0	64.7	5.6	61.6	4.2	12.9	7.2	65.4	5.6	61.6	1.7	11.3	25.6	55.7
0.090	24.1	31.6	9.1	53.2	4.4	10.5	21.5	43.2	11.6	50.0	5.3	12.4	10.6	54.8	9.1	53.2	4.0	11.7	24.1	31.6	9.1	53.2	2.9	11.3	21.5	43.2	11.6	50.0	4.1	13.8	10.6	54.8	11.6	50.0	4.4	6.9	24.1	31.6
0.063	23.8	7.7	33.1	20.0	5.8	4.8	30.6	12.6	26.2	23.9	6.7	5.7	32.0	22.8	33.1	20.0	6.5	5.2	23.8	7.7	33.1	20.0	6.4	4.9	30.6	12.6	26.2	23.9	7.2	6.6	32.0	22.8	26.2	23.9	4.7	2.1	23.8	7.7
0.053	5.9	1.8	16.6	3.4	2.8	2.2	10.6	2.0	16.9	7.0	4.0	1.7	16.5	6.2	16.6	3.4	2.4	2.8	5.9	1.8	16.6	3.4	3.5	1.3	10.6	2.0	16.9	7.0	3.6	3.0	16.5	6.3	16.9	7.0	1.8	0.6	5.9	1.8
0.045	0.4	1.5	1.5	1.9	0.2	2.0	0.7	1.3	5.1	1.8	0.6	1.1	3.1	3.2	1.5	1.9	1.8	1.0	0.4	1.5	1.5	1.9	0.3	1.1	0.7	1.3	5.1	1.8	1.6	1.4	1.4	3.1	3.2	5.1	1.8	0.0	0.4	1.5
0.038	0.6	0.8	1.0	1.0	1.2	0.7	0.6	0.7	1.2	0.6	0.4	0.7	2.3	0.9	1.0	1.0	0.3	0.6	0.6	0.8	1.0	1.0	0.6	0.4	0.6	0.7	1.2	0.6	0.7	0.7	2.3	0.9	1.2	0.6	0.1	0.4	0.6	0.8
0.025	0.8	0.0	1.0	0.0	0.7	0.0	0.7	0.0	0.6	0.0	0.7	0.0	0.9	0.0	1.0	0.0	0.6	0.0	0.8	0.0	1.0	0.0	0.4	0.0	0.7	0.0	0.6	0.0	0.7	0.0	0.9	0.0	0.6	0.0	0.4	0.0	0.8	0.0

SIEVE ANALYSIS FOR 1x13 mm at 2.7 kg/l																			
Sieve Size	FeSi	20.8			21.8			22.8			23.7			24.5			25.1		
		Feed	Overflow	Underflow	Feed	Overflow	Underflow	Feed	Overflow	Underflow	Feed	Overflow	Underflow	Feed	Overflow	Underflow	Feed	Overflow	Underflow
4.00	0	0.48	9.6	0	0.67	10.24	0	0.48	34.08	0	0.48	11.08	0	0.67	32.88	0	0.67	26.65	0
2.80	0	6.33	31.89	0	5.73	37.5	0	6.33	130.21	0	6.33	36.66	0	5.73	94.46	0	5.73	74.54	0
2.360	0	8.49	47.27	0	10.18	57.62	0	8.49	168	0.00	8.49	55.96	0	10.18	114.19	0.00	10.18	246.11	0
2.000	0	12.85	72.43	0	14.97	86.14	0	12.85	236.09	0	12.85	85.09	0	14.97	208.51	0	14.97	305.99	0
1.700	0	18.42	83.85	0	21.95	106.52	0	18.42	311.48	0	18.42	98.91	0	21.95	360.44	0	21.95	415.71	0
1.400	0	16.9	92.82	0	24.4	115.71	0	16.9	303	0	16.9	108.88	0	24.4	337.84	0	24.4	294.23	0
1.180	0	7.11	31.04	0	9.33	35.55	0	7.11	93.68	0	7.11	33.86	0	9.33	97.27	0	9.33	331	0
1.000	0	3.14	4.98	0	3	6.05	0	3.14	15.56	0	3.14	5.66	0	3	12.79	0	3	91.12	0
0.850	0	2.11	1.08	0	1.32	1.62	0	2.11	4.23	0	2.11	1.41	0	1.32	3.23	0	1.32	2.8	0
0.710	0	0	0	0	0	0	0	0	0	0	0	0	0	0	0	0	0	2.24	0
0.600	0	0	0	0	0	0	0	0	0	0	0	0	0	0	0	0	0	0	0
0.500	0	0	0	0	0	0	0	0	0	0	0	0	0	0	0	0	0	0	0
0.355	0	0	0	0	0	0	0	0	0	0	0	0	0	0	0	0	0	0	0
0.250	0	0	0	0	0	0	0	0	0	0	0	0	0	0	0	0	0	0	0
0.212	0	0	0	0	0	0	0	0	0	0	0	0	0	0	0	0	0	0	0
0.150	91.27	60.44	15.22	71.5	53	4.63	119.69	60.44	30.35	108.74	60.44	5	119.69	53	23.53	108.74	53	71.35	119.69
0.106	124.9	64.07	13.52	18.95	60.33	5.1	31.45	64.07	71.97	121.06	64.07	5.65	31.45	60.33	14.13	121.06	60.33	30.46	31.45
0.090	117.68	76.07	48.74	37.59	101.44	8.74	46.08	76.07	22.4	103.55	76.07	10.24	46.08	101.44	32.06	103.55	101.44	5.5	46.08
0.063	116.29	142.27	25.78	209.87	135.73	14	139.550	142.27	48.98	112.52	142.27	17.83	139.550	135.73	60.33	112.52	135.73	2.55	139.550
0.053	28.81	60.07	7.35	94.14	53.5	6.91	72.2	60.07	8.56	23.21	60.07	14.32	72.2	53.5	67.51	23.21	53.5	3.22	72.2
0.045	1.71	4.46	0.48	25.3	4.96	0.84	13.62	4.46	1.32	1.54	4.46	0.16	13.62	4.96	11.57	1.54	4.96	0.25	13.62
0.038	3.15	3.08	2.09	6.16	3.29	1.47	9.98	3.08	3.94	6.15	3.08	3.26	9.98	3.29	3.22	6.15	3.29	0.39	9.98
0.025	4.01	2.38	2.24	7.82	4.17	2.53	3.77	2.38	2.02	2.96	2.38	2.56	3.77	4.17	2.36	2.96	4.17	2.51	3.77
Sum	487.82	488.67	490.38	471.33	507.97	501.17	436.34	488.67	1485.87	479.73	488.67	496.53	436.34	507.97	1476.32	479.73	507.97	1906.62	436.34

Sieve Size	FeSi	20.8						21.8						22.8						23.7						24.5						25.1					
		Feed	Overflow	Underflow	Feed	Overflow	Underflow	Feed	Overflow	Underflow	Feed	Overflow	Underflow	Feed	Overflow	Underflow	Feed	Overflow	Underflow	Feed	Overflow	Underflow	Feed	Overflow	Underflow	Feed	Overflow	Underflow	Feed	Overflow	Underflow						
4.00	0.0	100.0	0.1	99.9	2.0	98.0	0.0	100.0	0.1	99.9	2.0	97.7	0.0	100.0	0.1	99.9	2.2	97.8	0.0	100.0	0.1	99.9	2.2	97.8	0.0	100.0	0.1	99.9	1.4	98.6	0.0	100.0					
2.80	0.0	100.0	1.3	98.6	6.5	91.5	0.0	100.0	1.1	98.7	7.5	90.5	0.0	100.0	1.3	98.6	8.8	88.9	0.0	100.0	1.3	98.6	7.4	90.4	0.0	100.0	1.1	98.7	3.9	94.7	0.0	100.0					
2.360	0.0	100.0	1.7	96.9	9.6	81.9	0.0	100.0	2.0	96.7	11.5	79.0	0.0	100.0	1.7	96.9	11.3	77.6	0.0	100.0	1.7	96.9	11.3	79.1	0.0	100.0	2.0	96.7	12.9	81.8	0.0	100.0					
2.000	0.0	100.0	2.6	94.2	14.8	67.1	0.0	100.0	2.9	93.8	17.2	61.8	0.0	100.0	2.6	94.2	15.9	61.7	0.0	100.0	2.6	94.2	17.1	62.0	0.0	100.0	2.9	93.8	14.1	69.5	0.0	100.0					
1.700	0.0	100.0	3.8	90.5	17.1	50.0	0.0	100.0	4.3	89.5	21.3	40.5	0.0	100.0	3.8	90.5	21.0	40.8	0.0	100.0	3.8	90.5	19.9	42.1	0.0	100.0	4.3	89.5	24.4	45.1	0.0	100.0					
1.400	0.0	100.0	3.5	87.0	18.9	31.1	0.0	100.0	4.8	84.7	23.1	17.4	0.0	100.0	3.5	87.0	20.4	20.4	0.0	100.0	3.5	87.0	21.9	20.1	0.0	100.0	4.8	84.7	15.4	28.5	0.0	100.0					
1.180	0.0	100.0	1.5	85.6	6.3	24.8	0.0	100.0	1.8	82.8	7.1	10.4	0.0	100.0	1.5	85.6	6.3	14.1	0.0	100.0	1.5	85.6	6.8	13.3	0.0	100.0	1.8	82.8	6.6	15.6	0.0	100.0					
1.000	0.0	100.0	0.6	84.9	1.0	23.8	0.0	100.0	0.6	82.2	1.2	9.1	0.0	100.0	0.6	84.9	1.0	13.0	0.0	100.0	0.6	84.9	1.1	12.2	0.0	100.0	0.6	82.2	0.9	14.8	0.0	100.0					
0.850	0.0	100.0	0.4	84.5	0.2	23.5	0.0	100.0	0.3	82.0	0.3	8.8	0.0	100.0	0.4	84.5	0.3	12.8	0.0	100.0	0.4	84.5	0.3	11.9	0.0	100.0	0.3	82.0	0.2	14.5	0.0	100.0					
0.710	0.0	100.0	0.0	84.5	0.0	23.5	0.0	100.0	0.0	82.0	0.0	8.8	0.0	100.0	0.0	84.5	0.0	12.8	0.0	100.0	0.0	84.5	0.0	11.9	0.0	100.0	0.0	82.0	0.0	14.5	0.0	100.0					
0.600	0.0	100.0	0.0	84.5	0.0	23.5	0.0	100.0	0.0	82.0	0.0	8.8	0.0	100.0	0.0	84.5	0.0	12.8	0.0	100.0	0.0	84.5	0.0	11.9	0.0	100.0	0.0	82.0	0.0	14.5	0.0	100.0					
0.500	0.0	100.0	0.0	84.5	0.0	23.5	0.0	100.0	0.0	82.0	0.0	8.8	0.0	100.0	0.0	84.5	0.0	12.8	0.0	100.0	0.0	84.5	0.0	11.9	0.0	100.0	0.0	82.0	0.0	14.5	0.0	100.0					
0.355	0.0	100.0	0.0	84.5	0.0	23.5	0.0	100.0	0.0	82.0	0.0	8.8	0.0	100.0	0.0	84.5	0.0	12.8	0.0	100.0	0.0	84.5	0.0	11.9	0.0	100.0	0.0	82.0	0.0	14.5	0.0	100.0					
0.250	0.0	100.0	0.0	84.5	0.0	23.5	0.0	100.0	0.0	82.0	0.0	8.8	0.0	100.0	0.0	84.5	0.0	12.8	0.0	100.0	0.0	84.5	0.0	11.9	0.0	100.0	0.0	82.0	0.0	14.5	0.0	100.0					
0.212	0.0	100.0	0.0	84.5	0.0	23.5	0.0	100.0	0.0	82.0	0.0	8.8	0.0	100.0	0.0	84.5	0.0	12.8	0.0	100.0	0.0	84.5	0.0	11.9	0.0	100.0	0.0	82.0	0.0	14.5	0.0	100.0					
0.150	18.7	81.3	12.4	72.1	3.1	20.4	15.2	84.8	10.4	71.5	0.9	7.9	27.4	72.6	12.4	72.1	2.0	10.7	22.7	77.3	12.4	72.1	1.0	10.9	27.4	72.6	10.4	71.5	1.6	12.9	22.7	77.3					
0.106	25.6	55.7	13.1	59.0	2.8	17.7	4.0	80.8	11.9	59.7	1.0	6.9	7.2	65.4	13.1	59.0	4.8	5.9	25.2	52.1	13.1	59.0	1.1	9.7	7.2	65.4	11.9	59.7	1.0	12.0	25.2	52.1					
0.090	24.1	31.6	15.6	43.4	9.9	7.7	8.0	72.8	20.0	39.7	1.7	5.1	10.6	54.8	15.6	43.4	1.5	4.4	21.6	30.5	15.6	43.4	2.1	7.7	10.6	54.8	20.0	39.7	2.2	9.8	21.6	30.5					
0.063	23.8	7.7	29.1	14.3	5.3	2.5	44.5	24.3	26.7	13.0	2.8	2.3	32.0	22.8	29.1	14.3	3.3	1.1	25.5	7.1	29.1	14.3	3.6	4.1	32.0	22.8	26.7	13.0	4.1	5.7	21.5	7.1					
0.053	5.9	1.8	12.3	2.0	1.5	1.0	20.0	8.3	10.5	2.4	1.4	1.0	16.5	6.3	12.3	2.0	0.6	0.5	4.8	2.2	12.3	2.0	2.9	1.2	16.5	6.3	10.5	2.4	4.6	1.2	4.8	2.2					
0.045	0.4	1.5	0.9	1.1	0.1	0.9	5.4	3.0	1.0	1.5	0.2	0.8	3.1	3.2	0.9	1.1	0.1	0.4	0.3	1.9	0.9	1.1	0.0	1.2	3.1	3.2	1.0	1.5	0.8	0.4	0.3						
0.038	0.6	0.8	0.6	0.5	0.4	0.5	1.3	1.7	0.6	0.8																											

SIEVE ANALYSIS FOR 1x12 mm at 1.9 kg/l															
Sieve Size	21.8			22.8			23.7			24.5			25.1		
	Feed	Overflow	Underflow	Feed	Overflow	Underflow	Feed	Overflow	Underflow	Feed	Overflow	Underflow	Feed	Overflow	Underflow
4.00	8.57	18.56	0	8.57	14.58	0	8.57	13.33	0	8.57	11.16	0	8.57	13.21	0
2.80	26.76	58.7	0	26.76	49.06	0	26.76	47.33	0	26.76	45.47	0	26.76	41.26	0
2.360	31.87	69.07	0	31.87	65.87	0	31.87	61.31	0	31.87	65.22	0	31.87	64.25	0
2.000	41.87	95.31	0	41.87	89.97	0	41.87	84.22	0	41.87	92.23	0	41.87	89.44	0
1.700	39.27	92.2	0	39.27	91.02	0	39.27	101.89	0	39.27	106.16	0	39.27	100.96	0
1.400	27.75	77.72	0	27.75	77.2	0	27.75	88.44	0	27.75	85.75	0	27.75	88.84	0
1.180	3.22	12.12	0	3.22	11	0	3.22	10.45	0	3.22	8.03	0	3.22	9.75	0
1.000	0.22	0.75	0	0.22	0.59	0	0.22	0.57	0	0.22	0.35	0	0.22	0.39	0
0.850	0	0	0	0	0	0	0	0	0	0	0	0	0	0	0
0.710	0	0	0	0	0	0	0	0	0	0	0	0	0	0	0
0.600	0	0	0	0	0	0	0	0	0	0	0	0	0	0	0
0.500	0	0	0	0	0	0	0	0	0	0	0	0	0	0	0
0.355	0	0	0	0	0	0	0	0	0	0	0	0	0	0	0
0.250	0	0	0	0	0	0	0	0	0	0	0	0	0	0	0
0.212	0	0	0	0	0	0	0	0	0	0	0	0	0	0	0
0.150	154.68	20.01	68.17	154.68	23.01	68.17	154.68	38.95	68.17	154.68	27.85	68.17	154.68	25.32	68.17
0.106	120.88	32.34	126.55	120.88	29.15	126.55	120.88	33.01	126.55	120.88	33.55	126.55	120.88	37.61	126.55
0.090	25.79	4.54	27.82	25.79	22.53	27.82	25.79	5.03	27.82	25.79	11.27	27.82	25.79	12.39	27.82
0.063	6.63	7.25	14.300	6.63	9.59	14.300	6.63	9.02	14.300	6.63	8.88	14.300	6.63	6.04	14.300
0.053	7.31	7.96	10.95	7.31	12.45	10.95	7.31	4.27	10.95	7.31	2.1	10.95	7.31	7.22	10.95
0.045	0.44	0.36	0.82	0.44	0.49	0.82	0.44	0.25	0.82	0.44	0.27	0.82	0.44	0.4	0.82
0.038	0.25	0.4	0.39	0.25	0.75	0.39	0.25	0.09	0.39	0.25	0.28	0.39	0.25	0.32	0.39
0.025	0.11	0.2	0.4	0.11	0.77	0.4	0.11	0.06	0.4	0.11	0.15	0.4	0.11	0.45	0.4
Sum	495.62	497.49	249.40	495.62	498.03	249.40	495.62	498.22	249.40	495.62	498.72	249.40	495.62	497.85	249.40

Sieve Size	21.8						22.8						23.7						24.5						25.1					
	Feed		Overflow		Underflow		Feed		Overflow		Underflow		Feed		Overflow		Underflow		Feed		Overflow		Underflow		Feed		Overflow		Underflow	
Sieve Size	%Retained	%Cum pass	%Retained	%Cum pass	%Retained	%Cum pass	%Retained	%Cum pass	%Retained	%Cum pass	%Retained	%Cum pass	%Retained	%Cum pass	%Retained	%Cum pass	%Retained	%Cum pass	%Retained	%Cum pass	%Retained	%Cum pass	%Retained	%Cum pass	%Retained	%Cum pass	%Retained	%Cum pass	%Retained	%Cum pass
4.00	1.7	98.3	3.7	96.3	0.0	100.0	1.7	98.3	2.9	97.1	0.0	100.0	1.7	98.3	2.7	97.3	0.0	100.0	1.7	98.3	2.2	97.8	0.0	100.0	1.7	98.3	2.7	97.3	0.0	100.0
2.80	5.4	92.9	11.8	84.5	0.0	100.0	5.4	92.9	9.9	87.2	0.0	100.0	5.4	92.9	9.5	87.8	0.0	100.0	5.4	92.9	9.1	88.6	0.0	100.0	5.4	92.9	8.3	89.1	0.0	100.0
2.360	6.4	86.4	13.9	70.6	0.0	100.0	6.4	86.4	13.2	74.0	0.0	100.0	6.4	86.4	12.3	75.5	0.0	100.0	6.4	86.4	13.1	75.6	0.0	100.0	6.4	86.4	12.9	76.2	0.0	100.0
2.000	8.4	78.0	19.2	51.4	0.0	100.0	8.4	78.0	18.1	55.9	0.0	100.0	8.4	78.0	16.9	58.6	0.0	100.0	8.4	78.0	18.5	57.1	0.0	100.0	8.4	78.0	18.0	58.2	0.0	100.0
1.700	7.9	70.1	18.5	32.9	0.0	100.0	7.9	70.1	18.3	37.7	0.0	100.0	7.9	70.1	20.5	38.2	0.0	100.0	7.9	70.1	21.3	35.8	0.0	100.0	7.9	70.1	20.3	37.9	0.0	100.0
1.400	5.6	64.5	15.6	17.3	0.0	100.0	5.6	64.5	15.5	22.2	0.0	100.0	5.6	64.5	17.8	20.4	0.0	100.0	5.6	64.5	17.2	18.6	0.0	100.0	5.6	64.5	17.8	20.1	0.0	100.0
1.180	0.6	63.8	2.4	14.8	0.0	100.0	0.6	63.8	2.2	19.9	0.0	100.0	0.6	63.8	2.1	18.3	0.0	100.0	0.6	63.8	1.6	17.0	0.0	100.0	0.6	63.8	2.0	18.1	0.0	100.0
1.000	0.0	63.8	0.2	14.7	0.0	100.0	0.0	63.8	0.1	19.8	0.0	100.0	0.0	63.8	0.1	18.2	0.0	100.0	0.0	63.8	0.1	16.9	0.0	100.0	0.0	63.8	0.1	18.0	0.0	100.0
0.850	0.0	63.8	0.0	14.7	0.0	100.0	0.0	63.8	0.0	19.8	0.0	100.0	0.0	63.8	0.0	18.2	0.0	100.0	0.0	63.8	0.0	16.9	0.0	100.0	0.0	63.8	0.0	18.0	0.0	100.0
0.710	0.0	63.8	0.0	14.7	0.0	100.0	0.0	63.8	0.0	19.8	0.0	100.0	0.0	63.8	0.0	18.2	0.0	100.0	0.0	63.8	0.0	16.9	0.0	100.0	0.0	63.8	0.0	18.0	0.0	100.0
0.600	0.0	63.8	0.0	14.7	0.0	100.0	0.0	63.8	0.0	19.8	0.0	100.0	0.0	63.8	0.0	18.2	0.0	100.0	0.0	63.8	0.0	16.9	0.0	100.0	0.0	63.8	0.0	18.0	0.0	100.0
0.500	0.0	63.8	0.0	14.7	0.0	100.0	0.0	63.8	0.0	19.8	0.0	100.0	0.0	63.8	0.0	18.2	0.0	100.0	0.0	63.8	0.0	16.9	0.0	100.0	0.0	63.8	0.0	18.0	0.0	100.0
0.355	0.0	63.8	0.0	14.7	0.0	100.0	0.0	63.8	0.0	19.8	0.0	100.0	0.0	63.8	0.0	18.2	0.0	100.0	0.0	63.8	0.0	16.9	0.0	100.0	0.0	63.8	0.0	18.0	0.0	100.0
0.250	0.0	63.8	0.0	14.7	0.0	100.0	0.0	63.8	0.0	19.8	0.0	100.0	0.0	63.8	0.0	18.2	0.0	100.0	0.0	63.8	0.0	16.9	0.0	100.0	0.0	63.8	0.0	18.0	0.0	100.0
0.212	0.0	63.8	0.0	14.7	0.0	100.0	0.0	63.8	0.0	19.8	0.0	100.0	0.0	63.8	0.0	18.2	0.0	100.0	0.0	63.8	0.0	16.9	0.0	100.0	0.0	63.8	0.0	18.0	0.0	100.0
0.150	31.2	32.6	4.0	10.7	27.3	72.7	31.2	32.6	4.6	15.2	27.3	72.7	31.2	32.6	7.8	10.4	27.3	72.7	31.2	32.6	5.6	11.3	27.3	72.7	31.2	32.6	5.1	12.9	27.3	72.7
0.106	24.4	8.2	6.5	4.2	50.7	21.9	24.4	8.2	5.9	9.4	50.7	21.9	24.4	8.2	6.6	3.8	50.7	21.9	24.4	8.2	6.7	4.6	50.7	21.9	24.4	8.2	7.6	5.4	50.7	21.9
0.090	5.2	3.0	0.9	3.3	11.2	10.8	5.2	3.0	4.5	4.8	11.2	10.8	5.2	3.0	1.0	2.7	11.2	10.8	5.2	3.0	2.3	11.2	10.8	5.2	3.0	2.5	2.9	11.2	10.8	
0.063	1.3	1.6	1.5	1.8	5.7	5.0	1.3	1.6	1.9	2.9	5.7	5.0	1.3	1.6	1.8	0.9	5.7	5.0	1.3	1.6	1.8	0.6	5.7	5.0	1.3	1.6	1.2	1.7	5.7	5.0
0.053	1.5	0.2	1.6	0.2	4.4	0.6	1.5	0.2	2.5	0.4	4.4	0.6	1.5	0.2	0.9	0.1	4.4	0.6	1.5	0.2	0.4	0.1	4.4	0.6	1.5	0.2	1.5	0.2	4.4	0.6
0.045	0.1	0.1	0.1	0.1	0.3	0.3	0.1	0.1	0.1	0.3	0.3	0.1	0.1	0.1	0.1	0.0	0.3	0.3	0.1	0.1	0.1	0.1	0.3	0.3	0.1	0.1	0.1	0.2	0.3	0.3
0.038	0.1	0.0	0.1	0.0	0.2	0.2	0.1	0.0	0.2	0.2	0.2	0.2	0.1	0.0	0.0	0.0	0.2	0.2	0.1	0.0	0.1	0.0	0.2	0.2	0.1	0.0	0.1	0.1	0.2	0.2
0.025	0.0	0.0	0.0	0.0	0.2	0.0	0.0	0.0	0.2	0.0	0.2	0.0	0.0	0.0	0.0	0.0	0.2	0.0	0.0	0.0	0.2	0.0	0.2	0.0	0.0	0.1	0.0	0.2	0.0	0.2

SIEVE ANALYSIS FOR 1x12 mm at 2.0 kg/l																
Sieve Size	21.8			22.8			23.7			24.5			25.1			
	Feed	Overflow	Underflow	Feed	Overflow	Underflow	Feed	Overflow	Underflow	Feed	Overflow	Underflow	Feed	Overflow	Underflow	
4.00	6.29	10.57	0	6.29	10.9	0	6.29	13.87	0	6.29	9.4	0	6.29	12.02	0	
2.80	23.5	39.61	0	23.5	44.6	0	23.5	42.6	0	23.5	38.26	0	23.5	37.63	0	
2.360	31.58	54.26	0	31.58	55.98	0	31.58	54.54	0	31.58	51.44	0	31.58	55.36	0	
2.000	35.27	81.45	0	35.27	84.12	0	35.27	79.15	0	35.27	80.74	0	35.27	75.29	0	
1.700	23.24	93.2	0	23.24	92.39	0	23.24	89.09	0	23.24	95.96	0	23.24	88.06	0	
1.400	46.85	101.03	0	46.85	93.69	0	46.85	85.03	0	46.85	85.18	0	46.85	77.63	0	
1.180	12.83	27.05	0	12.83	22.26	0	12.83	16.93	0	12.83	15.65	0	12.83	13.36	0	
1.000	0.93	2.07	0	0.93	1.72	0	0.93	0.98	0	0.93	1.08	0	0.93	0.87	0	
0.850	0	0	0	0	0	0	0	0	0	0	0	0	0	0	0	
0.710	0	0	0	0	0	0	0	0	0	0	0	0	0	0	0	
0.600	0	0	0	0	0	0	0	0	0	0	0	0	0	0	0	
0.500	0	0	0	0	0	0	0	0	0	0	0	0	0	0	0	
0.355	0	0	0	0	0	0	0	0	0	0	0	0	0	0	0	
0.250	0	0	0	0	0	0	0	0	0	0	0	0	0	0	0	
0.212	0	0	0	0	0	0	0	0	0	0	0	0	0	0	0	
0.150	192.9	30.05	114.71	192.9	27.85	114.71	192.9	45.29	114.71	192.9	48.86	114.71	192.9	66.39	114.71	
0.106	86.15	33.69	75.09	86.15	32.5	75.09	86.15	43.68	75.09	86.15	47.33	75.09	86.15	53.86	75.09	
0.090	20.81	5.65	41.23	20.81	8.98	41.23	20.81	10.8	41.23	20.81	10.42	41.23	20.81	6.89	41.23	
0.063	13.56	16.64	15.13	13.56	7.64	15.13	13.56	14.47	15.13	13.56	8.55	15.13	13.56	8.42	15.13	
0.053	1.93	2.04	2.21	1.93	13.84	2.21	1.93	0.97	2.21	1.93	2.72	2.21	1.93	0.97	2.21	
0.045	0.42	0.34	0.41	0.42	0.6	0.41	0.42	0.39	0.41	0.42	0.19	0.41	0.42	0.17	0.41	
0.038	0.21	0.5	0.51	0.21	0.63	0.51	0.21	0.28	0.51	0.21	0.27	0.51	0.21	0.15	0.51	
0.025	0.07	0.33	0.17	0.07	0.72	0.17	0.07	0.14	0.17	0.07	0.21	0.17	0.07	0.06	0.17	
Sum	496.54	498.48	249.46	496.54	498.42	249.46	496.54	498.21	249.46	496.54	496.26	249.46	496.54	497.13	249.46	

Sieve Size	21.8						22.8						23.7						24.5						25.1					
	Feed		Overflow		Underflow		Feed		Overflow		Underflow		Feed		Overflow		Underflow		Feed		Overflow		Underflow		Feed		Overflow		Underflow	
	%Retained	%Cum pass	%Retained	%Cum pass	%Retained	%Cum pass	%Retained	%Cum pass	%Retained	%Cum pass	%Retained	%Cum pass	%Retained	%Cum pass	%Retained	%Cum pass	%Retained	%Cum pass	%Retained	%Cum pass	%Retained	%Cum pass	%Retained	%Cum pass	%Retained	%Cum pass	%Retained	%Cum pass	%Retained	%Cum pass
4.00	1.3	98.7	2.1	97.9	0.0	100.0	1.3	98.7	2.2	97.8	0.0	100.0	1.3	98.7	2.8	97.2	0.0	100.0	1.3	98.7	1.9	98.1	0.0	100.0	1.3	98.7	2.4	97.6	0.0	100.0
2.80	4.7	94.0	7.9	89.9	0.0	100.0	4.7	94.0	8.9	88.9	0.0	100.0	4.7	94.0	8.6	88.7	0.0	100.0	4.7	94.0	7.7	90.4	0.0	100.0	4.7	94.0	7.6	90.0	0.0	100.0
2.360	6.4	87.6	10.9	79.0	0.0	100.0	6.4	87.6	11.2	77.6	0.0	100.0	6.4	87.6	10.9	77.7	0.0	100.0	6.4	87.6	10.4	80.0	0.0	100.0	6.4	87.6	11.1	78.9	0.0	100.0
2.000	7.1	80.5	16.3	62.7	0.0	100.0	7.1	80.5	16.9	60.8	0.0	100.0	7.1	80.5	15.9	61.8	0.0	100.0	7.1	80.5	16.3	63.8	0.0	100.0	7.1	80.5	15.1	63.7	0.0	100.0
1.700	4.7	75.9	18.7	44.0	0.0	100.0	4.7	75.9	18.5	42.2	0.0	100.0	4.7	75.9	17.9	43.9	0.0	100.0	4.7	75.9	19.3	44.4	0.0	100.0	4.7	75.9	17.7	46.0	0.0	100.0
1.400	9.4	66.4	20.3	23.7	0.0	100.0	9.4	66.4	18.8	23.4	0.0	100.0	9.4	66.4	17.1	26.9	0.0	100.0	9.4	66.4	17.2	27.3	0.0	100.0	9.4	66.4	15.6	30.4	0.0	100.0
1.180	2.6	63.8	5.4	18.3	0.0	100.0	2.6	63.8	4.5	19.0	0.0	100.0	2.6	63.8	3.4	23.5	0.0	100.0	2.6	63.8	3.2	24.1	0.0	100.0	2.6	63.8	2.7	27.7	0.0	100.0
1.000	0.2	63.7	0.4	17.9	0.0	100.0	0.2	63.7	0.3	18.6	0.0	100.0	0.2	63.7	0.2	23.3	0.0	100.0	0.2	63.7	0.2	23.9	0.0	100.0	0.2	63.7	0.2	27.5	0.0	100.0
0.850	0.0	63.7	0.0	17.9	0.0	100.0	0.0	63.7	0.0	18.6	0.0	100.0	0.0	63.7	0.0	23.3	0.0	100.0	0.0	63.7	0.0	23.9	0.0	100.0	0.0	63.7	0.0	27.5	0.0	100.0
0.710	0.0	63.7	0.0	17.9	0.0	100.0	0.0	63.7	0.0	18.6	0.0	100.0	0.0	63.7	0.0	23.3	0.0	100.0	0.0	63.7	0.0	23.9	0.0	100.0	0.0	63.7	0.0	27.5	0.0	100.0
0.600	0.0	63.7	0.0	17.9	0.0	100.0	0.0	63.7	0.0	18.6	0.0	100.0	0.0	63.7	0.0	23.3	0.0	100.0	0.0	63.7	0.0	23.9	0.0	100.0	0.0	63.7	0.0	27.5	0.0	100.0
0.500	0.0	63.7	0.0	17.9	0.0	100.0	0.0	63.7	0.0	18.6	0.0	100.0	0.0	63.7	0.0	23.3	0.0	100.0	0.0	63.7	0.0	23.9	0.0	100.0	0.0	63.7	0.0	27.5	0.0	100.0
0.355	0.0	63.7	0.0	17.9	0.0	100.0	0.0	63.7	0.0	18.6	0.0	100.0	0.0	63.7	0.0	23.3	0.0	100.0	0.0	63.7	0.0	23.9	0.0	100.0	0.0	63.7	0.0	27.5	0.0	100.0
0.250	0.0	63.7	0.0	17.9	0.0	100.0	0.0	63.7	0.0	18.6	0.0	100.0	0.0	63.7	0.0	23.3	0.0	100.0	0.0	63.7	0.0	23.9	0.0	100.0	0.0	63.7	0.0	27.5	0.0	100.0
0.212	0.0	63.7	0.0	17.9	0.0	100.0	0.0	63.7	0.0	18.6	0.0	100.0	0.0	63.7	0.0	23.3	0.0	100.0	0.0	63.7	0.0	23.9	0.0	100.0	0.0	63.7	0.0	27.5	0.0	100.0
0.150	38.8	24.8	6.0	11.9	46.0	54.0	38.8	24.8	5.6	13.0	46.0	54.0	38.8	24.8	9.1	14.2	46.0	54.0	38.8	24.8	9.8	14.0	46.0	54.0	38.8	24.8	13.4	14.2	46.0	54.0
0.106	17.4	7.5	6.8	5.1	30.1	23.9	17.4	7.5	6.5	6.5	30.1	23.9	17.4	7.5	8.8	5.4	30.1	23.9	17.4	7.5	9.5	4.5	30.1	23.9	17.4	7.5	10.8	3.4	30.1	23.9
0.090	4.2	3.3	1.1	4.0	16.5	7.4	4.2	3.3	1.8	4.7	16.5	7.4	4.2	3.3	2.2	3.3	16.5	7.4	4.2	3.3	2.1	2.4	16.5	7.4	4.2	3.3	1.4	2.0	16.5	7.4
0.063	2.7	0.5	3.3	0.6	6.1	1.3	2.7	0.5	1.5	3.2	6.1	1.3	2.7	0.5	2.9	0.4	6.1	1.3	2.7	0.5	1.7	0.7	6.1	1.3	2.7	0.5	1.7	0.3	6.1	1.3
0.053	0.4	0.1	0.4	0.2	0.9	0.4	0.1	2.8	0.4	0.9	0.4	0.4	0.1	0.2	0.2	0.9	0.4	0.4	0.1	0.5	0.1	0.9	0.4	0.4	0.1	0.2	0.1	0.9	0.4	
0.045	0.1	0.1	0.1	0.2	0.2	0.3	0.1	0.1	0.3	0.2	0.3	0.1	0.1	0.1	0.1	0.2	0.3	0.1	0.1	0.0	0.1	0.2	0.3	0.1	0.1	0.0	0.0	0.2	0.3	
0.038	0.0	0.0	0.1	0.0	0.1	0.0	0.0	0.0	0.1	0.1	0.1	0.0	0.0	0.0	0.0	0.1	0.0	0.2	0.1	0.0	0.0	0.1	0.0	0.0	0.0	0.0	0.0	0.0	0.2	0.1
0.025	0.0	0.0	0.0	0.0	0.0	0.0	0.0	0.0	0.0	0.0	0.0	0.0	0.0	0.0	0.0	0.0	0.0	0.0	0.0	0.0	0.0	0.0	0.0	0.0	0.0	0.0	0.0	0.0	0.0	0.0

SIEVE ANALYSIS FOR 1x12 mm at 2.2 kg/l																
Sieve Size	21.8			22.8			23.7			24.5			25.1			
	Feed	Overflow	Underflow	Feed	Overflow	Underflow	Feed	Overflow	Underflow	Feed	Overflow	Underflow	Feed	Overflow	Underflow	
4.00	8.15	5.46	0	8.15	7.78	0	8.15	10.91	0	8.15	11.68	0	8.15	10.35	0	
2.80	22.86	36.07	0	22.86	31.61	0	22.86	37.67	0	22.86	33.53	0	22.86	25.11	0	
2.360	32.58	47.93	0	32.58	48.20	0	32.58	50.88	0	32.58	48.17	0	32.58	40.16	0	
2.000	41.67	73.15	0	41.67	71.16	0	41.67	69.88	0	41.67	66.06	0	41.67	67.45	0	
1.700	40.56	93.36	0	40.56	92.88	0	40.56	84.89	0	40.56	82.89	0	40.56	71.91	0	
1.400	28.95	84.94	0	28.95	93.57	0	28.95	80.91	0	28.95	81.18	0	28.95	81.5	0	
1.180	10.02	27.81	0	10.02	29.14	0	10.02	20.79	0	10.02	20.95	0	10.02	27.2	0	
1.000	1.12	2.62	0	1.12	3.04	0	1.12	2.18	0	1.12	1.87	0	1.12	2.41	0	
0.850	0	0	0	0	0	0	0	0	0	0	0	0	0	0	0	
0.710	0	0	0	0	0	0	0	0	0	0	0	0	0	0	0	
0.600	0	0	0	0	0	0	0	0	0	0	0	0	0	0	0	
0.500	0	0	0	0	0	0	0	0	0	0	0	0	0	0	0	
0.355	0	0	0	0	0	0	0	0	0	0	0	0	0	0	0	
0.250	0	0	0	0	0	0	0	0	0	0	0	0	0	0	0	
0.212	0	0	0	0	0	0	0	0	0	0	0	0	0	0	0	
0.150	190.7	43.31	90.8	190.7	35.85	90.8	190.7	32.9	90.8	190.7	40.66	90.8	190.7	59.7	90.8	
0.106	92.08	34.87	85.69	92.08	33.2	85.69	92.08	59.58	85.69	92.08	60.22	85.69	92.08	56.18	85.69	
0.090	14.41	20.63	40.96	14.41	26.88	40.96	14.41	15.23	40.96	14.41	26.39	40.96	14.41	30.42	40.96	
0.063	9.13	9.96	25.05	9.13	20.18	25.05	9.13	13.98	25.05	9.13	20.14	25.05	9.13	10.26	25.05	
0.053	4.12	15.24	3.44	4.12	2.41	3.44	4.12	15.6	3.44	4.12	2.06	3.44	4.12	12.1	3.44	
0.045	0.16	0.79	1.66	0.16	0.34	1.66	0.16	0.3	1.66	0.16	0.57	1.66	0.16	0.63	1.66	
0.038	0.15	0.98	0.68	0.15	0.43	0.68	0.15	0.47	0.68	0.15	0.45	0.68	0.15	0.69	0.68	
0.025	0.08	0.34	0.82	0.08	0.54	0.82	0.08	0.26	0.82	0.08	0.2	0.82	0.08	0.33	0.82	
Sum	496.74	497.46	249.10	496.74	497.21	249.10	496.74	496.43	249.10	496.74	497.02	249.10	496.74	496.40	249.10	

Sieve Size	21.8						22.8						23.7						24.5						25.1						
	Feed		Overflow		Underflow		Feed		Overflow		Underflow		Feed		Overflow		Underflow		Feed		Overflow		Underflow		Feed		Overflow		Underflow		
	%Retained	%Cum pass	%Retained	%Cum pass	%Retained	%Cum pass	%Retained	%Cum pass	%Retained	%Cum pass	%Retained	%Cum pass	%Retained	%Cum pass	%Retained	%Cum pass	%Retained	%Cum pass	%Retained	%Cum pass	%Retained	%Cum pass	%Retained	%Cum pass	%Retained	%Cum pass	%Retained	%Cum pass	%Retained	%Cum pass	
4.00	1.6	98.4	1.1	98.9	0.0	100.0	1.6	98.4	2.2	97.8	0.0	100.0	1.6	98.4	2.4	97.6	0.0	100.0	1.6	98.4	2.1	97.9	0.0	100.0	1.6	98.4	2.1	97.9	0.0	100.0	
2.80	4.6	93.8	7.3	91.7	0.0	100.0	4.6	93.8	6.4	92.1	0.0	100.0	4.6	93.8	6.7	90.9	0.0	100.0	4.6	93.8	5.1	92.9	0.0	100.0	4.6	93.8	5.1	92.9	0.0	100.0	
2.360	6.6	87.2	9.6	82.0	0.0	100.0	6.6	87.2	9.7	82.4	0.0	100.0	6.6	87.2	10.2	80.0	0.0	100.0	6.6	87.2	8.1	84.8	0.0	100.0	6.6	87.2	8.1	84.8	0.0	100.0	
2.000	8.4	78.8	14.7	67.3	0.0	100.0	8.4	78.8	14.3	68.1	0.0	100.0	8.4	78.8	14.1	65.9	0.0	100.0	8.4	78.8	13.6	71.2	0.0	100.0	8.4	78.8	13.6	71.2	0.0	100.0	
1.700	8.2	70.6	18.8	48.6	0.0	100.0	8.2	70.6	18.7	49.4	0.0	100.0	8.2	70.6	17.1	48.8	0.0	100.0	8.2	70.6	16.7	51.2	0.0	100.0	8.2	70.6	14.5	56.7	0.0	100.0	
1.400	5.8	64.8	17.1	31.5	0.0	100.0	5.8	64.8	18.8	30.6	0.0	100.0	5.8	64.8	16.3	32.5	0.0	100.0	5.8	64.8	16.3	34.9	0.0	100.0	5.8	64.8	16.4	40.3	0.0	100.0	
1.180	2.0	62.8	5.6	25.9	0.0	100.0	2.0	62.8	5.9	24.7	0.0	100.0	2.0	62.8	4.2	28.3	0.0	100.0	2.0	62.8	4.2	30.7	0.0	100.0	2.0	62.8	5.5	34.8	0.0	100.0	
1.000	0.2	62.6	0.5	25.4	0.0	100.0	0.2	62.6	0.6	24.1	0.0	100.0	0.2	62.6	0.4	27.9	0.0	100.0	0.2	62.6	0.4	30.3	0.0	100.0	0.2	62.6	0.5	34.3	0.0	100.0	
0.850	0.0	62.6	0.0	25.4	0.0	100.0	0.0	62.6	0.0	24.1	0.0	100.0	0.0	62.6	0.0	27.9	0.0	100.0	0.0	62.6	0.0	30.3	0.0	100.0	0.0	62.6	0.0	34.3	0.0	100.0	
0.710	0.0	62.6	0.0	25.4	0.0	100.0	0.0	62.6	0.0	24.1	0.0	100.0	0.0	62.6	0.0	27.9	0.0	100.0	0.0	62.6	0.0	30.3	0.0	100.0	0.0	62.6	0.0	34.3	0.0	100.0	
0.600	0.0	62.6	0.0	25.4	0.0	100.0	0.0	62.6	0.0	24.1	0.0	100.0	0.0	62.6	0.0	27.9	0.0	100.0	0.0	62.6	0.0	30.3	0.0	100.0	0.0	62.6	0.0	34.3	0.0	100.0	
0.500	0.0	62.6	0.0	25.4	0.0	100.0	0.0	62.6	0.0	24.1	0.0	100.0	0.0	62.6	0.0	27.9	0.0	100.0	0.0	62.6	0.0	30.3	0.0	100.0	0.0	62.6	0.0	34.3	0.0	100.0	
0.355	0.0	62.6	0.0	25.4	0.0	100.0	0.0	62.6	0.0	24.1	0.0	100.0	0.0	62.6	0.0	27.9	0.0	100.0	0.0	62.6	0.0	30.3	0.0	100.0	0.0	62.6	0.0	34.3	0.0	100.0	
0.250	0.0	62.6	0.0	25.4	0.0	100.0	0.0	62.6	0.0	24.1	0.0	100.0	0.0	62.6	0.0	27.9	0.0	100.0	0.0	62.6	0.0	30.3	0.0	100.0	0.0	62.6	0.0	34.3	0.0	100.0	
0.212	0.0	62.6	0.0	25.4	0.0	100.0	0.0	62.6	0.0	24.1	0.0	100.0	0.0	62.6	0.0	27.9	0.0	100.0	0.0	62.6	0.0	30.3	0.0	100.0	0.0	62.6	0.0	34.3	0.0	100.0	
0.150	38.4	24.2	8.7	16.6	36.5	63.5	38.4	24.2	7.2	16.9	36.5	63.5	38.4	24.2	6.6	21.2	36.5	63.5	38.4	24.2	8.2	22.1	36.5	63.5	38.4	24.2	12.0	22.3	36.5	63.5	
0.106	18.5	5.6	7.0	9.6	34.4	29.1	18.5	5.6	6.7	10.2	34.4	29.1	18.5	5.6	12.0	9.2	34.4	29.1	18.5	5.6	12.1	10.0	34.4	29.1	18.5	5.6	11.3	11.0	34.4	29.1	
0.090	2.9	2.7	4.1	5.5	16.4	12.7	2.9	2.7	5.4	4.8	16.4	12.7	2.9	2.7	3.1	6.2	16.4	12.7	2.9	2.7	5.3	4.7	16.4	12.7	2.9	2.7	6.1	4.8	16.4	12.7	
0.063	1.8	0.9	2.0	3.5	10.1	2.6	1.8	0.9	4.1	0.7	10.1	2.6	1.8	0.9	2.8	3.3	10.1	2.6	1.8	0.9	4.1	0.7	10.1	2.6	1.8	0.9	2.1	2.8	10.1	2.6	
0.053	0.8	0.1	3.1	0.4	1.4	1.3	0.8	0.1	0.5	0.3	1.4	1.3	0.8	0.1	3.1	0.2	1.4	1.3	0.8	0.1	0.4	0.2	1.4	1.3	0.8	0.1	2.4	0.3	1.4	1.3	
0.045	0.0	0.0	0.2	0.3	0.7	0.6	0.0	0.0	0.1	0.2	0.7	0.6	0.0	0.0	0.1	0.1	0.7	0.6	0.0	0.0	0.1	0.1	0.7	0.6	0.0	0.0	0.1	0.2	0.7	0.6	
0.038	0.0	0.0	0.2	0.1	0.3	0.3	0.0	0.0	0.1	0.1	0.3	0.3	0.0	0.0	0.1	0.1	0.3	0.3	0.0	0.0	0.1	0.0	0.3	0.3	0.0	0.0	0.1	0.1	0.3	0.3	
0.025	0.0	0.0	0.1	0.0	0.3	0.0	0.0	0.0	0.1	0.0	0.3	0.0	0.0	0.0	0.1	0.0	0.3	0.0	0.0	0.0	0.0	0.0	0.3	0.0	0.0	0.0	0.0	0.1	0.0	0.3	0.0

SIEVE ANALYSIS FOR 1x12 mm at 2.3 kg/l															
Sieve Size	21.8			22.8			23.7			24.5			25.1		
	Feed	Overflow	Underflow	Feed	Overflow	Underflow	Feed	Overflow	Underflow	Feed	Overflow	Underflow	Feed	Overflow	Underflow
4.00	4.84	13.52	0	4.84	11.6	0	4.84	5.31	0	4.84	8.89	0	4.84	9.81	0
2.80	22.2	49.95	0	22.2	33.9	0	22.2	31.89	0	22.2	33.8	0	22.2	33	0
2.360	31.88	60.03	0	31.88	53.56	0	31.88	48.7	0	31.88	48.02	0	31.88	48.05	0
2.000	36.97	81.84	0	36.97	77.14	0	36.97	69.56	0	36.97	61.68	0	36.97	63.6	0
1.700	39.16	91.54	0	39.16	95.6	0	39.16	90.26	0	39.16	82.96	0	39.16	79.06	0
1.400	38.35	84.17	0	38.35	88.71	0	38.35	82.4	0	38.35	74.21	0	38.35	65.54	0
1.180	8.41	20.65	0	8.41	21.11	0	8.41	22.22	0	8.41	16.25	0	8.41	14.15	0
1.000	0.69	2.42	0	0.69	2.44	0	0.69	2	0	0.69	1.95	0	0.69	1.71	0
0.850	0	0	0	0	0	0	0	0	0	0	0	0	0	0	0
0.710	0	0	0	0	0	0	0	0	0	0	0	0	0	0	0
0.600	0	0	0	0	0	0	0	0	0	0	0	0	0	0	0
0.500	0	0	0	0	0	0	0	0	0	0	0	0	0	0	0
0.355	0	0	0	0	0	0	0	0	0	0	0	0	0	0	0
0.250	0	0	0	0	0	0	0	0	0	0	0	0	0	0	0
0.212	0	0	0	0	0	0	0	0	0	0	0	0	0	0	0
0.150	125.96	41.68	74.15	125.96	33.11	74.15	125.96	47.55	74.15	125.96	96.67	74.15	125.96	78.15	74.15
0.106	109.54	36.76	75.04	109.54	39.48	75.04	109.54	55.94	75.04	109.54	47.59	75.04	109.54	73.1	75.04
0.090	54.97	4.04	55.26	54.97	4.6	55.26	54.97	21.21	55.26	54.97	7.33	55.26	54.97	11.75	55.26
0.063	22.02	7.87	38.38	22.02	15.13	38.38	22.02	16.9	38.38	22.02	12.72	38.38	22.02	18.1	38.38
0.053	1.68	3.72	3.5	1.68	1.01	3.5	1.68	3.65	3.5	1.68	5.44	3.5	1.68	1.88	3.5
0.045	0.36	0.32	0.57	0.36	0.5	0.57	0.36	0.43	0.57	0.36	0.28	0.57	0.36	0.22	0.57
0.038	0.45	0.48	0.3	0.45	0.9	0.3	0.45	0.34	0.3	0.45	0.31	0.3	0.45	0.15	0.3
0.025	0.29	0.28	1.46	0.29	0.4	1.46	0.29	0.1	1.46	0.29	0.18	1.46	0.29	0.12	1.46
Sum	497.77	499.27	248.66	497.77	479.19	248.66	497.77	498.46	248.66	497.77	498.28	248.66	497.77	498.39	248.66

Sieve Size	21.8						22.8						23.7						24.5						25.1					
	Feed		Overflow		Underflow		Feed		Overflow		Underflow		Feed		Overflow		Underflow		Feed		Overflow		Underflow		Feed		Overflow		Underflow	
%Retained	%Cum pass	%Retained	%Cum pass	%Retained	%Cum pass	%Retained	%Cum pass	%Retained	%Cum pass	%Retained	%Cum pass	%Retained	%Cum pass	%Retained	%Cum pass	%Retained	%Cum pass	%Retained	%Cum pass	%Retained	%Cum pass	%Retained	%Cum pass	%Retained	%Cum pass	%Retained	%Cum pass	%Retained	%Cum pass	
4.00	1.0	99.0	2.7	97.3	0.0	100.0	1.0	99.0	2.4	97.6	0.0	100.0	1.0	99.0	1.1	98.9	0.0	100.0	1.0	99.0	1.8	98.2	0.0	100.0	1.0	99.0	2.0	98.0	0.0	100.0
2.80	4.5	94.6	10.0	87.3	0.0	100.0	4.5	94.6	7.1	90.5	0.0	100.0	4.5	94.6	6.4	92.5	0.0	100.0	4.5	94.6	6.8	91.4	0.0	100.0	4.5	94.6	6.6	91.4	0.0	100.0
2.360	6.4	88.2	12.0	75.3	0.0	100.0	6.4	88.2	11.2	79.3	0.0	100.0	6.4	88.2	9.8	82.8	0.0	100.0	6.4	88.2	9.6	81.8	0.0	100.0	6.4	88.2	9.6	81.8	0.0	100.0
2.000	7.4	80.7	16.4	58.9	0.0	100.0	7.4	80.7	16.1	63.2	0.0	100.0	7.4	80.7	14.0	68.8	0.0	100.0	7.4	80.7	12.4	69.4	0.0	100.0	7.4	80.7	12.8	69.0	0.0	100.0
1.700	7.9	72.9	18.3	40.5	0.0	100.0	7.9	72.9	20.0	43.3	0.0	100.0	7.9	72.9	18.1	50.7	0.0	100.0	7.9	72.9	16.6	52.8	0.0	100.0	7.9	72.9	15.9	53.1	0.0	100.0
1.400	7.7	65.2	16.9	23.7	0.0	100.0	7.7	65.2	18.5	24.8	0.0	100.0	7.7	65.2	16.5	34.2	0.0	100.0	7.7	65.2	14.9	37.9	0.0	100.0	7.7	65.2	13.2	40.0	0.0	100.0
1.180	1.7	63.5	4.1	19.5	0.0	100.0	1.7	63.5	4.4	20.4	0.0	100.0	1.7	63.5	4.5	29.7	0.0	100.0	1.7	63.5	3.3	34.6	0.0	100.0	1.7	63.5	2.8	37.2	0.0	100.0
1.000	0.1	63.3	0.5	19.1	0.0	100.0	0.1	63.3	0.5	19.9	0.0	100.0	0.1	63.3	0.4	29.3	0.0	100.0	0.1	63.3	0.4	34.2	0.0	100.0	0.1	63.3	0.3	36.8	0.0	100.0
0.850	0.0	63.3	0.0	19.1	0.0	100.0	0.0	63.3	0.0	19.9	0.0	100.0	0.0	63.3	0.0	29.3	0.0	100.0	0.0	63.3	0.0	34.2	0.0	100.0	0.0	63.3	0.0	36.8	0.0	100.0
0.710	0.0	63.3	0.0	19.1	0.0	100.0	0.0	63.3	0.0	19.9	0.0	100.0	0.0	63.3	0.0	29.3	0.0	100.0	0.0	63.3	0.0	34.2	0.0	100.0	0.0	63.3	0.0	36.8	0.0	100.0
0.600	0.0	63.3	0.0	19.1	0.0	100.0	0.0	63.3	0.0	19.9	0.0	100.0	0.0	63.3	0.0	29.3	0.0	100.0	0.0	63.3	0.0	34.2	0.0	100.0	0.0	63.3	0.0	36.8	0.0	100.0
0.500	0.0	63.3	0.0	19.1	0.0	100.0	0.0	63.3	0.0	19.9	0.0	100.0	0.0	63.3	0.0	29.3	0.0	100.0	0.0	63.3	0.0	34.2	0.0	100.0	0.0	63.3	0.0	36.8	0.0	100.0
0.355	0.0	63.3	0.0	19.1	0.0	100.0	0.0	63.3	0.0	19.9	0.0	100.0	0.0	63.3	0.0	29.3	0.0	100.0	0.0	63.3	0.0	34.2	0.0	100.0	0.0	63.3	0.0	36.8	0.0	100.0
0.250	0.0	63.3	0.0	19.1	0.0	100.0	0.0	63.3	0.0	19.9	0.0	100.0	0.0	63.3	0.0	29.3	0.0	100.0	0.0	63.3	0.0	34.2	0.0	100.0	0.0	63.3	0.0	36.8	0.0	100.0
0.212	0.0	63.3	0.0	19.1	0.0	100.0	0.0	63.3	0.0	19.9	0.0	100.0	0.0	63.3	0.0	29.3	0.0	100.0	0.0	63.3	0.0	34.2	0.0	100.0	0.0	63.3	0.0	36.8	0.0	100.0
0.150	25.3	38.0	8.3	10.7	29.8	70.2	25.3	38.0	6.9	12.9	29.8	70.2	25.3	38.0	9.5	19.8	29.8	70.2	25.3	38.0	19.4	14.8	29.8	70.2	25.3	38.0	15.7	21.1	29.8	70.2
0.106	22.0	16.0	7.4	3.3	30.2	40.0	22.0	16.0	8.2	4.7	30.2	40.0	22.0	16.0	11.2	8.6	30.2	40.0	22.0	16.0	9.6	5.3	30.2	40.0	22.0	16.0	14.7	6.5	30.2	40.0
0.090	11.0	5.0	0.8	2.5	22.2	17.8	11.0	5.0	1.0	3.7	22.2	17.8	11.0	5.0	4.3	4.3	22.2	17.8	11.0	5.0	1.5	3.8	22.2	17.8	11.0	5.0	2.4	4.1	22.2	17.8
0.063	4.4	0.6	1.6	1.0	15.4	2.3	4.4	0.6	3.2	0.6	15.4	2.3	4.4	0.6	3.4	0.9	15.4	2.3	4.4	0.6	2.6	1.2	15.4	2.3	4.4	0.6	3.6	0.5	15.4	2.3
0.053	0.3	0.2	0.7	0.2	1.4	0.9	0.3	0.2	0.2	0.4	1.4	0.9	0.3	0.2	0.7	0.2	1.4	0.9	0.3	0.2	1.1	0.2	1.4	0.9	0.3	0.2	0.4	0.1	1.4	0.9
0.045	0.1	0.1	0.1	0.2	0.2	0.7	0.1	0.1	0.1	0.3	0.2	0.7	0.1	0.1	0.1	0.1	0.2	0.7	0.1	0.1	0.1	0.2	1.4	0.9	0.3	0.2	0.4	0.1	1.4	0.9
0.038	0.1	0.1	0.1	0.1	0.6	0.1	0.1	0.2	0.1	0.1	0.6	0.1	0.1	0.1	0.1	0.1	0.6	0.1	0.1	0.1	0.1	0.6	0.1	0.1	0.1	0.1	0.1	0.1	0.6	0.1
0.025	0.1	0.1	0.1	0.0	0.6	0.0	0.1	0.0	0.1	0.0	0.6	0.0	0.1	0.0	0.0	0.6	0.0	0.1	0.0	0.1	0.0	0.6	0.0	0.1	0.0	0.1	0.0	0.0	0.6	0.0
0.025	0.1	0.0	0.1	0.0	0.6	0.0	0.1	0.0	0.1	0.0	0.6	0.0	0.1	0.0	0.0	0.6	0.0	0.1	0.0	0.1	0.0	0.6	0.0	0.1	0.0	0.0	0.0	0.0	0.6	0.0

SIEVE ANALYSIS FOR 1x12 mm at 2.45 kg/l															
Sieve Size	21.8			22.8			23.7			24.5			25.1		
	Feed	Overflow	Underflow	Feed	Overflow	Underflow	Feed	Overflow	Underflow	Feed	Overflow	Underflow	Feed	Overflow	Underflow
4.00	6.53	8.66	0	6.53	10.47	0	6.53	11.03	0	6.53	10.23	0	6.53	9.27	0
2.80	26.38	31.11	0	26.38	36.93	0	26.38	30.94	0	26.38	39.25	0	26.38	37.98	0
2.360	28.18	47.7	0	28.18	55.16	0	28.18	41.99	0	28.18	46.11	0	28.18	49.33	0
2.000	37.97	73.95	0	37.97	73.1	0	37.97	64.11	0	37.97	57.74	0	37.97	61.54	0
1.700	30.92	87.93	0	30.92	81.93	0	30.92	76.35	0	30.92	66.79	0	30.92	68.54	0
1.400	42.39	89.95	0	42.39	81.16	0	42.39	77.07	0	42.39	62.26	0	42.39	68.25	0
1.180	7.33	24.76	0	7.33	19.81	0	7.33	22.58	0	7.33	13.5	0	7.33	16.1	0
1.000	0.26	2	0	0.26	1.89	0	0.26	2.06	0	0.26	1.08	0	0.26	1.38	0
0.850	0	0	0	0	0	0	0	0	0	0	0	0	0	0	0
0.710	0	0	0	0	0	0	0	0	0	0	0	0	0	0	0
0.600	0	0	0	0	0	0	0	0	0	0	0	0	0	0	0
0.500	0	0	0	0	0	0	0	0	0	0	0	0	0	0	0
0.355	0	0	0	0	0	0	0	0	0	0	0	0	0	0	0
0.250	0	0	0	0	0	0	0	0	0	0	0	0	0	0	0
0.212	0	0	0	0	0	0	0	0	0	0	0	0	0	0	0
0.150	133.64	46.82	100.18	133.64	45.75	100.18	133.64	64.69	100.18	133.64	95.47	100.18	133.64	70.81	100.18
0.106	126.91	51.94	95.54	126.91	51.39	95.54	126.91	72.32	95.54	126.91	68.08	95.54	126.91	67.54	95.54
0.090	27.33	16.42	25.24	27.33	18.42	25.24	27.33	11.87	25.24	27.33	18.64	25.24	27.33	22.95	25.24
0.063	22.2	7.85	18.23	22.2	13.41	18.23	22.2	9.74	18.23	22.2	15.41	18.23	22.2	19.23	18.23
0.053	3.58	8.87	8.05	3.58	6.14	8.05	3.58	9.18	8.05	3.58	2.25	8.05	3.58	1.79	8.05
0.045	1.03	0.38	0.49	1.03	0.61	0.49	1.03	1.96	0.49	1.03	0.64	0.49	1.03	0.59	0.49
0.038	0.87	0.17	1.15	0.87	0.57	1.15	0.87	0.68	1.15	0.87	0.25	1.15	0.87	0.44	1.15
0.025	0.73	0.12	0.45	0.73	0.25	0.45	0.73	0.55	0.45	0.73	0.15	0.45	0.73	0.53	0.45
Sum	496.25	498.63	249.33	496.25	496.99	249.33	496.25	497.12	249.33	496.25	497.85	249.33	496.25	496.27	249.33

Sieve Size	21.8						22.8						23.7						24.5						25.1						
	Feed		Overflow		Underflow		Feed		Overflow		Underflow		Feed		Overflow		Underflow		Feed		Overflow		Underflow		Feed		Overflow		Underflow		
Sieve Size	%Retained	%Cum pass	%Retained	%Cum pass	%Retained	%Cum pass	%Retained	%Cum pass	%Retained	%Cum pass	%Retained	%Cum pass	%Retained	%Cum pass	%Retained	%Cum pass	%Retained	%Cum pass	%Retained	%Cum pass	%Retained	%Cum pass	%Retained	%Cum pass	%Retained	%Cum pass	%Retained	%Cum pass	%Retained	%Cum pass	
4.00	1.3	98.7	1.7	98.3	0.0	100.0	1.3	98.7	2.1	97.9	0.0	100.0	1.3	98.7	2.2	97.8	0.0	100.0	1.3	98.7	2.1	97.9	0.0	100.0	1.3	98.7	1.9	98.1	0.0	100.0	
2.80	5.3	93.4	6.2	92.0	0.0	100.0	5.3	93.4	7.4	90.5	0.0	100.0	5.3	93.4	6.2	91.6	0.0	100.0	5.3	93.4	7.9	90.1	0.0	100.0	5.3	93.4	7.7	90.5	0.0	100.0	
2.360	5.7	87.7	9.6	82.5	0.0	100.0	5.7	87.7	11.1	79.4	0.0	100.0	5.7	87.7	8.4	83.1	0.0	100.0	5.7	87.7	9.3	80.8	0.0	100.0	5.7	87.7	9.9	80.5	0.0	100.0	
2.000	7.7	80.0	14.8	67.6	0.0	100.0	7.7	80.0	14.7	64.7	0.0	100.0	7.7	80.0	12.9	70.2	0.0	100.0	7.7	80.0	11.6	69.2	0.0	100.0	7.7	80.0	12.4	68.1	0.0	100.0	
1.700	6.2	73.8	17.6	50.0	0.0	100.0	6.2	73.8	16.5	48.2	0.0	100.0	6.2	73.8	15.4	44.9	0.0	100.0	6.2	73.8	13.4	55.8	0.0	100.0	6.2	73.8	13.8	54.3	0.0	100.0	
1.400	8.5	65.3	18.0	32.0	0.0	100.0	8.5	65.3	16.3	31.8	0.0	100.0	8.5	65.3	15.5	39.4	0.0	100.0	8.5	65.3	12.5	43.3	0.0	100.0	8.5	65.3	13.8	40.6	0.0	100.0	
1.180	1.5	63.8	5.0	27.0	0.0	100.0	1.5	63.8	4.0	27.9	0.0	100.0	1.5	63.8	4.5	34.8	0.0	100.0	1.5	63.8	2.7	40.6	0.0	100.0	1.5	63.8	3.2	37.3	0.0	100.0	
1.000	0.1	63.7	0.4	26.6	0.0	100.0	0.1	63.7	0.4	27.5	0.0	100.0	0.1	63.7	0.4	34.4	0.0	100.0	0.1	63.7	0.2	40.4	0.0	100.0	0.1	63.7	0.3	37.1	0.0	100.0	
0.850	0.0	63.7	0.0	26.6	0.0	100.0	0.0	63.7	0.0	27.5	0.0	100.0	0.0	63.7	0.0	34.4	0.0	100.0	0.0	63.7	0.0	40.4	0.0	100.0	0.0	63.7	0.0	37.1	0.0	100.0	
0.710	0.0	63.7	0.0	26.6	0.0	100.0	0.0	63.7	0.0	27.5	0.0	100.0	0.0	63.7	0.0	34.4	0.0	100.0	0.0	63.7	0.0	40.4	0.0	100.0	0.0	63.7	0.0	37.1	0.0	100.0	
0.600	0.0	63.7	0.0	26.6	0.0	100.0	0.0	63.7	0.0	27.5	0.0	100.0	0.0	63.7	0.0	34.4	0.0	100.0	0.0	63.7	0.0	40.4	0.0	100.0	0.0	63.7	0.0	37.1	0.0	100.0	
0.500	0.0	63.7	0.0	26.6	0.0	100.0	0.0	63.7	0.0	27.5	0.0	100.0	0.0	63.7	0.0	34.4	0.0	100.0	0.0	63.7	0.0	40.4	0.0	100.0	0.0	63.7	0.0	37.1	0.0	100.0	
0.355	0.0	63.7	0.0	26.6	0.0	100.0	0.0	63.7	0.0	27.5	0.0	100.0	0.0	63.7	0.0	34.4	0.0	100.0	0.0	63.7	0.0	40.4	0.0	100.0	0.0	63.7	0.0	37.1	0.0	100.0	
0.250	0.0	63.7	0.0	26.6	0.0	100.0	0.0	63.7	0.0	27.5	0.0	100.0	0.0	63.7	0.0	34.4	0.0	100.0	0.0	63.7	0.0	40.4	0.0	100.0	0.0	63.7	0.0	37.1	0.0	100.0	
0.212	0.0	63.7	0.0	26.6	0.0	100.0	0.0	63.7	0.0	27.5	0.0	100.0	0.0	63.7	0.0	34.4	0.0	100.0	0.0	63.7	0.0	40.4	0.0	100.0	0.0	63.7	0.0	37.1	0.0	100.0	
0.150	26.9	36.8	9.4	17.2	40.2	59.8	26.9	36.8	9.2	18.3	40.2	59.8	26.9	36.8	13.0	21.4	40.2	59.8	26.9	36.8	19.2	21.2	40.2	59.8	26.9	36.8	14.3	22.8	40.2	59.8	
0.106	25.6	11.2	10.4	6.8	38.3	21.5	25.6	11.2	10.3	7.9	38.3	21.5	25.6	11.2	14.5	6.8	38.3	21.5	25.6	11.2	13.7	7.5	38.3	21.5	25.6	11.2	13.6	9.2	38.3	21.5	
0.090	5.5	5.7	3.3	3.5	10.1	11.4	5.5	5.7	3.7	4.2	10.1	11.4	5.5	5.7	2.4	4.4	10.1	11.4	5.5	5.7	3.7	3.8	10.1	11.4	5.5	5.7	4.6	4.5	10.1	11.4	
0.063	4.5	1.3	1.6	1.9	7.3	4.1	4.5	1.3	2.7	1.5	7.3	4.1	4.5	1.3	2.0	2.5	7.3	4.1	4.5	1.3	3.1	0.7	7.3	4.1	4.5	1.3	3.9	0.7	7.3	4.1	
0.053	0.7	0.5	1.8	0.1	3.2	0.8	0.7	0.5	1.2	0.3	3.2	0.8	0.7	0.5	1.8	0.6	3.2	0.8	0.7	0.5	0.2	3.2	0.8	0.7	0.5	0.4	0.3	3.2	0.8		
0.045	0.2	0.3	0.1	0.1	0.2	0.6	0.2	0.3	0.1	0.2	0.2	0.6	0.2	0.3	0.4	0.2	0.2	0.6	0.2	0.3	0.1	0.1	0.2	0.6	0.2	0.3	0.1	0.2	0.6	0.2	
0.038	0.2	0.1	0.0	0.0	0.5	0.2	0.2	0.1	0.1	0.1	0.5	0.2	0.2	0.1	0.1	0.1	0.5	0.2	0.2	0.1	0.1	0.0	0.5	0.2	0.2	0.1	0.1	0.1	0.5	0.2	
0.025	0.1	0.0	0.0	0.0	0.2	0.0	0.1	0.0	0.1	0.0	0.2	0.0	0.1	0.0	0.1	0.0	0.1	0.0	0.0	0.0	0.0	0.2	0.0	0.1	0.0	0.1	0.0	0.1	0.0	0.2	0.0

Appendix S: Mass balance

0.63x8.8 mm polyurethane panels at 2.45 kg/L slurry density															
Aperture size (microns)		0.63x8.8 mm													
	Feed	Oversize	Undersize												
STPH	21.84	3.89	17.95												
% weight	100	39.2	60.8												
% solids	70.8	94.07	70.8												
EXPERIMENTAL DATA, retained %				MASS BALANCED DATA, retained %											
STPH	21.84	17.947	3.89												
size (micron)	Feed	UF	OF	(fine-coarse)*(feed-coarse)	(fine-coarse)^2	Di	Feed	UF	OF	cumulative passing%					
										size (micron)	Feed	UF	OF	mean size (micron)	partition %
4000	0.35	0.00	1.69	2.3	2.9	0.05	0.32	0.02	1.71	4000	99.68	99.98	100.41		
2800	1.46	0.00	6.79	36.2	46.1	0.25	1.33	0.13	6.91	2800	98.35	99.85	93.49	3347	92
2360	2.40	0.00	12.43	124.6	154.5	0.20	2.30	0.10	12.53	2360	96.04	99.75	80.96	2571	96
2000	2.21	0.00	17.17	256.9	294.8	-0.83	2.62	-0.42	16.75	2000	93.42	100.16	64.21	2173	100
1700	3.49	0.00	19.61	316.3	384.7	0.02	3.48	0.01	19.62	1700	89.94	100.15	44.59	1844	100
1400	3.46	0.00	21.66	394.3	469.3	-0.37	3.65	-0.19	21.48	1400	86.29	100.34	23.11	1543	100
1180	2.32	0.00	7.59	40.0	57.6	0.97	1.83	0.49	8.08	1180	84.46	99.85	15.03	1285	100
1000	2.30	0.00	1.64	-1.1	2.7	2.01	1.30	1.01	2.65	1000	83.16	98.85	12.38	1086	100
850	0.00	0.00	0.00	0.0	0.0	0.00	0.00	0.00	0.00	850	83.16	98.85	12.38	922	100
710	0.00	0.00	0.00	0.0	0.0	0.00	0.00	0.00	0.00	710	83.16	98.85	12.38	777	100
600	0.00	0.00	0.00	0.0	0.0	0.00	0.00	0.00	0.00	600	83.16	98.85	12.38	653	100
500	0.00	0.00	0.00	0.0	0.0	0.00	0.00	0.00	0.00	500	83.16	98.85	12.38	548	100
355	0.00	0.00	0.00	0.0	0.0	0.00	0.00	0.00	0.00	355	83.16	98.85	12.38	421	100
250	0.00	0.00	0.00	0.0	0.0	0.00	0.00	0.00	0.00	250	83.16	98.85	12.38	298	100
212	0.00	0.00	0.00	0.0	0.0	0.00	0.00	0.00	0.00	212	83.16	98.85	12.38	230	100
150	13.89	24.52	1.88	271.9	512.8	-6.63	17.20	21.21	-1.43	150	65.96	77.64	13.82	178	0
106	20.96	16.33	2.22	264.5	199.2	7.13	17.40	19.90	5.78	106	48.56	57.74	8.03	126	6
90	20.19	16.11	1.11	286.0	224.8	6.73	16.82	19.47	4.48	90	31.74	38.27	3.55	98	5
63	21.95	26.58	3.54	424.0	530.5	-0.55	22.22	26.30	3.27	63	9.52	11.97	0.28	75	3
53	3.94	9.18	2.29	11.3	47.5	-4.03	5.95	7.17	0.28	53	3.57	4.80	0.00	58	1
45	0.19	4.62	0.08	0.5	20.5	-3.63	2.00	2.80	0.00	45	1.57	1.99	0.00	49	0
38	0.31	0.95	0.16	0.1	0.6	-0.50	0.56	0.70	0.00	38	1.01	1.29	0.00	41	0
25	0.59	1.71	0.12	0.7	2.5	-0.84	1.01	1.29	0.00	25	0.00	0.00	0.00	31	0
-25	0.00	0.00	0.00	0.0	0.0	0.00	0.00	0.00	0.00						
Sum	100.00	100.00	100.00	2428.42	2950.97										
				Fine/Feed ratio	82.3%										

Appendix T: Calculations for solid concentration

Pulp Calculations (Water Based)		Enter values in yellow cells			Key		
Specific Gravity of Solids		Ss =	6.10		Pw =	Percent Solids by Weight (Pulp Density)	
Specific Gravity of Pulp		Sp =	2.70		Pv =	Percent solids by Volume	
					Ss =	Specific Gravity of Solids	
Pw	Rws	Ss	Sp	Pv	Sp =	Specific Gravity of Pulp	
75.3%	0.33	6.10	2.70	33.33%	Rws =	Ratio of Water to Solids by Weight	
Percent Solids by Weight	Ratio of Water to Solids by	Specific Gravity of Solids	Specific Gravity of Pulp	Percent solids by Volume	Volume of ore for 340 L slurry	Volume of water for 340 L	Mass of ore= density*Volume
1.0%	99.00	6.10	1.008	0.17%	0.56	339.44	3.43
2.0%	49.00	6.10	1.017	0.33%	1.13	338.87	6.92
3.0%	32.33	6.10	1.026	0.50%	1.72	338.28	10.46
4.0%	24.00	6.10	1.035	0.68%	2.31	337.69	14.07
5.0%	19.00	6.10	1.044	0.86%	2.91	337.09	17.74
10.0%	9.00	6.10	1.091	1.79%	6.08	333.92	37.10
15.0%	5.67	6.10	1.143	2.81%	9.56	330.44	58.31
20.0%	4.00	6.10	1.201	3.94%	13.39	326.61	81.65
25.0%	3.00	6.10	1.264	5.18%	17.62	322.38	107.46
30.0%	2.33	6.10	1.335	6.56%	22.32	317.68	136.15
35.0%	1.86	6.10	1.414	8.11%	27.58	312.42	168.23
40.0%	1.50	6.10	1.502	9.85%	33.50	306.50	204.33
45.0%	1.22	6.10	1.603	11.83%	40.21	299.79	245.28
50.0%	1.00	6.10	1.718	14.08%	47.89	292.11	292.11
58.0%	0.72	6.10	1.941	18.46%	62.76	277.24	382.85
68.0%	0.47	6.10	2.318	25.84%	87.84	252.16	535.84
78.0%	0.28	6.10	2.875	36.76%	124.98	215.02	762.36
88.0%	0.14	6.10	3.784	54.59%	185.61	154.39	1132.21
98.0%	0.02	6.10	5.535	88.93%	302.36	37.64	1844.39
100.0%	0.00	2.70	2.700	100.00%	340.00	0.00	2074.00

$$\rho_m = \frac{100}{\left[\left(\frac{C_w}{\rho_s} \right) + \frac{100 - C_w}{\rho_l} \right]} \dots \dots \dots 7.1$$

Where

ρ_m - relative density of slurry (kg/m³)

C_w - percent solids by weight

ρ_s - density of solid (kg/m³)

ρ_l - density of liquid (water) (kg/m³)

However, with more than one solid in the slurry, the formula below was used:

$$SG_{slurry} = \frac{1}{\frac{XS_1}{SG_1} + \frac{XS_2}{SG_2} + \frac{X_l}{SG_l}} \dots \dots \dots 7.2$$

Where;

XS_1 and SG_1 - weight of first and specific gravity of first solid respectively.

XS_2 and SG_2 - weight of second and specific gravity of second solid respectively.

X_l and SG_l – weight and specific gravity of water respectively.

On the other hand, Percent solids (C_w) were calculated as follows:

$$C_w = \frac{M_s}{M_{sl}} * 100 \dots\dots\dots 7.3$$

Where

M_s - Weight of solids

M_{sl} -Weight of slurry (solids and liquid)

The term C_w represents the solid concentration by weight in the slurry. However, this parameter can be related to a corresponding value in terms of volume, i.e. C_v . The two parameters are related to slurry density as well as solid density by the equation below:

$$C_v = C_w * \left(\frac{\rho_m}{\rho_s} \right) \dots\dots\dots 7.4$$

Where

ρ_s - density of solid (kg/m³)

ρ_m - density of slurry (kg/m³)

Besides relating viscosity factor to stability test, this factor can also be described as relative to the viscosity of a liquid as follows:

$$\mu_r = \mu_l * \mu_r \dots\dots\dots 7.5$$

Where

μ_m -Viscosity of slurry, cP

μ_l - Viscosity of liquid, cP

μ_r -Relative viscosity, dimensionless

And

$$\mu_r = 1 + 2.5\phi + 10.05\phi^2 + 0.00273 \exp(16.6\phi) \dots\dots\dots 7.6$$

ϕ -Volume fraction

Volume fraction, in this case, is calculated using the concentration of solids in the slurry by volume (C_v) as follows:

$$\phi = \frac{C_v}{100} \dots\dots\dots 7.7$$